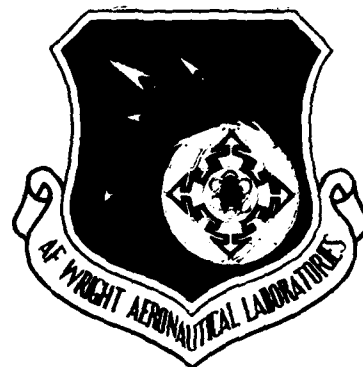


AFWAL-TR-82-4024

12

WA 126606

THE DYNAMIC PLASTIC DEFORMATION
OF METALS: A REVIEW



J. Duffy
Metals Behavior Branch
Metals and Ceramics Division

October 1982

Interim Report for Period: June 1981 - December 1981

DTIC
APR 11 1983
H

Approved for public release; distribution unlimited.

DTIC FILE COPY

MATERIALS LABORATORY
AIR FORCE WRIGHT AERONAUTICAL LABORATORIES
AIR FORCE SYSTEMS COMMAND
WRIGHT-PATTERSON AIR FORCE BASE, OHIO 45433

83 04 08 066

**Best
Available
Copy**

NOTICE

When Government drawings, specifications, or other data are used for any purpose other than in connection with a definitely related Government procurement operation, the United States Government thereby incurs no responsibility nor any obligation whatsoever; and the fact that the government may have formulated, furnished, or in any way supplied the said drawings, specifications, or other data, is not to be regarded by implication or otherwise as in any manner licensing the holder or any other person or corporation, or conveying any rights or permission to manufacture use, or sell any patented invention that may in any way be related thereto.

This report has been reviewed by the Office of Public Affairs (ASD/PA) and is releasable to the National Technical Information Service (NTIS). At NTIS, it will be available to the general public, including foreign nations.

This technical report has been reviewed and is approved for publication.

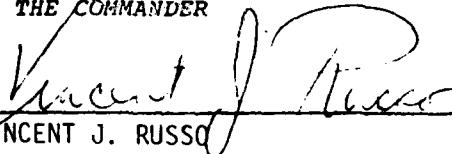


T. NICHOLAS
Project Engineer



J. P. HENDERSON
Chief, Metals Behavior Branch

FOR THE COMMANDER



VINCENT J. RUSSO
Chief, Metals and Ceramics Division

"If your address has changed, if you wish to be removed from our mailing list, or if the addressee is no longer employed by your organization please notify AFWAL/MLLN W-PAFB, OH 45433 to help us maintain a current mailing list".

Copies of this report should not be returned unless return is required by security considerations, contractual obligations, or notice on a specific document.

UNCLASSIFIED

SECURITY CLASSIFICATION OF THIS PAGE (When Data Entered)

REPORT DOCUMENTATION PAGE		READ INSTRUCTIONS BEFORE COMPLETING FORM
1. REPORT NUMBER AFWAL-TR-82-4024	2. GOVT ACCESSION NO. AN-A126 606	3. RECIPIENT'S CATALOG NUMBER
4. TITLE (and Subtitle) The Dynamic Plastic Deformation of Metals: A Review		5. TYPE OF REPORT & PERIOD COVERED Interim Report for period June 1981 - December 1981
7. AUTHOR(s) J. Duffy*		6. PERFORMING ORG. REPORT NUMBER
9. PERFORMING ORGANIZATION NAME AND ADDRESS Materials Laboratory (AFWAL/MLLN) Air Force Wright Aeronautical Laboratories (AFSC) Wright-Patterson Air Force Base, Ohio 45433		8. CONTRACT OR GRANT NUMBER(s)
11. CONTROLLING OFFICE NAME AND ADDRESS Materials Laboratory (AFWAL/MLLN) Air Force Wright Aeronautical Laboratories (AFSC) Wright-Patterson Air Force Base, Ohio 45433		10. PROGRAM ELEMENT, PROJECT, TASK AREA & WORK UNIT NUMBERS 2307P102 61028
14. MONITORING AGENCY NAME & ADDRESS (if different from Controlling Office)		12. REPORT DATE October 1982
		13. NUMBER OF PAGES 227
		15. SECURITY CLASS. (of this report) UNCLASSIFIED
16. DISTRIBUTION STATEMENT (of this Report) Approved for public release; distribution unlimited.		15a. DECLASSIFICATION DOWNGRADING SCHEDULE
17. DISTRIBUTION STATEMENT (of the abstract entered in Block 20, if different from Report)		
18. SUPPLEMENTARY NOTES *Division of Engineering Brown University Providence, R. I. 02912		
19. KEY WORDS (Continue on reverse side if necessary and identify by block number) High Strain Rate Dynamic Properties of Materials Structural Materials Dynamic Plasticity		
20. ABSTRACT (Continue on reverse side if necessary and identify by block number) This review covers the dynamic deformation of metals at strain rates from the quasi-static up to about 10^4 s^{-1} . The emphasis is on macroscopic material behavior as it is influenced by strain rate and temperature. The results of wave propagation experiments are discussed briefly, but greater weight is placed on tests with specimens short enough so the state of stress is homogeneous within the specimen. A brief review is presented of possible applications, such as armor penetration, metal forming, or machining.		

DTIC
SELECTED
APR 11 1983
H

DD FORM 1 JAN 73 1473

EDITION OF 1 NOV 65 IS OBSOLETE

UNCLASSIFIED

SECURITY CLASSIFICATION OF THIS PAGE (When Data Entered)

TABLE OF CONTENTS

SECTION	PAGE
I INTRODUCTION	1
II PLASTIC FLOW AND CONSTITUTIVE EQUATIONS ON THE MICROSTRUCTURAL SCALE	6
III CONSTITUTIVE EQUATIONS AND EARLY ANALYSES IN PLASTIC WAVE PROPAGATION	11
Strain Rate Independent (Time-Independent Constitutive Equations	11
IV EXPERIMENTS IN WAVE PROPAGATION	27
V IMPACT TESTS AND TESTS AT INTERMEDIATE STRAIN RATE	35
VI THE KOLSKY BAR (SPLIT-HOPKINSON BAR) AND TESTS AT HIGH RATES OF STRAIN	46
1. Critique of the Kolsky Bar	48
a. Inertial and Frictional Effects	48
b. Inhomogeneous Stress or Strain	51
c. Dispersion in the Loading Bars	56
d. Recording the Stress-Strain Curve	57
e. Tests at Elevated Temperatures	57
2. Results of Constant Strain Rate Tests with the Kolsky Bar	61
a. Strain Rates to 10^3 s^{-1}	61
b. Strain Rates Greater than 10^3 s^{-1}	63
3. The Torsional Kolsky Bar	68
VII HISTORY EFFECTS AND INCREMENTAL STRAIN RATE TESTS	77
1. Early Results and Investigations with FCC Metals	84
2. Investigations with BCC and HCP Metals	96
3. Microstructural Considerations in Dynamic Plasticity	115
VIII SHEAR BANDS	129

TABLE OF CONTENTS (Continued)

SECTION		PAGE
IX	EXPERIMENTAL TECHNIQUES FOR HIGHER STRAIN RATES	140
	1. The Plate Impact Experiment	141
	2. The Double-Notch Shear Test	146
	3. Machining and Metal Forming	146
X	COMPARISON OF THE STRAIN RATE SENSITIVITIES OF A NUMBER OF METALS	150
XI	DIRECTIONS FOR FUTURE INVESTIGATIONS	162
	REFERENCES	172
	BIBLIOGRAPHY	195

LIST OF ILLUSTRATIONS

FIGURE		PAGE
1	Schematic Diagram Showing the Effects of Temperature and Strain Rate on the Critical Resolved Shear Stress	9
2	Quasi-Static and Dynamic Shear Stress-Strain Curves for 1018 Cold-Rolled Steel	13
3	Idealized Uni-Axial Stress-Strain Curve for a Time Independent Material Showing Linear-Elastic and Work-Hardening Regions	16
4	Family of Characteristic Curves for "Instantaneous" Loading of Semi-Infinite Slender Elastic-Plastic Rod	16
5	Strain Distribution as a Function of Time for "Instantaneous" Loading of a Semi-Infinite Elastic-Plastic Rod	19
6	Family of Characteristic Curves for Ramp Loading of a Semi-Infinite Elastic-Plastic Rod	19
7	Bodner and Merzer's Calculated Stress-Strain Curves Compared to Results of Constant and Incremental Strain Rate Experiments	25
8	Theoretical and Experimental Strain Distribution Due to a Plastic Wave in an Annealed Copper Wire Specimen	32
9	Incremental Stress-Strain Curves from Tests on Short Specimens of Copper	32
10	Incremental Stress-Strain Curves from Tests on Short Specimens of Aluminum	32
11	Strain-Test Profiles at Various Stations Along an 1100F Aluminum Bar After Impact	34
12	Flow Stress Vs. Natural Strain at Different Strain Rates for a Low Carbon and a Medium Carbon Steel at Elevated Temperatures	39
13	Dynamic Stress-Strain Curves for Mild Steel at Constant Strain Rates and Constant Stress	42
14	Variation of Lower Yield Stress With Strain Rate in Mild Steel	42
15	Variations of Effective Stress with Effective Strain for 6061 Aluminum at Large Strains	45

LIST OF ILLUSTRATIONS (Continued)

FIGURE		PAGE
16	The Flow Stress of Two Steels as a Function of Strain Rate	45
17	Schematic Representation of Kolsky's Dynamic Compression Apparatus	50
18	Influence of Specimen's Fineness Ratio on Results Obtained With Kolsky Bar in Compression	50
19	Reference and Reconstituted Strain-Stress Curves for Trapezoidal and Triangular Incident Pulses	54
20	Calculated Transmitted Stress for a Specimen in a Kolsky Bar Subjected to Trapezoidal and Triangular Incident Pulses	54
21	Comparison of Experimental Values of $\epsilon_1 + \epsilon_R$ to ϵ_T for Equation (41)	55
22	Tapered Steel Torsional Kolsky Bar for Tests at 250°C	60
23	Strain Rate Sensitivity for Various Aluminum Alloys	64
24	Schematic Diagram of Torsional Kolsky Bar	69
25	Loading End of Explosively Loaded Torsional Kolsky Bar	71
26	Section Through Axial Mechanical Filter and Torsional Pulse Smoother Used in Explosively Loaded Torsional Kolsky Bar	71
27	Specimens Used in the Torsional Kolsky Bar	72
28	Typical Oscilloscope Records Obtained with the Torsional Kolsky Bar	73
29	Results of a Finite Element Analysis Showing the Growth of the Plastic Zone Within the Tubular Specimen Used in the Torsional Kolsky Bar	75
30	Schematic Representation of the Effect of Rapid Changes in Strain Rate or Temperature on Flow Stress for fcc Metals	80
31	Effect of Rapid Change in Temperature During Loading of Mild Steel	80

LIST OF ILLUSTRATIONS (Continued)

FIGURE		PAGE
32	Stress-Strain Curves for High Purity Aluminum at Various Strain Rates and Temperatures	82
33	Criterion for Existence of Equation of State	85
34	Cyclic Static-Dynamic-Static Loading for Aluminum	85
35	Cyclic Dynamic-Static-Dynamic Loading for Aluminum	87
36	Cyclic Dynamic Loading for Aluminum Showing Effect of Dwell Time Between Loading Cycles	87
37	The Results of an Interrupted Strain Rate Test from a High to a Low Strain Rate for Aluminum	88
38	The Results of an Interrupted Strain Rate Test from a Low to a High Strain Rate for Aluminum	88
39	Stopping Ring and Its Location in the Kolsky Bar	91
40	Results of Incremental Strain Tests in Brass	91
41	Equivalent Static Flow Curves for Different Strain Rates for Brass	94
42	Oscilloscope Record of Dynamic Portion of Incremental Strain Rate Test	94
43	Behavior of 1100-0 Aluminum Under Static Dynamic and Incremental Strain-Rate Loading in Shear	95
44	Behavior of 99.99% Pure Lead in Shear Under a Constant Low Strain Rate and Under Incremental Loading	97
45	Results of Incremental Strain-Rate Test Without Unloading for 1020 Steel	99
46	Results of Incremental Strain-Rate Test Without Unloading for 50-A Titanium	99
47	Stress-Strain Curves for Molybdenum	101
48	The Results of an Interrupted Strain Rate Test from a Low to a High Strain Rate for a High Purity Iron	101
49	Incremental Strain Rate Test Results for Copper at 24°C	104

LIST OF ILLUSTRATIONS (Continued)

FIGURE		PAGE
50	Temperature Dependence of Apparent and True Strain Rate Sensitivities of Copper	104
51	Temperatures Dependence of Apparent and True Strain Rate Sensitivities of Titanium	105
52	Incremental Strain Rate Test Results for Titanium at 24°C	105
53	Incremental Strain Rate Test Results for Mild Steel at -150°C	106
54	Incremental Strain Rate Test Results for Mild Steel at Room Temperature	106
55	Incremental Strain Rate Test Results for Mild Steel at 400°C	107
56	Temperature Dependence of Flow Stress of Mild Steel, at Low and High Strain Rate	107
57	Temperature Dependence of True Strain Rate Sensitivity of Mild Steel	110
58	Typical Stress-Strain Curves for Tests Involving Instantaneous Changes in Strain Rate for Stainless and Low Alloy Steels	110
59	Incremental Strain Rate Test Results for 1100-0 Aluminum at Various Temperatures	112
60	Incremental Strain Rate Test Results for OFHC Copper	112
61	Incremental Strain Rate Test Results for AZ31B Magnesium	113
62	Incremental Strain Rate Test Results for Commercially Pure Zinc	113
63	Incremental Strain Rate Test Results for 1020 Hot-Rolled Steel at 83 K	114
64	Incremental Strain Rate Test Results for 1020 Hot-Rolled Steel at 144 K	114
65	Incremental Strain Rate Test Results for 1020 Hot-Rolled Steel at 394 K	116

LIST OF ILLUSTRATIONS (Continued)

FIGURE		PAGE
66	The Predicted Flow Stress for an Annealed Low Carbon Steel at 200 K According to Klepaczko's Model	117
67	The Predicted Flow Stress for 1020 Hot-Rolled Steel at Room Temperature According to Klepaczko's Model	118
68	Stress-Strain Curves for Copper Single Crystals. Showing Results of Interrupted Strain Rate Tests	120
69	Flow Stress Vs. Strain Rate for Aluminum Single Crystals	122
70	Shear Stress Vs. Dislocation Cell Size for Aluminum Single Crystals Loaded Quasi-statically	123
71	Strain Rate Sensitivities, Apparent and True, as Functions of Dislocation Cell Size in Aluminum Single Crystals	124
72	Comparison of Macroscopic Activation Volume Evaluated on the Basis of Jump Tests and Microscopic Activation Volume Based on TEM Observations of Foil Samples of Aluminum Single Crystals	125
73	The Effects of a Sudden Reduction in Strain Rate on the Flow Stress of OFHC Copper	127
74	Static and Dynamic Shear Stress-Shear Strain Curves for 1020 Hot-Rolled Steel	132
75	Calculated Values of Stress, Strain and Temperature During Dynamic Deformation of Thin-Walled Tube With a Defect	134
76	Shear Stress-Strain Curves for OFHC Copper	138
77	Profiles of the Microhardness Across a Transformed Shear Band in AISI 1040 Quenched and Tempered at 200°C	138
78	Schematic of the Plate Impact Experiment	142
79	Schematic of Pressure-Shear Experiment	143
80	Dynamic Stress-Strain Curves for 1100-0 Aluminum Obtained in Pressure-Shear Experiments	145
81	Designs of Double-Shear Specimens	147

LIST OF ILLUSTRATIONS (Continued)

FIGURE		PAGE
82	Ratio of Dynamic Shear Stress, τ_2 , to Stress, τ_1 Plotted as a Function of Shear Strain	151
83	Apparent Strain Rate Sensitivity, μ_{12} , as a Function of Shear Strain	152
84	Ratio of Dynamic Shear Stress, τ_2 , to Static Shear Stress, τ_1 , Plotted as a Function of Shear Strain	153
85	Apparent Strain Rate Sensitivity, μ_{12} , as Function of Shear Strain	154
86	Ratio of Dynamic Shear Stress, τ_2 , to Static Shear Stress, τ_1 , Plotted as a Function of Shear Strain	155
87	Strain Rate Sensitivities for Various Metals Plotted as a Function of Strain Rate	156
88	The Variation of Flow Stress With Strain-Rate for Commercially Pure Titanium at 5% Plastic Strain	161
89	Variation of Activation Volume With Flow Stress in Commercially Pure Titanium at 0.2% Plastic Strain	161

SECTION 1

INTRODUCTION

The plastic deformation of metals under dynamic conditions, as opposed to quasi-static, is complicated not only by the presence of waves, both elastic, but by thermal and metallurgical processes which are potentially quite different from those that occur at low rates of deformation and which alter the material's mechanical response. As a result, dynamic plasticity continues to be a subject of great importance in practice and of great interest in research.

There are innumerable engineering applications which involve plastic deformation at high strain rates and often at temperatures far from the ambient. Dynamic plastic flow is encountered in many areas of ballistics, both internal and external. For instance, in penetration the impact of target and projectile produces a complicated pattern of elastic and plastic waves which propagate within the bodies, are reflected and interact with one another, the whole resulting in local and often extensive plastic deformation. In general, this process will be accompanied by rapid temperature changes as well. Our understanding of the phenomena involved in penetration ultimately will lead to more effective projectiles and simultaneously, of course, to targets more difficult to penetrate. The required improvements in the target may include changes in the material itself or else in the design of the structure, or both. Furthermore, since high-speed impacts may occur at any position in a structure, we need to study the response not only of plates but of beams, columns and other shapes leading to the field of structural dynamics. This in turn introduces the need for constitutive relations to represent material behavior at the appropriate temperature and strain rate. Unfortunately, our understanding of dynamic plasticity has not progressed to the point where the choice of the proper constitutive relation at any stage of a particular design is at all evident. This choice remains a matter of some uncertainty and even of controversy. Furthermore, it is complicated by strain rate history as well as by temperature history effects. Research in this domain, both experimental and analytic, is strongly

needed today. Indeed, the designer is often faced with a most frustrating situation: whereas he has available computer codes that are rapid and tailor-made to his needs, the choice of the proper constitutive relation is most difficult and remains today a matter of fine judgment.

The fracture process can also be viewed as an application of dynamic plasticity since it is frequently preceded by some and perhaps a considerable amount of plastic flow, particularly at elevated temperatures. This plastic flow may cover an extended volume or occur only locally at the root of the crack, in bands, or on the microscale between voids within the material. If the fracture process is rapid, then it generally involves complicated problems in dynamic plasticity. Numerous studies of this problem have been made and research is continuing very actively today.

A field of application which presents special structural problems is that of nuclear power. Nuclear radiation directly influences materials on the atomic scale. With continued exposure there often are large changes in static as well as in dynamic plastic behavior. In addition, the fracture behavior also is strongly affected. These property changes, combined with large dimensional changes, create serious design problems in structures where a failure can have the most serious consequences.

Among other applications one should mention conventional machining and forming processes. It is evident that dynamic effects are involved in explosive and electromagnetic forming, but it should also be pointed out that dynamic plastic deformation does not necessarily require these high speeds. For instance, in conventional machining, in forging, punching or extrusion, the strains are very large making for high strain rates even if the forming process itself is not rapid. Thus, the dynamic properties of the materials at temperature generally come into play. Estimating the strain rates in machining and forming operations is difficult. But for strip rolling, for instance, it is possible today for the material to travel at speeds in excess of 10,000 feet/min, leading to an estimated maximum strain rate in shear easily in excess of 1000 s^{-1} .

For machining at ordinary cutting speeds the strain rate may attain $10,000 \text{ s}^{-1}$, while in wire drawing at high speeds it is greater still. In each case there are temperature increases. Furthermore, drawing and rolling are frequently done hot, and at elevated temperatures the flow stress often becomes very sensitive to strain rate. For instance, this is true for most steels. All this must be of great interest to the production engineer, as well as to the metallurgist who is trying to attain desired properties through heat treatment. When these temperature and strain rate effects are combined with the difficult problem of friction and lubrication one even wonders at the value of detailed slip line solutions intended as descriptions of rolling or drawing operations.

In addition to the above applications, there are more fundamental reasons for studying rapid deformations over a temperature range. For some time, material scientists and engineers have been attempting to understand plastic flow on the metallurgical and indeed on the atomic level. The goal here is not limited to dynamic conditions, but dynamic plasticity does provide a challenge in that a complete understanding must include high rates of deformation over a range of temperatures. At the same time, results obtained through dynamic plasticity investigations provide a tool to aid in our basic understanding of material behavior. Starting with the atomic scale, there are many investigations which attempt to simulate the behavior of the crystal lattice through models consisting of regular arrays of particles with prescribed more or less realistic forces of interaction. Plastic deformation is represented by displacements of the particles within these arrays as functions of time and in accordance with the laws of classical or of quantum mechanics. This is a complex problem which has only been made tractable by the advent of the computer. At the next level, plasticity is studied on the basis of dislocation dynamics which is then generally applied to the deformation behavior of single crystals of relatively pure crystalline materials. The eventual goal of these studies is to understand the mechanical behavior of polycrystalline materials on the atomic and dislocation scales and relate this behavior to macroscopic deformation on an engineering scale. A parallel approach makes use of internal variables and the principles of thermodynamics to construct constitutive relations.

Clearly, these various approaches are interrelated and overlap. The hope is that the interrelations will grow stronger. Much has been done in this direction and many macroscopic phenomena already are explainable through mainly on a qualitative basis. Much additional work is necessary before mechanical behavior can be predicted with confidence under varieties of loading conditions, e.g. at different temperatures, over a range of strain rates, for multiaxial loading, at large strain, etc. The present report is intended to indicate some of the progress made to date in research, the emphasis being on the engineering scale and on experimental results.

A number of review papers, as well as proceedings of meetings devoted to particular aspects of the subject may be found in the literature. The most recent review is that of Nicholas (Reference 1) who covers the subject from a continuum mechanics viewpoint and who includes descriptions of the various experimental methods available today. The review of Campbell (Reference 2) and that of Sutterlin (Reference 3) cover not only experimental work and constitutive equations but also dislocation dynamics in its relation to dynamic plasticity. Lindholm's (Reference 4) review emphasizes experimental techniques and instrumentation in dynamic plasticity. The testing methods he describes cover the range from creep rates to the highest strain rates achievable. The review includes a critique of experimental methods and their bearing on the interpretation of results. Two excellent critical reviews but somewhat more specialized, are those of P. S. Symonds (References 5 and 6). The first, written in collaboration with T.C.T. Ting and D. N. Robinson, is directed toward structural dynamics. Unfortunately, these reviews are available only in report form. The subject of wave propagation is covered in the text by Kolsky (Reference 7) while more recent work in plastic waves is reviewed by Clifton (Reference 8). Applications of dynamic plasticity to metal forming and to machining were reviewed by Sellars and Tegart Bitans and Whitton and Oxley (References 9, 10 and 11). This area is also covered along with other applications and their relation to wave propagation phenomena in the text by W. Johnson (Reference 12). The subject of penetration has been reviewed very recently by Backman and Goldsmoth (Reference 13), who cover the mechanics of the problem in its various aspects. A review emphasizing two- and three-dimensional finite element studies of penetrator and target deformation

was presented by Jonas and Zukas (Reference 14). Finally, one should mention the proceedings of scientific meetings; all those devoted to dynamic plasticity cannot be cited but any list should include Lindholm, Rhode et al., Kawata and Shioriri and the two meetings at Oxford University, Harding, as well as Meyers and Murr which contains not only articles on high strain rates but on shock waves as well (References 15, 16, 17, 18, 19 and 20).

SECTION II

PLASTIC FLOW AND CONSTITUTIVE EQUATIONS ON THE MICROSTRUCTURAL SCALE

Over the years progress has been made in the investigation of dislocation mechanics and of the metallurgical aspects of plastic flow in general, starting with early work on single crystals. However, important and complicated questions remain to be answered before plastic flow can be understood fully and, particularly, before plastic flow on the dislocation scale can be related quantitatively to behavior on an engineering scale. Nonetheless, for engineering applications it is important today to acquire an understanding of the underlying microscopic and metallurgical phenomena since their relation to the phenomenological behavior is becoming clearer as research progresses. A detailed summary of the subject is not presented here since extensive descriptions are readily available in standard texts on metallurgy or on dislocation mechanics, e.g. Gilman, Kocks, et al., Honeycombe, also in the proceedings of various meetings, e.g. Rosenfield et al., and Kanninen et al (References 21, 22, 23, 24 and 25). Microstructural effects at high strain rates are treated in Rhode et al, as well as in review articles published on the subject, as for instance Campbell or Leslie (References 16, 26 and 27), also cite the book edited by Argon (Reference 28), which brings together microscopic and macroscopic viewpoints in the construction of constitutive equations.

Most studies of microstructural behavior concentrate on the ordered crystalline state, where deformation is viewed as due to the movement, generation and perhaps annihilation of dislocations. The rate at which plastic shear strain accumulates, $\dot{\gamma}_p$, depends then on the mean velocity, v , with which the dislocations move, on the density, N , of those dislocations that are mobile and on the Burgers vector, b , which defines the characteristic distance involved in the glide of one set of atoms relative to another. This provide the well-known equation

$$\dot{\gamma}_p = Nbv \quad (1)$$

which is applicable to slip along glide planes in a crystal. Unfortunately, making the transition from this equation to an understanding of the deformation process in the polycrystalline aggregate is no simple matter. The problem is far from solved even though it has occupied the attention of metal physicists and engineers for many years.

In applying Equation 1, it must be remembered that the quantity, $\dot{\gamma}^P$, represents a component of shear strain for a single crystal. As such it has a direction in space. Since the aggregate is composed of crystals with different orientations and since slip generally does not have the same magnitude on all planes nor occur on the same planes or directions in all crystals, the relation between $\dot{\gamma}^P$ in Equation 1 and the strain rate of the continuum is not obvious. It requires not only an averaging or summing process, but a means of specifying that during deformation equilibrium be satisfied at all points between crystals and simultaneously that the resulting displacements be compatible throughout the continuum. Further complications are introduced by unloading, by reverse loading, etc.

There are also difficulties in evaluating the terms on the right side of Equation 1. While N is believed to depend linearly on the magnitude of strain, except at elevated temperatures, the velocity v is a more complicated term. In general, it is a function of stress and of temperature and its functional form in turn varies according to the dominant dislocation mechanism or mechanisms. If a crystal were pure and free of dislocations then, in principle, very low stresses would introduce dislocations and set them in motion. Real crystals, however, contain alloying elements, impurities, other dislocations, etc., which serve as obstacles to dislocation motion. The relation between the velocity of a dislocation and the driving force on the one hand and therefore between the plastic strain rate and the applied loads on the other is determined largely by the mechanisms with which obstacles are overcome. These mechanisms are of many different types, and their study is complicated by the fact that several of them are generally acting simultaneously for any given set of conditions so that it is difficult to isolate one mechanism even for experimental purposes. This is

undoubtedly the principle reason why microscopic phenomena are difficult to relate to phenomenological behavior.

In general, different types of mechanisms operate over different ranges of temperature and stress. The current understanding is that a sufficiently high stress on the glide planes can produce plastic flow at any temperature by driving dislocations past all obstacles with no help from thermal fluctuations. This is represented by τ_1 in Figure 1. The only resistance to motion is then due to damping mechanisms, and when the stress on the glide planes exceeds τ_1 then it varies linearly with the strain rate. Lower stresses may also cause plastic flow but only with the help of thermal fluctuations. Under these conditions, the stress needed to produce plastic flow decreases, in general, with an increase in temperature: a typical variation being shown schematically in Figure 1. It may be noted that at 0°K, where thermal fluctuations are least important, the required stress for plastic flow is believed equal to τ_1 . As the temperature increases the dependence of stress on temperature decreases non-linearly depending on the crystal structure, the imposed strain rate, etc., and it is believed that the value of stress within various temperature ranges depends on the mechanism dominating the flow process within that range. In Region I, for instance, where stress decreases with temperature, the dominant deformation mechanisms are termed thermally activated. In this range of temperatures, for instance, dislocation motion is resisted by the intersection with other dislocations, by interstitials, by pinning points created perhaps by radiation, etc. The plastic strain rate in these thermally activated processes is generally taken as

$$\dot{\gamma}^P = \dot{\gamma}_0 \exp (- \Delta G/kT) \quad (2)$$

where k and T are respectively the Boltzmann constant and the temperature, $\dot{\gamma}_0$ is a pre-exponential factor, and ΔG is the free energy of activation. In general, ΔG and $\dot{\gamma}_0$ are functions of the applied shear stress, the temperature and a number of microstructural parameters. The specific form taken for these functions depends on which of the thermally activated mechanisms is believed dominant. One should note at this point that

It is evident from the above that research towards a better understanding of the microstructural basis of plastic flow and its relation to flow on an engineering scale should be continued very actively. The better one understands the influence of metal composition, heat treatment, temperature, etc., the easier it will be to design adequately against impact and wave propagation phenomena. From the engineering viewpoint, however, it is also evident that research on the phenomenological scale must continue, and when necessary even independently of microstructural considerations, so that structural design may progress. As will be seen in the next section, the early development of constitutive equations in viscoplasticity was based almost entirely on observations of macroscopic behavior. This is no longer the case today, since dislocation mechanics frequently serves as a guide at least to the form of the constitutive relation. It is to be expected that future investigations will more frequently span disciplines until quantitative relations are established covering at least certain ranges of temperature or strain rate for certain materials.

SECTION III

CONSTITUTIVE EQUATIONS AND EARLY ANALYSES IN
PLASTIC WAVE PROPAGATION

As mentioned in the previous section, much of the early work on the derivation of constitutive equations was based on the continuum viewpoint rather than on the microscopic. In dynamic plasticity the first attempts to understand and predict plastic wave propagation phenomena involved, therefore, an extension of elastic wave analyses to include plastic stress-strain relations. The plasticity representations employed were those previously developed for static work and, generally, were time-independent. Soon thereafter, however, viscoplastic relations were adopted in order to determine whether they might better represent observed phenomena. A further change which occurred simultaneously was in the method of solution of the wave equations. Whereas waves in linear elastic bodies are described by linear partial differential equations, the corresponding equations for plastic bodies are only quasi-linear due to the nonlinearities of the constitutive equations. As a result the method of characteristics generally has been adopted for their solution. Since Symonds et al (References 5 and 8) have reviewed the subject of plastic waves including the method of characteristics, the present review will treat the subject but briefly. Furthermore, a number of excellent texts are available, as for instance those by Cristescu, Rakhmatulin and Dem'yanov or by Nowacki to mention only a few (References 30, 31 and 32).

1. STRAIN RATE INDEPENDENT (TIME-INDEPENDENT) CONSTITUTIVE EQUATIONS

One of the simplest of constitutive equations for uniaxial loading in the plastic range is

$$\sigma = f(\epsilon) \quad (3)$$

where σ and ϵ are uniaxial components of stress and strain, respectively. Equation 3 is used frequently in spite of the fact that it does not account for changes in temperature or strain rate. Depending on the particular application and metal involved, it may be quite good enough,

especially if there are no large changes in strain rate and if the temperature remains nearly constant.

Specific examples of Equation 3 are well-known since they are generally the same as in quasi-static investigations. In working with cold-rolled steel, for instance, one often employs the elastic-perfectly plastic representation, since cold-rolled steel does not work-harden appreciably except at very large strains. Unfortunately, this is not a satisfactory representation for cold-rolled steel under dynamic conditions, as can be seen for instance in the results obtained by Costin and Duffy (Reference 33) shown in Figure 2. Thus, for dynamic conditions a better constitutive equation might be

$$\sigma = A\epsilon^n \quad (3a)$$

where n is the work-hardening exponent and A is a constant. Equation 3a is often used in static work as well, e.g. for hot-rolled steel, for aluminum, etc. Other specific examples of Equation 3 are the well-known rigid-plastic relation, good for large strains, and the bilinear relation which retains the simplicity of straight lines but includes work-hardening. The last was employed by Donnell (Reference 34) in the first study made of plastic wave propagation in slender rods. Other early analyses of this important problem also made use of rate-independent equations of the type of Equation 3. Such analyses were presented by Von Karman, Taylor, Rakhmatulin, and White and Griffis (References 35, 36, 37 and 38). For a critique of these contributions the reader is referred to the review by Symonds et al (Reference 5).

In order to provide some physical basis for later discussion, the solution of a simple wave propagation problem is presented below. However, the reader is referred to the texts mentioned in the previous paragraph for the method of solution and all details.

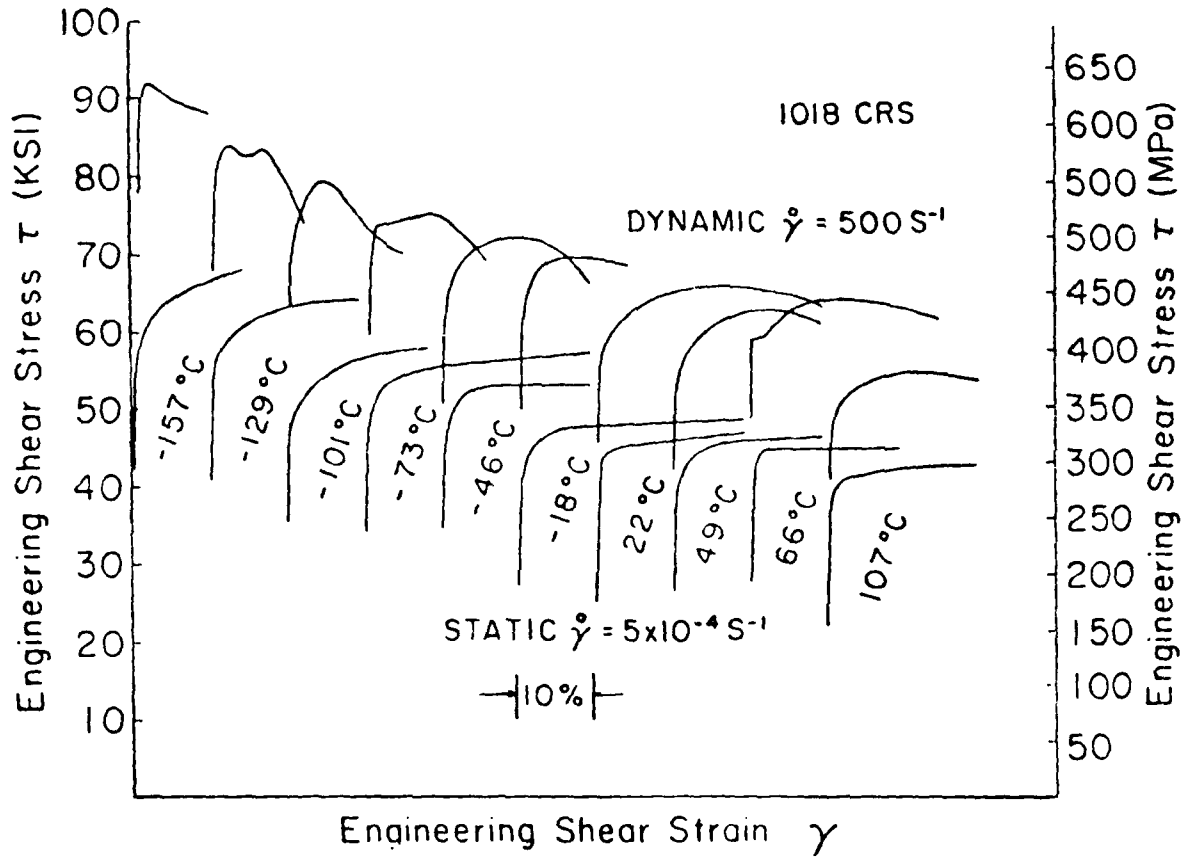


Figure 2. Quasi-Static and Dynamic Shear Stress-Strain Curves for 1018 Cold-Rolled Steel

Early experiments and analyses invariably involved the propagation of axial waves along thin rods, and it may be shown on the basis of conservation of linear momentum of a material element that the equation of motion for a slender cylindrical rod lying parallel to the x-axis is given by

$$\frac{\partial \sigma}{\partial x} = \rho \frac{\partial^2 u}{\partial t^2} \quad (4)$$

In this equation x represents a Lagrangian coordinate for the material element at time t , while $\sigma = \sigma(x, t)$ and $u = u(x, t)$ represent respectively the axial components of stress and displacement and ρ represents the mass density of the rod. For elastic behavior

$$\sigma = E \epsilon = E \frac{\partial u}{\partial x} \quad (5)$$

which, inserted in Equation 4, provides the well-known wave equation

$$c^2 \frac{\partial^2 u}{\partial x^2} = \frac{\partial^2 u}{\partial t^2} \quad (6)$$

where

$$c = \sqrt{\frac{E}{\rho}} \quad (7)$$

represents the velocity of propagation. Equation 6 is linear since E , the elastic modulus, and hence c are constant.

For plastic bodies, however, Equation 5 does not apply, and we have recourse instead to Equation 3. In this instance, it may be shown that Equation 6 may still be used to describe wave propagation if now

$$c = \sqrt{\frac{d\sigma/d\epsilon}{\rho}} \quad (8)$$

However, c is no longer constant, since its value depends on the slope of the stress-strain curve which, for plastic bodies, will generally be a function of the strain or stress level. The solution is found more easily if Equation 6 is rewritten as a pair of first order partial differential equations

$$c^2 \frac{\partial \epsilon}{\partial x} = \frac{\partial v}{\partial t} \quad \text{and} \quad \frac{\partial \epsilon}{\partial t} = \frac{\partial v}{\partial x} \quad (9)$$

where $v = \partial u / \partial t$ is the nominal velocity of a material element. Since we can consider $c = c(\epsilon)$, Equations 9 constitute a pair of quasi-linear equations in the independent variables $\epsilon(x, t)$ and $v(x, t)$. Their solution for particular boundary and initial conditions is generally effected by the method of characteristics. The mathematical bases of this method are given by Courant and Hilbert (Reference 39) for instance, and examples of particular solutions in wave propagation may be found in the texts cited above or in various papers, such as that of Davids and Kumar (Reference 40). The present review will give only the results of a single problem. Suppose the slender rod is made of a time-independent material whose stress-strain curve is as shown in Figure 3: during loading the material behaves elastically up to some yield stress σ_y above which the function $f(\epsilon)$ is concave toward the strain axis. During unloading the material behaves elastically so that MN, for instance, is parallel to the elastic portion of the original loading curve starting at the origin.

If the end of a semi-infinite bar is loaded "instantaneously" then, as shown by Von Karman and Duwez (Reference 41) both ϵ and v depend on the ratio x/t , rather than on x and t independently. The characteristics for this problem are shown in Figure 4 and the strain distribution at any time in Figure 5. Karman and Duwez showed that the strain distribution is divided into three regimes:

- 1) For $c_0 < x/t < \infty$, the material is undisturbed.
- 2) For $c_m < x/t < c_0$, the strain increases from the yield strain, ϵ_y , which propagates at c_0 , up to the maximum strain imposed at the end of the bar, ϵ_{max} , which propagates at c_m . Between these two values of wave velocity, it can be shown that

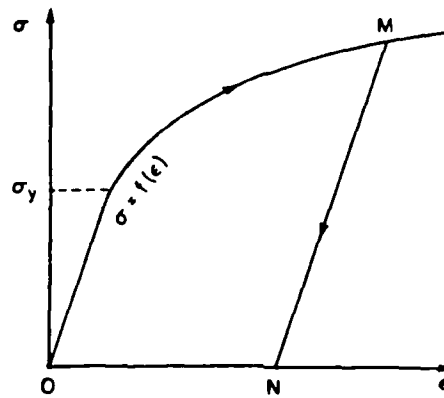


Figure 3. Idealized Uni-Axial Stress-Strain Curve for a Time Independent Material Showing Linear-Elastic and Work-Hardening Regions

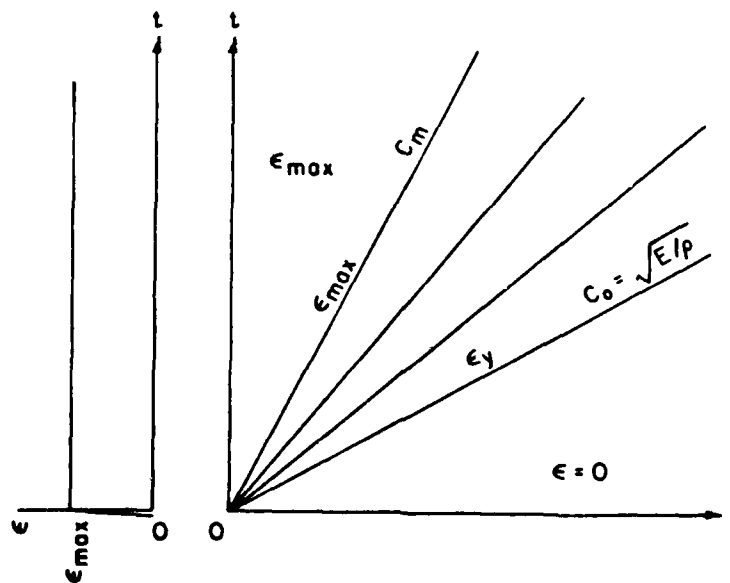


Figure 4. Family of Characteristic Curves for "Instantaneous" Loading of Semi-Infinite Slender Elastic-Plastic Rod

$$c^2 = \frac{1}{\rho} \frac{d\sigma}{d\epsilon} = \left(\frac{x}{t} \right)^2 \quad (10)$$

Hence, when the function $\sigma = f(\epsilon)$ is known it can be substituted into Equation 10 to give the strain at any x and t . This provides the values of ϵ along the curved portion of the plot in Figure 5. Finally,

3) The maximum strain, ϵ_{\max} , imposed at the end of the bar propagates at the smallest velocity, c_m , as shown in the figure.

It is also possible to relate the velocity, v_1 , at the end $x = 0$ of the bar to the maximum strain, ϵ_{\max} . Since, in this example, v_1 is constant, we have

$$v_1 = \frac{u(0, t)}{t} \quad (11)$$

where $u(0, t)$ is the displacement at the end $x = 0$. This displacement can be found by integrating the strain from the fixed end of the bar to its moving end, so that

$$u(0, t) = - \int_{\infty}^0 \epsilon dx \quad (12)$$

where the sign indicates that positive u is directed along the $+x$ axis. This integral represents the area under the curve in Figure 5 and can be obtained as well by changing coordinates so that

$$u(0, t) = \int_0^{\epsilon_{\max}} x d\epsilon = t \int_0^{\epsilon_{\max}} \frac{x}{t} d\epsilon = t \int_0^{\epsilon_{\max}} c(\epsilon) d\epsilon \quad (13)$$

the last being found by using Equation 10. Combining Equations 11 and 13 gives the velocity at the free end in term of ϵ_{\max} as

$$v_1 = \int_0^{\epsilon_{\max}} c(\epsilon) d\epsilon \quad (14)$$

This equation corresponds to

$$\sigma = \rho v_1 c \quad (15)$$

which gives the stress at any point in terms of particle velocity for the propagation of an elastic pulse.

Von Karman and Duwez (Reference 41) also studied the finite bar by taking into account reflections from a fixed end. The solution can be extended in other ways. Thus the boundary condition at the free end can be changed from an instantaneous application of strain to a ramp function, and then, in the expressions for ϵ and v , x and t become independent. The resulting characteristics are shown in Figure 6. Rakhmatulin (Reference 37) has studied the problem of subsequent unloading. As long as the stress at any point along the bar is increasing, i.e. as long as

$$\frac{\partial \sigma}{\partial t} > 0 \quad (16)$$

then the constitutive equation for the material is given by Equation 3, $\sigma = f(\epsilon)$, as illustrated in Figure 3. However, as soon as any unloading occurs i.e. as soon as

$$\frac{\partial \sigma}{\partial t} < 0 \quad (17)$$

then the constitutive equation for the material at that point shifts to

$$d\sigma = E d\epsilon \quad (18)$$

Analyses which include unloading are complicated since it is now known a priori when the shift occurs from one constitutive equation to the other for any given point along the bar. In general, it occurs at a different time for each point. Put differently, we do not know the shape of the loading-unloading curve in the $x - t$ diagram. It is only by solving the complete problem, including the loading problem, that the shape of this curve can be found. Examples of problems in the propagation of elastic-plastic waves can be found in the literature, as for instance in the texts by Cristescu or Rakhmatulin and Dem'yanov, as well as in numerous published papers (References 30 and 31).

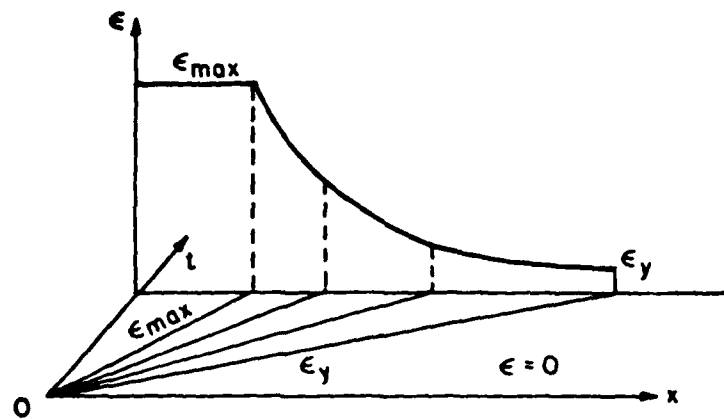


Figure 5. Strain Distribution as a Function of Time for "Instantaneous" Loading of a Semi-Infinite Elastic-Plastic Rod

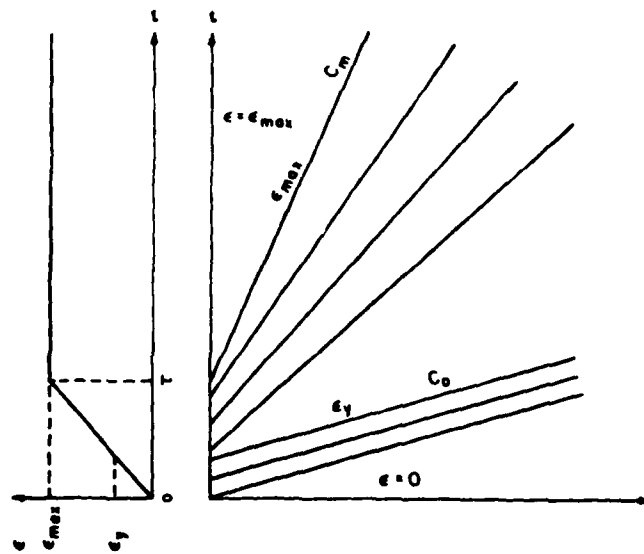


Figure 6. Family of Characteristic Curves for Ramp Loading of a Semi-Infinite Elastic-Plastic Rod

2. STRAIN RATE DEPENDENT (TIME-DEPENDENT) CONSTITUTIVE EQUATIONS

A constitutive equation which includes strain rates effects is one of the type

$$E \frac{\partial \epsilon}{\partial t} = \frac{\partial \sigma}{\partial t} + g(\sigma, \epsilon_p) \quad (19)$$

where ϵ_p is the plastic strain component defined as

$$\epsilon_p = \epsilon - \sigma/E \quad (20)$$

and the equation is used for monotonic loading when the stress, σ , exceeds the yield stress, σ_y . An additional condition, sometimes imposed, is that the stress, σ , exceed the stress given by the quasi-static loading curve. Specific examples of the function $g(\sigma, \epsilon_p)$ had been in use for some time to describe material behavior, when Malvern (Reference 42, 43) presented the more general form of the function, and went on to use Equation 19 to solve the problem of longitudinal waves in a slender bar of a rate-sensitive material.

One of the most frequently used functions for $g(\sigma, \epsilon_p)$ is $f(\sigma - \sigma_y)$, where $(\sigma - \sigma_y)$ is termed the overstress. For the specific case of

$$f(\sigma - \sigma_y) = k(\sigma - \sigma_y) \quad (21)$$

where k is a constant having units of $(\text{time})^{-1}$, Malvern (Reference 42) showed that the solution to the wave-propagation problem for a semi-infinite rod can be obtained in closed form. Other relations which have been used are

$$g(\sigma, \epsilon_p) = k\sigma_y [\sigma/\sigma_y - 1]^m \quad (22)$$

or

$$g(\sigma, \epsilon_p) = k\sigma_y \sinh [(\sigma - \sigma_y)/m\sigma_y] \quad (23)$$

Clearly, a large number of possible functions can be devised for $g(\sigma, \epsilon_p)$, to include an overstress, work-hardening, etc. In addition, the resulting viscoplastic constitutive relations have been generalized to three-dimensional states of stress, as for instance in the work of Perzyna (References 44 and 45). Obviously, if the functions in these equations contain a larger number of arbitrary parameters, then mechanical response can be better represented over a larger variety of test conditions. Unfortunately, however, a large number of parameters does not necessarily give a function that predicts behavior when one departs from test conditions or employs a different material. As mentioned above, simple equations based on dislocation dynamics can be used as a guide to the form of the function $g(\sigma, \epsilon_p)$, or more generally for the inclusion of viscoplastic effects. This is an important subject of research today in metallurgy, physics and engineering. The book by Argon (Reference 28) covers this subject in general and presents various approaches to it. Its application to dynamic plasticity is included in the reviews of Campbell and Clifton (References 26 and 8).

One should point out that constitutive relations of the type of Equation 19 does not include temperature-history or strain rate-history effects. Though these history effects are reviewed in more detail in a later section, a few general statements can be made at this point. There are today but few rules that can be invoked to predict the importance of history effects during the loading of a given material. In general, temperature-history effects are greater the higher the temperature; at low temperatures they can often be ignored. Broadly speaking, and looking only at the stress-strain curve, a sudden decrease (increase) in temperature has an effect similar to a sudden increase (decrease) in strain rate. It is not clear, however, how far this parallel can be carried. In mild steel, and bcc metals it is generally recognized that an increase in strain rate can raise the flow stress by a factor of two or even three, and recent results indicate that history effects can be quite large. This is particularly true for steels at low temperatures. In fcc metals, as for instance in aluminum and copper, the situation is quite different; strain rate history effects are relatively large though of small practical importance, since strain rate effects themselves are small. On the other hand, strain rate and strain rate history effects are both of importance in fundamental studies

of the micromechanisms of plastic flow. Progress in understanding these phenomena on the microscopic scale should aid considerably in the development of constitutive equations and in our general understanding of deformation on an engineering scale.

Hereditary stress-strain laws constitute another approach to dynamic plasticity. Kelly (Reference 46) showed that history effects could be included by employing an integral operator functional and Rabotnov (Reference 47) employed a constitutive relation with a non-linear hereditary integral to study the delayed yield phenomenon in steel, while Rabotnov and Survorova (Reference 48) used it to study plastic wave propagation. These constitutive equations can also be made to include the effects of history, as was shown by Survorova (Reference 49) and Rabotnov and Survorova (Reference 50). For instance, Bell, Sternglass and Stuart found that an incremental dynamic load applied to a specimen already deforming plastically will produce a wave traveling at the elastic speed (References 51 and 52). This result cannot be predicted by a time-independent constitutive relation, while time-dependent relations, of the type given by Equation 19, predict that the entire stress increment travels at the elastic wave velocity. Rabotnov and Survorova's analysis is consistent with experimental results which show that the stress increment propagates partly at the elastic wave speed and partly at lower speeds. Their analysis was also applied to the results obtained by Lindholm in which strain rate is changed suddenly from a quasi-static to a dynamic value then back to the quasi-static, as well as the results of Frantz and Duffy (References 53 and 54). In the latter investigation, involving short specimens of aluminum in a torsional Kolsky bar, an upper and lower yield point was observed following a sudden increase in strain rate. The hereditary integral can reproduce this upper and lower yield point.

Bodner and colleagues have derived constitutive relations which they apply with considerable success to study the results of experiments at various strain rates and, in particular, to those of incremental strain rate tests. The constitutive relations they propose contain a number of parameters, adjusted for each material according to test results.

However, the derivation of their constitutive equations has considerable justification, based in part on dislocation mechanics and in part on a general three-dimensional formulation of the laws of plasticity. Thus Bodner and Partom (Reference 55) separate elastic and plastic components of deformation rate and retain the elastic component throughout their analysis. This is essential to their analysis since it allows for incremental loading, in which one component of the deformation rate, the elastic or the plastic, may suddenly increase while the other decreases. They then relate the plastic deformation rate to the state of stress by use of the relation

$$D_2^P = f(J_2) \quad (24)$$

where D_2^P is the second invariant of the plastic deformation rate tensor and J_2 is the second invariant of the elastic stress deviator. The use of invariants in this equation is essential from a mechanics standpoint and the use of deformation rate allows for greater than infinitesimal strains in the deformation. The particular relation they choose for Equation 24 is

$$D_2^P = D_0^2 \exp \left[-\left(\frac{1}{3} Z^2\right)^n \left(\frac{n+1}{n}\right) / J_2^n \right] \quad (25)$$

where D_0 and n are material constants and Z is an internal variable. At its origin this equation is based on the experimental determination of dislocation velocity, v , made by Johnston and Gilman (References 56 and 57). The equation in question

$$v = v^* \exp (-D/\tau) \quad (26)$$

later modified to

$$v = v^* \exp (-D/\tau)^n \quad (27)$$

includes also the characteristic drag stress, D , on the moving dislocation. Thus in Equation 25, D_0^2 is a limiting term on D_2^P and n is a constant which depends upon temperature, strain rate sensitivity, etc. Bodner and Partom express the internal variable Z , through

$$Z = Z_1 + (Z_0 - Z_1) e^{-mW_P}$$

where Z_0 , Z_1 and m are new material constants independent of temperature and W_p is the plastic work. This constitutive equation was first applied by Bodner and Partom to the results of a series of experiments they conducted on specimens of commercially pure titanium loaded at strain rates of $1.6 \cdot 10^{-3} \text{ s}^{-1}$, and also to incremental strain rate tests between these two strain rates. Later Bodner and Merzer applied this equation to the results obtained by Senseny et al., Figure 7 (References 58 and 59). The constants in the constitutive equation are determined by the constant strain rate tests, so that the measure of success for this constitutive equation depends on the degree of agreement with incremental tests.

An example of an approach to constitutive equations which holds much promise is that of Patel and Bieniek (Reference 60). These investigators start with relations applicable to a single slip system in a single crystal and in a step by step analysis go from this level to the polycrystalline aggregate. In their work, they apply Equation 1 to the single slip system. For the value of the mobile dislocation density, N , they make use of the relation due to Gilman (Reference 61) namely

$$N = N_0 + M\dot{\gamma} \quad (28)$$

where N_0 may represent initial dislocation density and M a dislocation multiplication parameter. The dislocation velocity is expressed as

$$v = \left(\frac{\tau - H\dot{\gamma}}{\tau_0} \right)^n \quad (29)$$

where H is a strain hardening coefficient, τ_0 is the resolved shear stress for unit velocity and n is a constant. Thus one obtains

$$\dot{\gamma} = b(N_0 + M\dot{\gamma}) \left(\frac{\tau - H\dot{\gamma}}{\tau_0} \right)^n \quad (30)$$

for the single slip system, a relation first derived by Gilman and Johnston used by Hahn to explain yield point phenomena in bcc metals, and by Gillis and Gilman (References 62, 63 and 64). As it stands, this constitutive relation is applicable only to monotonically increasing stress and strain, but Patel and Bieniek include non-monotonic loading by appropriate changes in the signs of the stress and strain terms. The equation

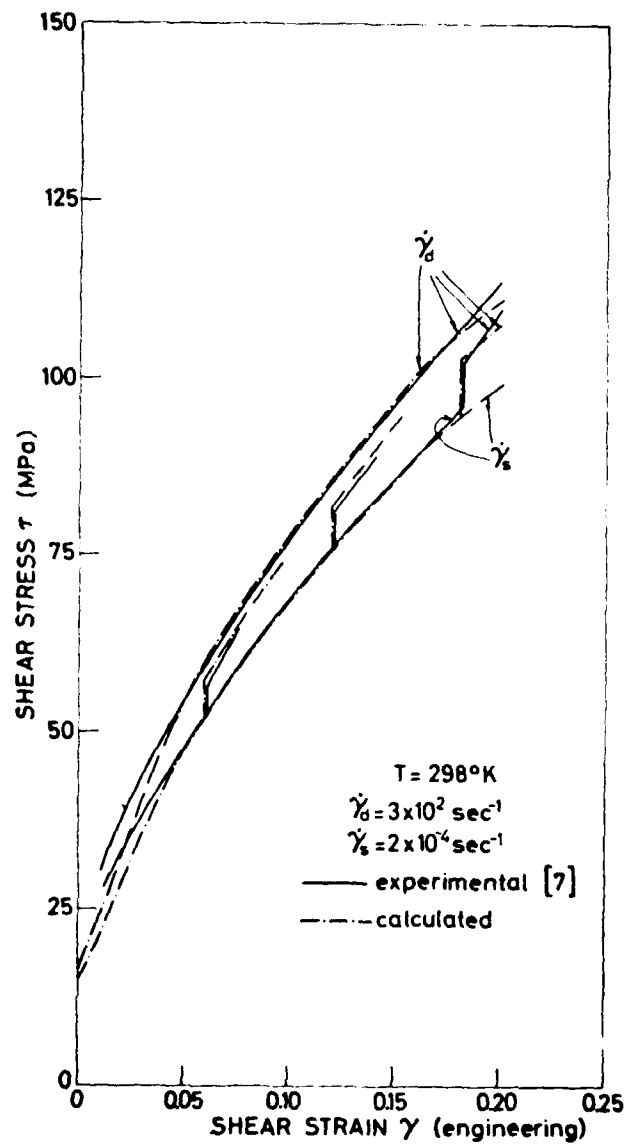


Figure 7. Bodner and Merzer's Calculated Stress-Strain Curves Compared to Results of Constant and Incremental Strain Rate Experiments. The Experimental Results are Due to Senseny et al.

is also generalized to include further slip systems within the crystal. Finally, by a summation process they are able to apply it to the polycrystalline aggregate. Their summation process necessarily involves a number of simplification, e.g. a matrix with spherical grains, uniform stress throughout the specimen, etc. The end result is applied to fcc metals by including the proper number of slip systems, at the correct orientations. One should note that Equation 30 constitutes an ordinary differential equation which must be integrated with respect to time in order to obtain an expression for γ . The authors apply the resulting constitutive equations to experimental results in dynamic plasticity as well as to the results of relaxation tests.

The point of view adopted in the paper by Patel and Bieniek seems to this reviewer to be most promising. At the present time many investigators are combining microscopic and macroscopic approaches in too-limited a sense. A frequently seen procedure, for instance, is to calculate activation volume from the results of macroscopic experiments on a particular metal and for certain conditions, and then to compare the values thus obtained with those of previous investigators who generally used a different experimental technique. Though this procedure is clearly worth the effort, since it does provide some substantiation for the test results, even very close agreement does not go far in identifying with certainty the particular microstructural deformation mechanism that is dominant, its proper mathematical description or the interpretation of the experimental technique. Nor does it show whether the results can be extended to other metals or indeed to other loading paths or testing conditions for the same metal. Patel and Bieniek's approach has the disadvantage of giving far more elaborate constitutive equations than previous analyses. However, in view of modern computational facilities it no longer seems necessary to limit the form of constitutive relations to those providing simple, even closed-form, solutions. The approach of Patel and Bieniek should provide a better test of existing theories in dislocation dynamics, of their relation to macroscopic deformation and of experimental techniques.

SECTION IV

EXPERIMENTS IN WAVE PROPAGATION

Although the Charpy machine had been used in fracture testing and the Guillery rotary machine in dynamic plasticity before the turn of the century, the first experiments attempting to understand dynamic effects on a more rational basis appear to be those of J. and B. Hopkinson. In his plasticity tests, B. Hopkinson (Reference 65) employed the apparatus that had been used some thirty years before his father for fracture studies. A falling mass delivered a blow on the lower and free end of a wire the upper end of which was fixed. Both iron and copper wires were used as specimens. The falling mass was threaded on the wire and its downward movement stopped by a sleeve attached to the free end. The tensile pulse thus initiated traveled up the wire to the attachment at a large iron block. Measurements included the dimensions and density of the wire, the weight of the dropping mass, and the height through which it fell. In addition, B. Hopkinson measured the residual strain near the top end of the wire where the stresses are high due to the fact that the reflected tensile pulse is for some time superposed on the incident. He showed that for a brief period the wire can support without yielding a stress considerably higher than the static yield stress. This constituted the first evidence of delayed yield in metals. Taylor (Reference 66) presented a review of this work which included a correction showing that the dynamic stresses were even higher than Hopkinson had supposed, since Hopkinson failed to realize that with his arrangement the stresses are higher on the second reflection from the support than on the first.

As mentioned above, by the early 1940's a number of analyses had been presented of plastic wave propagation in slender bars. These analyses made use of time-independent constitutive equations to predict the stress, strain, and particle velocity distributions along the bar during the passage of the plastic wave as well as the permanent strain distributions. The results of these analyses could be compared with those obtained in experiments in which a plastic wave travels along a slender bar. Von Karman and Duwez (Reference 41) who were among the early investigators

to perform experiments of the nature, used specimens of a copper wire about 100 inches long suspended vertically. Marks were made every inch along the wire in order to measure the distribution of permanent strain after the test. The bottom and free end of the wire was struck by a hammer which could impart a maximum velocity of 200 ft/sec. The duration of impact was controlled by means of a brittle disk which fractured at the instant when impact was terminated, allowing the hammer to continue to travel freely. This arrangement allows the duration of impact to be prescribed for each test. Hence, experiments can be performed all with the same impact velocity but covering a range of impact durations. It also furnishes a nearly constant impact velocity throughout the application of load, as the kinetic energy of the hammer is sufficiently large so it is reduced by only a small percent before the disk fractures.

Karman and Duwez drew a number of important conclusions from their experiments. First, they present a series of graphs showing the residual plastic strain in the bar as a function of distance. These graphs were obtained from tests performed with different durations of impact but the same impact velocity. They are similar in general appearance to that of Figure 5. They show that the elastic wave front propagating along the bar is followed by gradually increasing strain into the plastic regime. Furthermore, any particular level of plastic strain propagates with a nearly constant velocity, demonstrating the wave character of dynamic plastic deformation. The increasing strain continues until a maximum value, ϵ_{\max} , is attained referred to as the plateau. In experiments all with the same impact velocity, the levels of the plateaus, i.e. the value of ϵ_{\max} , are all the same. However, the length of the plateau is greater, the greater the duration of impact. One might observe that the plateaus in the tests of Karman and Duwez all appear to be perfectly flat and at the same strain level. This seems surprising in view of the inevitable small differences in material properties between specimens and the usual small variations one obtains in experimental work. The appearance of these results suggests that only the length of the plateau was measured starting at a set value of ϵ_{\max} . The later experiments of Kolsky and Douch would seem to confirm this, as does DeVault's analysis which takes into account radial inertia (References 67 and 68). Secondly, Karman and

Duvez present a graph showing the variation of ϵ_{max} with impact velocity, v_1 . This graph is the result of a series of tests at various impact velocities. Agreement with predicted values based on Equation 14 is fairly good though strains are greater than predicted at the lower impact velocities and less at the higher. Lastly, Karman and Duwez compare measured values of the distribution of strain along the length of the wire to those predicted by Equation 10, Figure 8. They found that predicted values deviate considerably from experimental and they attribute this deviation to some inaccuracy in the measured value of the duration of impact, and to perturbing effects due to the sudden stopping. These tests by Karman and Duwez showed that existing analyses were qualitatively right: plastic deformation propagates in waves and leaves a residual strain with a distribution approximately as shown in Figure 5. However, discrepancies in magnitude do exist; they are attributed by Karman and Duwez to rate of strain effects. The results of similar experiments, performed mainly at the California Institute of Technology, Duwez and Clark, induced Malvern to include strain rate effects in the constitutive equation when studying plastic wave propagation; although, more positive experimental evidence did not come until the experiments of Bell, Sternglass, Stuart and Bianchi (References 42, 43, 51, 52, 69, 70 and 71).

Bell propagated a small incremental tensile wave along a steel bar stretched beyond its elastic limit. He found that the wave travels at the velocity rather than at a velocity given by $\frac{1}{\rho} \frac{d\sigma}{d\epsilon}$, thus indicating that dynamic loading raised the elastic limit. The experiments of Sternglass and Stuart (Reference 52) provided additional evidence. These investigators used a standard testing machine to pull long flat strips of copper or steel, as well as rods of brass. After loading to a strain beyond the knee in the stress-strain curve, a hammer strikes a blow at a platform attached to the metal strip or rod. The resulting tensile wave is monitored by means of strain gages placed at four stations along the length of the strip. These gages provide measures of wave shape as well as wave velocity. In each case it was found that the wave traveled at the velocity of elastic waves in that material. This was true whether or not loading of the specimen was continued or stopped during the impact. They concluded that

"the experimental evidence ... indicate that in so far as the transient phenomenon is concerned, the existing theory neglecting strain-rate effects cannot describe the propagation of plastic strain satisfactorily. The assumption that the ordinary engineering stress-strain curve can be used to describe the dynamic aspects of plastic wave propagation does not seem tenable in the light of the observed propagation velocity and the apparent absence of a dependence of dispersion upon amplitude. Thus, the assumption that the instantaneous tangent modulus is only a function of the strain and not the strain rate it cannot be maintained if transient phenomena are to be described."

Yet, based only on the results of wave propagation experiments, the evidence in factor of strain rate effects was perhaps not quite as convincing as Sternglass and Stuart believed. Craggs (References 72 and 73) pointed out that three-dimensional effects in experiments with axial waves in bars might have an influence on results which might be interpreted as a strain rate effect. In this he was perhaps anticipating the results of combined stress wave tests such as those performed by Clifton (Reference 74). As Lee (Reference 75) showed, waves of combined stress offer an alternative explanation for the results of Sternglass and Stuart. In any case, Craggs urged that torsional wave propagation tests be made. Baker and Yew, Yew and Richardson, and Convery and Pugh (1968) tested tubular specimens of copper and mild steel in torsion (References 75, 76, 77 and 78). Their results showed that if the tube is being preloaded plastically in torsion then a superposed torsional wave has a component traveling at the elastic wave speed. Campbell and Dowling (Reference 79) performed both incremental wave tests and incremental strain rate tests in torsion on tubular specimens of copper, aluminum and a mild steel. In the incremental wave tests the tubes were first prestressed into the plastic range and, while quasi-static stressing continued, a torsional pulse was superposed and its velocity measured. It was found that a wave traveled at the elastic velocity in both aluminum and in mild steel. This was true over the entire range of prestrains. For copper, the fastest wave observed was somewhat slower than the elastic, its speed dropping gradually with the amount of prestrain, so that at a prestrain of 24.3% the speed was 92.5% of the elastic. The reason for this drop is not clear but the overall conclusion is that a

superposed pulse has a component traveling at or near the elastic wave speed, a phenomenon not explainable on the basis of a time-independent constitutive relation. Similarly, Campbell and Dowling (Reference 79) in tests on short specimens employing a Kolsky (split-Hopkinson) bar, showed that a rapid change in strain rate from 10^{-3} s^{-1} to 90 s^{-1} results in an increment in flow stress. This is shown in Figures 9 and 10, in which the slope of the stress-strain curve immediately after the change in strain rate appears to be near that of the elastic, followed by plastic flow at a higher stress level. Incremental strain rate experiments such as these which involve no intermediate unloading appear to give strong evidence for the existence of strain rate effects. This evidence is particularly persuasive since it does not require comparisons between different specimens. Even when specimens are cut from the same bar stock, machined with identical techniques and heat-treated in close contact with one another, there are differences in their mechanical behavior. Although these differences generally are small, it is always more convincing to see the results of an experiment in which a single specimen is loaded at two very different strain rates without removing it from the apparatus or making any change other than speed of loading.

Undoubtedly the most detailed and extensive series of tests on wave propagation in bars are those of J. F. Bell (Reference 80). In his tests, Bell employs a diffraction grating to measure the strain distribution in the specimen during the passage of the plastic wave. His specimens are cylindrical bars of metal having a diameter of 25.4 mm. They are struck at one end by a hitter bar. The diffraction grating is applied to the surface of the bar by using a special lathe which can scribe up to 35,000 lines/inch ($\sim 1,400$ lines/mm). By this means detailed measures of strain and particle velocity can be obtained for any station along the bar. Bell has employed his technique in studies of many different metals over a wide range of temperatures. On the basis of his results, Bell claims that plastic deformation is not sensitive to strain rate. Indeed, he puts forward the following general expression for stress during plastic deformation

$$\sigma = (2/3)^{1/2} \mu(0) B_0 (1 - T/T_m)(\epsilon - \epsilon_h)^{1/2} \quad (31)$$

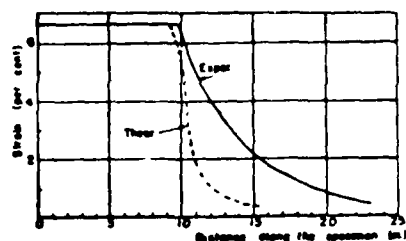


Figure 8. Theoretical and Experimental Strain Distribution Due to a Plastic Wave in an Annealed Copper Wire Specimen

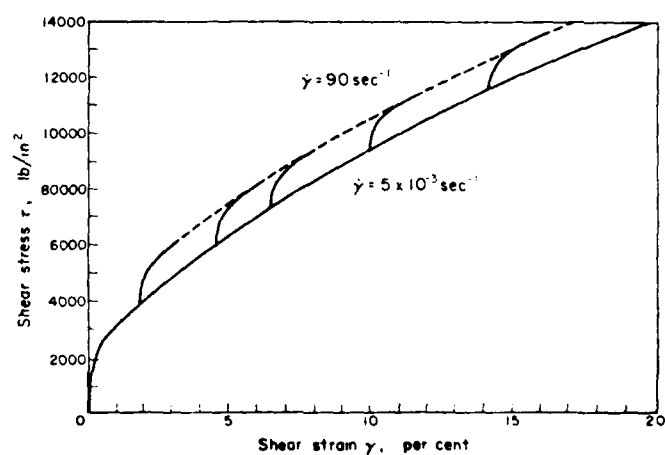


Figure 9. Incremental Stress-Strain Curves from Tests on Short Specimens of Copper

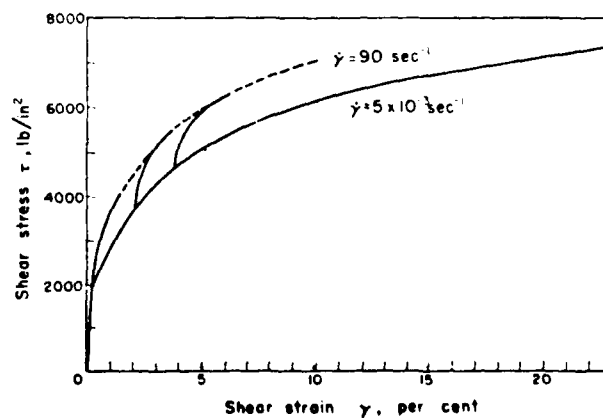


Figure 10. Incremental Stress-Strain Curves from Tests on Short Specimens of Aluminum

where $\mu(0)$, B_0 , T_m , and r_h are known constants for the material and r is an integral parameter. Bell's interpretation of his results is contested by many investigators on the grounds that the results of wave-propagation experiments such as he obtains are not sufficiently sensitive to material behavior to enable the investigator to distinguish between constitutive relations. If one plots strain-time profiles as shown in Figure 11, they agree just as well with strain rate dependent theories as with the strain rate independent, particularly when one takes into account experimental variations due perhaps to dispersion of the waves or imperfect impact at the end of the specimens. A detailed study by Ripperger and Watson (Reference 81) employing various constitutive equations of the type of Equation 19, showed that strain rate dependent theories predict results as near to the experimental as the strain rate independent. Ripperger and Watson also showed that it is not possible to distinguish from among the various strain rate dependent constitutive relations on the basis of strain-time or velocity-time profiles of the type shown in Figure 11. Thus, it would seem promising to employ entirely different experimental techniques to supplement the wave propagation studies. It should be added, that it seems unlikely that success can be achieved by means of tests in which a flat-ended projectile is fired at a rigid target. Tests of this sort were performed by Taylor and Whiffin (Reference 82 and 83). However, measurements of the lateral expansion constitute another measure of strain distribution as a function of length and therefore are unlikely to be sensitive to the precise form of the constitutive relation of the material. On the other hand, wave propagation experiments performed by plate impact as described below, would seem to hold great promise.

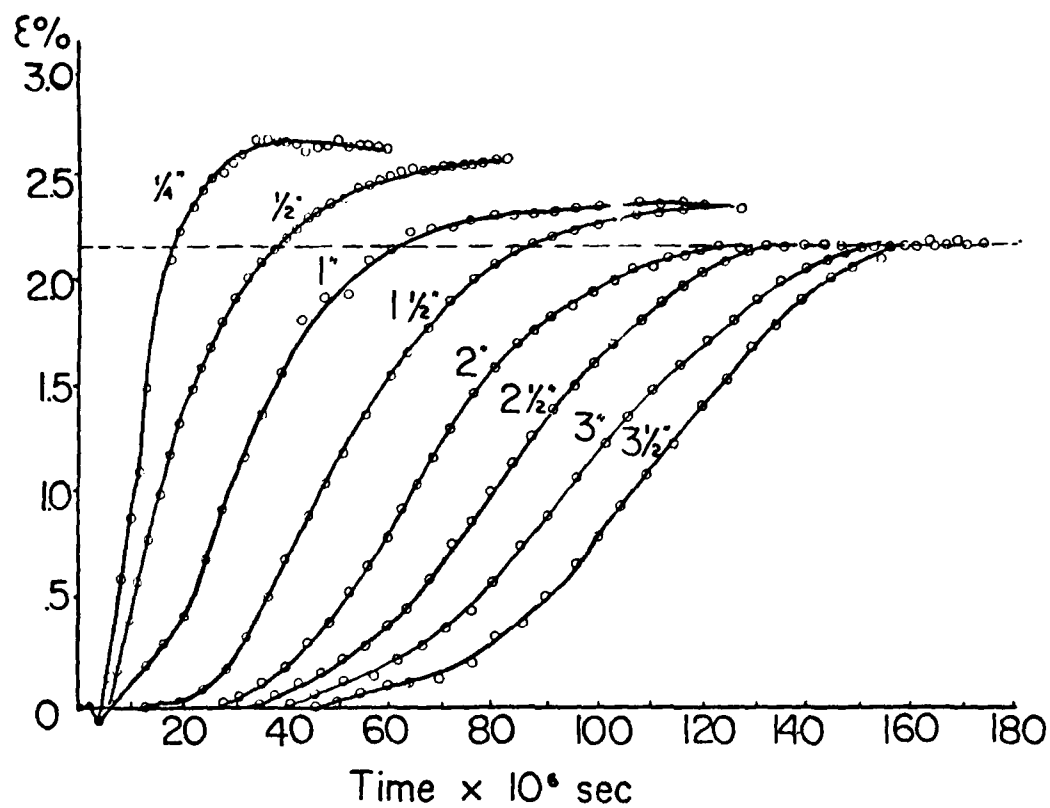


Figure 11. Strain-Time Profiles at Various Stations Along an 1100F Aluminum Bar After Impact

SECTION V

IMPACT TESTS AND TESTS AT INTERMEDIATE STRAIN RATES ($\dot{\epsilon} < 10^2 \text{ s}^{-1}$)

Concurrently with the early research in dynamic plasticity by wave propagation experiments, a number of investigators were performing tests at somewhat lower strain rates but with substantially homogeneous stress and strain distributions in the specimens. The practical motivation for much of this work came from metal forming and machining applications. For some period of time as a result, the most frequently used specimen material was steel and its properties were determined at room and at elevated temperatures. One need hardly point out that though the strain rates attained in these early experiments may not be as great as those encountered in plastic wave propagation they represent a considerable increase over strain rates achieved in a conventional testing machine, and that the problems encountered in performing a good quality test at 10^2 s^{-1} are far from trivial.

The first tests in this range of strain rates used the impact provided by a dropping mass or a spinning flywheel. Excellent examples are provided by the work of Manjoine and Nadai, Nadai and Manjoine and Sokolov or the many articles by the group at the California Institute of Technology, such as Johnson, Wood and Clark (References 84, 85 and 86). By these methods it was established that the plastic flow stress of metals increases at higher loading rates and that this effect generally is quite pronounced in the softer steels. It was also shown that temperature, grain size and heat-treatment all play crucial roles in this respect. Furthermore, it was found that there is a small delay between the time of application of the load and the onset of yield in the specimen. Although delayed yield was first discovered in steels, it has been established since that it occurs in other metals, probably being present whenever thermal activation assists the applied stress. Clark and Wood (Reference 88) showed that the duration of the delay time is strongly dependent on applied stress: for higher stresses it lies in the millisecond range while for stresses near the yield stress it is measured in seconds. Campbell and Duby (Reference 89) provided a criterion to evaluate the delay time. Later

experiments performed to study delayed yield used the Kolsky bar in compression, or modifications of it. Thus Krafft and Sullivan (Reference 90) tested short specimens of mild steel at successively greater loads and measured the decreasing delay time. Campbell and Marsh (Reference 91) on the other hand, used a hydraulic machine to conduct a study of the effects of grain size on delayed yield.

The advantages inherent in torsional loading were already appreciated by Work and Dolan (Reference 92). As these authors point out, during twisting of a circular bar its length and diameter will remain nearly constant up to large plastic strains. In other words, there is no reduction in area as in the later stages of the tension test. Accordingly, these investigators tested specimens of a 1018 hot-rolled steel in torsion using a specially constructed apparatus having a motor and a flywheel. Their specimens were in the form of round bars, rather than tubes, so that results are given in terms of torque and twisting rate rather than stress and strain rate. However, they did calculate the outer surface strain rate which for their tests ranged from $\dot{\gamma} = 10^{-4} \text{ s}^{-1}$ to $\dot{\gamma} = 12.5 \text{ s}^{-1}$. The results show an increase in stress at high strain rates and a decrease with an increase in temperature. Work and Dolan conclude that at constant temperature the torque is a power function of strain rate.

The impact tests mentioned above, in the form in which they were first developed, had a number of disadvantages which led Orowan and Los (Reference 93) to design the cam plastometer. The main criticisms leveled at the dropping mass experiment were three: (1) that the strain rate during a test generally cannot be held constant, (2) that the magnitude of strain rate depends on the mass employed, so that for a series of specimens each offering a different resistance, as would be encountered in testing one material over a temperature range, each specimen will be tested at a different strain rate unless the mass dropped is varied appropriately, and (3) that the impact produces resonant vibrations making interpretation of result difficult, if not questionable. These criticisms are valid; but, aside from the last, are not as telling as might seem at first. Thus, by increasing the inertia of the dropping mass it is possible to achieve a nearly constant strain rate, certainly

over the early stages of the deformation. The second criticism only implies that a larger number of tests must be conducted. Furthermore, the first two criticisms can also be made of the Kolsky bar unless certain precautions are taken. As pointed out below, in testing work-hardening materials in the Kolsky bar a constant strain rate is achieved only by imposing a sufficiently large impact or using a sufficiently large stored-torque. This corresponds precisely to an increase in the mass of the dropping weight or an increase in the inertia in the cam plastometer. However, the oscillations mentioned in the third criticism are most undesirable, partly because of interpretation difficulties but mainly because of strainrate history effects which can be quite strong particularly for a drop in strain rate.

The cam plastometer consists of a spinning flywheel with a logarithmically shaped cam to provide constant true strain rate and avoid the sudden impact of load application. It was first used by Alder and Phillips (Reference 94) who tested specimens of a commercially pure aluminum over the temperature range -190°C to 550°C , copper from room temperature to 900°C and a low carbon steel from 930°C to 1200°C . The tests were performed in compression at strain rates up to about 40 s^{-1} . The specimens measured 12 to 18 mm in diameter and 25 mm in length. Powdered glass was used as the lubricant between specimen and platens at the high temperatures. Heating or cooling was done outside the testing machine and the specimens put into place rapidly while contained in a special insulating box. Apparently, Alder and Phillips encountered stability problems in compressing their specimens to the larger strains, particularly at lower temperatures, and discarded results in which the stress-strain curve was not smooth. Their results were plotted using both a semi-logarithmic relation of the type

$$\sigma = A \ln \dot{\epsilon} + \sigma_0 \quad (32)$$

and a power law

$$\sigma = \sigma_0 \dot{\epsilon}^n \quad (33)$$

with apparently fairly good agreement using either relation, although somewhat better with the latter. It is clear from their results that, of the three metals tested, steel is the one whose flow stress is by far the most sensitive to strain rate. This is in agreement with succeeding work. Today, there is also rather clear evidence that the semi-logarithmic relation, Equation 32, can describe quite satisfactorily the behavior of fcc metals at least up to strain rates in the neighborhood of 10^3 s^{-1} . This is shown by the results reviewed below as well as those in the next section. For steel, on the other hand, the situation is not as clear. It is customary, whatever the material, to present experimental results by a plot of flow stress, at one value of strain and temperature, as a function of the logarithm of strain rate. On such a plot, results for steel generally do not provide a linear relation: the flow stress at the lower strain rate is often found to be independent of strain rate or nearly so, but at higher strain rates may rise rapidly so that a power relation (Equation 33), often fits results better than the semi-logarithmic.

The cam plastometer was also used by Cook (Reference 95) who altered the design of the cam to allow for testing up to a strain rate of 100 s^{-1} . He had in mind metal-working operations, particularly hot-working, where temperatures are high and where the flow stress for most steels is strongly dependent on both temperature and strain rate. He tested a dozen different steels from low carbon to stainless. Typical of his results are the graphs in Figure 12, which show a large strain rate effect. Thus, for low carbon steel there is an increase of about 50% in the flow stress between strain rates of 1.5 s^{-1} and 100 s^{-1} at 900°C . At 1200°C the difference is almost a factor of two. Unfortunately, Cook does not include curves showing the behavior of his steels at room temperature and at conventional strain rates, nor was it clear to him whether his results fitted better a relation of the type of Equation 32 or 33. One should add that Cook's temperatures are greater than about $0.6 T_m$, where T_m is the melting temperature of his materials, and that different microstructural deformation mechanisms may be governing from those at lower temperatures.

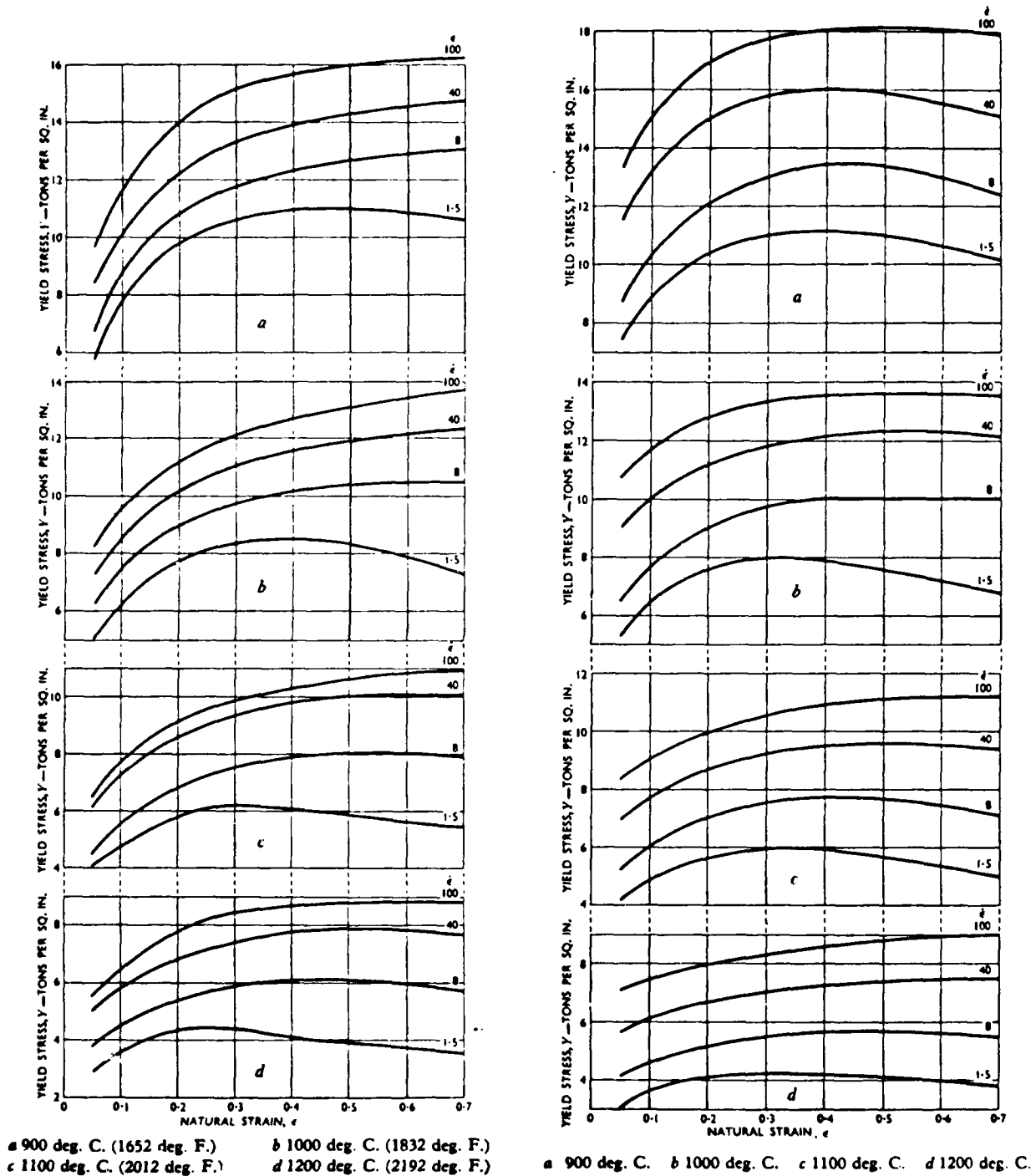


Figure 12. Flow Stress Vs. Natural Strain at Different Strain Rates for a Low Carbon and a Medium Carbon Steel at Elevated Temperatures. Figures Under $\dot{\epsilon}$ are in sec⁻¹.

Lueg and Muller (Reference 96) performed tests similar to those of Cook but involving only one steel (containing 0.45% carbon); however they tested both in compression and in shear. The imposed strain rates, whether in compression or shear, covered the range from 0.01 s^{-1} to 10 s^{-1} and the testing temperatures chosen ranged from 700°C to 1100°C . Qualitatively, the results are not very different from those obtained by Cook with his medium-carbon steel, although they are well-represented by a power relation, Equation 33. A similar conclusion was reached by Zoteev (Reference 97) on the basis test results obtained in tension with Armco iron and with three steels of varying carbon content. Zoteev also concluded that the strain rate sensitivity decreased with an increase in carbon content.

An interesting series of experiments on mild steel are those of Marsh and Campbell (Reference 98). Having a study of Malvern's rate-dependent constitutive relation, Equation 19 in mind, these investigators performed two series of tests, one in which strain rate was held constant and one in which stress was constant. The purpose of the constant stress tests was to evaluate the function $g(\sigma, \epsilon_p)$ appearing in Equation 19. During deformation at a constant stress

$$g(\sigma, \epsilon_p) = \frac{1}{E} \frac{\partial \epsilon}{\partial t}$$

so that a record of strain rate during deformation gives the function $g(\sigma, \epsilon_p)$ directly. The experiments were performed in compression by employing a rapid-loading hydraulic machine capable of imposing strain rates of nearly 10 s^{-1} . Typical results are shown in Figure 13, where the dotted lines represent constant stress results and the solid lines results at constant strain rates. On the basis of their analysis, Marsh and Campbell concluded that Malvern's Equation 19 was consistent with results. However, a simpler and frequently used version of this equation in which $g(\sigma, \epsilon_p) = g(\sigma - \sigma_s)$, where $\sigma_s = f(\epsilon_p)$ represents the static stress-strain relation, does not describe the observed behavior except within a limited range of strains in the work-hardening region. In this latter range a power relation, (Equation 33) fits results more closely. Campbell and Ferguson (Reference 99) attempted to broaden the range of strain rates in order to determine whether a different deformation

mechanism might be operating for steel at rates above about 10^3 s^{-1} . They employed three different experimental techniques, depending on the strain rate. For the highest rates they put the specimen in double shear and measured stress and strain with an adaptation of Kolsky's method. By this method they attained strain rates of $4 \cdot 10^4 \text{ s}^{-1}$. Results are shown plotted in Figure 14 where the s-rain rates must be divided by a factor of at least $\sqrt{3}$ in order to obtain an effective axial strain rate (and stress values multiplied by $\sqrt{3}$). It is evident from the figure that there is a rather sharp increase in the strain rate sensitivity at a value of strain rate of about $5 \cdot 10^3 \text{ s}^{-1}$. The question which arises is whether this is evidence of a different deformation mechanism dominating at the higher strain rates or whether it might not be due to the change in experimental technique. The conclusion reached by Campbell and Ferguson is that viscous resistance to dislocation motion becomes rate-controlling in steel at these high strain rates.

Bailey and Singer (Reference 100) employed the cam plastometer to test specimens of various aluminum alloys and of lead. Their strain rates ranged from 0.4 to 300 s^{-1} and the natural strains attained a value greater than 2. Since these investigators were interested in hot-working applications they performed experiments at temperatures up to 0.95 of the melting temperature, heating the specimen in a separate oven and preheating the dies before moving the specimens. Plots of their results show that the dependence of stress on strain rate fits a power relation remarkably well although the values of the exponent are somewhat greater than those of Alder and Phillips (Reference 94) over most of the temperature range. Even larger strains were attained by Bailey et al (Reference 101) who tested three aluminum alloys (including commercially pure aluminum) over a wide range of temperatures and strain rates. Their specimens were thin-walled tubes loaded in torsion by means of a special screw machine which could impose strain rates from 10^{-2} s^{-1} up to 10^2 s^{-1} . The stress-strain curves are presented for each metal at the various temperatures and strain rates. Typical results are shown in Figure 15, where a, b, c, d and e refer to strain rates of 0.01, 0.1, 1.3, 8 and 100 s^{-1} , respectively. The authors explain their results at the large strains attained in these tests on the basis of competing work-hardening and thermal softening effects.

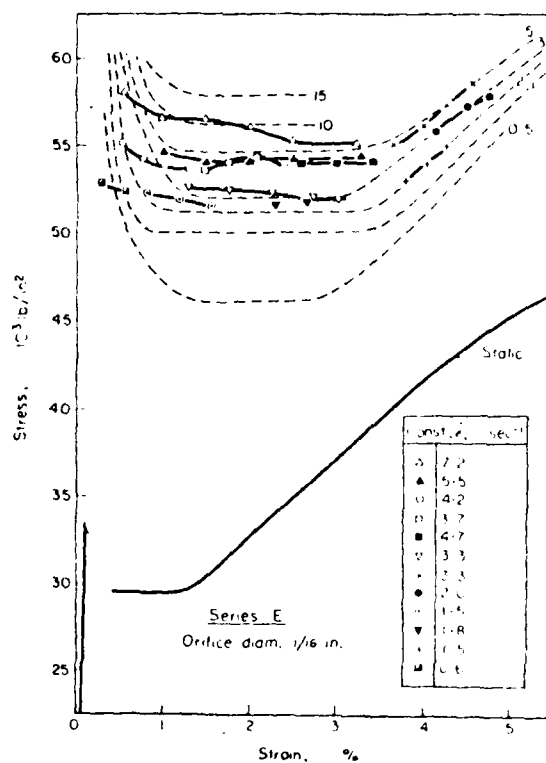


Figure 13. Dynamic Stress-Strain Curves for Mild Steel at Constant Strain Rates (Solid Lines) and Constant Stress (Dotted Lines)

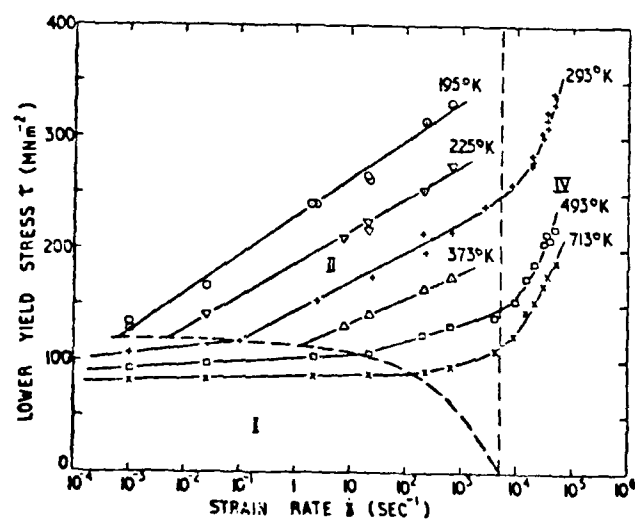


Figure 14. Variation of Lower Yield Stress With Strain Rate in Mild Steel

This presumes a homogeneous strain distribution. The analysis of results is made first in terms of the two constitutive relations given in Equation 32 and 33, and then in terms of a relation of the form

$$\dot{\epsilon} = A_1 [\sinh(\alpha \bar{\sigma})]^n \exp(-Q/RT) \quad (34)$$

first proposed by Sellars and Tegart (1966), who also carried their tests to large strains. Throughout their analysis, Bailey et al. used effective stress and strain, $\bar{\sigma}$ and $\bar{\epsilon}$, these being defined as $\sqrt{3}$ and $1/\sqrt{3}$ times the shear stress and shear strain respectively. They found that their results provided linear relations between the stress or strain rate functions in Equations 33 or 34; with the former the slope of the straight lines depended on temperature whereas Equation 34 gave parallel straight lines. On the other hand, on a semi-logarithmic plot straight lines were obtained only at the higher stresses (or lower temperatures). Hockett (Reference 102) used the cam plastometer to test 1100 aluminum in the temperature range 223-673K and at strain rates up to 200 s^{-1} . He found that a relation of the type of Equation 32 fitted his data quite closely, even though he attained a true strain of 70% in his tests.

The dropping mass referred to above continues to be used by a number of investigators, probably in part because of the large strains that can be achieved with it, and in part because of the ease with which specimens can be tested at temperature. Thus, Samanta (Reference 103) tested various steels with this method, dropping a mass of 41 kilograms through a distance of over 5 meters to achieve strain rates in compression of about 550 s^{-1} , and true strains of 50% and 80%. He heated his specimens in a separate platinum furnace, placed only 20 cm away, and transported them rapidly along a highly polished channel to the compressive platen. Temperatures in the range 20C were attained. Similarly, Samanta (Reference 104) tested an aluminum-copper alloy by using this drop-hammer technique. In all cases he found that the flow stress depends linearly on the logarithm of strain rate. Suzuki et al. (Reference 105) also used this technique to test a variety of metals from steels to aluminum, zinc, magnesium, copper and titanium. More recently, Harding (Reference 106) has employed a dropping mass to test a variety of steels in the temperature range 77K to

225K at strain rates from 10^{-3} s^{-1} to 2500 s^{-1} . Typical results, shown in Figure 16, clearly indicate that the flow stress is independent of strain rate for strain rates less than about 10 s^{-1} , but thereafter increases rapidly. For the milder steel, the strain rate sensitivity is quite large. Based on these results and on the temperature dependence of the flow stress, Harding concludes that the strain rate is predicted quite satisfactorily by a single thermally activated deformation mechanism, i.e. by Equation 2, for temperatures below 225K and strain rates from 100 s^{-1} to 2500 s^{-1} .

High strength steels have been tested by Kendall and Davidson and Kendall (References 107 and 108). The purpose of their tests was to determine the initial yield stress as a function of the elastic strain rate. Tests were conducted on 4340 steel, H-11 tool steel and maraging steel, as well as 1018 steel. Temperatures extended from 200 to 590K.

Since much of the above work involves steel, one can draw tentative conclusions as to its plastic behavior under dynamic loading even without reference to the results obtained with the Kolsky bar (described in the next section). First, it is clear that the flow stress of steel for strain rates above about 10 s^{-1} , is far more sensitive to strain rate than is the case for fcc metals. In this respect, Harding's results, Figure 16, are typical of the dependence of flow stress on strain rate at room temperature and below. The highest strain rate sensitivity is found in the mild steels and particularly at elevated temperatures.

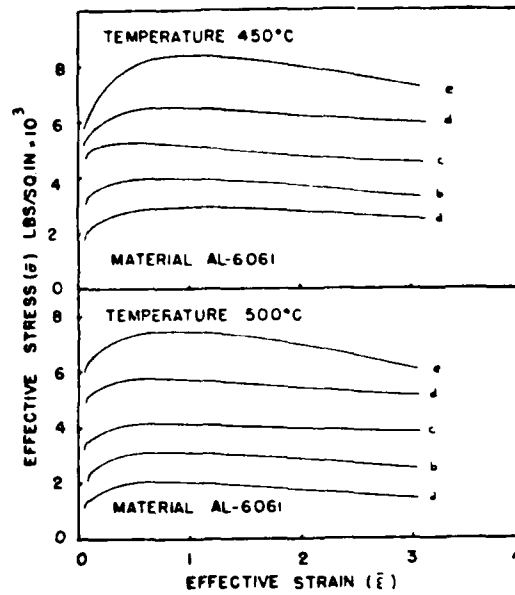


Figure 15. Variations of Effective Stress With Effective Strain for 6061 Aluminum at Large Strains. Strain Rates are:
 $a = 0.01 \text{ s}^{-1}$, $b = 0.1 \text{ s}^{-1}$, $c = 1.3 \text{ s}^{-1}$, $d = 8 \text{ s}^{-1}$,
 $e = 100 \text{ s}^{-1}$.

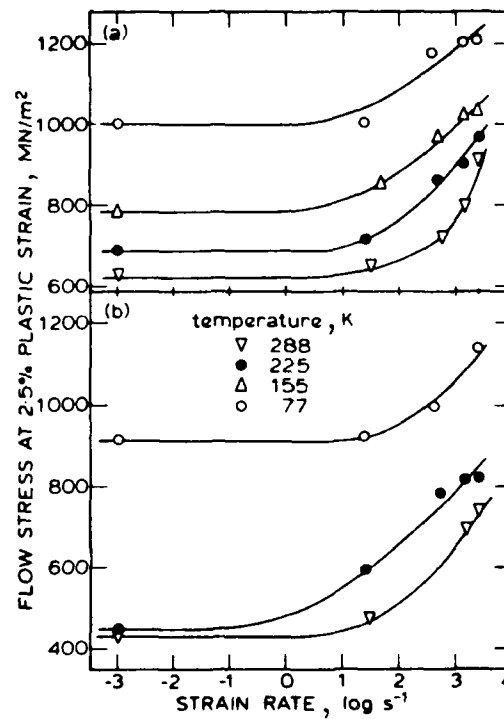


Figure 16. The Flow Stress of Two Steels as a Function of Strain Rate
 (a) HY 80 and (b) BS 968

SECTION VI

THE KOLSKY BAR (SPLIT-HOPKINSON BAR) AND TESTS AT
HIGH RATES OF STRAIN (10^{-2} s^{-1} to 10^4 s^{-1})

The cam plastometer or the hydraulic testing machine can impose strain rates up to perhaps 10^2 s^{-1} and still retain a homogeneous state of strain in the specimen. To achieve homogeneous conditions at higher strain rates and simultaneously obtain reliable measures of stress and strain posed a difficult problem, which was solved by Kolsky (Reference 109) by a most ingenious idea. Kolsky placed a thin wafer-shaped specimen of the material to be tested between two long elastic bars as shown schematically in Figure 17. Loading of the specimen is accomplished by propagating a compressive pulse along one of these bars toward the specimen. This pulse is partially transmitted into the second elastic bar and partially reflected by the specimen. Kolsky showed that the transmitted pulse provides a direct measure of the average stress in the specimen, $\sigma_s(t)$. Thus, if P_I and P_T are, respectively, the forces acting at the interfaces with the incident and transmitter bars then the average stress in the specimen is given by

$$\sigma_s = \frac{P_I + P_T}{2A_s} \quad (35)$$

where A_s is the cross-sectional area of the specimen. Since the bars remain elastic, the forces P_I and P_T are proportional to the respective axial strains in the bars. For a homogeneous state of stress in the specimen, and for bars of the same cross-sectional areas, A_T , and equal elastic moduli, E_T , this gives

$$\sigma_s(t) = \frac{A_T}{A_s} E_T \epsilon_T(t) \quad (36)$$

where $\epsilon_T(t)$ is the axial strain in the transmitter bar, a quantity which is relatively easy to measure. Thus by employing Equation 36 the Kolsky bar provides a measure of the axial stress in the specimen as a function of time. Kolsky evaluated $\epsilon_T(t)$ by using a parallel-plate condenser microphone to measure the displacement at the free end of the bar, a technique employed earlier by Davies (Reference 110). Today $\epsilon_T(t)$ is

measured directly by means of electric resistance strain gages cemented to the surface of the transmitter bar.

Kolsky next showed that the reflected pulse provides a measure of the axial strain in the specimen, ϵ_s , or rather of the strain rate $d\epsilon_s/dt$, as a function of time. However, by a single integration, the latter provides $\epsilon_s(t)$. As can be seen from Figure 17, the strain in the specimen is given by

$$\epsilon_s = (u_2 - u_1)/l \quad (37)$$

where u_1 and u_2 are the displacement at the ends of the incident and transmitter bars, respectively, and l is the undeformed length of the specimen. Now u_2 can be found from the transmitted strain since

$$\epsilon_T = \frac{\partial u_2}{\partial x} = \frac{1}{c} \frac{\partial u_2}{\partial t}$$

so that

$$u_2 = c \int_0^t \epsilon_T dt \quad (38)$$

Similarly u_1 can be found from the strains due to the incident and reflected pulses through

$$u_1 = c \int_0^t (\epsilon_I - \epsilon_R) dt \quad (39)$$

where the negative sign is necessary because the reflected pulse travels in the $-x$ direction. If we differentiate Equation 37 and make use of 38 and 39 we have

$$\dot{\epsilon}_s = \frac{c}{l} [\epsilon_T - (\epsilon_I - \epsilon_R)] \quad (40)$$

where the strains are all functions of time. For a homogeneous state of strain in the specimen $\epsilon_T = \epsilon_I + \epsilon_R$, so that

$$\dot{\epsilon}_s(t) = \frac{2c\epsilon_R(t)}{l}$$

Since ϵ_R is measured as a function of time, Equation 41 can be integrated to give $\epsilon_S(t)$, the strain in the specimen. Kolsky evaluated $\epsilon_R(t)$ indirectly by measuring the change in diameter of the loading bar using a specially designed condenser microphone. Today it is measured directly by means of strain gages. Thus, Equation 36 and 41 provide stress and strain in the specimen as functions of time. Furthermore, by eliminating time between $\sigma_S(t)$ and $\epsilon_S(t)$ one obtains the stress-strain curve for the material at a strain rate provided through Equation 41 by the record of $\epsilon_R(t)$.

1. CRITIQUE OF THE KOLSKY BAR

Kolsky's method evidently has numerous advantages. It can be employed to attain strain rates in the range 10^2 s^{-1} to 10^4 s^{-1} . The apparatus is simple and inexpensive, and yet gives detailed records of stress, strain, and strain rate, all as functions of time. Data acquisition and recording require only commercially available equipment, mainly oscilloscopes, though it is essential that their frequency response be adequate. Almost any material can be tested, and experiments have been performed on metals and plastics, as well as on geological and biological materials. The method has been and remains one of the most widely used for dynamic testing. It has been adapted to tensile loading by Lindholm and Yeakley (Reference 111) to uniaxial strain by Bhushan and Jahsman (Reference 112) and lastly, to torsional loading by a number of investigators as described further in greater detail.

In view of its significance, both in material testing and in research, the Kolsky bar has been analyzed in great detail to determine its limitations and any possible errors. These can be classified as follows:

a. Inertial and Frictional Effects

When an axial pulse, say a compressive pulse, propagates along a bar, whether elastic or plastic, it is accompanied by a radial expansion of the bar. This lateral motion is resisted by a radial inertia which is greater the shorter the pulse and the larger its amplitude. In the specimen this effect results in a radial stress component superposed on the axial.

Hence, with the Kolsky bar the state of stress in the specimen is not uniaxial and, furthermore, the radial component of stress is difficult to evaluate since it depends on dynamic material properties which have not yet been determined. In addition, a radial traction component is imposed at the two interfaces between the specimen and the loading bars. This traction, whose magnitude depends upon friction is due to the fact that Poisson's ratio for the specimen, particularly when it is deforming plastically, is not the same as for the elastic loading bars. Though lubricants are used, estimates of these frictional forces are still necessary and are difficult to make.

Davies and Hunter (Reference 113) performed quasi-static and dynamic experiments employing the Kolsky bar. Unfortunately, they do not specify the rates in their quasi-static tests so that calculations of strain rate sensitivities is uncertain. However, even presuming a very low quasi-static strain rate their results, for aluminum, copper, magnesium and zinc, show larger strain rate sensitivities than any measured since. These authors also studied the inertial and frictional effects in the compressional Kolsky test, and pointed out that for Kolsky's wafer-thin specimens the inertial effects are small but the frictional effects may be quite large. They present a detailed analysis of these effects to show that an optimum length to diameter ratio for the specimen is given by $\sqrt{3}\nu/2$ where ν is Poisson's ratio for the specimen material. On the other hand, Lindholm (Reference 53) showed by experiment that variations of dimensions within reasonable bounds do not adversely affect results (Figure 18). On the basis of his experiments, he suggested that the length to diameter ratio be approximately one half to unity. However, he pointed out the importance of maintaining a constant length to diameter ratio within any one series of tests. Thus, in his work, whenever he reduces the length of his specimen to achieve higher strain rates, he simultaneously reduces the diameters of his loading bars. The importance of proper lubrication is emphasized in this paper, as it is again by Lindholm and Yeakley (Reference 111).

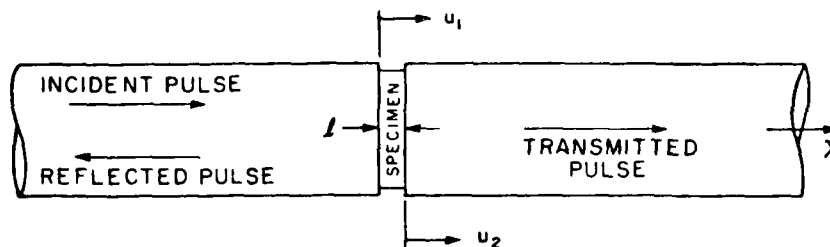


Figure 17. Schematic Representation of Kolsky's Dynamic Compression Apparatus

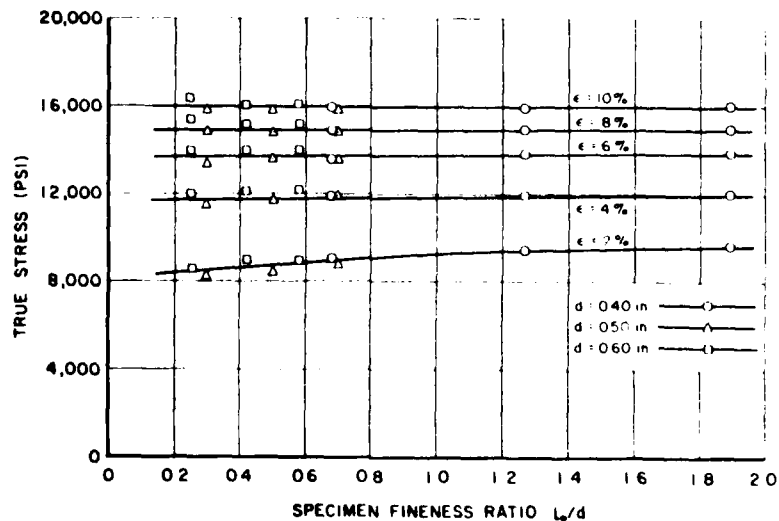


Figure 18. Influence of Specimen's Fineness Ratio on Results Obtained With Kolsky Bar in Compression

In spite of these results, inertial and frictional effects continued to create doubt as to the magnitude of the dynamic yield stress. Indeed, a few investigators claimed that the difference between quasi-static and dynamic flow curves could be explained entirely by friction and inertia, and that in reality material behavior was rate-independent. This position became more difficult to hold with the advent of the torsional Kolsky bar, described in a later section. In the torsional test, radial inertial and frictional effects are absent; yet results obtained in torsion with a variety of metals show strain rate effects of about the same relative magnitude as found in axial tests.

b. Inhomogeneous Stress or Strain

The idea behind the Kolsky bar is to make the specimen short enough so the stress and strain distributions are homogeneous. Indeed, the analysis of results in the Kolsky bar and hence the resulting stress-strain curves are predicated on homogeneity of the stress and strain distributions. Unfortunately, the strain distribution in the specimen is difficult to measure directly during a dynamic test because the specimen is short and the event rapid.

For the first few microseconds of loading, i.e., for low strains, the Kolsky bar cannot provide reliable records of stress and strain. Deformation of the specimen is first produced by elastic waves. Since these are rapid, they will suffer multiple reflections from the ends of the specimen within the first few microseconds after the arrival of the pulse. In spite of that, however, one cannot measure the dynamic elastic modulus of metals by using a Kolsky bar. On the other hand, after a few microseconds have elapsed following the arrival of the pulse, and depending on its rise-time, substantially uniform states of stress and strain are achieved within the specimen so that a reliable measure of flow stress is obtained, including that of the initial yield stress.

While the above implies that a nearly homogeneous state of strain obtains after a few wave reflections, it does not follow that the strain distribution need remain homogeneous with further straining. Barrelling of the specimen may occur in axial testing and shear bands have been observed in the torsional test. Either of these phenomena must be guarded against very carefully since their presence completely vitiates results, unless, of course, the purpose of the tests is to study shear bands, as in the work of Wulf or of Costin et al. (References 114 and 115). Fortunately, shear bands generally are not encountered until some perceptible strain has accumulated. Thus in torsional loading, Costin et al. (Reference 115) have observed shear bands with 1018 cold-rolled steel, but only after a strain of 8 or 10%. Shear bands are not seen with 1020 hot-rolled steel or with aluminum or copper. Their presence is easy to detect in the tubular specimens used in torsional testing. This is done by scribing fine axial lines on the walls of the specimen before loading. If the strain is homogeneous then, after testing, each of these lines is tilted at the shear angle within the gage length of the specimen, but remains straight. A curved line on the other hand is immediate evidence of non-homogeneous strain. As a matter of fact, in the experience of the author, when non-uniform strain is present the lines depart drastically from straight lines, due undoubtedly to instability effects (shear banding).

Jahsman (Reference 116) investigated the quality of results that can be obtained with the Kilsky bar. He compared the known or reference stress-strain curve of a hypothetical specimen to the reconstituted curve as determined in a typical test. His analysis takes into account the multiple elastic and plastic wave reflections within the specimen. To perform the calculations, he presumed that the reference stress-strain relation was bi-linear, with the work-hardening rate having a slope $1/25$ as large as the elastic slope. He considered two input pulses, a trapezoidal one designated in Figure 19 by (a), and a triangular one designated (b). He fixed the rise time, τ , of these pulses in relation to the thickness, h , of the specimen according to the equation

$$c\tau = 5h$$

where c is the elastic wave speed in the specimen, and τ designates the time for the stress to attain first yield. Thus this equation represents five passes of the elastic wave before the specimen becomes plastic. For steel or aluminum specimens it provides a rise-time of 25 microseconds if the specimen is one inch thick. The reconstituted stress-strain curves compared to the reference are shown in Figure 20, where (a) and (b) again refer to trapezoidal and triangular input pulses, respectively. It may be seen that general agreement is quite good, particularly with the trapezoidal input pulse which is considerably nearer to the pulse shapes generally imposed. But even with the triangular pulse, results in the early stages are not far wrong. This analysis illustrates graphically the importance of maintaining consistently the same shape of (trapezoidal) input pulse, since a change could be interpreted as a strain rate effect. Nicholas (Reference 117) made a somewhat similar analysis for the torsional Kolsky bar and a rate-dependent material. His results depend upon the choice of a particular relation between stress and strain rate, but agreement between the reconstituted stress-strain relation and the reference can be quite satisfactory.

Lindholm et al (Reference 118) performed experiments to check whether the relation $\epsilon_T = \epsilon_I + \epsilon_R$, used in the derivation of Equation 41, held during a particular test. They employed specimens of a 7075-T6 aluminum alloy at 500°F. The results (Figure 21) appear quite satisfactory, the disagreement being no greater than one would expect from experimental inaccuracies. As they point out, their test was fairly severe because the value of $d\sigma/d\epsilon$ for an aluminum alloy at this temperature is small so that plastic waves propagate at a relatively low velocity. However, even if $\epsilon_T = \epsilon_I + \epsilon_R$, one does not have an acceptable test unless the strain rate in the specimen is held constant, (or otherwise specified). For this purpose it is not sufficient that the input pulse be "square," since it is the reflected pulse that establishes strain rate (Equation 41). In Lindholm's example ϵ_T was nearly constant, because this material does not work-harden rapidly. Yet ϵ_R decreased rather quickly with time so that the strain rate was not constant. In order to obtain a more nearly constant value of strain rate in this example, it would be necessary to increase the magnitude of ϵ_I until it is considerably larger than that of ϵ_T . In general,

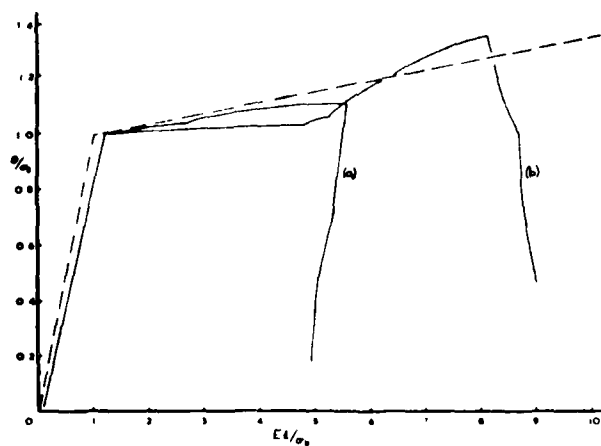


Figure 19. Reference (Dashed LINES) and Reconstituted (Solid Lines) Stress-Strain Curves for (a) Trapezoidal and (b) Triangular Incidence Pulses

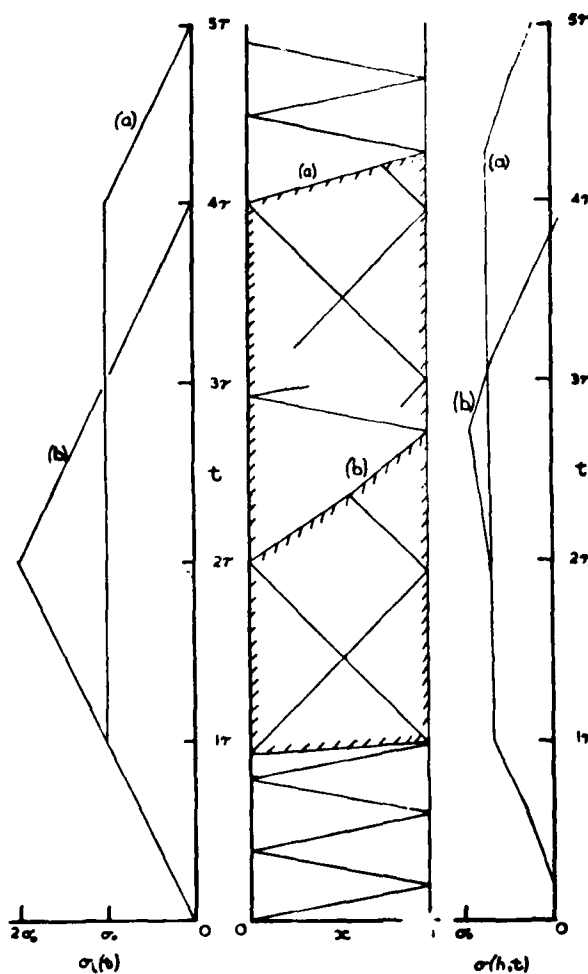


Figure 20. Calculated Transmitted Stress for a Specimen in a Kolsky Bar Subjected to (a) Trapezoidal and (b) Triangular Incident Pulses

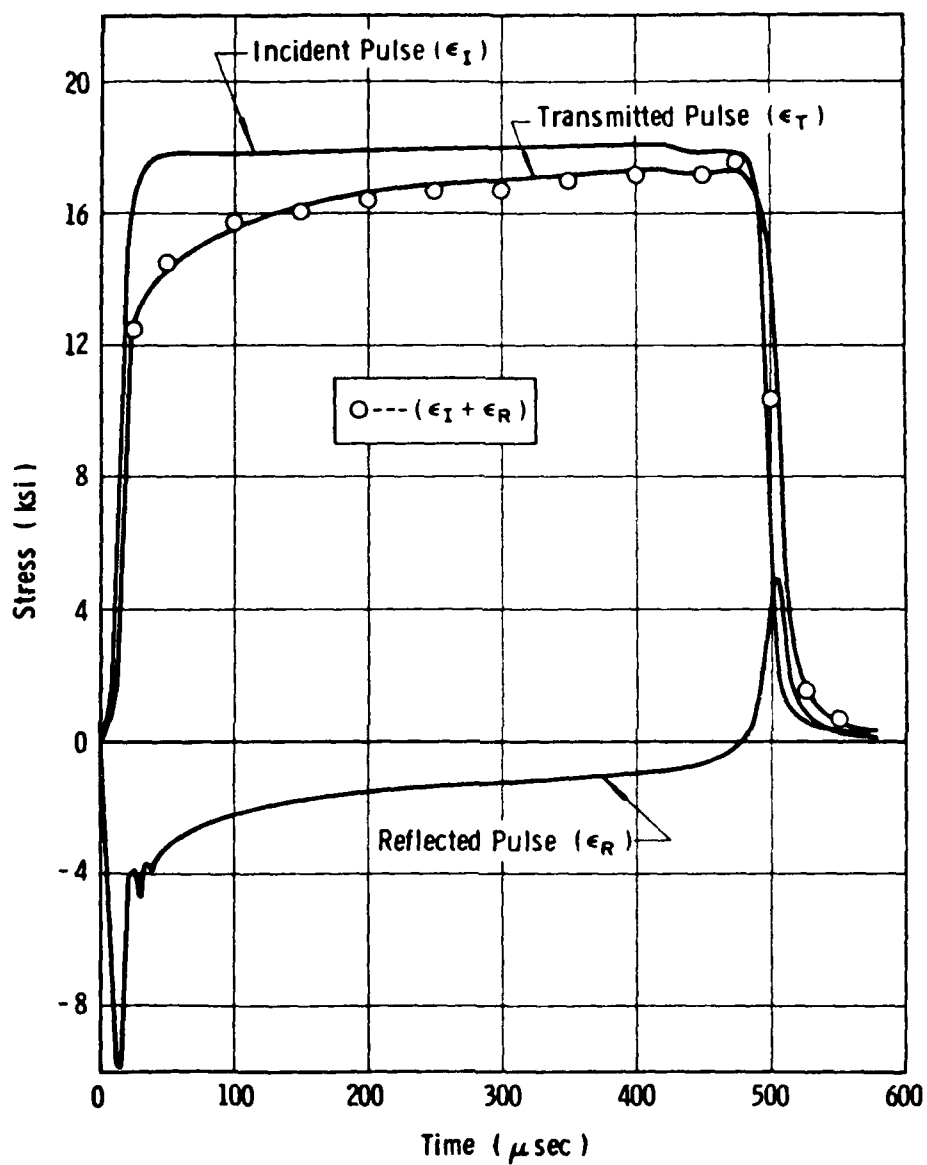


Figure 21. Comparison of Experimental Values of $\epsilon_I + \epsilon_R$ to ϵ_T for Equation (41)

depending on the rate of work-hardening, the ratio $\dot{\epsilon}_I/\dot{\epsilon}_T$ cannot be less than five or ten to one, thus imposing a lower limit on the strain rates that can be attained with the Kolsky bar. This is true whenever loading is effected by means of a striker bar (or, in torsion, by a stored torque), since this provides a nearly constant input pulse. With explosive loading, the input pulse reaching the specimen generally is not quite "square," often showing a gradually increasing amplitude near the start of the pulse; it is sometimes possible to take advantage of this increasing amplitude to obtain a constant reflected pulse, since the rate of increase often matches approximately the initial work-hardening rate.

c. Dispersion in the Loading Bars

Compressive (or tensile) waves propagating in an elastic bar will suffer geometric dispersion. In the case of the Kolsky bar, this dispersion has a number of effects, not all deleterious:

- 1) In Kolsky's original test the pulse was initiated at one end of the bar by the detonation of an explosive charge. In general, when explosives are used there is a short rise-time followed by a pulse with large variations in amplitude. If a pulse of varying amplitude were to reach the specimen then the resulting strain rate would include these variations and be far from constant. However, as a result of geometric dispersion the high frequency components in the incident pulse travel more slowly than the main pulse so that the pulse has acquired a relatively constant magnitude by the time it reaches the specimen. Thus, the explosive impact in Kolsky's original experiment resulted in constant strain rates. The situation is completely different in the case of the torsional Kolsky bar, because a torsional pulse in the primary mode propagates without dispersion. Hence, with the torsional bar any high-frequency components that appear immediately after the explosive detonation will persist essentially unchanged all the way to the specimen, no matter how long the bar. The investigator who wants to use an explosive detonation rather than stored-torque to initiate the torsional pulse must employ a pulse smoother as well (see below).

2) Geometric dispersion lengthens the rise-time of the axial pulse. For a one inch diameter incident bar the minimum rise-time is about 20 or 25 microseconds. Hence, torsional loading with an explosive detonation provides a potential advantage since the rise-time for a one inch bar has been reduced to about eight microsecond and to three to four microseconds in an incremental strain rate test.

3) The pulse transmitted through the specimen, as well as the one reflected, suffer some dispersion before they reach the strain gage stations. This influences to some extent the records of ϵ_T and ϵ_R and hence influences both stress and strain rate records. As a result, with the axial bar it is customary to place the gage stations fairly near the specimen in order to diminish the effects of dispersion in these records. Again, in torsional loading this effect is absent so that the strain gages may be placed at any convenient distance.

d. Recording the Stress-Strain Curve

In early applications of the Kolsky bar there was a purely practical difficulty in the interpretation of records. From the oscilloscope records of stress-time and strain rate-time one had to eliminate time in order to find the stress-strain curve. It was difficult to match the initial points on the curves; an error of a few microseconds would displace in time one variable relative to the other for the whole record. Lindholm (Reference 53) showed that this difficulty can be overcome by placing the gage stations at equal distances to either side of the specimen and using electronic integration and an X-Y oscilloscope to eliminate time. It is a relatively easy matter to locate a strain gage properly, and an error of one millimeter in its location produces an error in time of only one fifth of a microsecond.

e. Tests at Elevated Temperatures

The Kolsky bar is not as easily adapted to testing at elevated temperatures as might at first appear. The apparatus is very long so it is difficult to bring it all to temperature; furthermore, electric resistance strain gages cannot be heated above a certain temperature.

The alternative is to enclose only the specimen in the furnace, but this creates a problem since the loading bars, in contact with the specimen, will have a temperature gradient to either side of the specimen. Such gradients produce variations in the elastic modulus of the bars and hence variations in the wave velocity. As a result, elastic pulses propagating along the bars suffer continuously from partial reflections and from a change in amplitude. Various investigators have solved this temperature gradient problem as follows:

1) Green and Babcock (Reference 119) heated the specimen, then inserted the cold pressure bars rapidly into the furnace. This is the simplest solution but may result in considerable error if not done rapidly and skillfully. It cannot be used in torsional loading since mounting the specimen in that case takes considerable time.

2) The specimen is heated after mounting and the thermal gradients in the bars are ignored. If this method is adopted, it is advantageous to employ loading bars made of steel, or other material for which a temperature gradient does not produce too great a difference in impedance. The method is generally satisfactory to at most 200°C to either side of the ambient, depending on the accuracy sought; for larger differences in temperature the error becomes quite large. Furthermore, it is not correct to argue, as do some investigators, that the error is negligible because the temperature gradients are symmetric to either side of the specimen. The truth is that unwanted reflections occur on both sides of the specimen creating errors in both the stress-time and strain rate-time records, and that these errors do not compensate each other in the stress-strain diagram. For instance, on the transmitter side the apparent stress is too low, at least during the first few microseconds, because the pulse transmitted through the specimen is partly reflected back toward the specimen before it reaches the gage station. On the incident and reflected side, on the hand, the strain rate appears larger than it should because the incident pulse is partly reflected before it ever reaches the specimen. Spurious signals result which precede the pulse reflected from the specimen and then are superposed on it. Unfortunately, in plotting the stress-strain curve, an error that makes the strain rate appear too large cannot compensate for another error making the stress too small.

3) The thermal gradients are accepted in the experiment but corrected for in the analysis. This was the method adopted by Chiddister and Malvern, Lindholm and Yeakley and Campbell and Ferguson (Reference 99, 111, and 120). Thus Chiddister and Malvern measured the temperature gradients along the Kolsky bars then calculated the corrections necessary to account for the impedance change; they simplified these corrections by changing the impedance sharply at every inch of the bar rather than continuously. In this way they would calculate the reflected and transmitted pulses at each impedance change and modify their records accordingly. This technique is cumbersome but provides quite satisfactory records of stress and strain.

4) Eleiche's solution was to preserve a constant impedance along the loading bars by tapering them appropriately for each test temperature. The method is described in detail for the case of torsional waves by Eleiche and Duffy (Reference 121). As in the method of Chiddister and Malvern, it is first necessary to measure the temperature gradients. On the basis of the temperature distribution in a similar but dummy bar, it is possible to calculate the necessary taper in order to preserve a constant impedance. For torsional loading this taper is very gradual. Thus, for a specimen at 250C and a steel bar it amounts only to a change in diameter of 1.43%, Figure 22. After the tapered Kolsky bar is machined it can be tested to insure that the new profile is correct. This is easily done in a test at temperature by employing a dummy specimen of the same material as the bars. For these conditions and at the appropriate temperature there should be no reflected pulse whatsoever either from the specimen, which remains elastic, or from the tapered bar which now has a constant impedance at that temperature. Furthermore, strain gages placed at any position along the bars give correct incident, reflected and transmitted pulses. Eleiche and Duffy show this by presenting an analysis of the propagation of torsional elastic waves along a slender bar for which the wave velocity, the material density and the geometry are all functions of the axial coordinate subject to the constraints that the impedance remain constant. A solution of the wave propagation problem under these conditions shows that the characteristics are curved lines but that torque and angular velocity propagate unchanged along these lines. Hence, strain gages may be placed at any position along the length of the bar to give the same

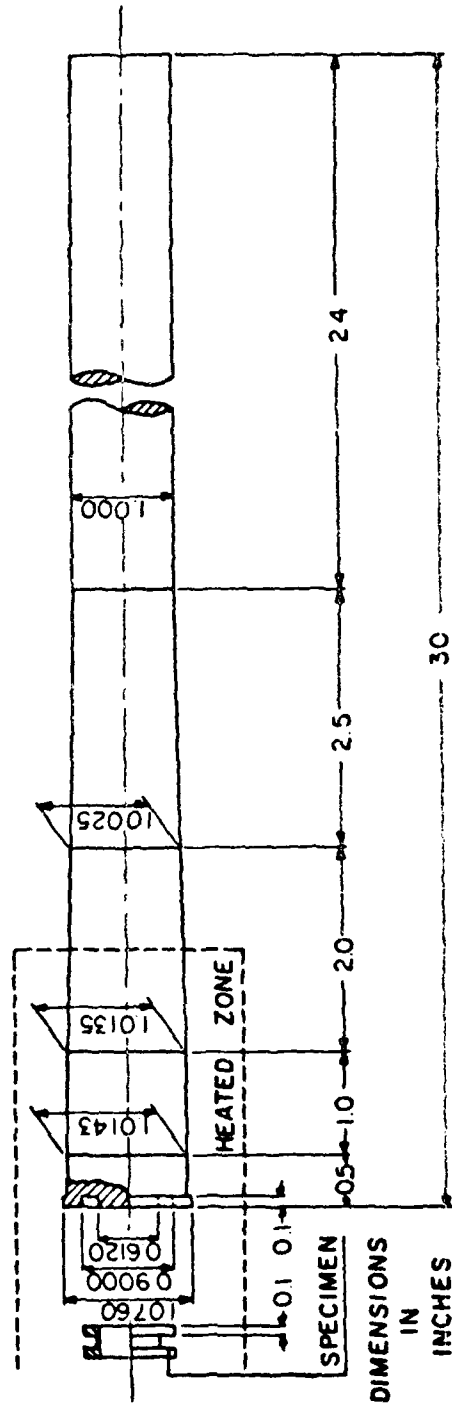
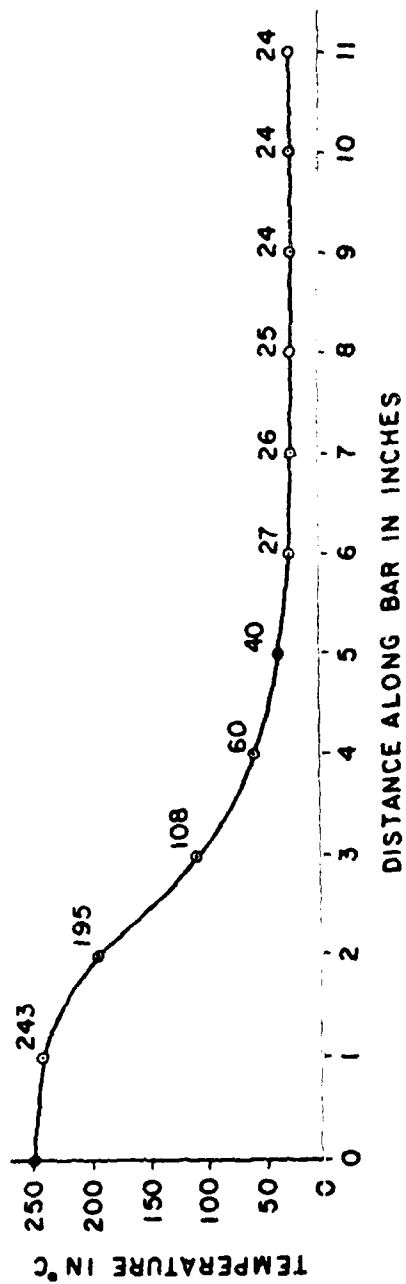


Figure 22. Tapered Steel Torsional Kolisky Bar for Tests at 250°C

pulse shape as imposed on the specimen. Similarly, the transmitted pulse is also a correct measure of stress-time.

Summary View of the Kolsky Bar

The above comments relative to the use of Kolsky's split-Hopkinson bar can be summarized as follows. The Kolsky bar is a convenient, relatively inexpensive technique which provides reliable curves of flow stress as a function of strain at strain rates in the range 10^2 s^{-1} to 10^4 s^{-1} . The important questions regarding inertial and frictional effects in the axially loaded configuration that were raised shortly after the method was first devised seem far less important today, as long as the length to diameter ratio of the specimen is maintained constant within a series of tests and approximately in the range of unity, and as long as care is exercised in lubricating the surfaces. However, attempts to attain very high strain rates by employing extremely short specimens seem questionable because of the presence of end effects. Unfortunately, use of the Kolsky bar for tests at temperatures far from the ambient is more difficult than had been anticipated because of the temperature gradients along the bars and the attendant wave dispersion. However, as outlined below, recent work shows that the Kolsky bar is useful in studies of strain rate history effects.

2. RESULTS OF CONSTANT STRAIN RATE TESTS WITH THE KOLSKY BAR

a. Strain Rates to 10^3 s^{-1}

It is not possible to comment critically upon all the experiments that have been performed with the Kolsky bar nor even to attempt a complete list. Furthermore, such a task is unnecessary since much of this work is already discussed in a number of other reviews, as for instance those by Lindholm and Bessey, Eleiche, the two reviews by Campbell or the one by Bitans and Whitton (Reference 2, 26, 10, 122 and 123). It might, however, be useful to mention a few of the published papers, omitting references to the work of Campbell, Lindholm, or Klepaczko, whose results are commented upon elsewhere in this review.

A large number of tests in the early years were performed at the University of California in Berkeley. Among the papers published one should cite Larsen (Reference 124) who tested single crystals of Ag_2Al both in compression and tension, and Hauser (Reference 125) who performed experiments in tension and presented a general review of experiment 1 techniques to cover a large range of strain rates. But perhaps the paper with the most influence on later work is that of Hauser et al. (Reference 126). These investigators made two major changes in the Kolsky bar: they employed electric resistance strain gages instead of capacitance gages to measure the transmitted and reflected pulses, and they initiated their pulse by means of the impact provided by a Hyge ram rather than by explosive loading. Their specimens were of a high purity aluminum machined into short tubes which were compressed axially during testing. Both the impact velocity of the ram and the gage length of the specimen were varied during these tests to cover the range of strain rates from 2s^{-1} to $12 \cdot 10^3 \text{s}^{-1}$. Tests were conducted at three temperatures 295, 194, and 78K. The results indicate a linear relation between stress and strain rate (Equation 32) at least up to rates of 10^3s^{-1} . For higher strain rates the flow stress increases more rapidly than predicted by Equation 32 and it is surmised by the authors that there exists a limiting maximum strain rate which corresponds to the limiting achievable velocity of dislocations.

At the General Motors Research Laboratories the Kolsky bar has been used to study the behavior in compression of a large variety of different metals. Among the various papers published one should cite Maiden and Green, Green and Babcock, Holt et al. Kumar et al. Babcock and Perkins, and Green et al. (References 119, 127, 128, 129, 130 and 131). Their results for various fcc metals are particularly interesting. They found that the semi-logarithmic relation (Equation 32) comes closest to describing the dependence of flow stress on strain rate, at least up to rates of about 10^3s^{-1} , so that a simple thermally activated mechanism can explain material behavior. Furthermore, in a detailed study of aluminum and its alloys, they demonstrated that impurity content is an important factor in determining the degree of strain rate sensitivity, with the purer metals showing greater sensitivity to strain rate. These results are presented graphically by showing the variation of the strain rate sensitivity

as a function of the quasi-static flow stress (Figure 23). According to these investigators the principal influence of an alloying element is to increase the value of σ_0 in Equation 32, which they associate with an athermal stress component due to long range stress fields.

Samanta (Reference 132), whose work has already been referred to above, also has employed the Kolsky bar. He performed compressive tests on specimens of aluminum and copper at elevated temperatures and over a range of strain rates extending to values exceeding 10^3 s^{-1} . In his tests the impact at the end of the loading bar was provided by means of a sawed-off anti-aircraft gun. Needless to say, large deformations were achieved, attaining values of true strain greater than 50%. Samanta presents stress-strain curves for the two metals; these show an initial work-hardening region followed, at all temperatures and strain rates, by continued straining with no apparent further increase in flow stress. For aluminum the stabilized flow stress occurs at about 40% strain and for copper nearer to 30% or even 20%. Samanta then analyzes the results by plotting the stabilized value of flow stress as a function of strain rate. For aluminum, the stress is a linear function of the logarithm of strain rate, in accordance with Equation 32. For copper, better agreement is obtained with Equation 34. This is in agreement with the work mentioned above of Sellars and Tegart and of Bailey et al. (References 101 and 133). Thus Equation 34 seems to represent quite well large strain behavior of copper. For aluminum, Samanta and Hockett (References 132 and 102) seem to prefer the semi-logarithmic relation, (Equation 32) while Bailey et al. and Sellars and Tegart (References 101 and 133) find closer agreement with Equation 34.

b. Strain Rates Greater than 10^3 s^{-1}

A number of investigators have attained strain rates in the range 10^3 s^{-1} to 10^4 s^{-1} . One purpose of these tests is to determine whether in that range there is not a change in the form of the dependence of flow stress on strain rate. Such a change might imply that the dominant deformation mechanism was one of viscous resistance to the motion of dislocations rather than a thermally-activated deformation mechanism. As mentioned above, evidence to support this change in behavior had been

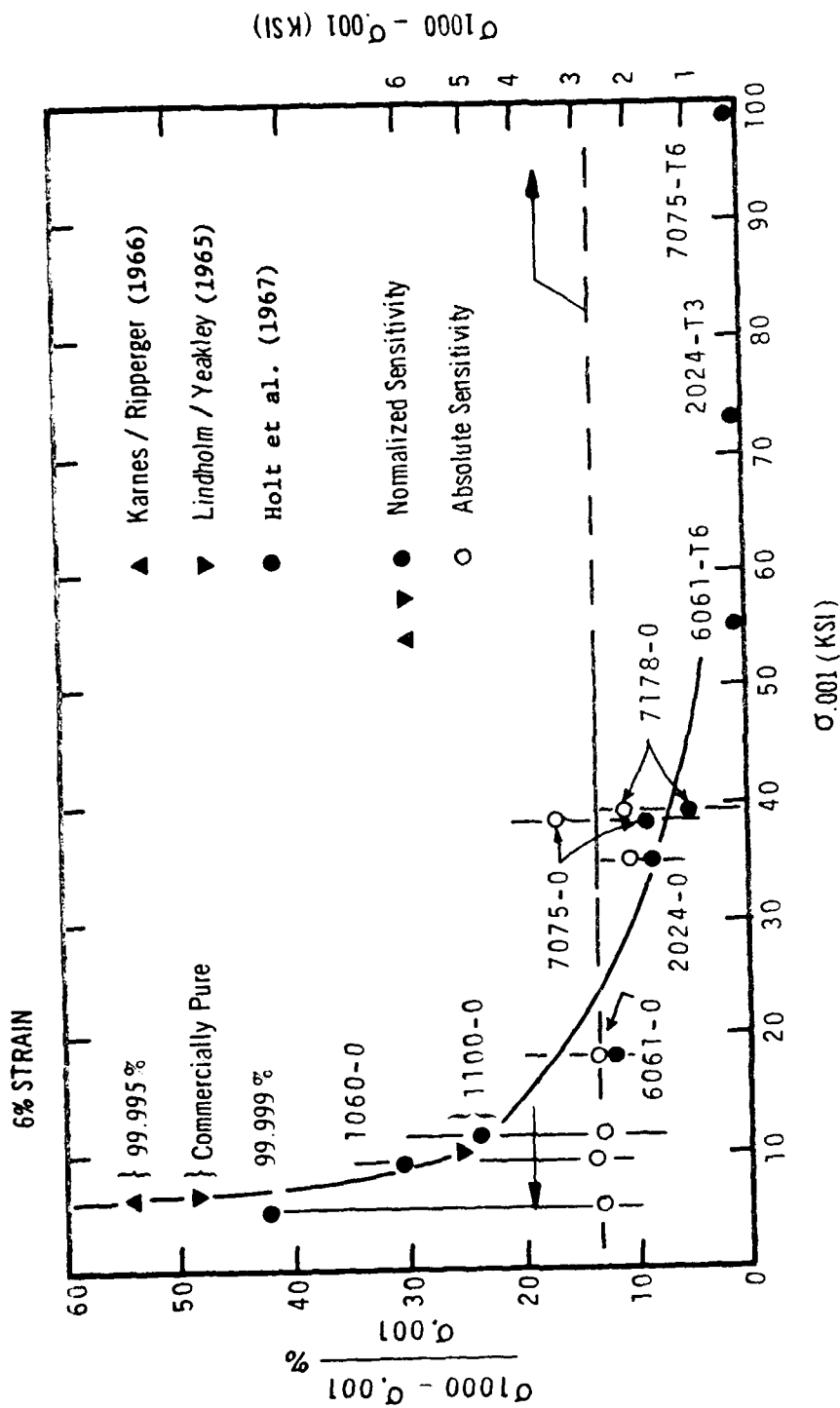


Figure 23. Strain Rate Sensitivity for Various Aluminum Alloys
 Flow Stress at $\dot{\epsilon} = 10^3 \text{ s}^{-1}$ (σ_{1000}) and $\dot{\epsilon} = 10^{-3} \text{ s}^{-1}$ ($\sigma_{.001}$)
 are Values at $\epsilon = 6\%$

seen in the results of the shear tests performed by Campbell and Ferguson (Reference 99) with a mild steel (Figure 14). Their results indicate a sharp upward turn in the curve flow stress as a function of $\log \dot{\gamma}$ for strain rates above $5 \cdot 10^3 \text{ s}^{-1}$. At these high strain rates the flow stress varies linearly with strain rate, implying a linear viscous deformation mechanism. A similar behavior had been seen by Kumar and Kumble, with OFHC copper specimens, by Ferguson et al. with aluminum single crystals, and by Edington with single crystals of copper. Edington employed specimens of two different length (References 134, 135 and 136). His long specimens had a length to diameter ratio of unity, while for the short specimens the length was reduced so the ratio was less than 0.2. Both the long and short specimens were used in tests at strain rates from the quasi-static to 10^3 s^{-1} . In this range the strain rate dependence is small for either length of specimen, although the shorter ones consistently showed a higher flow stress, presumably due to frictional effects and radial inertia. For strain rates above 10^3 s^{-1} only short specimens were tested. This is the region in which the flow stress increased much more rapidly with strain rate.

More recently, other groups of investigators have tested single crystals at strain rates above 10^3 s^{-1} and with similar results. Dormeal et al. and Stelly and Dormeal conducted tests on single crystals of high-purity copper (References 137 and 138). Their results show a dramatic increase in the strain rate sensitivity of copper at strain rates just exceeding 10^3 s^{-1} . They attribute this to a viscous damping mechanism, because the dependence of flow stress on strain rate becomes linear in this range. Dusek and Dusek et al. tested a number of materials: aluminum, copper, silicon and zinc, in the form of single crystals (References 139, 140 and 141). Their highest strain rate was 10^4 s^{-1} and in general they obtain a linear relation between flow stress and strain rate in the range 10^3 s^{-1} to 10^4 s^{-1} . Tanaka and Ogawa have investigated in detail the behavior of polycrystalline and single crystal specimens of high purity zinc over the temperature range -200C to 200C (References 142, 143 and 144). In dynamic tests they attain constant strain rates in compression of $6 \cdot 10^3 \text{ s}^{-1}$ by using a Kolsky bar. Their single crystals are oriented for deformation either by slip parallel to the basal plane or by twinning. In the former

case they show that the flow stress increases linearly with strain rate for rates in the range 10^3 s^{-1} to $6 \cdot 10^3 \text{ s}^{-1}$. A similar result had been seen by Ferguson et al. (1967b), although there is disagreement as to the temperature dependence of the viscosity coefficient.

Muller (Reference 145) investigated the plastic behavior of high purity polycrystalline specimens of iron and nickel at temperatures between 20°C and 500°C and at strain rates to 10^4 s^{-1} . His results show a linear dependence of stress on strain rate at all testing temperatures. He concludes also that his results are consistent with a viscous deformation mechanism for this range of strain rates. Wulf (Reference 114) modifies the Kolsky bar to test specimens in compression at strain rates in the range 10^3 s^{-1} to $25 \cdot 10^3 \text{ s}^{-1}$. He eliminates the incident bar and he strikes the specimen directly with a projectile fired from a gas gun. This projectile consists of a hardened steel rod 50 mm long and 12.5 mm in diameter. The specimen is mounted at the near end of a long transmitter bar, and the compressive stress in the specimen is measured as a function of time in the usual way by a pair of gages on opposite sides of the transmitter bar. Strain in the specimen is determined by monitoring the position of the back face of the projectile by means of a stationary coaxial capacitor through which the projectile slides during impact. The analysis does not account for the deformation of the loading bars but, since the true strains imposed on the specimen may be as great as 50 or 100%, this simplification would seem to be inconsequential. By eliminating the incident bar in Kolsky's experiment, the rise-time of the pulse can be made much shorter and the strain rates far greater. Wulf (Reference 114) first investigated the behavior of annealed 1045 aluminum, and OFHC copper and a 70/30 brass. In later work, he extended his studies to an aluminum alloy two steels and to titanium and two of its alloys (References 146, 147 and 148). In all these metals, for strain rates exceeding $\sim 10^3 \text{ s}^{-1}$, he found that the flow stress increases directly with strain rate; he attributes this to a viscous drag deformation mechanism. However, at a strain rate of about $12 \cdot 10^3 \text{ s}^{-1}$, Wulf finds a break in this dependence of flow stress on strain rate. For strain rates in the range 12 to $25 \cdot 10^3 \text{ s}^{-1}$ the functional relation apparently continues to be linear but at a much smaller slope, implying a change from one viscous mechanism to another.

An exception seems to be the hardened 4130 steel for which stress increases linearly with strain rate over the entire range. Wulf's experiments involve strains up to 100%. At strains of this magnitude, the friction conditions on the specimen's surfaces, as well as possible material instabilities, seem likely to create an inhomogeneous state of strain and strain rate. It is obvious that unless the strain distribution is uniform, or nearly so, measured values of stress and strain lose much of their significance. Wulf has used the inhomogeneities to advantage in order to observe shear bending in aluminum and titanium. A further difficulty in these tests, however, in view of the very high strain rates, lies in possible radial inertia effects. Qualitatively, Wulf's results appear consistent with those of Dharan and Hauser who tested specimens of a 99.999% purity aluminum at strain rates ranging up to 10^5 s^{-1} , but who limited their tests to a maximum strain of 20% (References 149 and 150). These investigators found a linear dependence of stress on strain rate up to a critical strain rate $\dot{\epsilon}_c$, whose value increased gradually with strain. They calculate a viscous drag coefficient of 3.0 kPa s at $\epsilon = 20\%$ and $\dot{\epsilon}_c \approx 13 \cdot 10^3 \text{ s}^{-1}$, as compared with Wulf's calculated value of 0.9 kPa s . Above this strain rate, the flow stress at first appears independent of strain rate and then for greater strain rates increases more and more rapidly so that at 10^5 s^{-1} it is about ten times greater than at 10^3 s^{-1} . Dharan and Hauser applied a correction factor to account for inertia effects.

Lindholm (Reference 151) has raised interesting questions relative to the behavior of materials at high strain rates. He conducted tests with an 1100-0 aluminum and with a high purity copper at strain rates from the quasi-static to 10^5 s^{-1} . When using the Kolsky bar he was careful to preserve a constant value of the length to diameter ratio for the specimen. As mentioned above, there is some latitude in the choice of this ratio before frictional and inertial effects or the effects of a non-homogeneous strain distribution become important. However, Lindholm preserves a constant ratio throughout his series of tests. He attains high highest rates by reducing the specimen length from 1.25 cm to 4 mm and simultaneously reducing the diameter of the Kolsky bars by the same ratio. The results for these two metals indicate no change to a viscous damping mechanism at the higher strain rates. Indeed, in the case of copper the flow stress remains almost insensitive to any change in

strain rate throughout the range 10^{-4} s^{-1} to 10^5 s^{-1} . This evidence contradicts the previous results and thus raises a serious question as to the nature of the strain rate dependence at strain rates above 10^3 s^{-1} and hence as to the dominant deformation mechanism in that range.

3. THE TORSIONAL KOLSKY BAR

The original reason for developing a torsional version of the Kolsky bar was to eliminate the transverse stresses due to radial inertia and friction that are present in axial loading. Today, this reason no longer seems as important since the results of torsional tests have been found consistent with those of axial. However, torsional loading has other advantages as described below.

A number of investigators have developed a torsional Kolsky bar, starting with Baker and Yew, Nicholas, Duffy et al., Lewis and Campbell, and Lewis and Goldsmith (References 76, 152, 153, 154 and 155). Either explosive charges or a stored torque can be used to initiate the pulse. The former has the advantage that it produces a shorter rise-time and the latter that it gives potentially larger strains. Generally, for torsional loading the wafer specimen used with the axial Kolsky bar is converted into a short thin-walled tube.

A schematic diagram of the torsional bar employed by Duffy et al. (Reference 153) is shown in Figure 24. The stress pulse is initiated by an impulsive torque applied at the top end of the bar (Figure 25). For this purpose two explosive charges are used, and it is essential that they provide equal impulses and be detonated simultaneously. The first requirement is met by employing equal weights of explosive and the second by using a single detonator connected to the explosive charges by means of "leaders" also made of the explosive. These leaders have equal lengths, and tests show that the explosive charges are detonated less than 0.1 microseconds apart. This method assures that the stress pulse initiated is almost entirely torsional, although some low amplitude axial and bending stress pulses are initiated as well. These are monitored in each test and are so small that generally they can be disregarded. However, a mechanical filter, resembling a rather stiff

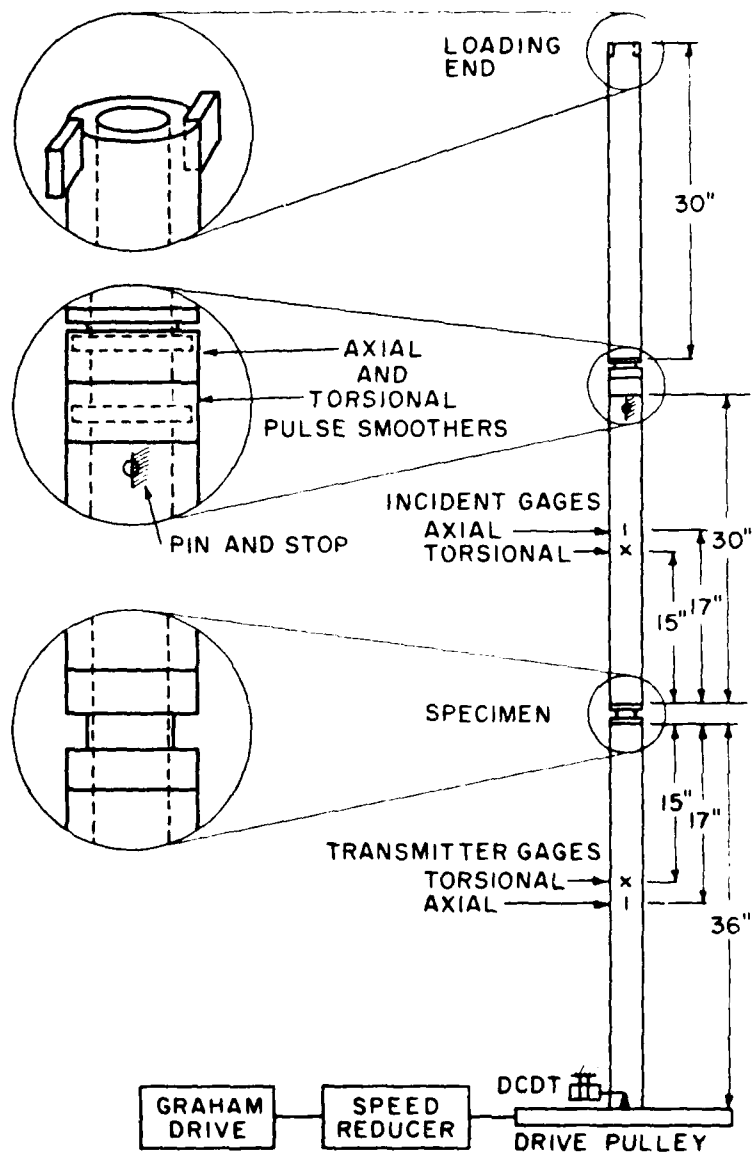


Figure 24. Schematic Diagram of Torsional Kolsky Bar

bellows, is used to decrease their magnitude further. This filter, shown at the top in Figure 26, is made of an aluminum alloy with a relatively high yield stress.

A second mechanical filter, at the bottom in Figure 26, is required in a torsional Kolsky bar for quite a different purpose. The pulse produced at the loading end by the explosion is neither "square" nor "smooth": its rise-time is short, as desired, but the amplitude of the main pulse varies considerably with time. This variation in amplitude is undesirable since it would result in loading the specimen at a variable strain rate. As explained above, this is not a problem in the axial Kolsky bar since the high frequency components of an axial pulse travel more slowly than the main pulse, so that an axial pulse is smoothed by geometric dispersion in propagating from the impact end of a bar to the specimen. No such smoothing occurs during the propagation of a torsional pulse because all frequency components travel at the same speed in torsional waves of the first mode. Consequently, a filter or pulse-smoother is needed. It consists essentially of a short length of tubing with a narrow neck made of 1100-0 aluminum so it deforms plastically during passage of the pulse. The presence of this filter reduces the magnitude of the higher frequency components thus smoothing the pulse. As shown in Figure 26, the two filters are placed next to each other in the Kolsky tube. It should be pointed out that the strain gages used to monitor the pulses incident on the specimen are located at stations between these filters and the specimen.

The specimen consists of a short length of tubing with a thin wall (Figure 27). During passage of the pulse the narrow section deforms plastically. Typical incident and reflected pulses are shown at the top of Figure 28. Also shown in this figure are the transmitted pulse and the stress-strain diagram; for the test shown the strain rate varies from about 810 s^{-1} to 850 s^{-1} . The same apparatus has also been used to test materials at low and elevated temperatures. As may be seen in Figure 24, it is equipped with a variable speed drive to allow testing of specimens with the same geometric configuration at quasi-static rates.



Figure 25. Loading End of Explosively Loaded Torsional Kolsky Bar

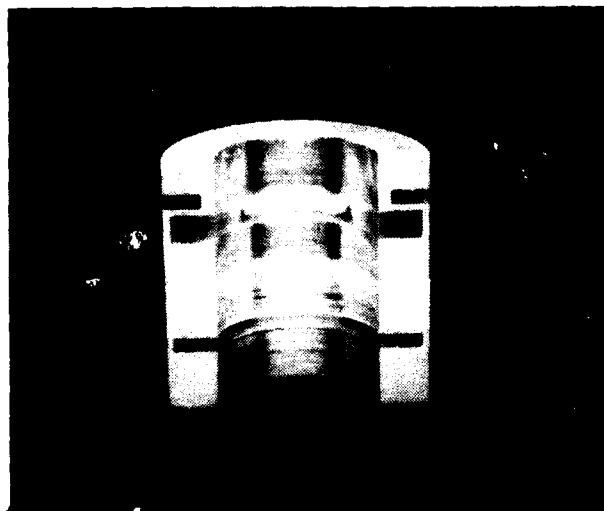
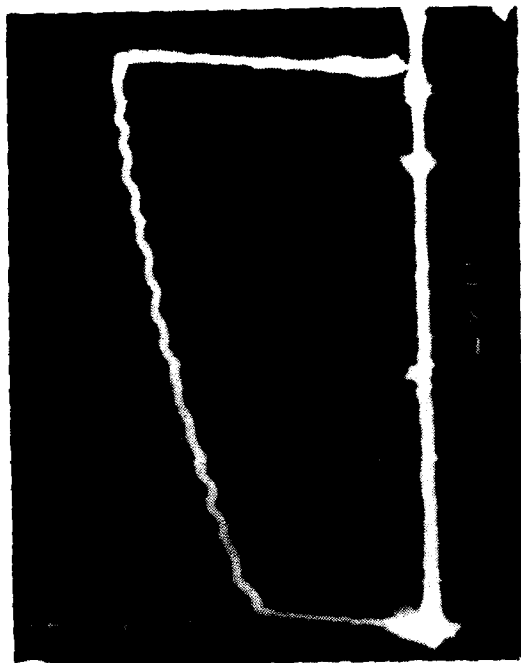


Figure 26. Section Through Axial Mechanical Filter (Top) and Torsional Pulse Smoother (Bottom) Used in Explosively Loaded Torsional Kolsky Bar



Figure 27. Specimens Used in the Torsional Kolsky Bar



(b)



(a)

Figure 28. Typical Oscilloscope Records Obtained With the Torsional Kolsky Bar
(a) Incident and Reflected Pulses (Upper Trace) and Transmitted Pulse (Lower Trace); (b) Stress Strain Curve

This drive is also used in incremental strain rate testing, as described in the next section.

Leung (Reference 156) presented a finite element analysis of the strain distribution within the wall thickness of the tubular specimen used with the torsional Kolsky bar. To represent material properties he took a bilinear elastic-plastic stress-strain relation with an elastic modulus and a plastic hardening rate approximately equal to those of commercially pure aluminum. His results show the growth of the plastic zone at various stages of deformation (Figure 29). In this figure, the dark areas represent the plastic zone. It starts at the reentrant corner between the thin-walled tube and the flange and from there spreads gradually throughout the thickness of the wall. Each diagram in the figure represents one quarter of the tube's cross-section plus the adjacent part of the flange; thus, the central axis of the specimen would lie below in each diagram, and because of symmetry only half of the length of the wall's cross-section is shown. The values of ϕ_0 are proportional to the applied torque. It can be seen that the growth of the plastic zone at first proceeds radially toward the inside wall surface then across the gage length along the outside surface of the specimen. Fortunately, the plastic zone remains contained until almost the whole specimen begins to flow. Leung's results are based on a static analysis but, since the wave length of the pulse is very much longer than the specimen, they can be applied to dynamic deformation and, indeed, seem to agree quite well with experimental results. Thus, the analysis shows a gradual spreading out of the plastic zone into the flanges. This effect is observed experimentally although not to quite as great an extent: at a final strain of 10%, aluminum specimens of the dimensions used by Leung show a plastic strain in the flanges which effectively increases the gage length by about 5% as measured on the inside surface of the specimen. It might be expected that a lower work-hardening rate would increase the danger of shear banding at the reentrant corners. Apparently, this is not always the case; the tests of Costin et al. (Reference 115) with cold-rolled steel, while they do produce shear bands, do not show such bands occurring at the reentrant corners.

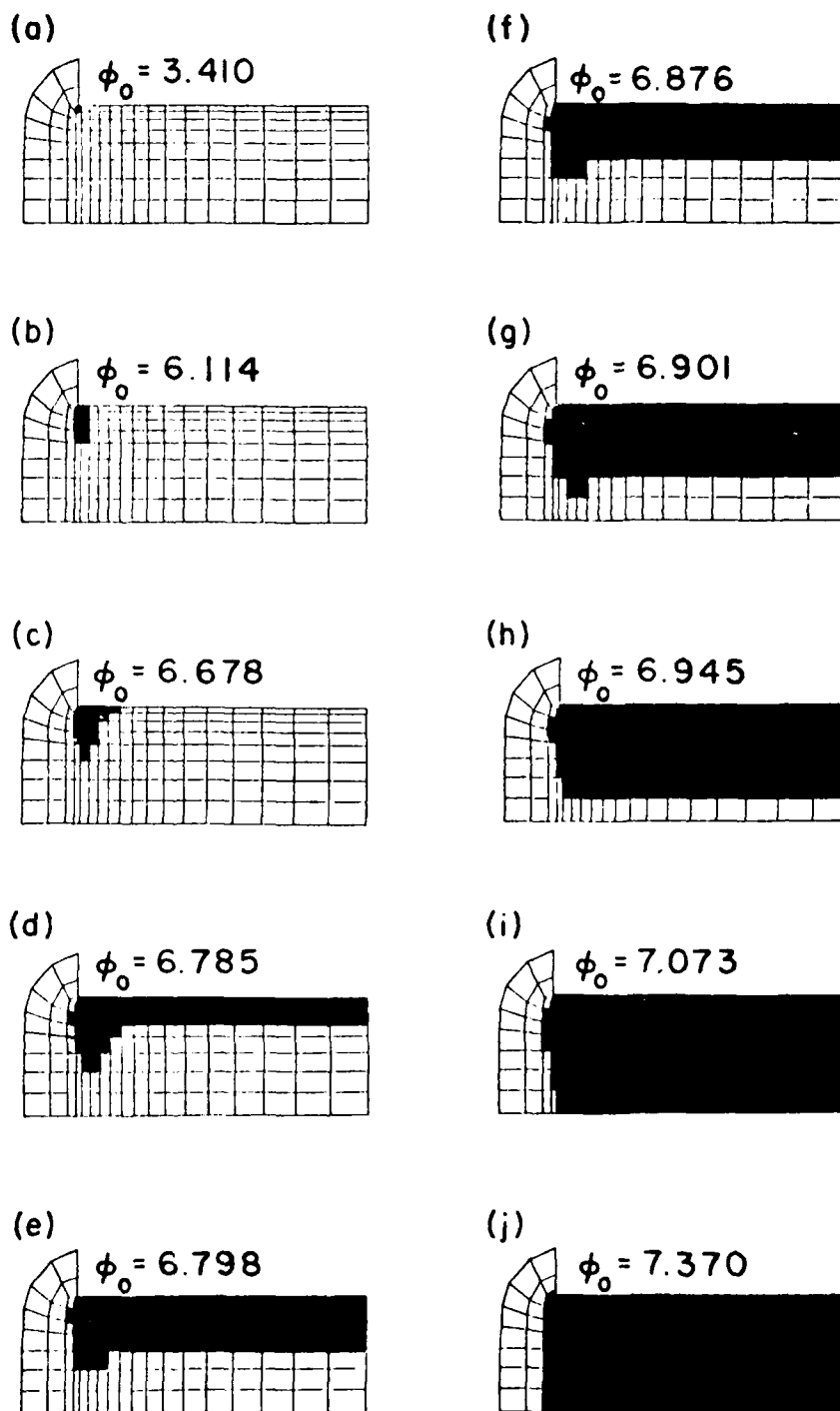


Figure 29. Results of a Finite Element Analysis Showing the Growth of the Plastic Zone Within the Tubular Specimen Used in the Torsional Kolsky Bar. Each Diagram Shows a Cross-Section Through Half the Length of the Tube's Wall, Plus the Adjacent Flange. The Plastic Zone is Represented by the Dark Area and the Applied Torque, $T = 2\pi\phi_0$.

In general, the torsional Kolsky bar is more difficult to construct than is the axial bar. Specimens are more expensive and it takes longer to perform a test. On the other hand, it is easier to adapt the torsional bar to testing at incremental strain rates and this is probably its main advantage. In addition due to the absence of geometric dispersion during pulse propagation in an elastic bar the rise-time of the pulse can be much shorter than with an axial bar: about eight microseconds in torsion as compared to 20 or 25 microseconds in an axial test. In practice, the eight microseconds has been achieved only with explosive loading, the stored-torque bar giving about 25 microseconds. The torsional bar also presents an advantage for tests at high temperatures. Since elastic resistance strain gages cannot be applied to a surface heated beyond a certain temperature, the gages usually cannot be placed near the heated specimen. For an axial bar, dispersion of the pulse then causes an error which, however, does not occur with the tapered torsional bar. Finally, under specialized conditions the torsional bar may prove useful where there may be an advantage to loading in shear, e.g., the testing of single crystals.

SECTION VII

HISTORY EFFECTS AND INCREMENTAL STRAIN RATE TESTS

It has long been known that the plastic behavior of metals is influenced by previous plastic flow and, generally, by the strain rate and temperature at which that flow occurred. The magnitude of these history effects depends among other factors on the particular material; and they can be made evident by experiments in which a rapid change in strain rate or in temperature is imposed during deformation. Experiments of this nature may involve either single crystals or polycrystals and until recently the strain rates imposed generally lay below the dynamic range. Figure 30 illustrates schematically the effects of a sudden increase in strain rate, or decrease in temperature, on the stress-strain curve of an fcc metal. (Similar results frequently are obtained whether one imposes a sharp increase in strain rate or a sharp decrease in temperature. However, as will be seen below, a sudden decrease in strain rate does not produce an immediate corresponding change in stress.) In the figure, the lowest curve represents the behavior observed during loading of the specimen at a relatively low constant strain rate, say $\dot{\gamma}_l = 10^{-4} \text{ s}^{-1}$, whereas the upper curve represents a high constant strain rate, say $\dot{\gamma}_r = 10^3 \text{ s}^{-1}$. An incremental test consists in loading initially at the low strain rate $\dot{\gamma}_l$ up to a specified strain $\dot{\gamma}_i$ at which point the strain rate is increased suddenly to the upper value $\dot{\gamma}_r$. The resulting stress-strain curve, at least for fcc metals, follows a path such as ABCD. On this path the line BC represents the instantaneous response of the specimen, and it is believed that with continued straining CD gradually attains the upper stress-strain curve. With the possible exception of steel, the behavior of bcc and hcp metals has not been investigated as thoroughly; it appears, however, that history effects in bcc metals may be quite different from those found in fcc metals as discussed later.

Incremental strain rate tests or incremental temperature tests of the type shown in Figure 30 are performed with either of two related purposes in mind:

- 1) To obtain evidence as to the current state of a material. In this case, tests are performed at a constant strain rate and the stress-strain behavior is compared to that found in an incremental test, typically the path ABCD in Figure 30. No test is required at the upper strain rate. Tests of this nature have been performed for many years, particularly with single crystals. Their purpose is to distinguish between the action of various microstructural deformation mechanisms. It is difficult to do this when testing is limited to constant strain rates and temperatures, since the deformation mechanisms occur simultaneously with steady or only slowly varying rates. In incremental tests, the changes in strain rate or temperature are presumed to occur "instantaneously," and hence with no change in the microstructural parameters.

- 2) To study the effect of strain rate or temperature history. In early investigations, this meant determining the applicability of an equation of state. In this instance, we require a test involving a rapid variation in strain rate (or temperature) and, for comparative purposes, tests at constant values of both strain rates (or temperatures). The precise method of comparison, however, is still a subject of active research as will be seen in the remainder of this section.

Historically, rapid changes in temperature were achieved in the laboratory before rapid changes in strain rate. This is probably because they are easier to effect since the range of temperatures required lies well within the capacity of most standard laboratory equipment. On the other hand, to produce a convincing demonstration of the effect of rapid changes in strain rate may require a change of six or seven orders of magnitude; this has not been possible until recent years for strain rates outside the creep or quasi-static range. The earliest incremental temperature tests are probably those of Zener and Holloman (Reference 159). Other early work in this area is that of Dorn et al., Trozera

et al., and Sylwestrowicz (References 157, 160 and 161). All of these investigators changed the temperature of the specimen rapidly during deformation and compared the results to those of constant temperature tests.

Zener and Holloman (Reference 159) for instance, conducted a series of investigations to determine whether the mechanical behavior of metals could be described by an equation of state. They limited their investigations to lower temperatures where the possibilities of grain growth, recovery and recrystallization are lessened, and adopted the equation

$$\dot{\epsilon} = \dot{\epsilon}(\epsilon, \sigma, T) \quad (42)$$

which contains the strain, ϵ , explicitly. Today, of course, plastic strain is considered a result of the history of loading rather than a state variable. Zener and Holloman conducted tensile tests on mild steel specimens in which they imposed a rapid temperature change during straining. The resulting stress-strain curves, Figure 31, show that if the temperature is lowered rapidly from the ambient to -77°C at a given strain during the test, then the flow stress jumps to the same value of stress as is obtained at the same strain for a similar specimen tested entirely at -77°C , i.e. as would be predicted by an equation of state. This seemed to confirm the applicability of an equation of state to plastic deformation. Zener and Holloman went further and suggested that a single parameter, P , determined the dependence of stress on strain rate and on temperature and proposed that

$$P = \dot{\epsilon} \exp Q/RT \quad (43)$$

where Q is the activation energy and R is the gas constant. In other words, rewriting Equation 42 by solving for stress would give

$$\sigma = \sigma(\dot{\epsilon}, P) \quad (44)$$

so that stress is not a function of three independent variables, since $\dot{\epsilon}$ and T are no longer independent of each other. Unfortunately, later work, e.g.

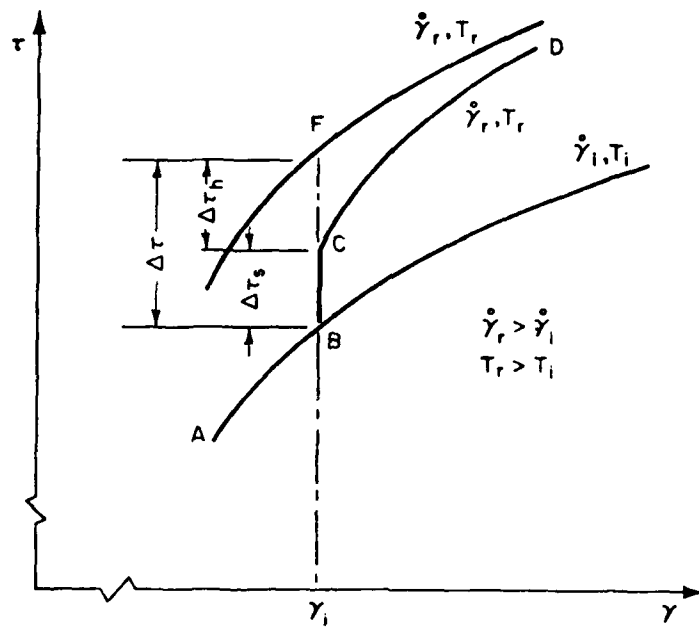


Figure 30. Schematic Representation of the Effect of Rapid Changes in Strain Rate or Temperature on Flow Stress for fcc Metals

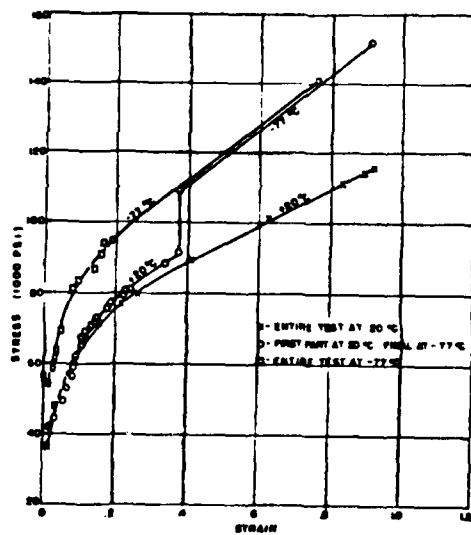


Figure 31. Effect of Rapid Change in Temperature During Loading of Mild Steel

Trozero et al. (Reference 157) showed that an equation of state of the above form is not applicable for most metals. Temperature history and strain rate history effects will influence the subsequent stress-strain behavior. Trozero et al. attempted to take into account these history effects by making a small change in Zener and Holloman's formulation. They preserved the Zener-Holloman parameter in the form

$$Z = \dot{\epsilon} \exp \Delta H/RT \quad (45)$$

where ΔH is an activation enthalpy, but with the stress given by

$$\sigma = \sigma(\epsilon) \quad (46)$$

a formulation identical with that of Zener and Holloman's only if ΔH is constant. Trozero et al. performed experiments in tension with specimens of a high purity aluminum. Their results, Figure 32, covered strain rates in the range from 10^{-6} s^{-1} to 0.17 s^{-1} and temperatures from -295°C to 445°C . Their stress-strain curves show an apparent coincidence, in that they can all be made to lie one upon another by changing the stress scale appropriately. This means that any particular curve can be duplicated by an increase (decrease) in $\dot{\epsilon}$ if it is accompanied by a decrease (increase) of the right magnitude in T . The authors conclude that the same microstructural state can be obtained by loading along alternative strain rate and temperature paths. They found, furthermore, that the value of ΔH is constant only for the lowest stress-strain curves; for high stresses it drops off sharply. As indicated by Wiedersich (Reference 158) in the discussion of this paper, if σ is plotted as a function of T , then the resulting curves are approximately linear and, if the deformation can be described by a thermally activated mechanism, the constitutive equation becomes

$$\sigma = B(\epsilon)(1 - T/T_{cr}) + C \quad (47)$$

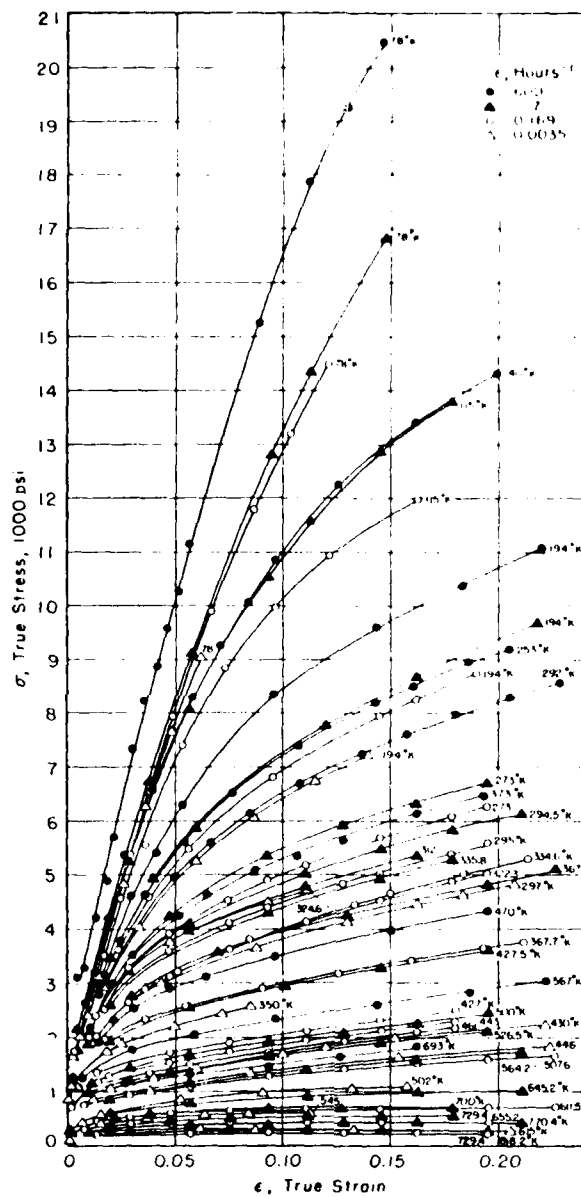


Figure 32. Stress-Strain Curves for High Purity Aluminum at Various Strain Rates and Temperatures

This equation is similar to the one proposed by Bell, Equation 31, with one important difference: T_{Cr} is now a function of strain rate.

It does not appear that the ideas of Trozera et al. have been pursued by other investigators except for applications in which the temperature exceeds $\frac{1}{2} T_m$, as in hot-forming, see for instance Barraclough and Sellars (Reference 162). However, the principal point made by Trozera et al. seemed by then to be accepted: namely, that current response depends upon history, i.e. upon the strain rate and temperature imposed during the previous loading. As a result, an equation of state cannot be used to describe material behavior. This last statement is now being modified by some investigators to say that an equation of state of the form

$$f(\sigma, \dot{\epsilon}, T) = 0 \quad (48)$$

cannot be used, but that the addition of microstructural parameters, α_i , leads to a new form of the equation which can be employed to represent material behavior. Thus one obtains

$$f(\sigma, \dot{\epsilon}, T, \alpha_i) = 0 \quad (49)$$

where i might be one or many. This equation is then viewed as an equation of state in the sense that the history of temperature and of strain rate determine the present microstructure, and that the present microstructure as specified by the α_i determines mechanical response. In particular, Hart (Reference 163) proposes an equation of state of the form

$$\sigma = \sigma(y, \dot{\epsilon}) \quad (50)$$

where $\dot{\epsilon}$ is the plastic strain rate and where y is a parameter representing the hardness state; here the word hardness refers to the work-hardening state. Operationally, in Hart's formulation the hardness at any point of a stress-strain curve is obtained by a load relaxation test effected after loading the material to the desired strain.

Dorn et al. (Reference 160) in their investigation as to the existence of an equation of state, assumed an equation of the form

$$\sigma = \sigma(\epsilon, \dot{\epsilon}, T) \quad (51)$$

where ϵ represents true strain. They conducted a series of experiments involving temperature increments. Their criterion to determine whether or not an equation of state exists is illustrated in Figure 33. A series of three tests is made all at the same strain rate. In the figure the stress-strain curve indicated by A is the result of a test at temperature T_1 , curve B is obtained at temperature T_2 , where $T_1 < T_2$, and finally a test is conducted which starts at T_2 up to a strain ϵ_1 , where the temperature is dropped rapidly to T_1 . If the stress-strain curve in this last test rejoins curve A, and does this with no lag in strain, then Equation 51 is an equation of state for the material, otherwise it is not. The experiments were performed in tension, initially on commercially pure aluminum, and the results show that the criterion for an equation of state is not met (Figure 33). Dorn et al. performed additional experiments with high purity aluminum, copper and stainless steel, with the same qualitative results. They conclude that "The flow stress for plastic deformation of metals is not a simple function of the instantaneous values of the strain, strain rate and temperature; it is sensitive to the entire thermal-mechanical history."

1. EARLY RESULTS AND INVESTIGATIONS WITH FCC METALS

The first study of strain rate history effects in the dynamic range of strain rates is that of Lindholm (Reference 53). He performed interrupted tests, in which complete unloading of the specimen precedes reloading at the new strain rate. Employing specimens of a high purity aluminum at room temperature, Lindholm imposed alternately a quasi-static strain rate, $\dot{\epsilon} \approx 10^{-4} \text{ s}^{-1}$, and a dynamic strain rate, $\dot{\epsilon} \approx 10^3 \text{ s}^{-1}$. His results are shown in Figures 34 and 35, where the solid lines are the actual loading paths. In Figure 34, initial loading from the annealed condition is done quasi-statically, while in Figure 35, it is dynamic. The dotted lines in the figure represent the stress-strain relations that would obtain for loading entirely at the

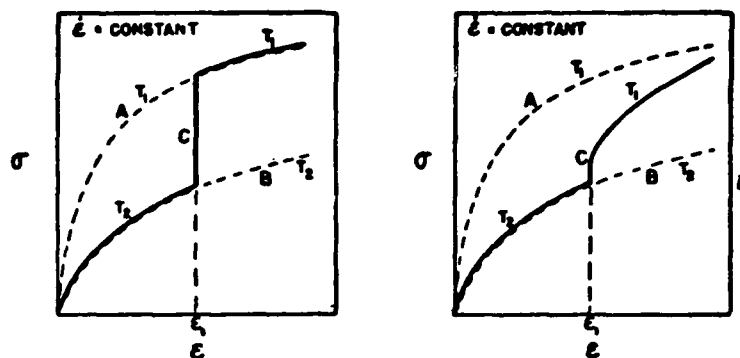


Figure 33. Criterion for Existence of Equation of State

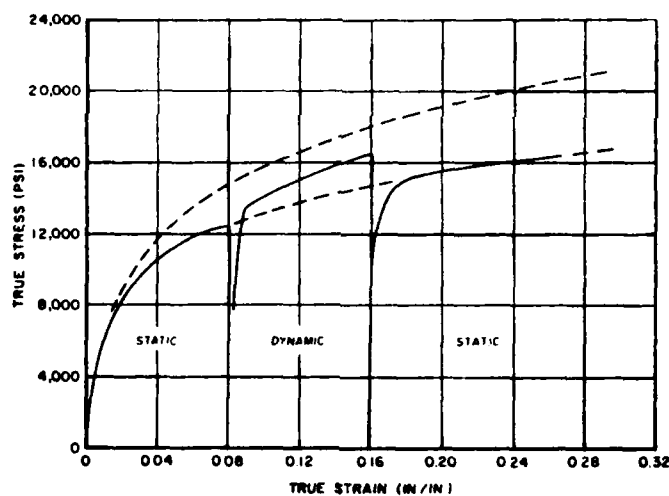


Figure 34. Cyclic Static-Dynamic-Static Loading for Aluminum.
Solid Lines are the Actual Loading Paths

quasi-static or at the dynamic rate. If the material behavior were not sensitive to strain rate history then the solid line would coincide with one or the other of the dotted lines. As part of this study, Lindholm also performed tests in which the dwell time at zero load was three minutes and others in which it was 450 microseconds. This last was achieved by reloading the specimen with the reflected incident pulse. The results (Figure 36) indicate that the time interval at zero load is of considerable importance in the subsequent behavior: apparently some recovery occurs during the longer dwell time.

With the same purpose in mind, Yoshida and Nagata (Reference 164) performed interrupted strain rate tests in compression on high purity polycrystalline aluminum. For dynamic loading they employed a Kolsky bar and attained strain rates lying between 100 s^{-1} and 300 s^{-1} . Two series of tests were conducted; in one series the strain rate was decreased rapidly, in the other the strain rate was increased, but in either case complete unloading took place before a change in strain rate.

Klepaczko performed interrupted strain rate tests in torsion on tubular specimens of aluminum at five different values of strain rate ranging from $1.66 \cdot 10^{-5} \text{ s}^{-1}$ to a high rate of 0.624 s^{-1} (References 165 and 166). Just as in the preceding experiments, in order to effect the change in strain rate Klepaczko unloaded his specimens completely before resuming straining at the new rate. There were two series of interrupted tests: the first involving a drop from a high to a low strain rate and the second involving an increase in strain rate. Typical results for the two types of tests are shown respectively in Figures 37 and 38, which also show the results of test at the corresponding constant strain rates. Thus the upper stress-strain curve in Figure 37 is obtained in a test entirely at the high rate. Each interrupted strain rate test follows the same curve to a specified value of shear strain where unloading occurs. The curves for reloading at the quasi-static rate are shown, as well as the stress-strain curve obtained entirely at the lower rate. It is evident from these tests that there are two values of flow stress for straining at the lower rate, and that these two values depend on the

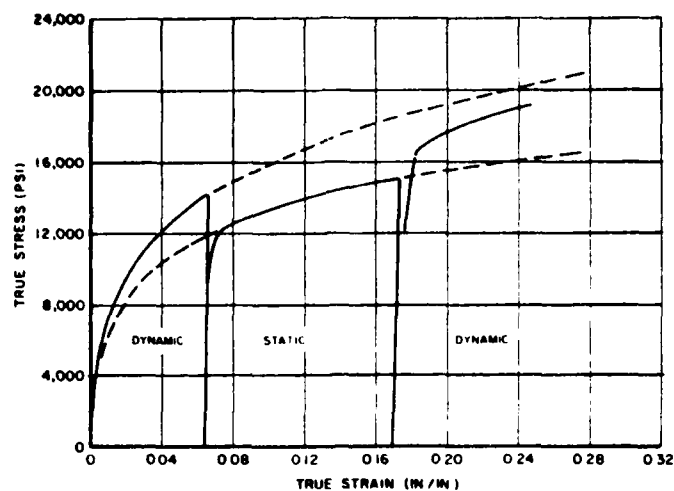


Figure 35. Cyclic Dynamic-Static-Dynamic Loading for Aluminum .
Solid Lines are Actual Loading Paths

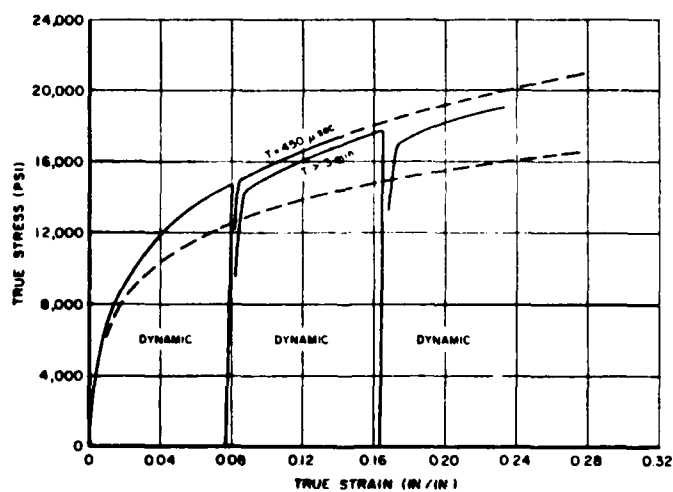


Figure 36. Cyclic Dynamic Loading for Aluminum Showing Effect of
Dwell Time Between Loading Cycles

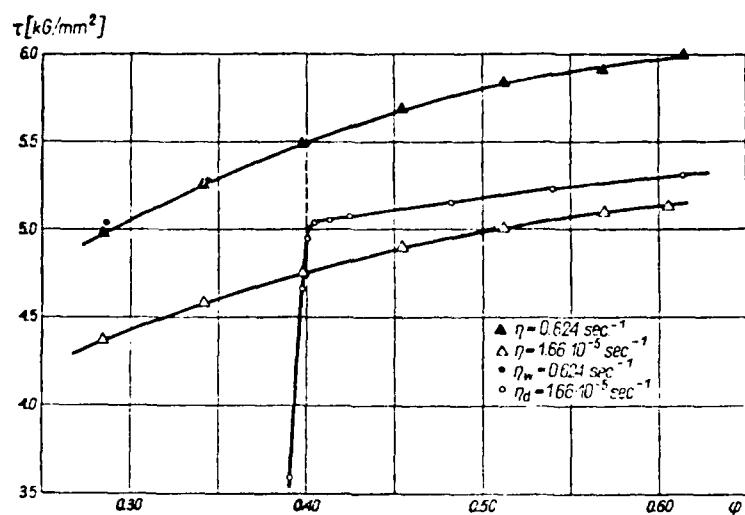


Figure 37. The Results of an Interrupted Strain Rate Test from a High to a Low Strain Rate for Aluminum

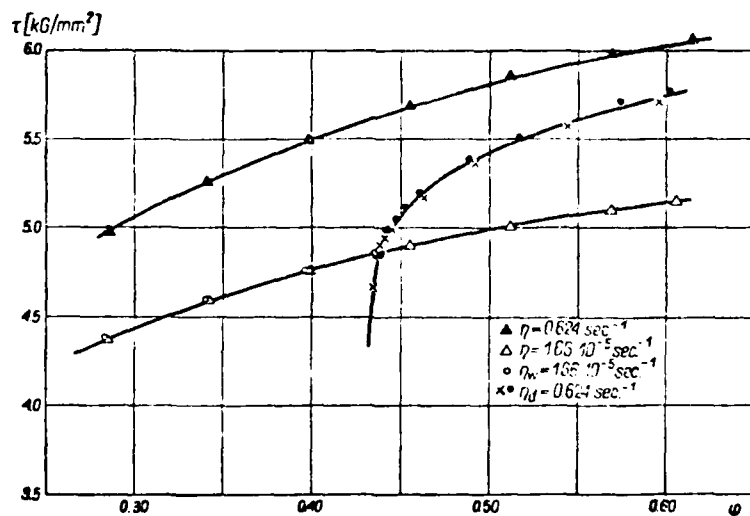


Figure 38. The Results of an Interrupted Strain Rate Test from a Low to a High Strain Rate for Aluminum

previous strain rate. This history or memory effect diminishes or fades with continued straining at the new strain rate. Similarly, Figure 38 show the results of a rapid increase in strain rate. Again a strain rate history effect is evident as well as a fading memory.

The first incremental strain rate tests involving no unloading during the change in strain rate are those of Campbell and Dowling (Reference 79). Since it includes wave propagation experiments, this investigation was cited in Section IV. The incremental strain rate experiments on short specimens, which formed part of this study, employed copper and aluminum specimens deformed at two strain rates, the higher rate being 90 s^{-1} . The conclusion drawn was that strain rate history influences the subsequent stress-strain curve.

Shirakashi and Usui (Reference 167) carried out an important study of strain rate effects which in many respects was ahead of its time. Unfortunately it was published in a Japanese journal seldom read in the Western World. Their work involved extensive interrupted experiments performed in compression with a Kolsky bar. Three fcc metals, namely, aluminum, α -brass, and copper were tested and a detailed analysis is presented. On the basis of their experimental results, they proposed a constitutive equation in which stress is represented by the product of three terms: one involving strain rate history, another representing the direct strain rate effect, and lastly a term involving temperature. Since their constitutive equation includes history effects, it applies to loading at variable strain rates. The equation they propose for the stress, σ , is given by

$$\sigma = A \left[\int_C (\dot{\epsilon} / \dot{\epsilon}_0)^{n_1} d\epsilon \right]^m (\dot{\epsilon} / \dot{\epsilon}_0)^n \exp \alpha / \theta \quad (52)$$

where A , m , n_1 , n , ϵ_0 , $\dot{\epsilon}_0$ and α represent material constants evaluated experimentally by the authors, θ is the temperature, and the integration in the history term follows the path C given by $\dot{\epsilon} = h(\epsilon)$. For instance, for deformation preceeding at a constant strain rate

$$\sigma = A_1 (\dot{\epsilon}/\dot{\epsilon}_0)^{n_0} (\epsilon/\epsilon_0)^m \exp \alpha/\theta \quad (53)$$

where $n_0 = mn_1 + n$, and $A_1 = A\epsilon_0^m$. In order to be able to vary total strain independently of strain rate, the authors placed a stop ring around the specimen to limit the total strain (Figure 39). Two series of tests were performed, one involving positive increments in strain rate, i.e., from a low to a higher strain rate, and the other involving negative increments (Figure 40). The latter were performed as follows: loading proceeded at a rapid strain rate, 10^3 s^{-1} up to a strain, $\epsilon_s = 0.5$, point B_0 in Figure 40(b). After reaching that point the specimen was unloaded completely and then reloaded quasi-statically (10^{-3} s^{-1}) to point B_1 in the figure; the authors designate the stress at that point as the equivalent static flow stress, σ_{ES} , at $\dot{\epsilon} = 10^3 \text{ s}^{-1}$. Similar tests following the same procedure are made for different values of ϵ_s , leading to a curve composed of points of the type B_1 , called the equivalent static flow curve. The authors' proposal is that a measure of history effects is provided by the difference in stress point B_1 and a point B_2 at the same value of strain but lying on the stress-strain curve obtained at the constant strain rate 10^{-3} s^{-1} . This is consistent with the understanding given above, e.g. (Figure 31). A series of curves for σ_{ES} at different value of $\dot{\epsilon}$ can be obtained and compared to the same quasi-static reference curve (Figure 41). Furthermore, their experimental results show that $\ln \sigma_{ES}/\sigma$ varies linearly with $\ln \dot{\epsilon}/\dot{\epsilon}_0$, so that

$$\sigma_{ES}/\sigma = B_1 (\dot{\epsilon}/\dot{\epsilon}_0)^{n_1} \quad (54)$$

where B_1 and n_1 are known constants, and ϵ_s is the strain on the reference curve at a strain rate of 10^{-3} s^{-1} . In addition, the results of their tests at constant rates indicate that

$$\sigma = A_1 (\epsilon/\epsilon_0)^m (\dot{\epsilon}/\dot{\epsilon}_0)^{n_0} \exp \alpha/\theta \quad (55)$$

where the constants are all evaluated on the basis of experimental results. It follows that

$$\sigma_{ES} = A_1 (\epsilon/\epsilon_0)^m (\dot{\epsilon}/\dot{\epsilon}_0)^{mn_1} \quad (56)$$

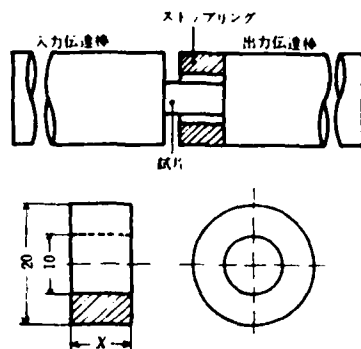


Figure 39. Stopping Ring and Its Location in the Kolsky Bar

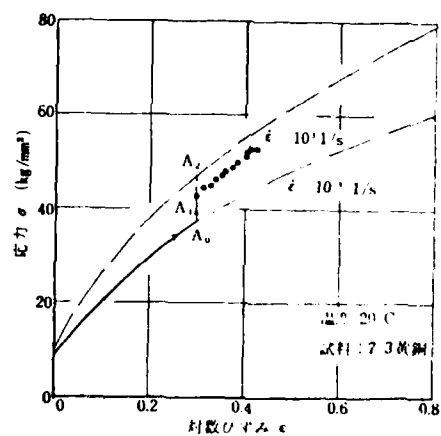


図 1 (a) 変形途中で歪み速度が増した場合の応力・歪みの関係

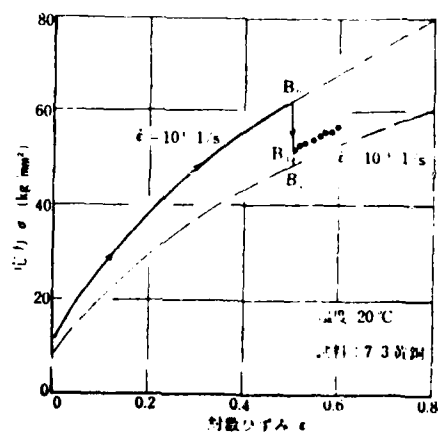


Figure 40. Results of Incremental Strain Tests in α Brass.
(a) Increase in Strain Rate (b) Decrease in Strain Rate

Differentiation of the last equation gives

$$\frac{d\sigma_{ES}}{d\epsilon} = \frac{m\Lambda_1}{\epsilon_o} (\epsilon/\epsilon_o)^{m-1} (\dot{\epsilon}/\dot{\epsilon}_o)^{mn-1} = \frac{m\Lambda_1}{\epsilon_o} (\dot{\epsilon}/\dot{\epsilon}_o)^{n_1} \sigma_{ES}^{(1-1/m)} \quad (57)$$

where for a given history of strain rate, $\dot{\epsilon} = h(\epsilon)$, results in

$$\sigma_{ES} = \frac{\Lambda_1}{\epsilon_o^m} \left[\int_C (\dot{\epsilon}/\dot{\epsilon}_o)^{n_1} d\epsilon \right]^m \quad (58)$$

Equation 58, when combined with Equation 55 leads to Shirakashi and Usui's constitutive relation, Equation 52, for loading at a variable strain rate. Tests in which a positive strain rate increment is imposed are used as a check. Clearly, this analysis requires a large number of tests of high precision in order to have sufficiently dependable data for the various curves. Shirakashi and Usui collected large quantities of data for all three metals at a large number of different strain rates. They also performed numerous incremental strain rate tests, and on the basis of all these results they evaluated the parameters in their equations. The approach of Shirakashi and Usui seems most promising. It would now be of value to check their results with different, and perhaps somewhat more complicated histories of strain rate. It would also be of value to see whether the same or similar results could be obtained on the basis of experiments in which the increment in strain rate is imposed without unloading the specimen.

Frantz and Duffy (Reference 54) performed incremental strain rate experiments with the torsional Kolsky bar using an explosive charge to initiate the pulse (Figure 24). By this means the rise-time can be made as brief as 8 or 10 microseconds for a test at a constant strain rate, while in the incremental test the rise-time is only about 4 microseconds. During the quasi-static portion of an incremental test, the entire length of the Kolsky bar up to the pin-stop is twisted slowly and the specimen is strained to any desired value of shear strain. At that point, the explosive charges are detonated initiating the torsional pulse which superposes additional strain at a higher strain rate, thus effectively changing the strain rate, thus effectively changing the strain rate from about 10^{-4} s^{-1} to 10^3 s^{-1} . In incremental strain rate

tests of this nature, the Kolsky bar provides an important advantage: the transmitted signal furnishes a measure not of the total stress in the specimen but of the excess stress imposed by the stress pulse above the existing as a result of loading at the quasi-static strain rate. Thus one obtains directly the stress increment due to the sudden change in strain rate rather than having to depend on finding a small difference between two large numbers. A typical oscillograph record of the stress-strain relation is shown in Figure 42, in which the origin represents the maximum static stress, τ_s , and the maximum static strain, γ_s , just before the strain rate is increased to its dynamic value.

The results of Frantz and Duffy for polycrystalline 1100-0 aluminum are shown in Figure 43. It is evident that a sharp increment in strain rate raises the flow stress rapidly from its quasi-static value. The increment in flow stress, however, is not large enough to make the new value of flow stress immediately equal to that of a like specimen strained entirely at the higher strain rate. However, as straining continues at the new rate, the flow stress does tend to approach the value it would have if the entire test were performed at this rapid strain rate. Thus the effects of strain rate history apparently are erased with additional strain.

Klepaczko (Reference 168) presented an analysis of strain rate and history effects based on a thermally activated mechanism of deformation. His ideas can be explained more simply by referring back to Figure 30, which shows schematically the stress-strain curves obtained in three tests on similar specimens. The significance of the incremental test lies in the fact that $\Delta\tau_s$ provides a truer measure of the strain rate effect at that strain than does $\Delta\tau$, which also includes a history effect, represented by $\Delta\tau_h$. Klepaczko presumes that the change in strain rate, $\dot{\gamma}_i$ to $\dot{\gamma}_r$, occurs rapidly enough so there is essentially no change in microstructure during the stress increment $\Delta\tau_s$ see also (Reference 169). On the other hand, $\Delta\tau_h$ is a reflection of the difference in the microstructures occurring at the same strain γ_i , due to the different strain rate histories. Klepaczko then assumes that the deformation at the higher strain rate $\dot{\gamma}_r$ occurs so rapidly that there is not enough time

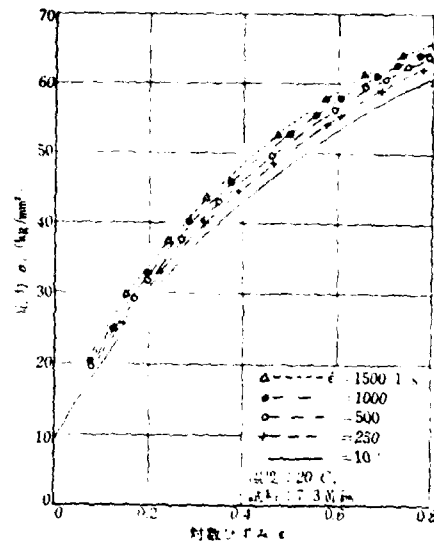


Figure 41. Equivalent Static Flow Curves for Different Strain Rates for α Brass

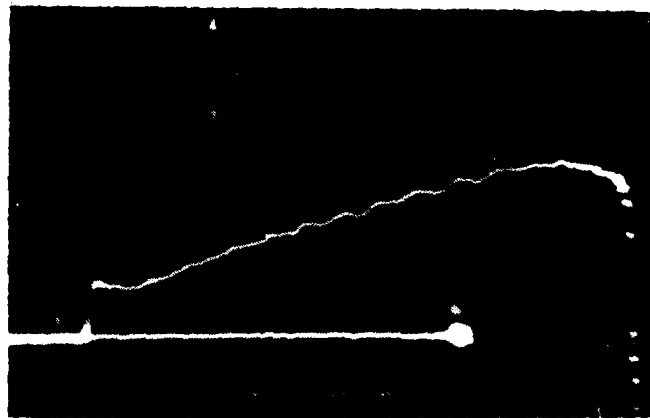


Figure 42. Oscilloscope Record of Dynamic Portion of Incremental Strain Rate Test. Vertical Deflection Represents Excess Stress τ_s , the Maximum Static Stress. Horizontal Deflection Represents Excess Strain Over γ_s

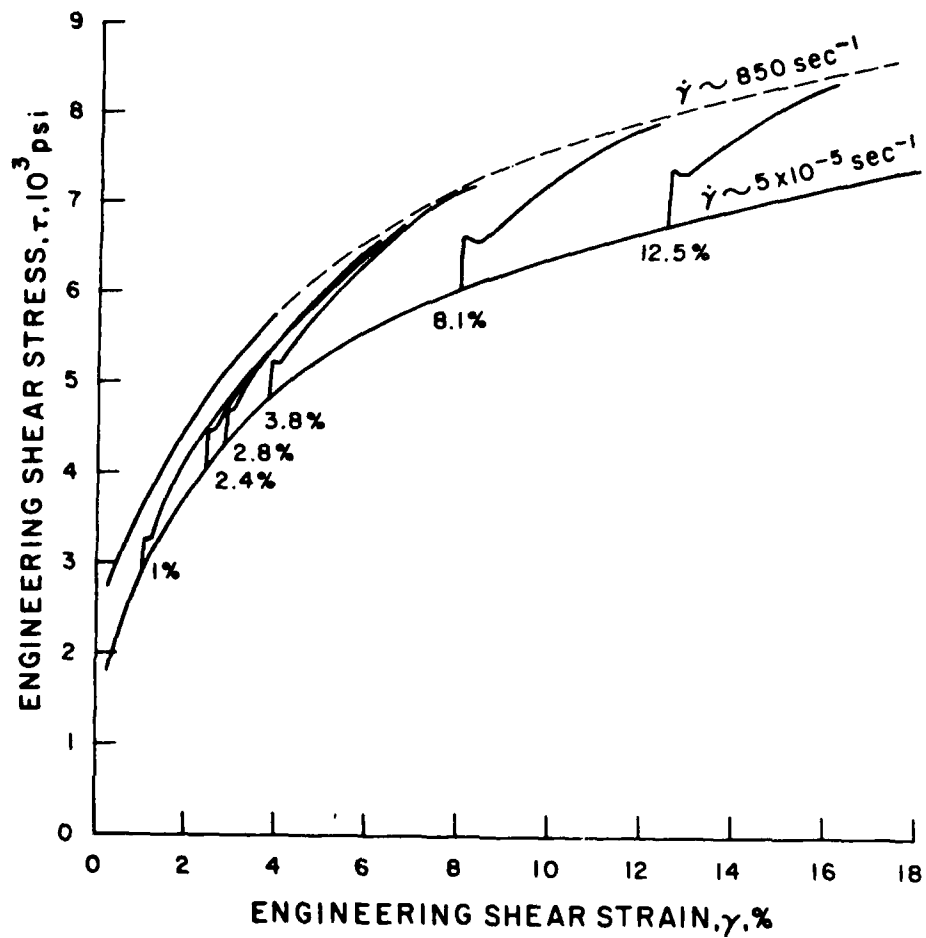


Figure 43. Behavior of 1100-0 Aluminum Under Static Dynamic and Incremental Strain-Rate Loading in Shear.

Strain Rate Changes from $5 \times 10^{-5} \text{ s}^{-1}$ to 850 s^{-1} in all Incremental Rate Tests.

for relaxation processes to occur, whereas at $\dot{\epsilon}_f$ the flow stress level is due to a combination of two competing processes: work-hardening and recovery. By taking a simple thermally-activated mechanism for flow and presuming that recovery is linear in accumulated strain, Klepaczko is able to estimate the density of dislocations annihilated during recovery. He shows that for aluminum and copper the results are close to those found by measurement in an electronic microscope. He followed up this work with a later paper, Klepaczko et al. (Reference 170) in which results of experimental performed on lead by R. A. Frantz are presented (Figure 44). Klepaczko's analysis shows that recovery processes are most important in lead tested quasi-statically at room temperature than they are for aluminum or copper.

Glenn and Bradley performed interrupted strain rate tests, obtaining results qualitatively similar to those of Lindholm and Klepaczko (Reference 53, 165, 166, and 171). However, Glenn and Bradley used OFHC copper as the specimen material and, more important, they reversed the sequence of strain rates in loading so that their specimens were first compressed dynamically and then reloaded quasi-statically, with full unloading preceding the quasi-static deformation. The strain rate sensitivity which they observed agrees very well with the previous results of Lindholm, though they give a dynamic flow stress somewhat greater than that of Green et al. (References 53 and 131). Their explanation, to account for the increase in flow stress generally observed with an increase in strain rate, is that higher strain rates generate a larger number of dislocations which, however, move on the average over shorter distances. In support of this explanation, they cite observations with the electron microscope performed by Korbel and Swiatkowski (Reference 172) with polycrystalline aluminum at strain rates of $6 \cdot 10^{-6} \text{ s}^{-1}$ to about 70 s^{-1} . The TEM photographs presented by these investigators show a rather dramatic difference in the dislocation structure between specimens tested quasi-statically and dynamically. Their significance is discussed later in this section under subsection C.

2. INVESTIGATIONS WITH BCC AND HCP METALS

Far fewer experiments have been conducted into history effects at dynamic strain rates for bcc and hcp metals than for the fcc metals.

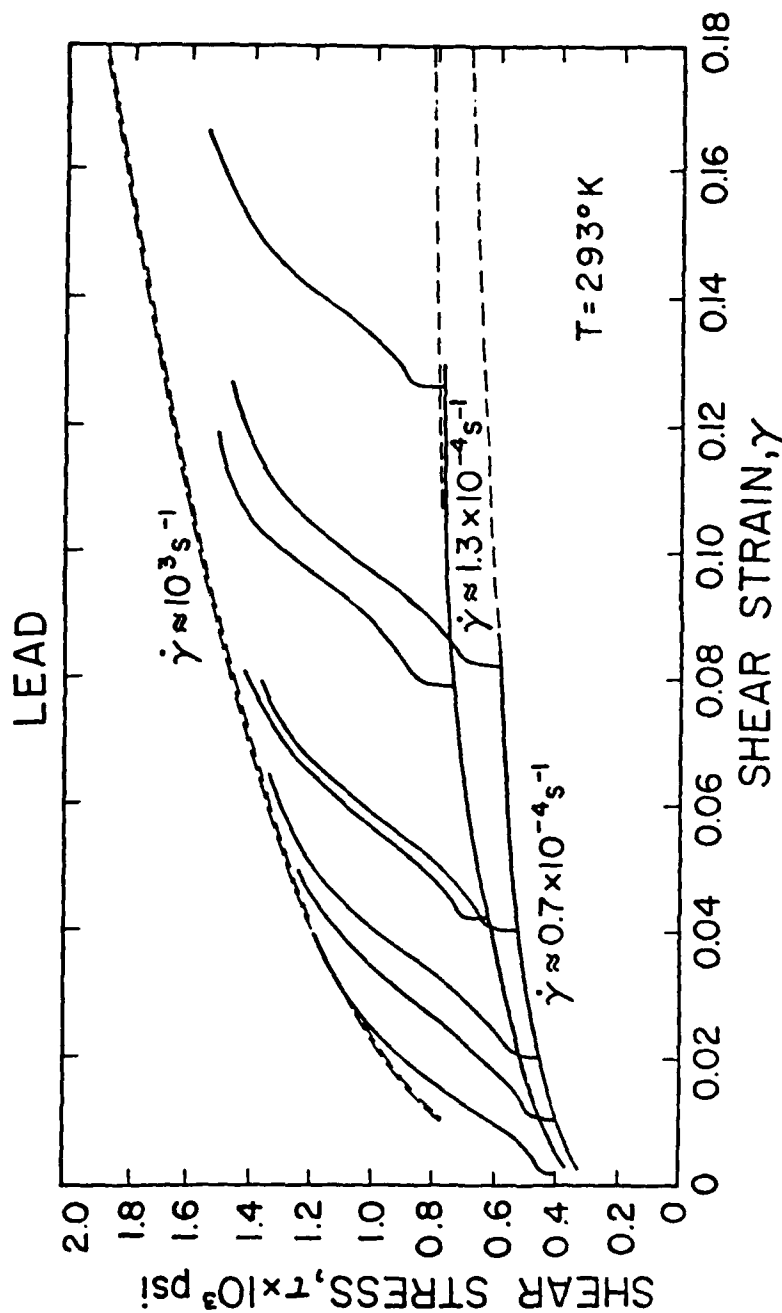


Figure 44. Behavior of 99.99% Pure Lead in Shear Under a Constant Low Strain Rate, a Constant High Strain Rate and Under Incremental Loading from $\dot{\gamma}_i = 0.7 \times 10^{-4} \text{ s}^{-1}$ and $\gamma_i = 1.3 \times 10^{-4} \text{ s}^{-1}$ to $\dot{\gamma}_r \approx 10^3 \text{ s}^{-1}$

The one exception perhaps is steel. It has been found that the yield and the flow stress of iron and steel depend quite strongly on strain rate. Furthermore, temperature and strain rate history effects can be quite large. This is not unexpected since iron and steel are readily subject to strain ageing effects due mainly to the presence of carbon and nitrogen as interstitial solutes. Their high diffusion rates account for the marked strain ageing seen in steels even at relatively low temperatures. In particular, dynamic strain ageing implies that the yield or flow stress will be greater after a prestrain than in the unstrained material and thus is in itself a history effect. At low strain rates, strain ageing can also produce a negative strain rate effect, as was demonstrated by MacGregor and Fisher (Reference 173) with AISI 1020 hot-rolled steel deformed in the strain rate range $5 \cdot 10^{-5} \text{ s}^{-1}$ to $5 \cdot 10^{-3} \text{ s}^{-1}$. In addition, strain ageing can be made evident by the presence of a relative maximum in the curve of flow stress as a function of temperature, for a particular value of strain. Manjoine (Reference 174) showed that the temperature at which this relative maximum occurs is strain rate dependent: for a strain rate of $8.5 \cdot 10^{-4} \text{ s}^{-1}$ it occurs at about 250°C at 300 s^{-1} it occurs at 550°C . This strain rate dependence can be explained on the basis of dislocation motion since a sufficiently high strain rate forces the dislocations to travel faster than impurities can travel at that temperature.

The first study of strain rate history effects that includes bcc and hcp metals was presented by Nicholas (Reference 152). The tests were performed in torsion on thin tubular specimens using a pneumatic drive to attain a maximum strain rate of 25 s^{-1} . The metals tested were 1100-0 aluminum, 1020 hot-rolled steel and 50A titanium. For the last two of these, a comparison was made between the flow stress obtained at the constant dynamic rate with that found in incremental strain rate tests. These results (Figure 45 and 46) indicate that the flow stress for these two metals is sensitive to strain rate but not particularly sensitive to strain rate history. Later work seems to show that history effects are not significant in the deformation of titanium but of great importance in steel, except perhaps at room temperature. Although, the values of flow stress found for mild steel vary considerably from one investigation to another, the strain rate sensitivity found by Nicholas agrees closely with that found later by Costin et al. (Reference 115).

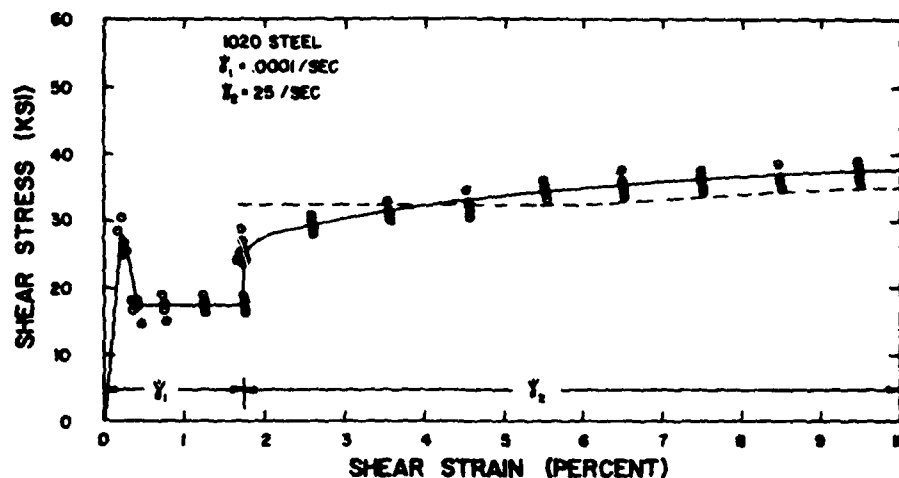


Figure 45. Results of Incremental Strain-Rate Test Without Unloading for 1020 Steel

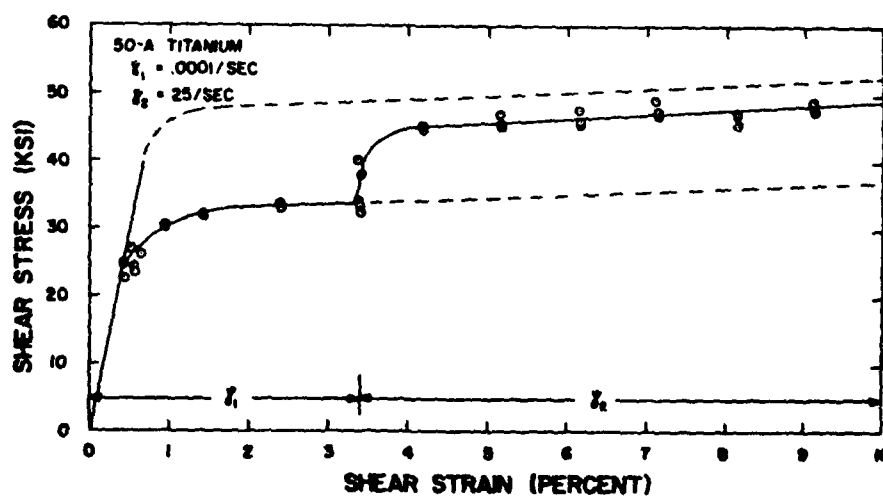


Figure 46. Results of Incremental Strain-Rate Test Without Unloading for 50-A Titanium

At about this time, Campbell initiated a most interesting series of experiments on history effects and their relation to crystallographic structure. On the basis of constant strain rate experiments with niobium and molybdenum, Briggs and Campbell (Reference 175) had suspected that history effects in bcc metals would be quite different from those seen in fcc metals. Accordingly, a series of incremental strain rate tests was undertaken: the first were performed with niobium and molybdenum, Campbell and Briggs followed by tests on copper and titanium, Eleiche and Campbell, and later tests with steel and other metals (References 176 and 177). In the experiments on niobium and molybdenum, strain rate increments were imposed during deformation at low and intermediate strain rates. The results for molybdenum are shown in Figure 47. It may be seen that when the strain rate is increased from $1.7 \cdot 10^{-4} \text{ s}^{-1}$ to $8.3 \cdot 10^{-3} \text{ s}^{-1}$, the results appear similar to those reported for aluminum, copper, etc., that is, the increment in stress raises the total stress level to a value less than the flow stress obtained in an all dynamic test at the higher strain rate. On the other hand, if the strain rate increment is from 0.51 s^{-1} to 4.25 s^{-1} then the total stress exceeds the value found in the all-dynamic test at 4.25 s^{-1} . Campbell and Briggs suggested that different deformation mechanisms may be dominant within different ranges of strain rates for bcc metals. As additional evidence, they cited the incremental strain rate experiments of Nicholas (Reference 152), described above, who had shown that the flow stress of steel following a quasi-static prestrain lies somewhat above the all-dynamic stress level; however, the overshoot occurs only after some additional straining at the dynamic rate.

Further evidence as to the presence of history effects during the deformation of bcc metals was provided by Harding (Reference 178). Using specimens of annealed high-purity iron, he showed that the dynamic flow stress following a small quasi-static prestrain is greater than the flow stress in an all-dynamic test at the same strain rate. His results are shown in Figure 48, where curve A represents the interrupted test. The initial prestrain of 1.6% is imposed at a strain rate of 10^{-3} s^{-1} , followed by continued deformation at about 10^3 s^{-1} . For curve B, the strain rate remains constant at about 10^3 s^{-1} throughout the test.

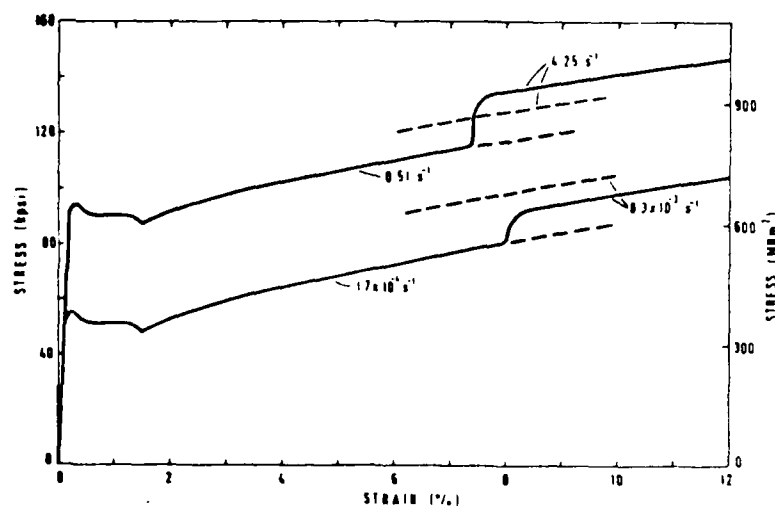


Figure 47. Stress-Strain Curves for Molybdenum (Initial Temperature 292 K). Full Lines: Results of Strain-Rate Change Tests; Dashed Lines: Curves Expected for Constant Results

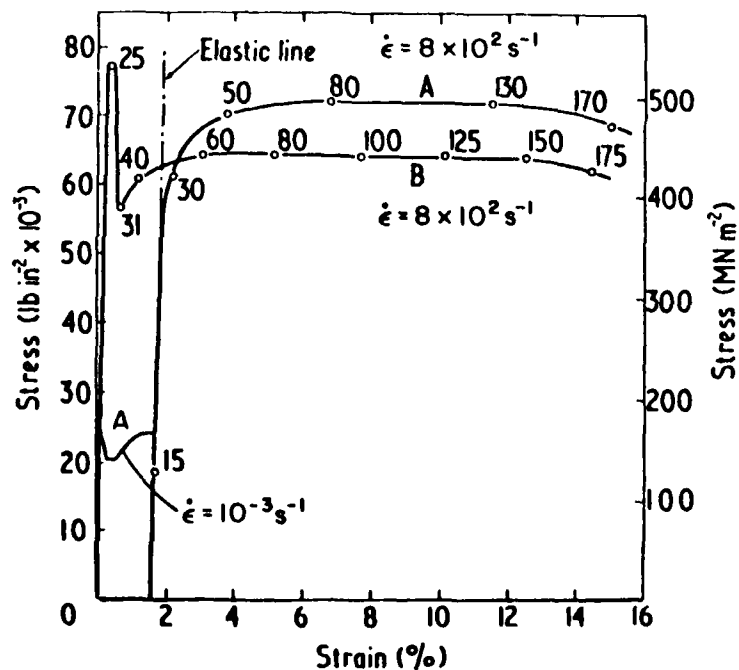


Figure 48. The Results of an Interrupted Strain Rate Test from a Low to a High Strain Rate for a High Purity Iron

Since the specimen in these tests are composed of high purity iron, it would appear that the bcc structure itself might be responsible for the overshoot in flow stress. However, this is not entirely clear. The degree of purity of the iron apparently is of consequence, since strain ageing effects have been seen in iron containing only small amounts of carbon or nitrogen. On the other hand, a further complicating factor is the possibility of twinning and its influence on flow stress. Hockett and Zukas (Reference 179) showed that twinning in pure iron will occur whenever the strain rate is high enough or the temperature is sufficiently low. They place the boundary between twinning and no twins at $\log \dot{\epsilon} = -1744/T + 5.9031$, where $\dot{\epsilon}$ is in units of reciprocal seconds and T is in degrees Kelvin. By this criterion twinning should occur in Harding's test. However, as was pointed out later by Eleiche and Campbell (Reference 180) the effects of twinning do not correlate in a simple manner with applied stress, since less twinning is observed in specimens after an incremental strain rate test than after an all-dynamic test, in spite of the higher stresses occurring in the former.

The contrasting behavior of copper (fcc), titanium (hcp) and steel (bcc) is brought out most clearly by the tests reported by Eleiche and Campbell and published in part by Campbell et al. and in part by Eleiche (References 180, 181, 182 and 183). These tests were performed in a stored-torque Kolsky bar over temperatures ranging from -150 C to 400 C and at strain rates of approximately 10^{-3} s^{-1} and 10^3 s^{-1} . Based on their results, the authors calculate an apparent strain rate sensitivity defined by

$$\mu_{12} = \frac{\partial \tau}{\partial \ln \dot{\gamma}} \approx \frac{\tau_2 - \tau_1}{\ln \dot{\gamma}_2 / \dot{\gamma}_1} \quad (59)$$

where τ_1 and τ_2 are respectively the flow stresses in shear obtained from tests at two constant strain rates $\dot{\gamma}_1$ and $\dot{\gamma}_2$. Since the purpose of this investigation was to study the effects of strain rate history, incremental strain rate tests were performed at each temperature investigated for a range of values of prestrain. Based on the

incremental strain rate tests, the authors calculate an intrinsic or true strain rate sensitivity,

$$\bar{\mu}_{12} = \frac{\tau_j^{-1} - \tau_1^{-1}}{\ln \dot{\gamma}_2 / \dot{\gamma}_1} \quad (60)$$

where τ_j represents the flow stress immediately after the increment in strain rate from $\dot{\gamma}_1$ to $\dot{\gamma}_2$. Figure 49 shows the stress-strain behavior of copper at room temperature. Values of μ_{12} and $\bar{\mu}_{12}$ are calculated from curves such as these. Of the three metals tested copper clearly shows the least sensitivity to strain rate, although it becomes more sensitive at the higher temperatures (Figure 50). History effects were found at all temperatures during the deformation of copper but decrease as the test temperature is increased. Titanium is more strongly sensitive to strain rate than copper. Its strain rate sensitivity depends on temperature and seems to reach a maximum at about 500°K (Figure 51). However, the stress-strain curves of titanium show very little in the way of strain rate history effects (Figure 52). The behavior of steel is quite different from that of the other two metals. To begin with, the stress-strain behavior makes it evident that the strain rate sensitivity is quite large (Figures 53-55). It should be remembered also, that steel is the only one of the three metals whose behavior, at the quasi-static rate, is affected by dynamic strain ageing. This is seen in Figure 56 which shows the flow stress as a function of temperature. The strain rate sensitivity of steel decreases with temperature (Figure 57), and is quite small at 400°C, the maximum temperature in these tests. Strain rate history effects are also present, although markedly different from those seen in the other two metals. As will be seen below, one of the reasons for evaluating μ_{12} or $\bar{\mu}_{12}$ is that it leads to an estimated activation volume, Equation 63. If, as is the case with steel at low and strain ageing temperatures, the flow stress after an increment in strain rate exceeds the all-dynamic value, then μ_{12} becomes negative and hence loses much of its meaning. Accordingly, the jump test and μ_{12} become more reliable indicators of behavior on the microscopic scale.

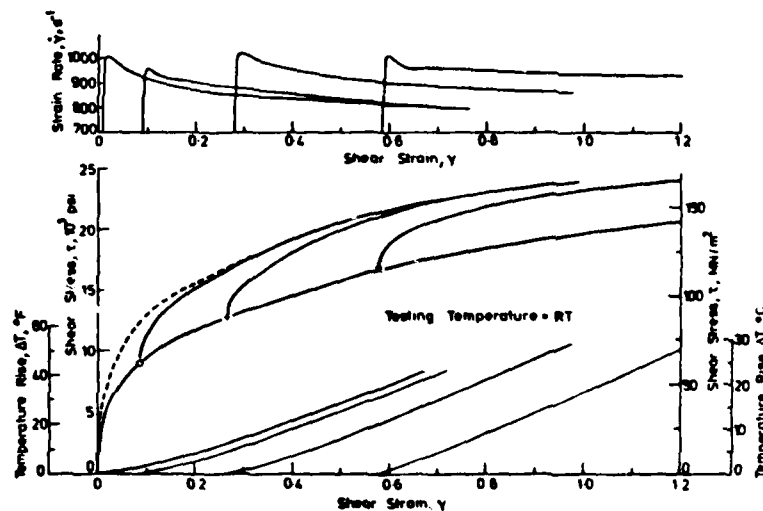


Figure 49. Incremental Strain Rate Test Results for Copper at 24°C

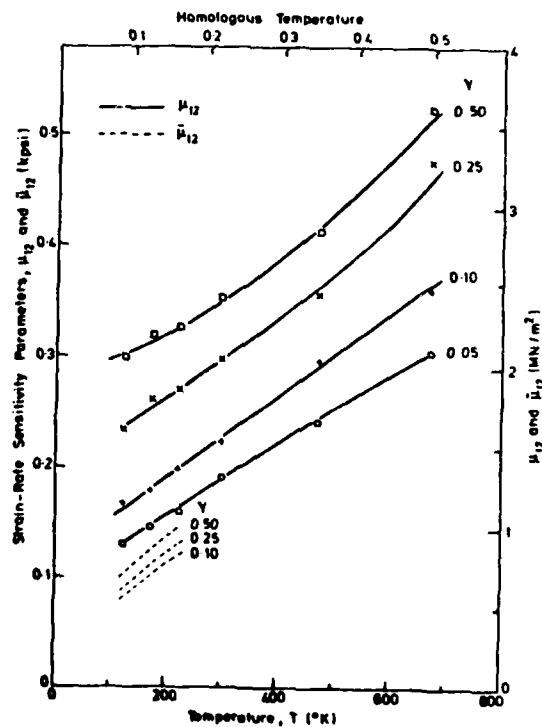


Figure 50. Temperature Dependence of Apparent and True Strain Rate Sensitivities of Copper

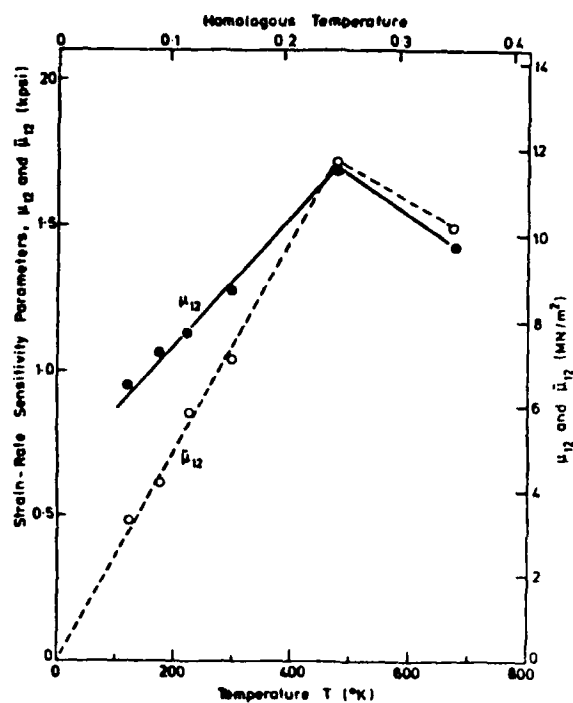


Figure 51. Temperatures Dependence of Apparent and True Strain Rate Sensitivities of Titanium

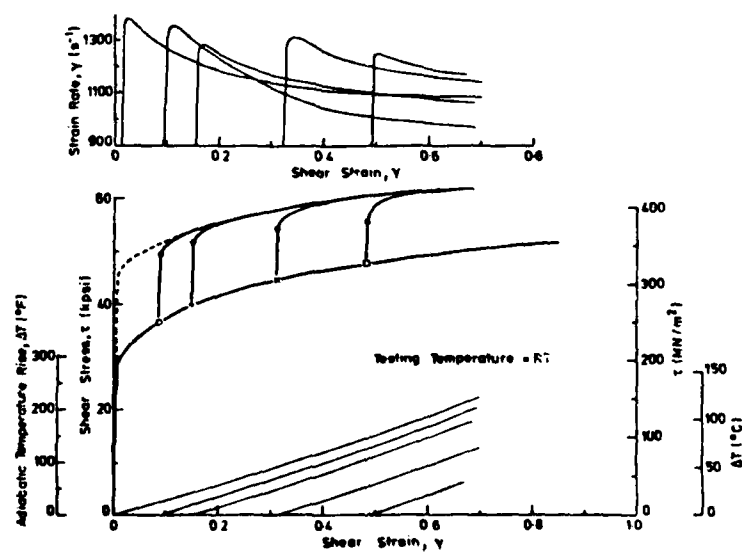


Figure 52. Incremental Strain Rate Test Results for Titanium at 24°C

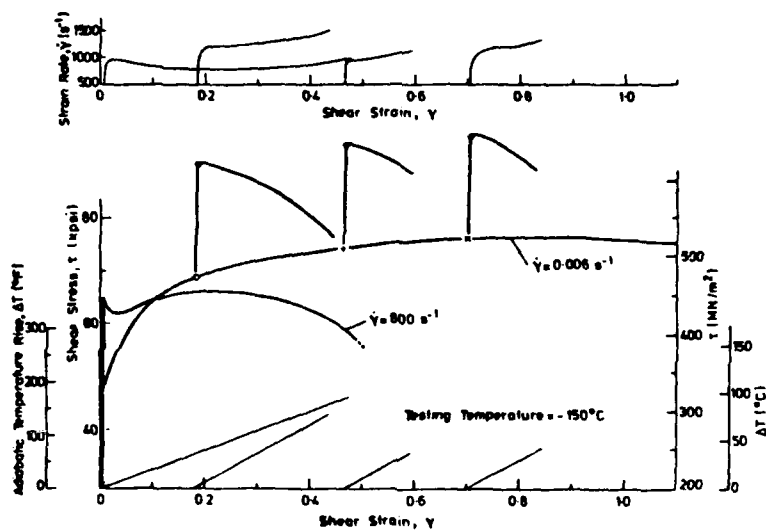


Figure 53. Incremental Strain Rate Test Results for Mild Steel at -150°C

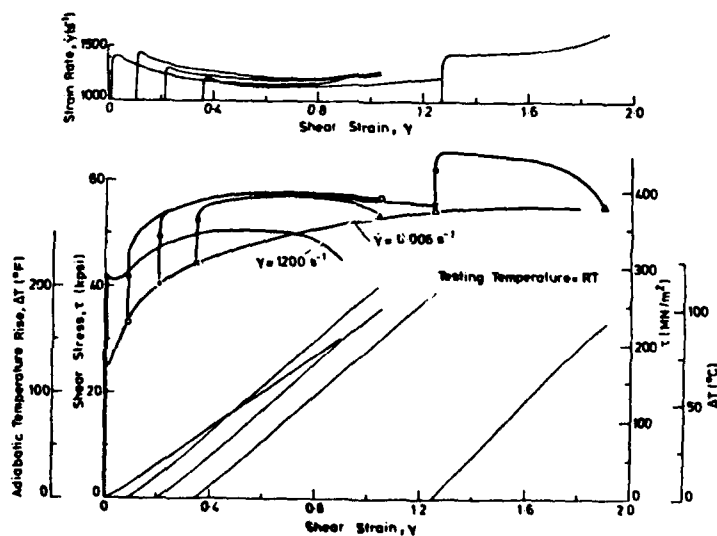


Figure 54. Incremental Strain Rate Test Results for Mild Steel at Room Temperature

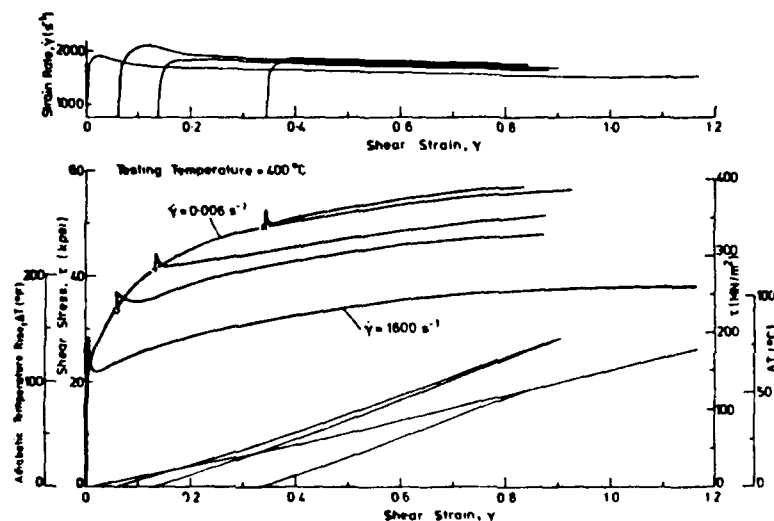


Figure 55. Incremental Strain Rate Test Results for Mild Steel at 400°C

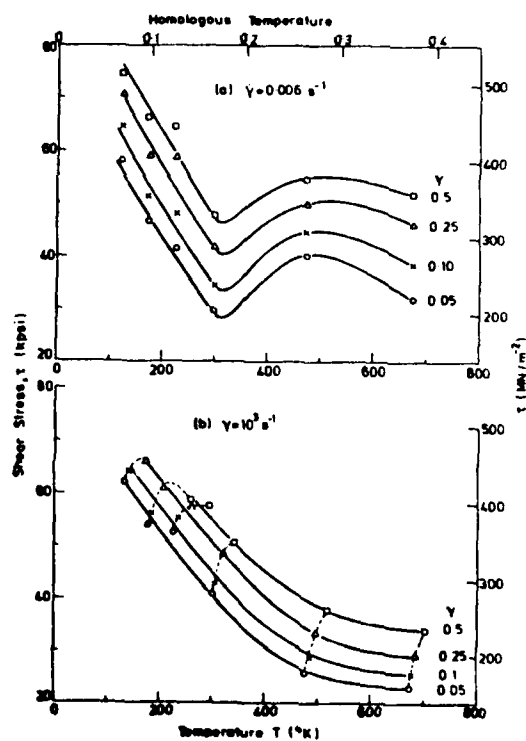


Figure 56. Temperature Dependence of Flow Stress of Mild Steel, at (a) Low and (b) High Strain Rate

The experimental results of Eleiche and Campbell can be summarized by saying that while strain rate effects occur in all three metals they are more pronounced in titanium and in steel than in copper. However, strain rate history effects appear to be absent or nearly so in titanium, while they produce quite a different behavior in steel than in fcc metals. In steel, constant strain rate tests over a range of strain rates show an apparent negative strain rate effect. Jumps in strain rate give a positive strain rate effect which is strongly dependent on temperature. The most likely explanation for the behavior of steel lies in the dynamic strain ageing occurring during quasi-static deformation. However, this conclusion is not entirely certain as yet, since the bcc lattice structure itself may be playing a considerable role. The evidence for this lies in the results of tests with high purity iron described previously (Reference 178) Harding and in the anomolous behavior of niobium and molybdenum, found by Campbell and Briggs (Reference 176). The intrinsic behavior of iron, as opposed to the influence of impurities, continues to be a subject of research interest involving elaborate attempts at purification, Tseng and Tangri (Reference 184).

Eleiche and Campbell also calculated the temperature rise expected to occur during rapid straining of their specimens; they presume homogenous deformation, no heat flow to the surroundings and that all work done is converted to heat. For copper at a strain of 50% the temperature rise would be less than 20°C. On the basis of the thermal sensitivity of copper, they estimate that this would produce only a small drop in the value of the flow stress so that adiabatic heating is not an important factor in the observed history and memory effects in the case of copper. For titanium and steel, however, the calculated temperature rise at 50% strain is about 80°C, and 50°C, respectively. In view also of the greater thermal sensitivity of these two metals, this increase in temperature probably is enough to reduce the flow stress during rapid straining. Furthermore, judging by the rapid drop in stress seen in some of the stress-strain curves (Figures 53 and 54), it is possible that the state of strain was not always homogeneous during dynamic deformation of steel. Eleiche and Campbell do not comment on this point.

Campbell et al. (Reference 181) also propose possible constitutive relations for these three metals. For titanium, strain rate history appears not to be of consequence so that equation of the form

$$F(\tau, \gamma, \dot{\gamma}) = 0$$

can describe deformation at a constant temperature, and the authors propose

$$\tau = f(\gamma) + g(\dot{\gamma})$$

In the case of copper they employ

$$\tau = A\dot{\gamma}^n \{1 + m \ln(1 + \dot{\gamma}/B)\} \quad (61)$$

for behavior at a constant strain rate and temperature. According to this equation, when $\dot{\gamma}/B \gg 0$ then $\tau \approx A\dot{\gamma}^n$, which frequently represents very satisfactorily the quasi-static stress-strain relation for an fcc metal. They evaluate the other constants in the equation from a plot of τ against $\ln \dot{\gamma}$. To represent behavior at a variable strain rate in copper or steel, they make use of a hereditary integral. For a jump in strain rate from $\dot{\gamma}_1$ to $\dot{\gamma}_2$, they show that

$$\tau = A[1 + m \ln(1 + \dot{\gamma}_1/B)]\dot{\gamma}_1^n + mA[\ln(B + \dot{\gamma}_2)/(B + \dot{\gamma}_1)](\tau - \sigma)^n \quad (62)$$

represents quite well the behavior of copper except at very large strains, strains in excess of 80%. For steel the behavior is more complicated.

Incremental strain rate experiments at temperature mainly in the range 950°C to 1165°C for very large strains (up to 200%) and strain rate ranging from about 10^{-2} s^{-1} to 20 s^{-1} were carried out by Barraclough and Sellars (Reference 162). The tests were performed in torsion on solid bars of two types of steel, a stainless steel, AISI 304, and a low alloy steel, AISI 5140. The results (Figure 58) indicate that a change in strain rate is followed by a transition period before the flow stress adopts the value obtained in constant strain rate test. This transition period represents a strain of some 20 to 50%, becoming larger as the prestrain increases. It is interesting to note that in some instances the stress overshoots, while in others it is less than the expected value of stress at the new strain rate. Based on this investigation, one can conclude that the flow stress of these steels at elevated temperature is quite strongly dependent on strain rate but that the history of strain rate plays a lesser role. On the scale shown and for the conditions described, these materials appear to have very little memory.

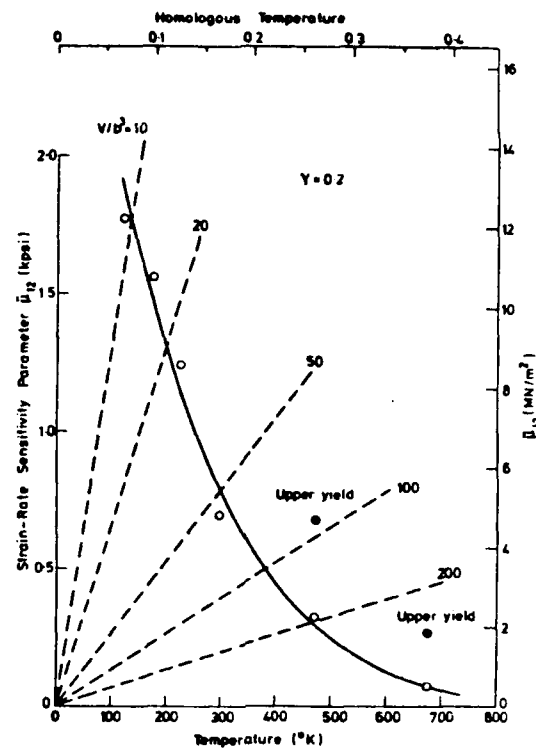


Figure 57. Temperature Dependence of True Strain Rate Sensitivity of Mild Steel

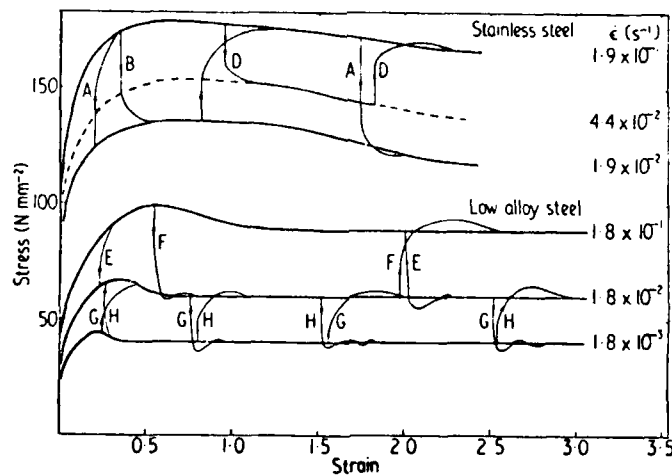


Figure 58. Typical Stress-Strain Curves for Tests Involving Instantaneous Changes in Strain Rate for Stainless and Low Alloy Steels

Senseny et al. (Reference 59) extended the work of Frantz and Duffy to cover other metals and a range of temperature. Again, explosive loading was used to initiate the torsional pulse. Results were obtained for two fcc metals, aluminum and copper, and two hcp metals, magnesium and zinc (Figures 59-62). In this connection, one must cite the work of Basinski (Reference 185), who's results are relevant even though the strain rates involved did not attain the dynamic range. Basinski performed two series of tests; in the first, increments in temperature were imposed during deformation of the specimen at a constant strain rate, while in the second tests, strain rate was varied at constant temperature. Specimens of polycrystalline aluminum were tested as well as single crystals of the following fcc metals: aluminum, copper and silver. The temperature in these tests ranged from 1.70K and the strain rates from 10^{-5} s^{-1} to 10^{-3} s^{-1} . Basinski noted that in either type of test the increment in stress increased with the stress level at which the strain rate or temperature increment was imposed. He also noted that the ratio of stress increment to stress level remained constant for incremental tests performed over a range of strain at one strain rate and one temperature. Basinski and Christian (Reference 186) performed similar experiments with iron and found that the stress increment for this metal does not depend on the stress level. They concluded that fcc and bcc metals behave differently in this respect. As near as one can tell, though, the evidence is far from conclusive. In any case, the results of Senseny et al. for fcc metals would seem to agree with those of Basinski, in that for both sets of experiments the stress increment increases with the stress level. For the hcp metals the stress increments seem nearer to being constant.

Klepackzo and Duffy (Reference 187) reviewed strain rate history effects in bcc metals including steels, and also presented new data obtained as the result of incremental strain rate tests with 1020 hot-rolled steel (Figure 63 and 64). These show that at low temperatures, 83K, strain rate history effects are quite pronounced. For constant strain rates the strain rate sensitivity is positive, but incremental strain rate tests show an overshoot, as did those of Eleiche and Campbell (Reference 180). However, at 144K and at room temperature, history

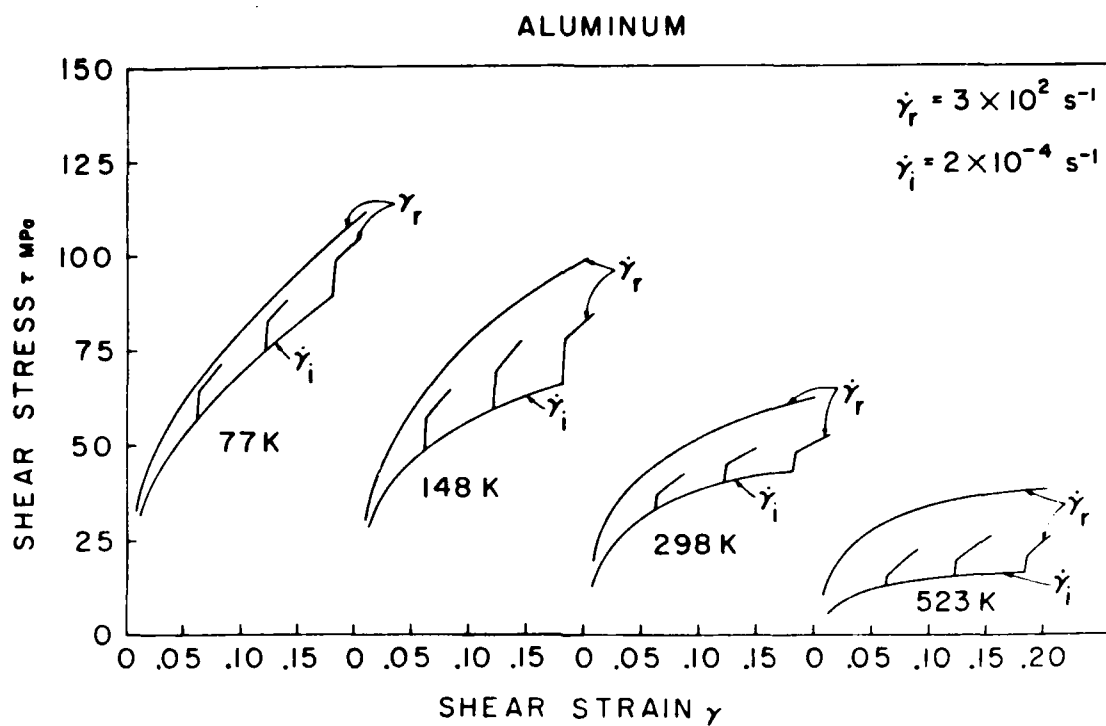


Figure 59. Incremental Strain Rate Test Results for 1100-0 Aluminum at Various Temperature

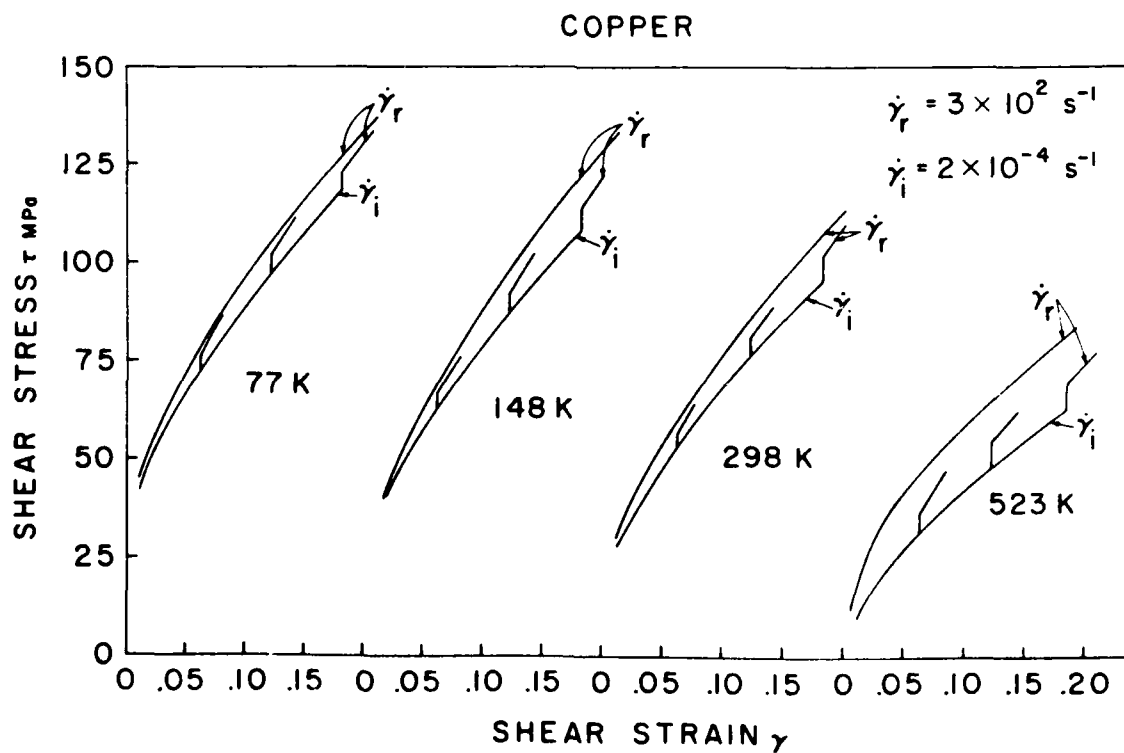


Figure 60. Incremental Strain Rate Test Results for OFHC Copper

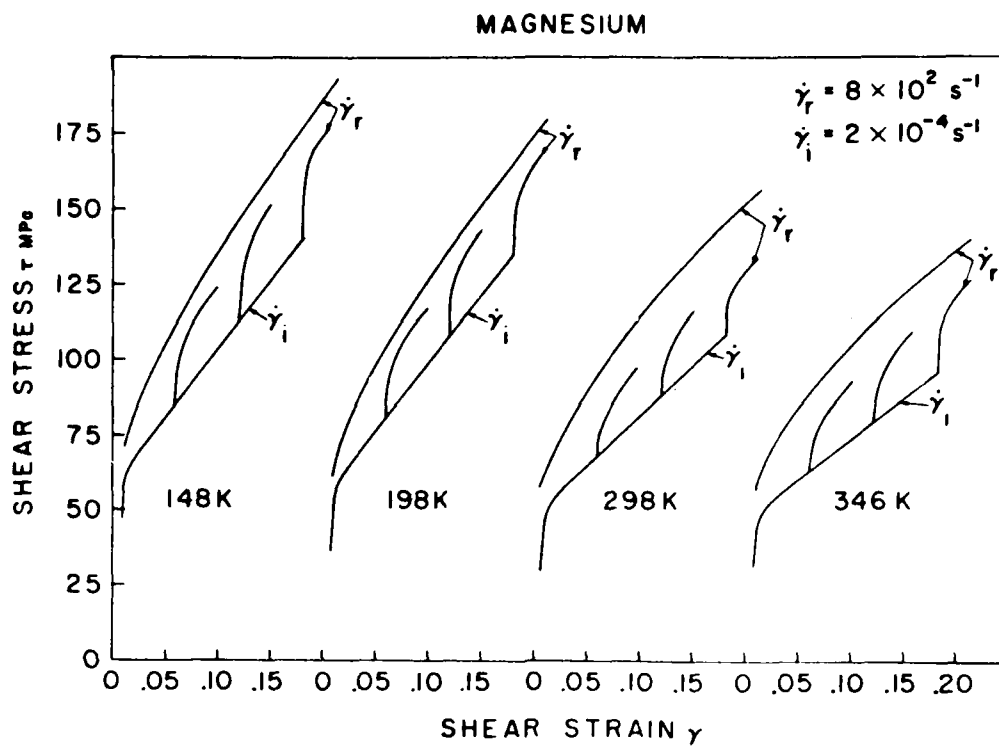


Figure 61. Incremental Strain Rate Test Results for AZ31B Magnesium

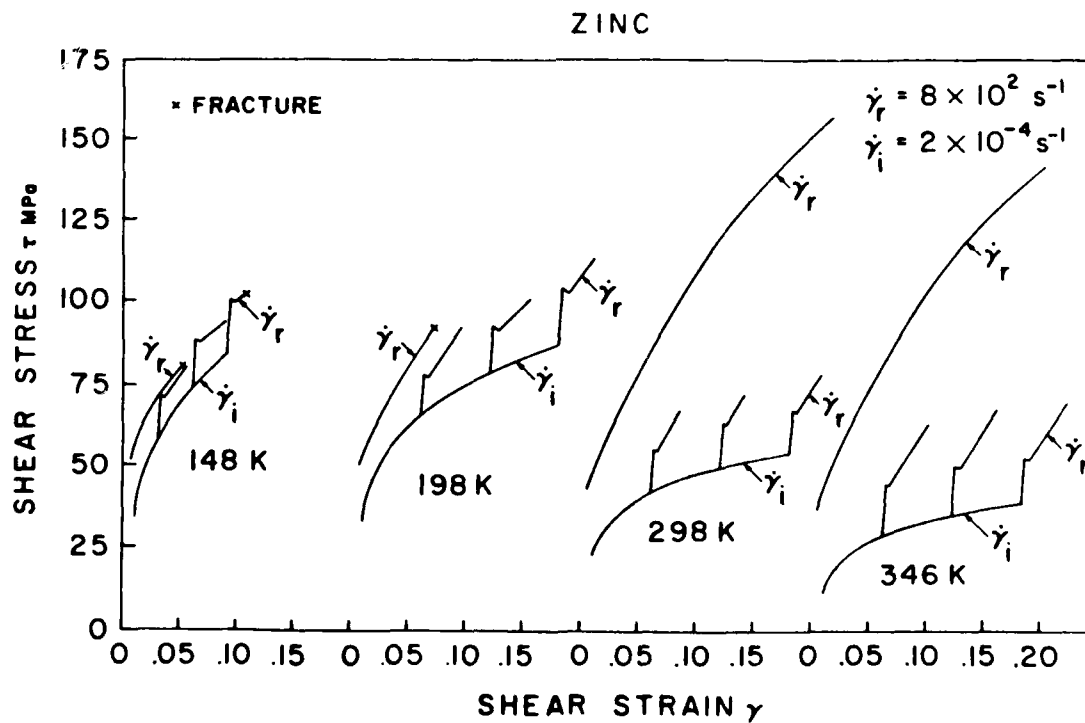


Figure 62. Incremental Strain Rate Test Results for Commercially Pure Zinc

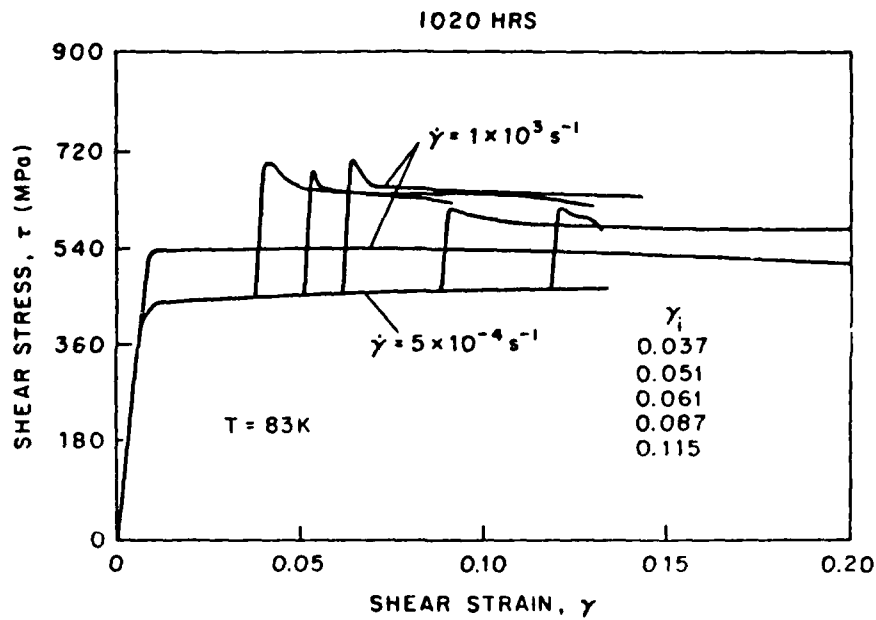


Figure 63. Incremental Strain Rate Test Results for 1020 Hot-Rolled Steel at 83 K

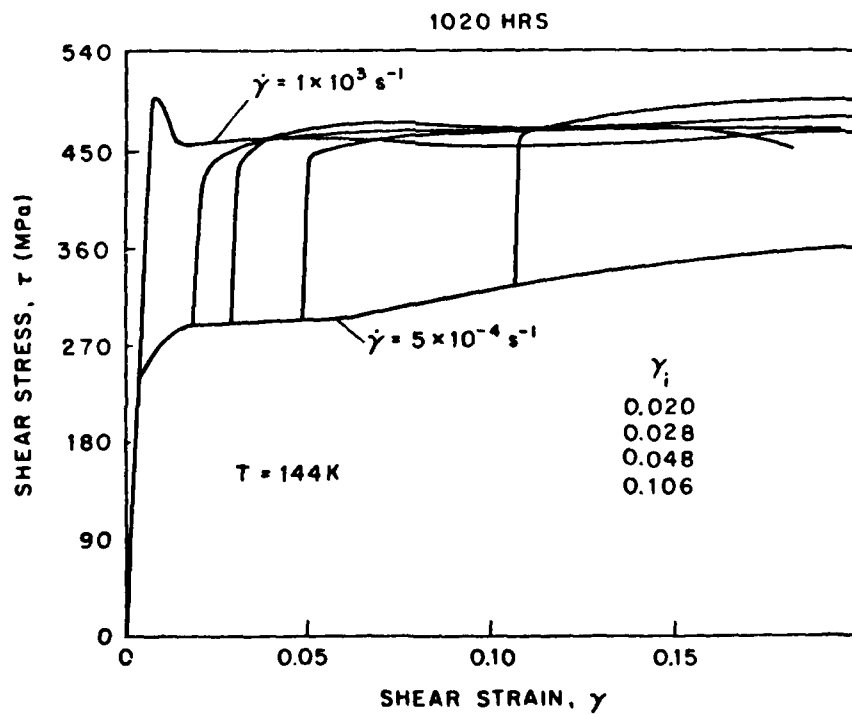


Figure 64. Incremental Strain Rate Test Results for 1020 Hot-Rolled Steel at 144 K

effects disappear in this particular test. This may be due in part to a positive strain rate effect which is balanced by dynamic strain ageing at the low rates. In any case, results show that the overshoot reappears at the higher temperatures (Figure 65) where results are influenced by adiabatic coupling. Indeed, adiabatic coupling plays a role whenever large strains at high strain rates are involved. In related work, Klepaczko (Reference 188) has presented a model for yielding and flow of steel. It is based on a thermally activated deformation mechanism in which the Peierls stress is overcome by the nucleation of kink pairs. Klepaczko combines this mechanism with an evolutionary equation, so that the final model contains one structural parameter representing total dislocation density. He employs this model to predict material behavior at constant strain rates in two steels and obtains very close agreement with experimental results (Figures 66 and 67), although, in the latter figure some experimental points are not quite in agreement with the analytic predictions.

3. MICROSTRUCTURAL CONSIDERATIONS IN DYNAMIC PLASTICITY

A large number of incremental strain rate experiments has been performed with single crystals, but in nearly all of these experiments the strain rates are low. Among the earliest dynamic tests are those of Lindholm and Yeakley (Reference 189) on single crystal and polycrystal specimens deformed in compression at strain rates up to 500 s^{-1} . Activation volumes were calculated as a function of strain using the theory of the thermally activated deformation of metals. For single crystals, results indicate that the activation volume depends on the direction of the loading axis relative to the crystallographic orientation. Furthermore, for polycrystalline specimens of the same purity aluminum the activation volume is approximately equal to the average found for the single crystals. Ferguson et al. (Reference 135) performed their tests in shear on single crystals of aluminum in the temperature range 200K to 500K . They showed that the flow stress in the strain rate range 10^3 s^{-1} to 10^4 s^{-1} varies linearly with strain rate, thus implying that deformation at these high strain rates is dominated by a viscous mechanism which, furthermore, offers a resistance almost independent of temperature. Dormeal et al. and Stelly and Dormeal

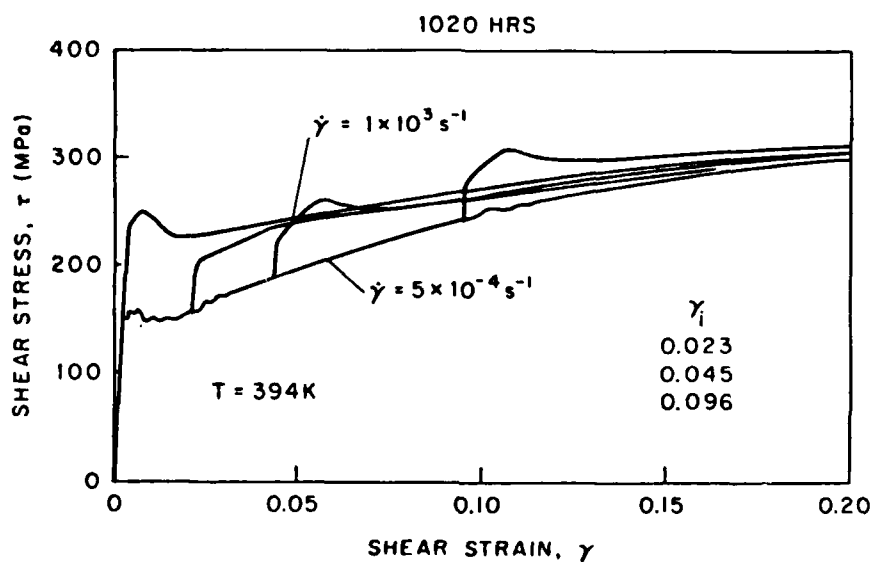


Figure 65. Incremental Strain Rate Test Results for 1020 Hot-Rolled Steel at 394 K

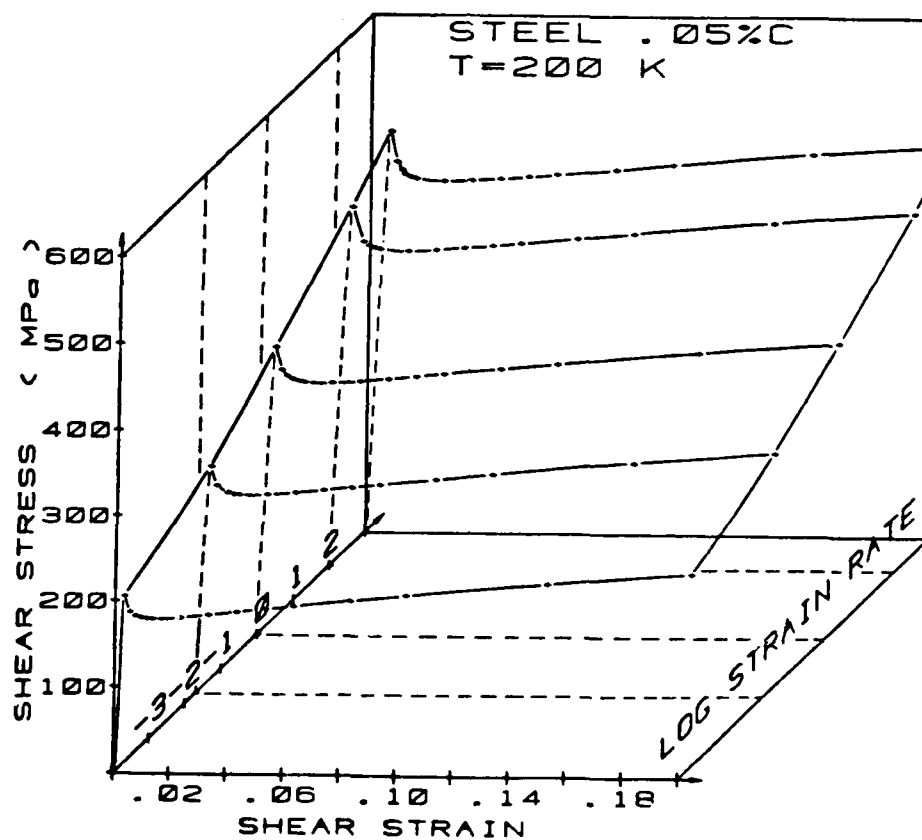


Figure 66. The Predicted Flow Stress for an Annealed Low Carbon Steel at 200 K According to Klepaczko's Model

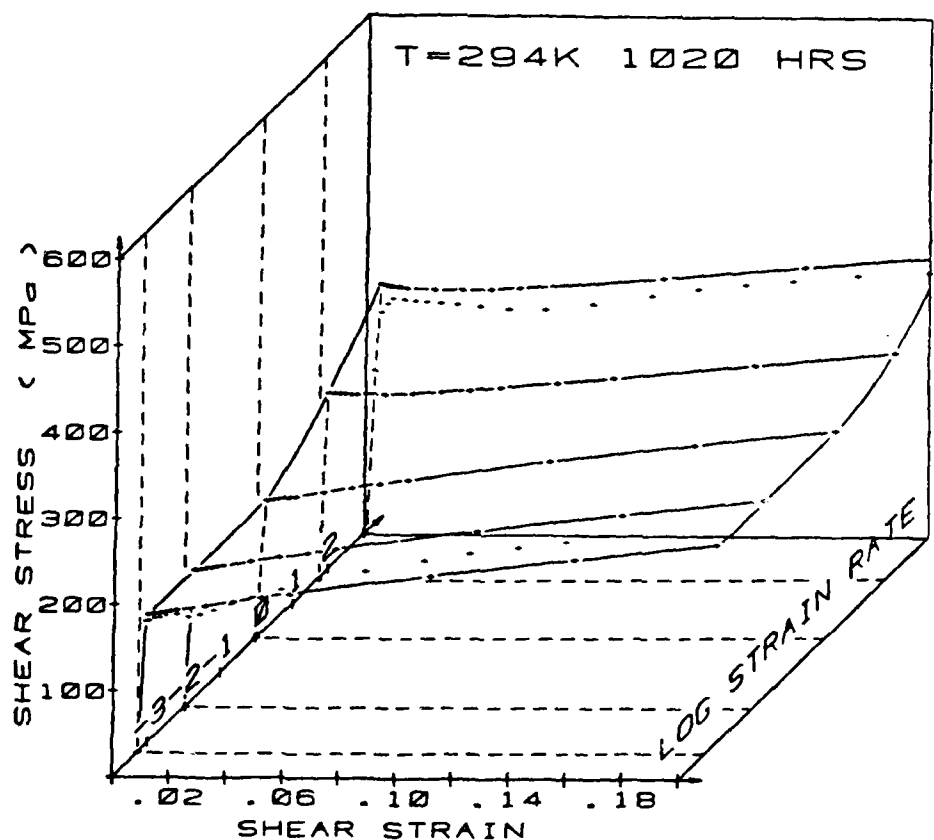


Figure 67. The Predicted Flow Stress for 1020 Hot-Rolled Steel at Room Temperature According to Klepaczko's Model.
Experimental Points are Indicated for $\dot{\gamma} = 5 \times 10^{-4} \text{ s}^{-1}$
and $\dot{\gamma} = 10^3 \text{ s}^{-1}$

conducted interrupted tests as well as the constant rate tests described in Section VI (References 137 and 138). In their interrupted tests, the prestrain was imposed either quasi-statically or dynamically and the reloading at a rate either lower or higher than for prestraining. Their results for copper single crystals show a strong strain rate history effect which is not erased by continued straining (Figure 68). This contrasts with the behavior of polycrystalline copper which exhibits a fading memory (References 59 and 181). Chiem and Duffy (References 190 and 191) performed incremental strain rate experiments with single crystals of lithium fluoride and aluminum loaded in shear. At low values of prestrain there is a fading memory, but as prestrain increases the memory effect becomes more permanent.

The development of transmission electron microscopy creates a promising new approach to studies in dynamic plasticity and some investigators are attempting to relate strain rate effects and, more recently, strain rate history effects to the changes in dislocation substructure that occur during deformation. The experiments of Edington with single crystals of copper and niobium have already been described in Section VI (References 192 and 193). However, in addition to the macroscopic tests, Edington performed detailed TEM observations to determine dislocation distribution and density as functions of strain rate. In the case of the copper crystals, a cellular dislocation substructure formed after about 13% strain in either quasi-static or dynamic deformation. For niobium the cellular structure occurred only as a result of quasi-static deformation. Similar results were observed in polycrystalline aluminum specimens by McQueen and Hockett and by Korbel and Swiatkowski (References 172 and 194). In the first of these investigations 1100 aluminum was deformed at strain rates of 0.1 s^{-1} to 220 s^{-1} in a cam plastometer at temperatures ranging from 200°C to 500°C . It was found that the cell size (at a given strain) increased with testing temperature and decreased with strain rate, and that the flow stress varied inversely as the cell diameter. Korbel and Swiatkowski tested high purity polycrystalline aluminum and found that a higher strain rate produces a much smaller cell size as well as an increase in the relative misorientation between the subgrains. Using the latter as a measure of

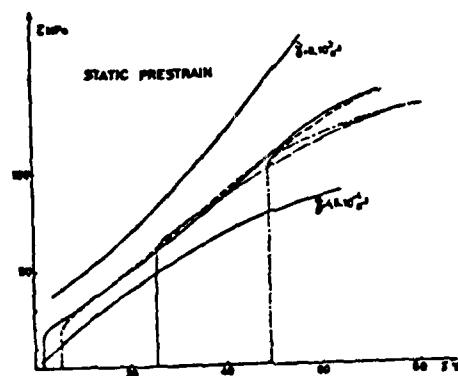


Figure 68. Stress-Strain Curves for Copper Single Crystals, Showing Results of Interrupted Strain Rate Tests from $4.5 \cdot 10^{-4} \text{ s}^{-1}$ to $8 \cdot 10^3 \text{ s}^{-1}$

dislocation density, they showed that the flow stress increased linearly with the square root of dislocation density, and inversely as the square root of the subgrain size, in accordance with the Hall-Petch relation, but in disagreement with McQueen and Hockett's results. As mentioned previously, Chiem and Duffy (Reference 191) performed a series of incremental strain rate tests with single crystals of aluminum. The specimens were deformed in shear at strain rates in the range 10^{-4} s^{-1} to 1600 s^{-1} and to strains of about 20%. A plot of flow stress as a function of strain rate gives evidence of a change in the deformation mechanism at a strain rate of about 500 s^{-1} (Figure 69). TEM observation after deformation at quasi-static strain rates reveals a cellular dislocation arrangement even at low values of strain that develops into well-outlined subgrains as strain increases. Cells are also visible after dynamic deformation, but these cells are about one quarter the size of those produced by quasi-static deformation and their walls are not as well-defined. Thus, for the strain rates covered by these tests, the results indicate that as cell size is reduced both the flow stress and the strain rate sensitivity increase (Figures 70 and 71). The jump tests performed by Chiem and Duffy show a pronounced strain rate history effect and permit the calculation of an activation volume applicable to quasi-static straining. Results of this calculation, which is based on macroscopic measurements and on the theory of thermally activated deformation of metals, compares quite favorably to an activation volume based on the dislocation densities measured after deformation (Figure 72).

The results of the dynamic tests and of the incremental strain rate tests described above for polycrystalline specimens are tabulated and compared with one another in Section X. A few general conclusions are also presented in that section and the following. It is important to add, however, that a sudden increase in strain rate does not constitute the only test available for studies of history effects, even in uniaxial loading. Eleiche and Campbell (Reference 195) prestrained specimens in shear by loading in one direction and then suddenly reversing the straining direction. Their tests were performed with a torsional Kolsky bar on specimens of a magnesium alloy. In each test the

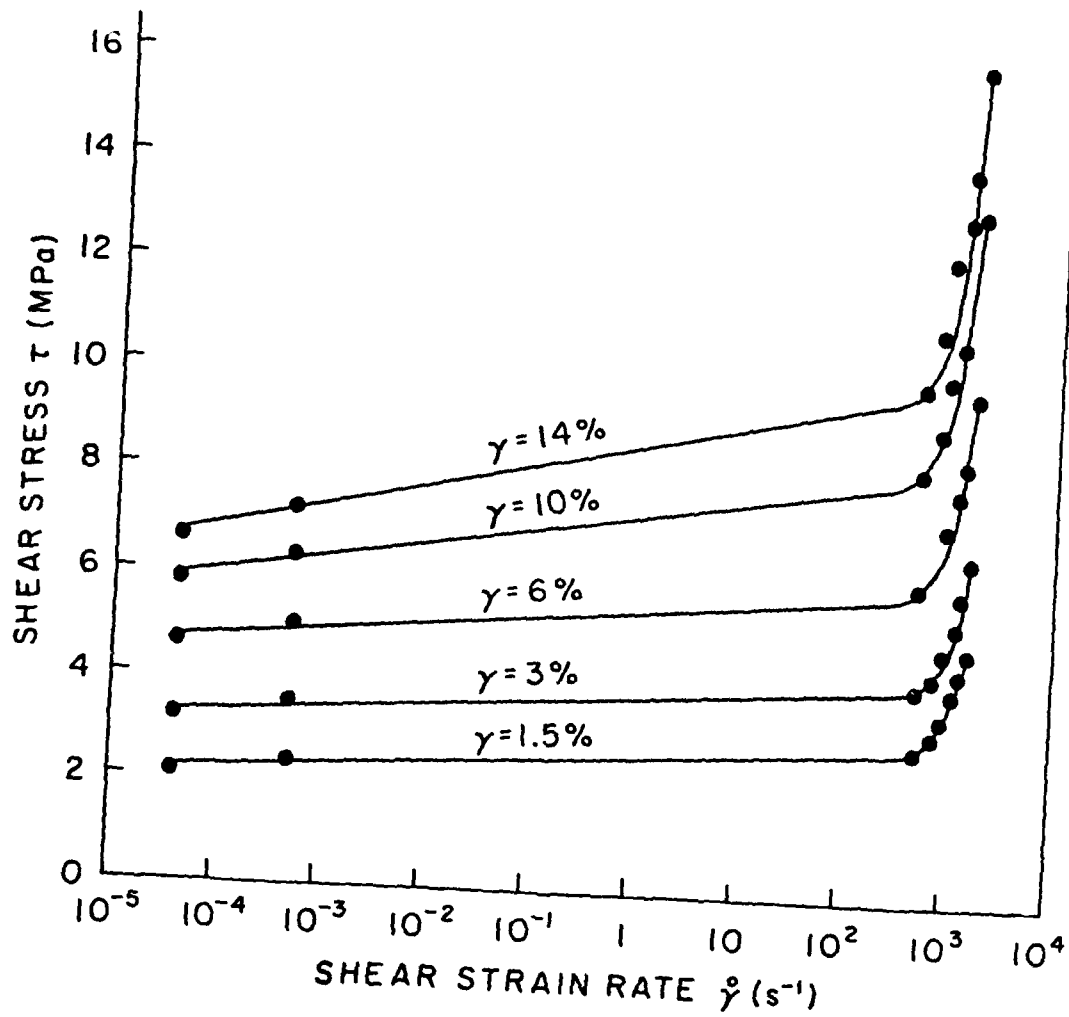


Figure 69. Flow Stress Vs. Strain Rate for Aluminum Single Crystals

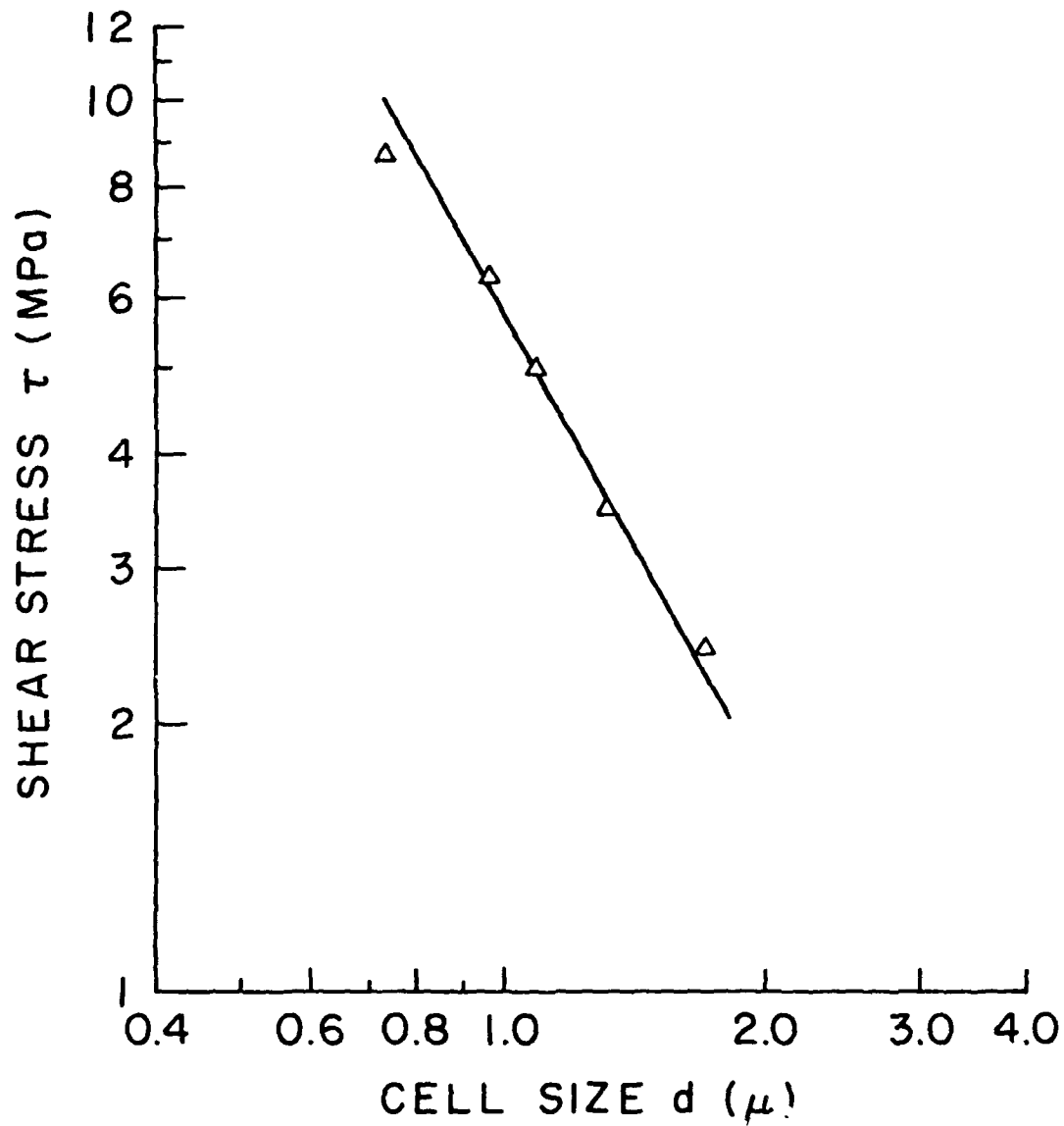


Figure 70. Shear Stress Vs. Dislocation Cell Size for Aluminum Single Crystals Loaded Quasi-statically

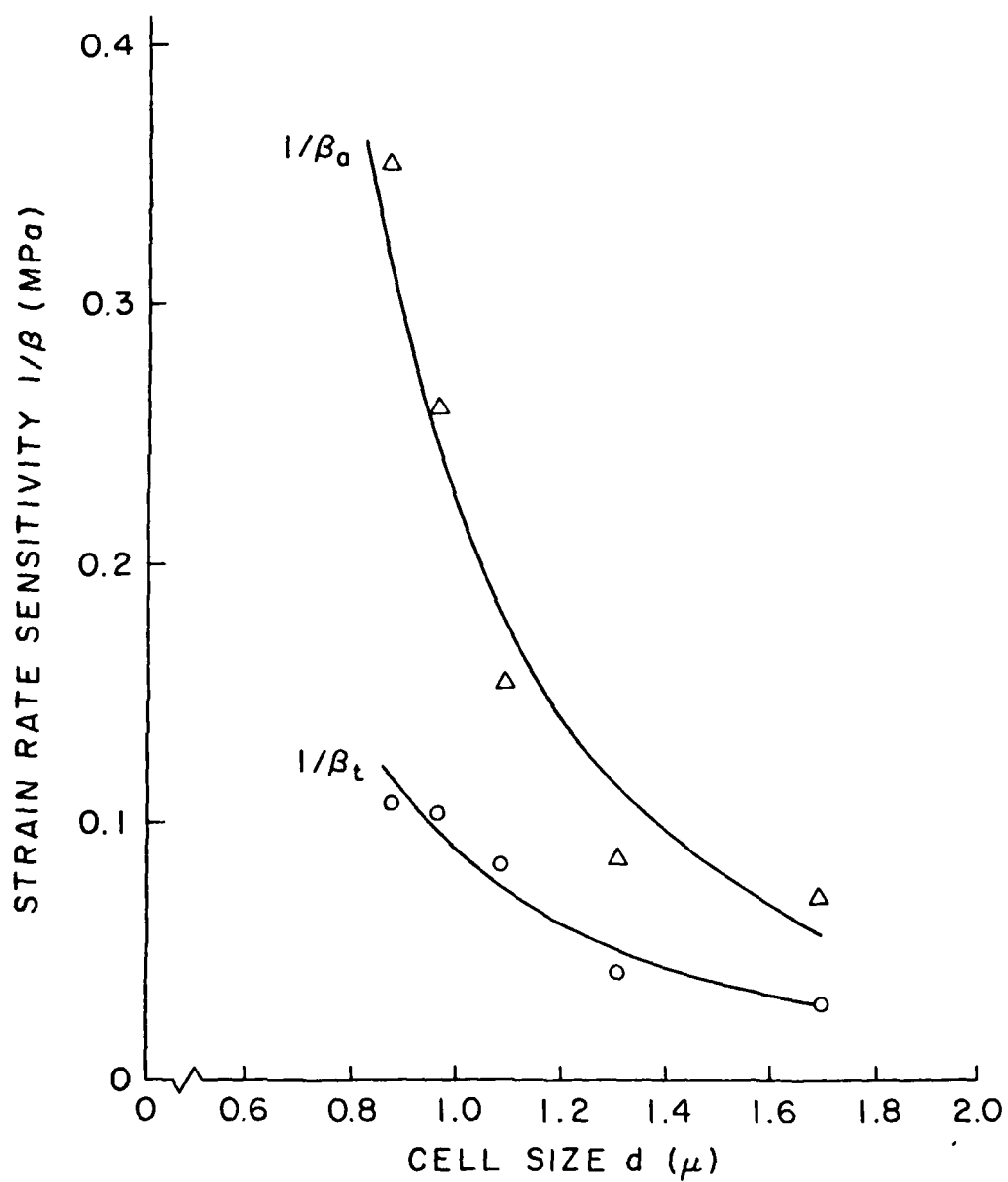


Figure 71. Strain Rate Sensitivities, Apparent and True, as Functions of Dislocation Cell Size in Aluminum Single Crystals

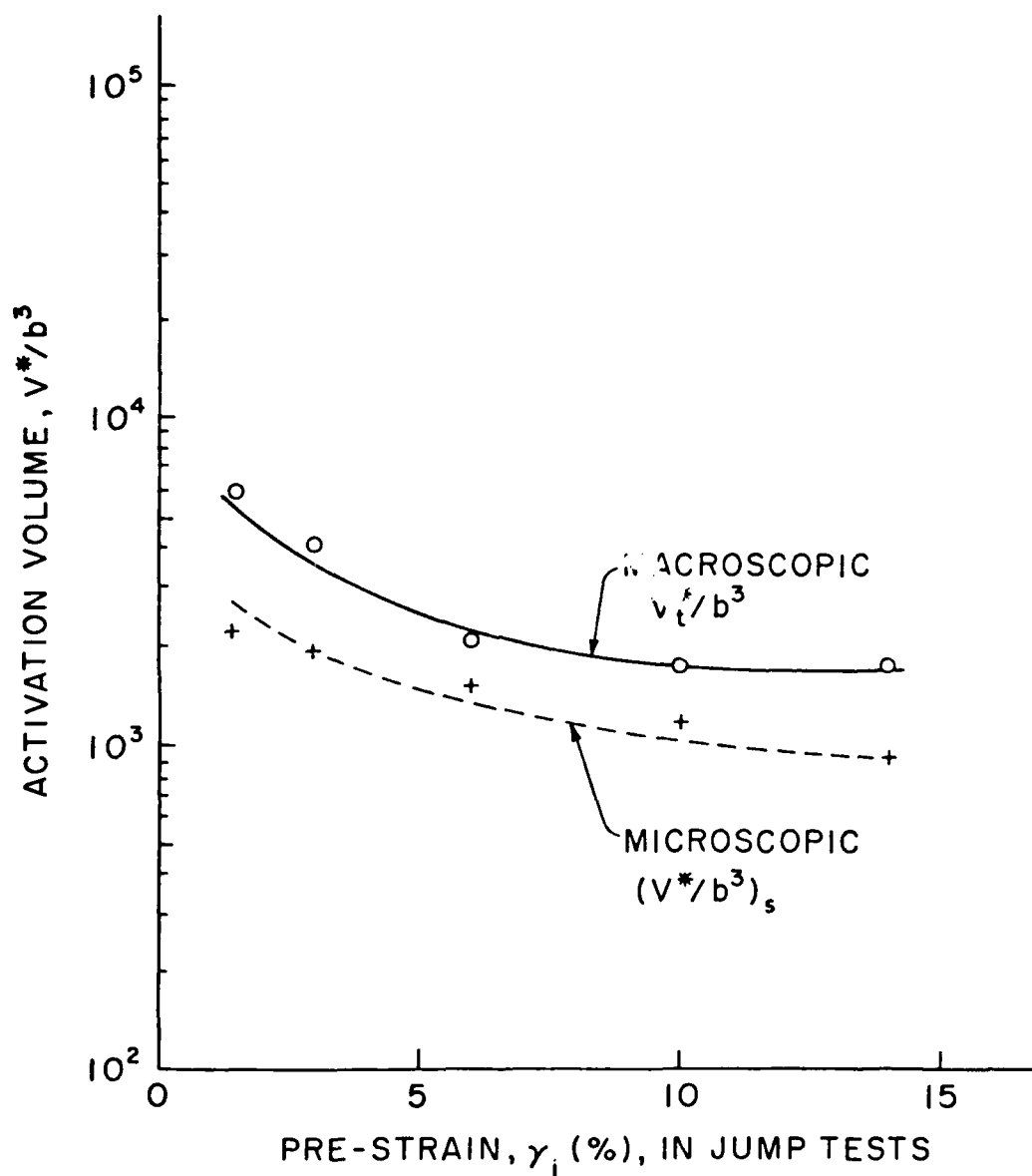


Figure 72. Comparison of Macroscopic Activation Volume Evaluated on the Basis of Jump Tests and Microscopic Activation Volume Based on TEM Observations of Foil Samples of Aluminum Single Crystals

initial prestrain, which ranged from about 5% to 35%, was imposed at a strain rate of $6 \times 10^{-3} \text{ s}^{-1}$. The reverse loading was applied either at the quasi-static rate or at a dynamic rate of 250 s^{-1} or 1100 s^{-1} . Reverse loading at the quasi-static rate produces the usual Bauschinger effect: the reverse yield stress is greater the larger the amount of prestrain. In contrast, for reverse loading at the dynamic rate the yield stress decreases as the amount of prestrain is increased. Eliche and Campbell present constitutive equations to describe this behavior.

Another method available for the study of history effects was presented by Lipkin et al. (Reference 196). In this investigation, OFHC copper specimens were deformed at an initial dynamic strain rate which was reduced very rapidly after about 15% strain to a lower, constant dynamic rate. The results are most interesting and are explained quite convincingly by the authors in terms of changes they believe may be occurring in the microscopic substructure. A torsional Kolsky bar is used in this investigation, and the reduction in the dynamic strain rate is effected by making use of the partial reflections from an external tube attached to the incident bar. The results provide stress, strain and strain rate as functions of time (Figure 73a), and stress and strain rate as function of strain (Figure 73b). In the tests shown in the figure, the initial strain rate is about 850 s^{-1} and drops within 30 or 40 seconds to about 200 s^{-1} . It is immediately evident that the stress continues to increase for a brief time after the drop in strain rate and then adopts approximately a constant value. This delay in the response apparently was observed in all the tests performed. To describe the behavior, the authors propose a constitutive relation involving a superposition integral. Of greater interest from a materials viewpoint is the hypothesis they present describing the delay in terms of a dislocation rearrangement. According to their explanation, the initial deformation produces a dislocation arrangement which is thermodynamically stable under the initial deformation conditions but unstable after the change in strain rate. An instability of this nature had been predicted by Holt and discussed by Alden (References 197 and 198). For the experiments of Lipkin et al., the implication presumably would be that a homogeneous distribution of dislocations becomes cellular as a result of

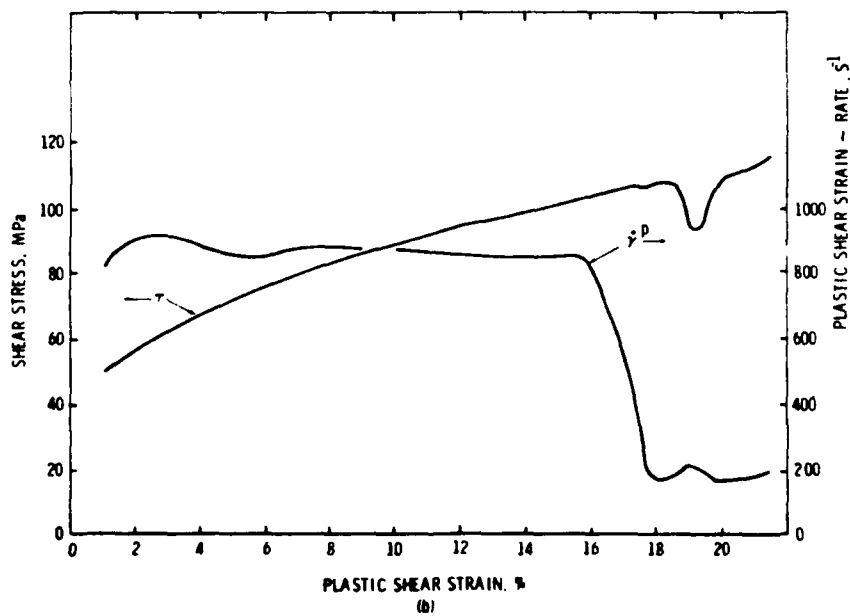
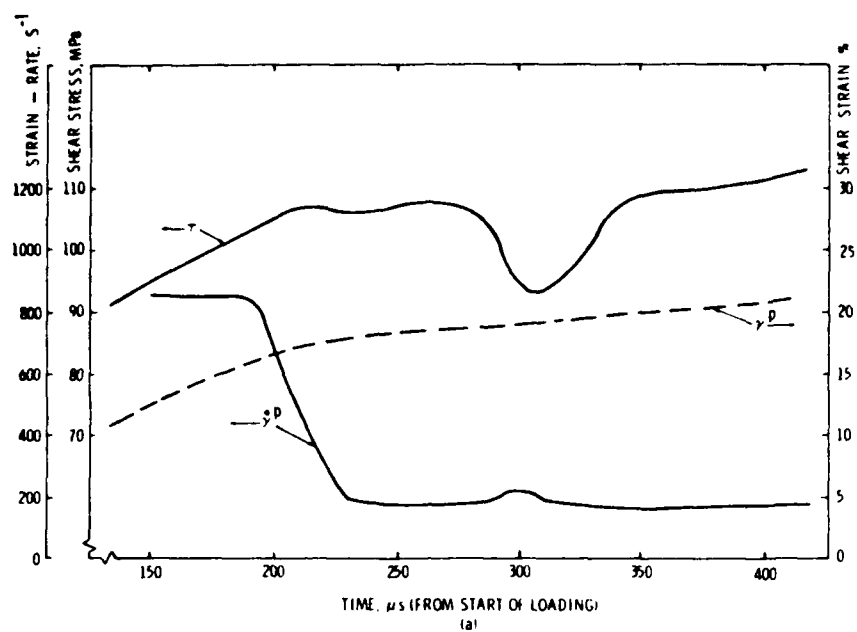


Figure 73. The Effects of a Sudden Reduction in Strain Rate on the Flow Stress of OFHC Copper

an instability existing after the change in strain rate. This would be consistent with the results of Korbel and Swiatkowski (Reference 172) mentioned previously. A modification of this explanation would require only that a change in the size of the dislocation cells accompany the change in strain rate. Chiem and Duffy (Reference 191) show that the cell size in dynamic deformation varies inversely with strain rate, so that a reduction in strain rate would require an increase in cell size to achieve thermodynamic stability. The conclusion to be drawn from these investigations is that material response depends not only on dislocation density but also on dislocation arrangement. Furthermore, the dislocation arrangement depends not only on strain rate but on the accumulated strain as well. This is consistent with the finding of Keh and Weissman (Reference 199), who showed that cell formation in iron requires a minimum total strain and that this minimum strain varies inversely with deformation temperature. It is evident that future research into history effects should include tests with a reduction in strain rate, such as those of Lipkin et al., but coupled with microscopic observations of the substructure. Future inquiry into the cellular structure should also introduce effects of temperature, since Staker and Holt (Reference 200) showed that cell size increases with an increase in temperature. If future investigations can establish that cell size indeed is increased either by an increase in temperature or by a reduction in strain rate (followed by sufficient time and deformation under the new conditions) then the view generally held that changes in temperature and changes in strain rate play opposing roles would be based not only on macroscopic behavior but on microscopic grounds as well. It might then also become possible to combine temperature and strain rate effects in a single variable, such as perhaps $T \ln \dot{\epsilon}_0 / \dot{\epsilon}$, suggested by MacGregor and Fisher (Reference 173) to describe strain ageing effects.

SECTION VIII

SHEAR BANDS

Dynamic deformation, whether in tension, compression or in shear, can produce shear bands or other unstable inhomogeneous deformation. Shear bands are an important phenomenon, because they can weaken metal components rapidly and because they often precede fracture. They appear often in high speed machining and are a frequent cause of failure in armament hardware, see for instance Samuels and Lamborn (Reference 201). Unfortunately, present understanding of shear bands is far from satisfactory in spite of considerable research on the subject. Although shear bands do not constitute the main topic of the present paper, they are given a brief review since they have been observed in dynamic plasticity experiments. Among recent papers on various aspects of the subject one might cite Chakrabarti and Spretnak, Nowacki and Zarka, Needleman and Rice, Hutckinson and Neale, Smith et al., Asaro Kocks et al., as well as the recent reviews of Rogers and Clifton (References 202, 203, 204, 205, 206, 207 and 208, 209 and 210. Of particular interest to studies of penetration and perforation by projectiles are the papers of Woodward and associates, see for instance Woodward, Woodward and Aghan and Yellup and Woodward (References 211, 212, 213 and 214).

In the case of steel, shear bands are divided into two classes: deformed bands and transformed bands. The latter generally appear white when etched with a nital solution. Examples of both types of shear bands are given by Beckman and Finnegan (Reference 215) who studied the formation of shear bands in a number of structural steels. Culver (Reference 216) performed an important series of tests in torsion on thick-walled tubes of three metals: commercially pure titanium, mild steel and 6061-T6 aluminum. He used a torsional impact machine with which he could attain strain rates between 74 s^{-1} and 320 s^{-1} . He found that strain localization occurred in all three materials at a value of strain near the static fracture strain. He compared his results with those predicted on the basis of a criterion which includes the work-hardening rate and the variation in flow stress with temperature as well as the heating effects

due to the plastic work. Agreement with experimental results is particularly good when the instability strain is not too great, as in the case of titanium. When the instability strain is large, the change in the work-hardening rate during straining probably should be taken into account. Culver shows that a low work-hardening rate is favorable to the formation of shear bands in steel and titanium, as is also a rapid variation in flow stress with temperature.

The temperature changes which occur during deformation at high strain rates can be determined only by the use of a high-speed detection system. A temperature detector which depends on heat conduction, e.g. a thermocouple, cannot provide an adequate response time. To date, however, only a few investigators have attempted temperature measurements with high speed equipment; in all these cases they employ a radiant energy detection system. Moss and Pond (Reference 217) performed tensile tests on specimens of copper at strain rates from 0.56 to 172 s⁻¹. They measured the radiant energy emitted by employing a photoconductive detection system calibrated so as to account for the changes in surface finish occurring as a result of the plastic strain. Afzali and later Costin et al., observed shear bands in thin-walled tubular specimens of cold-rolled steel after testing in a torsional Kolsky bar (References 115 and 218). To measure the change in temperature of their specimens during dynamic testing, Costin et al. used high-speed infrared radiation system whose essential element was an indium-antimonide photovoltaic detector. In this way they ascertained that the plastic work done is almost completely converted into heat, resulting in a temperature rise of 40 C or 50 C at a strain of about 20%. This result is consistent with the more detailed temperature measurements on aluminum and copper made by Hayashi et al. (Reference 219) also employing an indium-antimonide detector. These investigators had found that the temperature change during dynamic compression corresponded to 50 to 90 percent of the plastic work done, depending on the material, and that the maximum temperature occurred after a short time lag.

Costin et al (Reference 115) tested specimens quasi-statically and at a strain rate of 500 s⁻¹; their tests covered the temperature range -

157 C to 107 C. The shear band in these tests was made visible in two ways: first, as described in Section VI, by means of fine scribe lines, and secondly, by giving the specimen a high polish before testing. The latter method is only qualitative, but since at large strains the material loses its polish within the region of the shear band, the method shows that the bands in this test extend around the entire circumference of the specimen. The scribe lines, of course, provide quantitative information. They furnish a measure of strain as a function of the axial dimension. Thus they show that after a dynamic test there is some permanent strain along the entire length of the specimen; for AISI 1018 cold-rolled steel the strain outside the shear band is 10% to 15%, in tests at room temperature. However, within the region of the shear band the strain is much greater. Costin et al., found that the shear stress increased with the nominal strain, attaining a maximum at a nominal shear strain of about 12% before starting to decrease (Figure 2). Furthermore, if the test is interrupted at a nominal strain of about 8%, then no shear band is produced; in the latter case, the scribe lines remain straight though they are now tilted at an angle about equal to the final shear strain angle. These investigators found no shear bands under similar conditions in a hot-rolled steel, where the strain hardening rate is greater (Figure 74). They analyzed the results of their experiments by making use of a model developed by Litonski (Reference 220) for the torsion of a thin-walled tube with a defect. Litonski represents the defect by a local thinning of the tube's wall. His constitutive equation is of the form

$$\tau = c(1 - aT)(1 + b\dot{\gamma})^m \gamma^n$$

which takes into account at least approximately both strain rate and temperature effect. In this equation a, b, c, m and n are parameters that are easily evaluated if a set of stress-strain curves is available covering a range of temperatures and strain rates. For this purpose, Costin et al. used the stress-strain curves shown in Figures 2 and 74. A numerical integration of the constitutive equation then gives the stress, strain and temperature as functions of nominal strain. For the region of the defect, strain and temperature are designated γ_B and T_B , while for the remainder of the specimen γ_A and T_A are used. The results

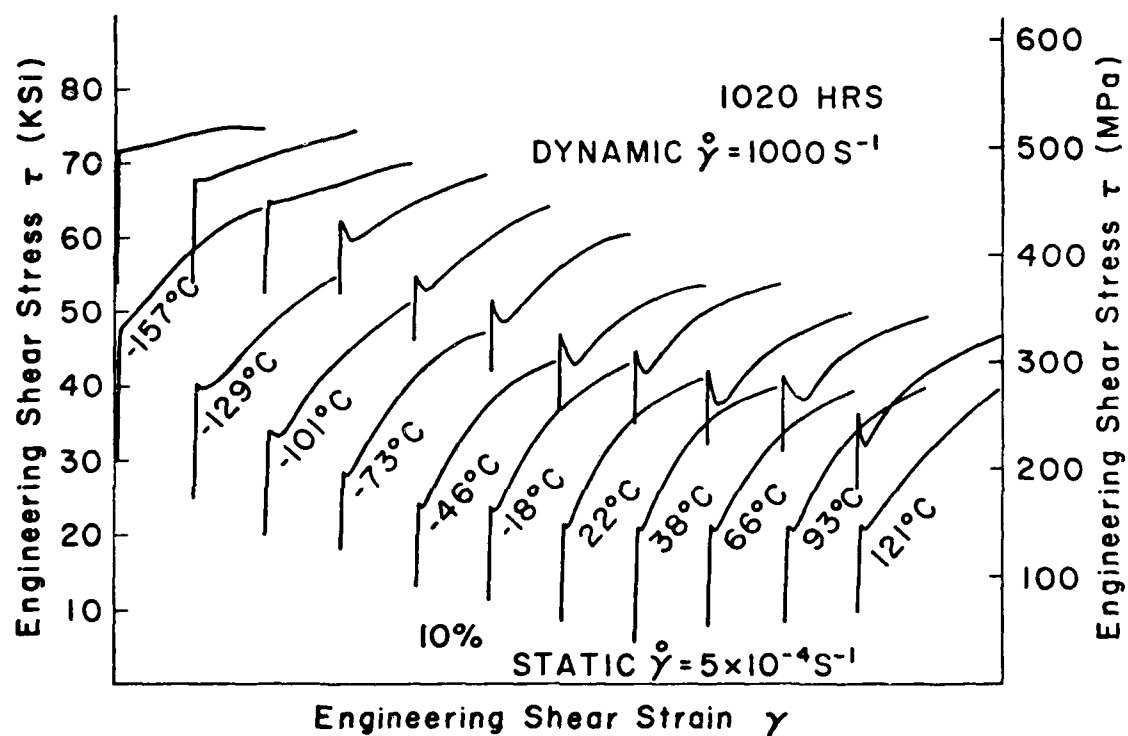


Figure 74. Static and Dynamic Shear Stress-Shear Strain Curves for 1020 Hot-Rolled Steel

are shown in Figure 75. Evidently, in the cold-rolled steel the strain and temperature within the thinned region begin to increase rapidly at a nominal strain of about 10% or 15%. In the remainder of the specimen the increase continues nearly linearly. For the hot-rolled steel, whose strain hardening rate is much steeper, this analysis predicts an almost equal rise in strain and temperature inside and outside the defect region. The temperature measurements in cold-rolled steel made by Costin et al. showed an increase in temperature within the thinned region of approximately 40 or 50°C at 20% nominal strain, which agrees closely with the value predicted by the analysis (Figure 75). After allowing their specimen sufficient time to cool, Costin et al. performed a second test to examine the subsequent shear strength of the metal within the shear band. The second test consisted simply in reloading quasi-statically those specimens which showed a shear band after the initial loading. In all cases the reloading produced considerable additional plastic strain outside the shear band region but none within it. This would seem to indicate that the material within the shear band region was relatively weaker when deformation was proceeding dynamically, probably because it was at a temperature somewhat greater than that of the remainder of the specimen; this, in spite of the fact that the large strain within the shear band results in a relatively stronger material once it has had time to cool. They conclude that the formation of shear bands in cold-rolled steel is due to the low-strain hardening rate of this material combined with the near adiabatic conditions that exist during dynamic testing.

The results of Costin et al. are in general agreement with those of Culver's experiments and with the analysis presented by Clifton (Reference 210). In his analysis, Clifton imposes a simple shear stress as a boundary condition on a body made of a rate-sensitive material and containing a geometric inhomogeneity. The shear stress is applied at the boundary by a traction $\sigma(t)$, which is a specified function of time. It results in a shear strain rate $\dot{\gamma}(t)$ which may be divided into elastic and plastic components, $\dot{\gamma}^e$ and $\dot{\gamma}^p$. In addition there is a thermoelastic volume change. For the plastic shear strain rate, Clifton takes an Arrhenius type relation

$$\dot{\gamma}^p = \dot{\gamma}_0 \exp \left[-\frac{H(1, T, P)}{KT} \right]$$

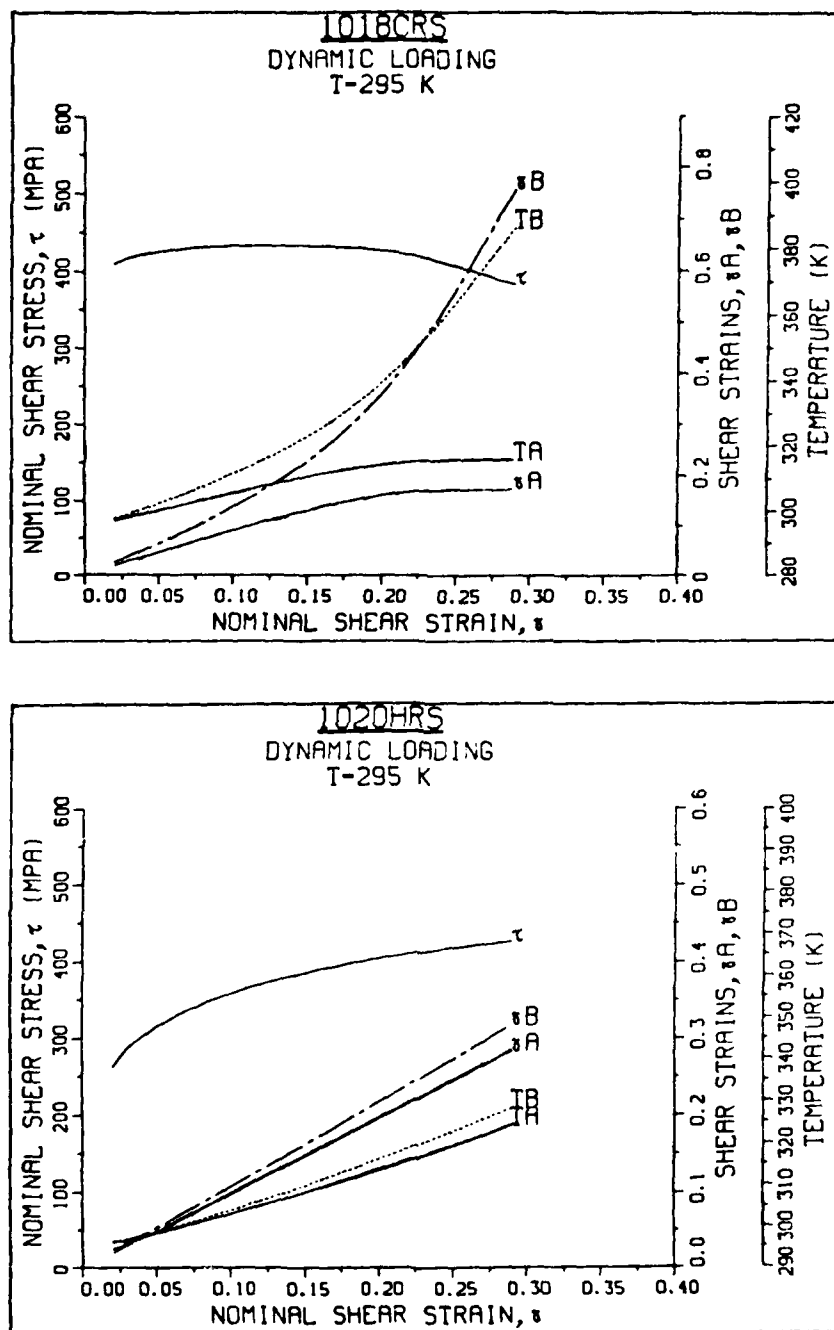


Figure 75. Calculated Values of Stress, Strain and Temperature During Dynamic Deformation of Thin-Walled Tube With a Defect (Thin Section), Showing Contrasting Behavior of 1018 Cold-Rolled Steel and 1020 Hot-Rolled Steel. Strain and Temperature Are Identified, Respectively, by γ_A and T_A for the Region of the Specimen Outside the Defect Section and by γ_B and T_B Within the Defect Section

where γ_0 is a constant, H is an activation enthalpy, K is Boltzmann's constant and T is absolute temperature. The activation enthalpy is assumed to depend on the applied shear stress τ , a shear stress τ_f that represents the resistance of the material to plastic deformation, and the hydrostatic pressure p which is related to the change in temperature. Clifton then employs a perturbation technique, simultaneously satisfying equations of compatibility of displacements, heat conduction as well as heat production due to the plastic deformation. By this method he shows that the deformation process is unstable whenever the following quantity is positive

$$- m \dot{\gamma}^{op} \left[\frac{1}{\tau_f} \frac{\partial \tau_f}{\partial \gamma} + \frac{\beta}{\rho c} \frac{\partial \tau_f}{\partial T} \right] - \frac{k \epsilon^2}{l^2 c}$$

In this expression, m is a strain rate sensitivity parameter defined by

$$m = \frac{\partial \ln \dot{\gamma}^p}{\partial \ln \tau}$$

while c is the specific heat of the material, k its thermal conductivity, ρ its mass density, $\dot{\gamma}^{op}$ the homogeneous plastic strain rate, l/ϵ is the wavelength of the inhomogeneity, and β is the fraction of plastic work converted into heat; β generally lies in the range 0.9 to 1.0. It should be noted also that $\partial \tau_f / \partial \gamma > 0$ for most materials so that the two terms within the brackets are of opposite sign. The expression presented above is a simplification of Clifton's original criterion to the case of a material for which the pressure sensitivity of the plastic resistance is assumed to be negligible. The first two terms in this criterion are the ones most likely to vary depending on the material and its condition. Their relative magnitude is thus most important, and the quantity most likely to vary by a large amount is the strain hardening rate, $\partial \tau_f / \partial \gamma^p$. A large strain hardening rate, according to this criterion, will tend to a stable deformation process, while a vanishingly small strain hardening rate may make the second term dominant. Hence, shear bands are more likely in cold-rolled steel than in hot-rolled steel. The value of the product $m \dot{\gamma}^{op}$ is also important since it multiplies two terms in expression (5). Thus a large value of $m \dot{\gamma}^{op}$ combined with a relatively large strain hardening rate would imply a very strong instability.

Johnson (Reference 221) has presented a detailed analysis of the behavior of a thin-walled tube during torsion. The analysis includes strain rate effects, strain hardening and heat conduction. The results of the analysis are compared to the behavior of copper specimen deformed in a new high speed torsional testing machine built by Lindholm et al. (Reference 222). This machine is able to impose very high strains, allowing a rotation $\theta = 3.3$ radians. It can impose this large strain rate from the quasi-static to 330 s^{-1} . With this apparatus tubular specimens of OFHC copper were tested at seven different strain rates covering the range of strain rates from 0.009 s^{-1} to the maximum of 330 s^{-1} . If one defines shear strain as $\gamma = \theta R/L$ where R is the mean radius of the specimen and L is its length, then the maximum shear strain in these experiments was 7. The results show that the strain hardening rate remains positive over the entire deformation range up to strain rates of 10 s^{-1} , (Figure 76). Furthermore, strain rate effects are positive in this range of strain rates. However, for strain rates in the range $174\text{--}330 \text{ s}^{-1}$, and starting at $\gamma \approx 2$ the hardening rate is lower than in quasi-static deformation and becomes negative above $\gamma \approx 5$. Lindholm et al. attribute this decrease in hardening rate to thermal effects due to the plastic work. They estimate, for instance, that at $\dot{\gamma} = 7$ and $\dot{\gamma} = 10 \text{ s}^{-1}$ the increase in temperature will be 447°C presuming 90% of the plastic work is converted to heat. Furthermore, if $d\sigma/dT = -0.22 \text{ MPa}/^\circ\text{C}$ for this copper, then by a simple analysis they show that the critical instability strain is $\gamma_c = 3.71$. Metallographic observation of the specimens after testing reveals both surface and cross-sectional effects within a narrow shear band region for those specimens exhibiting a drop in flow stress. Johnson (Reference 221) presents a detailed finite element analysis of the deformation in these copper specimens. His analysis shows good agreement with experimental results including a softening of the material for deformation at the higher strain rates. However, his analysis does not predict the relatively sharp drop in flow stress found experimentally at $\gamma \approx 5$.

Rogers and Shastry (Reference 223) performed impact tests on specimens of a number of different steels. Examination of the specimens after testing showed shear bands of the transformed type (white-etching)

are preceded by deformation type shear bands. Microhardness profiles tests across the width of the shear bands provided two results. First, that the hardness within the transformed bands varies linearly with the carbon content and does not depend on impact velocity. This result does not appear to hold for deformed bands, for which hardness increases the greater the deformation. Secondly, the microhardness traverse of the specimen showed that hardness decreases to either side of the transformed band, but that this decrease may not be monotonic (Figure 77). Thus an AISI 1040 steel, quenched and tempered at 200°C, shows a drop in hardness separating the transformed band region from the two deformation bands to either side of it. Rogers and Shastry surmise that the trough represents a heat-affected zone in which recovery and recrystallization have softened the material and that this trough will be found in steels that are less stable thermally. Hence, the trough is not found in the 1040 steel tempered at 400°C.

Additional investigations into shear bands are needed to establish more firmly both their cause and their nature. These should include temperature measurements as well as studies of possible metallurgical effects. As pointed out by Olson et al. (Reference 224) all the factors producing shear instabilities are not well understood. For instance, the role of pressure dependence and the presence of microvoids should be investigated, in addition to the more customary factors, e.g. strain hardening rate of thermal softening. Indeed, Hartmann et al. (Reference 225) bring in the possibility of local melting. Moss (Reference 226) questions the usual explanation of an austenitic transformation as the reason for the white-etched appearance. His experiments were performed by punching shear plugs in nickel-chrome steel plate. He employs the metals prior texture, resulting from the forming process, as reference bands to measure the large shear strains in the region of flow localization. In general, among the experimental methods available the Kolsky bar is well-suited for investigations into shear bands since it can be used to impose high strain rates and large strains either axially or in shear. However, a number of other methods are available as well and these need to be explored, as for instance the explosive expansion of hollow cylinders (Reference 227). In addition to the experimental

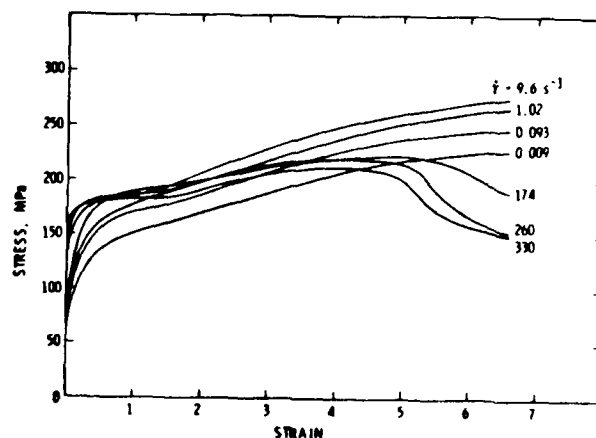


Figure 76. Shear Stress-Strain Curves for OFHC Copper

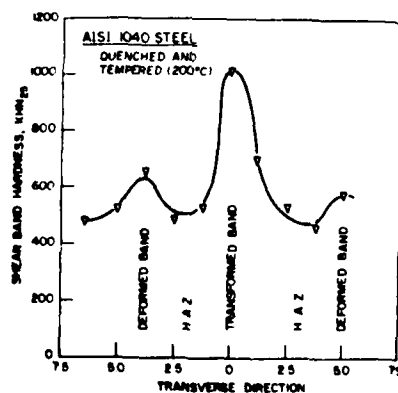


Figure 77. Profiles of the Microhardness Across a Transformed Shear Band in AISI 1040 Quenched and Tempered at 200°C

AFWAL-TR-82-4024

investigations, detailed analyses of the stability problem are needed which include finite deformations, temperature effects, strain rate sensitivity, strain hardening, etc.

SECTION IX

EXPERIMENTAL TECHNIQUES FOR HIGHER STRAIN RATES

As mentioned previously, there is strong interest today in studying the deformation of materials at ever greater strain rates. This interest stems in part from a number of immediate practical applications, including machining, metal forming and armor penetration. Furthermore, from a scientific viewpoint, the dependence on strain rate is of great importance in any attempt to determine the governing deformation mechanism. In particular, it appears that for strain rates greater than about 10^3 s^{-1} the deformation process may be governed by a viscous mechanism. In order to examine this possibility, some investigators have extended their use of the Kolsky bar to higher strain rates, as described above in Section VI. However, a strain rate of 10^4 s^{-1} is probably the maximum that can be attained with this technique and even then may involve a sacrifice in the accuracy of results. For instance, the modification most frequently used to increase the strain rate is to decrease the length of the specimen. Any end effects present during deformation will then be magnified, whether the loading in the Kolsky bar be axial or torsional. In addition, at these high strain rates because of the length of the rise-time a constant strain rate is not established until considerable strain has accumulated. A simple calculation illustrates the last point most quickly. If the rise-time is 25 microseconds then, presuming a ramp input, a strain of 12.5% will accumulate before a strain rate of $10,000 \text{ s}^{-1}$ is reached. This compares with a strain of 1.25% for a strain rate of $1,000 \text{ s}^{-1}$. The difference, actually, may be greater since the rise-time tends to increase the larger the input pulse. (An exception is the torsional Kolsky bar with explosive loading which, due in part to the absence of dispersion during torsional wave propagation, can provide a rise-time of 8 microseconds, i.e. a strain of only 0.4% to reach a strain rate of 1000 s^{-1}). One concludes from the above that in deformation at strain rates of 10^4 s^{-1} the Kolsky bar becomes useful mainly for studies involving large deformations, and, furthermore, that for strain rates greater than 10^4 s^{-1} it becomes necessary to adopt other experimental methods.

1. THE PLATE IMPACT EXPERIMENT

Plate impact experiments provide the highest strain rates attainable today in essentially one-dimensional deformation and, as mentioned above, show great promise, particularly in efforts to relate macroscopic behavior to microstructural changes. A full description of the experiment is provided by Karnes by Berkowitz and Cohen by Clifton and by Clifton and Kumar (References 228, 229, 230 and 231). The apparatus can be modified to accomplish one of a number of different purposes. For instance, by subjecting the specimen to normal impact (Figure 78), and by supplementing the impact test with microscopic observations one can perform investigations into dislocation dynamics. On the other hand, the specimen may be struck obliquely, thus leading to pressure-shear loading. The purpose of the latter test is the determination of stress-strain behavior at strain rates beyond the range that can be attained conveniently with the Kolsky bar. As such, therefore, it is closely related to the subject of the present review. The apparatus for oblique impact used by Kim and Clifton (Reference 232) is shown schematically in Figure 79. In principle this experiment resembles Kolsky's in that a thin specimen is mounted between two loading plates hard enough to remain elastic throughout impact. Since the plates are tilted relative to the direction of propagation of the flyer, the impact imposes both a normal and shear traction on the specimen's surface. As in Kolsky's experiment, the instrumentation provides measures of stress and strain rate in the specimen. Both are determined from measurements made on the back face of the target plate upon arrival of the stress pulses which originated at the interface with the specimen. It can be shown on the basis of elastic wave theory that the normal and tangential components of stress at this interface are given by

$$\sigma = -\frac{\rho c_1}{2} u_{fs} \quad \tau = -\frac{\rho c_2}{2} v_{fs}$$

where u_{fs} and v_{fs} are the normal and tangential components of particle velocity of the back face of the target, ρ is the mass density and c_1 and c_2 are the longitudinal and shear wave speeds of the target

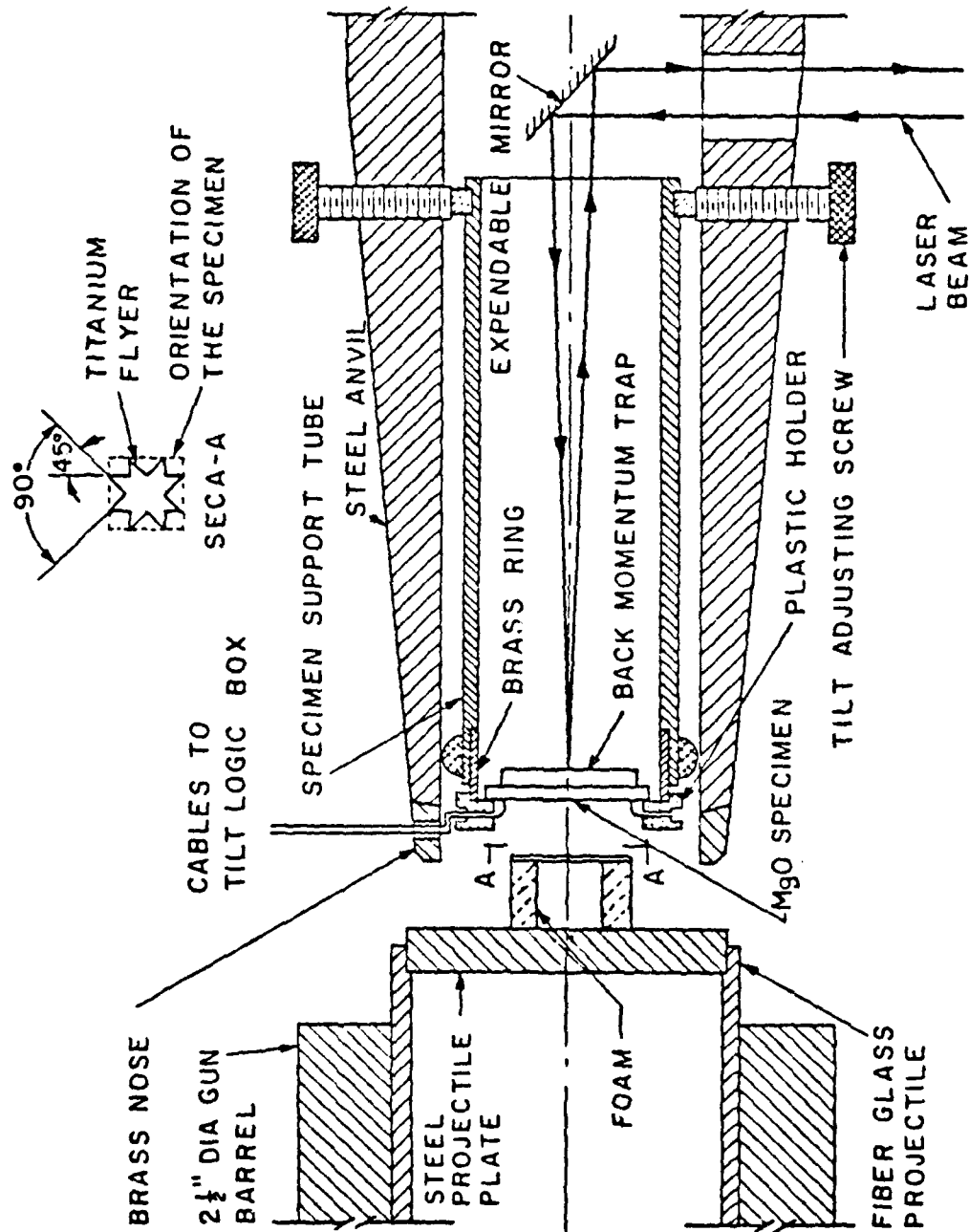


Figure 78. Schematic of the Plate Impact Experiment

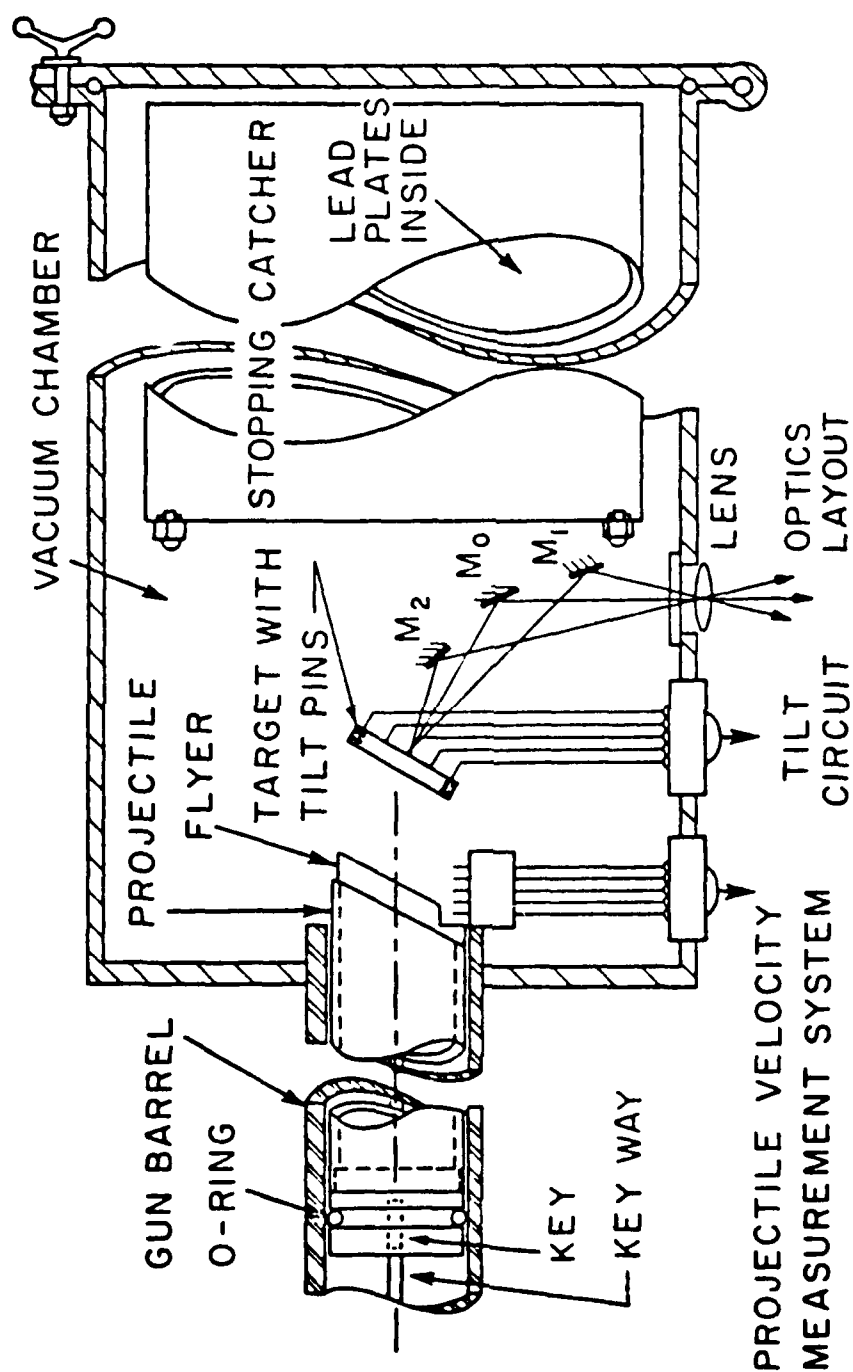


Figure 79. Schematic of Pressure-Shear Experiment

material. In order to obtain homogeneous conditions within the specimen it is necessary, just as with the Kolsky bar, to allow for a few reflections of the loading pulses. However, the much shorter rise-time achieved with plate-impact results in a very brief period from first impact to a nominally constant strain rate. The strain rate, in a specimen of thickness h , is calculated from

$$\dot{\gamma} = \frac{v_0 - 2v}{h}$$

where v_0 is the transverse component of the initial flyer plate velocity and $v = v_{fs}/2$ is the particle velocity at the interface. Thus the technique described requires in the experiment that u_{fs} and v_{fs} be measured as function of time. Clifton uses two laser interferometers for this purpose, one to measure velocity components normal to the surface and the other displacement components within the plane of the surface. Li and Clifton (Reference 233) tested 1100-0 aluminum and their results are shown in Figure 80, where a comparison is made with the results of Frantz and Duffy (reference 54) obtained at lower strain rates with a Kolsky bar. In order to account for the pre-compression in the pressure-shear experiment, the curves of Frantz and Duffy have been shifted by 2.5%. It is evident from the figure that flow stress increases far more rapidly with strain rate at the higher rates than in the range from quasi-static to 10^3 s^{-1} . This is taken as an indication that a transition occurs in the rate controlling mechanism for plastic flow between strain rates of 10^3 s^{-1} and 10^5 s^{-1} .

The advantages of the plate-impact experiment are numerous, not the least of which is the range of investigations for which it is useful. When employed for pressure-shear loading it allows for the deformation of specimens at strain rates up to 10^5 s^{-1} in an experiment of great precision and reliability. The technique undoubtedly will prove of great use in the future. When supplemented by quasi-static experiments and tests with the Kolsky bar, it makes possible a determination of material behavior over an extended span of strain rates.

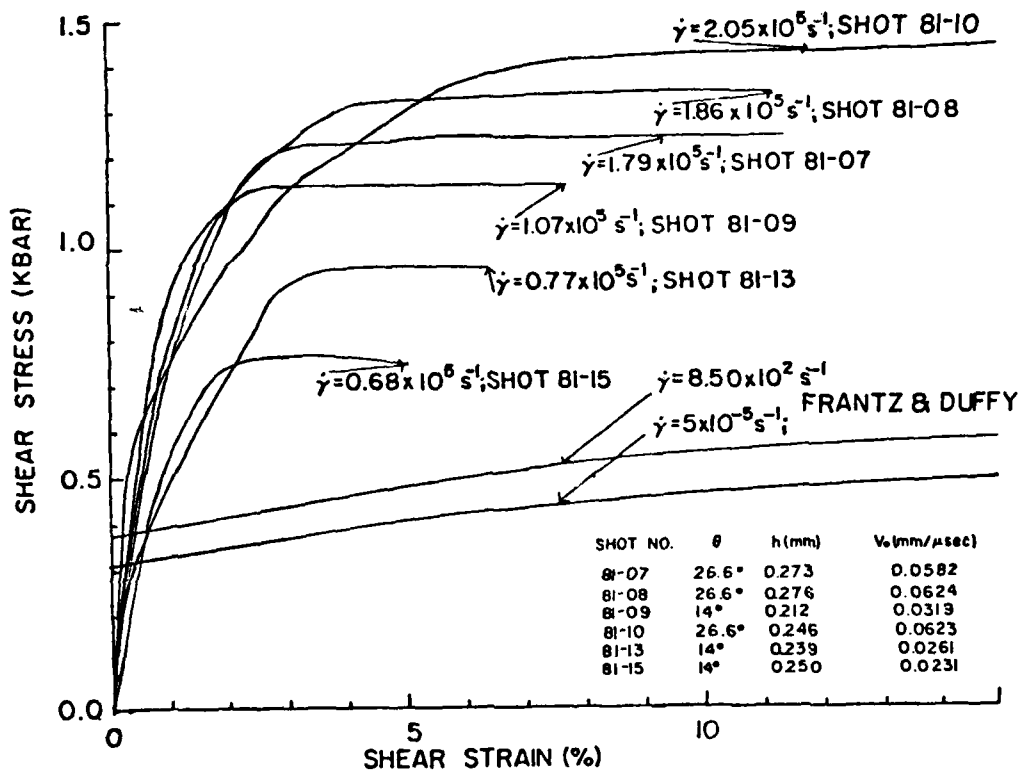


Figure 80. Dynamic Stress-Strain Curves for 1100-0 Aluminum Obtained in Pressure-Shear Experiments. Results are Compared with Those of Frantz and Duffy for the Same Material Deformed at Lower Strain Rates

2. THE DOUBLE-NOTCH SHEAR TEST

The double-notch shear test dates back to the work of J.E. Dorn and associates at the University of California, where it was used principally to deform single crystals at high strain rates, see for instance Ferguson et al. (Reference 135). It was also the method adopted by Campbell and Ferguson (Reference 99) in their tests on steel. For experiments at high strain rates, the double-notch shear test makes use of a compressional Kolsky bar. Its characteristic feature, however, is the geometry of the specimen (Figure 81a). The two end pieces of the specimen are held in the Kolsky apparatus and the center piece is given a transverse motion by the impact of the incident bar. In this way the notched regions, which constitute the gage length, are given a deformation in shear. Until recently, the disadvantage of this method has been the nonuniform state of strain within the gage length of the specimen and the fact that considerable plastic strain and rotation occur in the end pieces. Harding and Huddart (Reference 234), however, have modified the shape of the specimen to reduce considerably the deformation outside the gage length (Figure 81b). They also presented a detailed analysis of the state of strain based on a slip-line-field solution for the shear deformation within the notched region. They supplemented this analysis by a experimental determination of the strain field, made by depositing a photographic grid of small squares on the specimen's surface. As a result of these modifications and analyses, the double-notch shear test now appears to have become a considerably more reliable experimental method for tests to strain rates of 10^4 s^{-1} , as long as the strains do not exceed about 20%. The method has been used to determine the effects of strain rate on the flow properties of α -uranium, Harding and Huddart (Reference 234).

3. MACHINING AND METAL FORMING

Judging by the increasing number of publications relating dynamic plasticity to machining and forming processes, it is clear that research in this area is growing. This seems entirely warranted in view of the importance of metal removal and metal forming processes and also in view of their potential for more basic studies. The work of Ghosh (Reference 235) for instance, illustrates the application of dynamic plasticity to sheet metal forming.

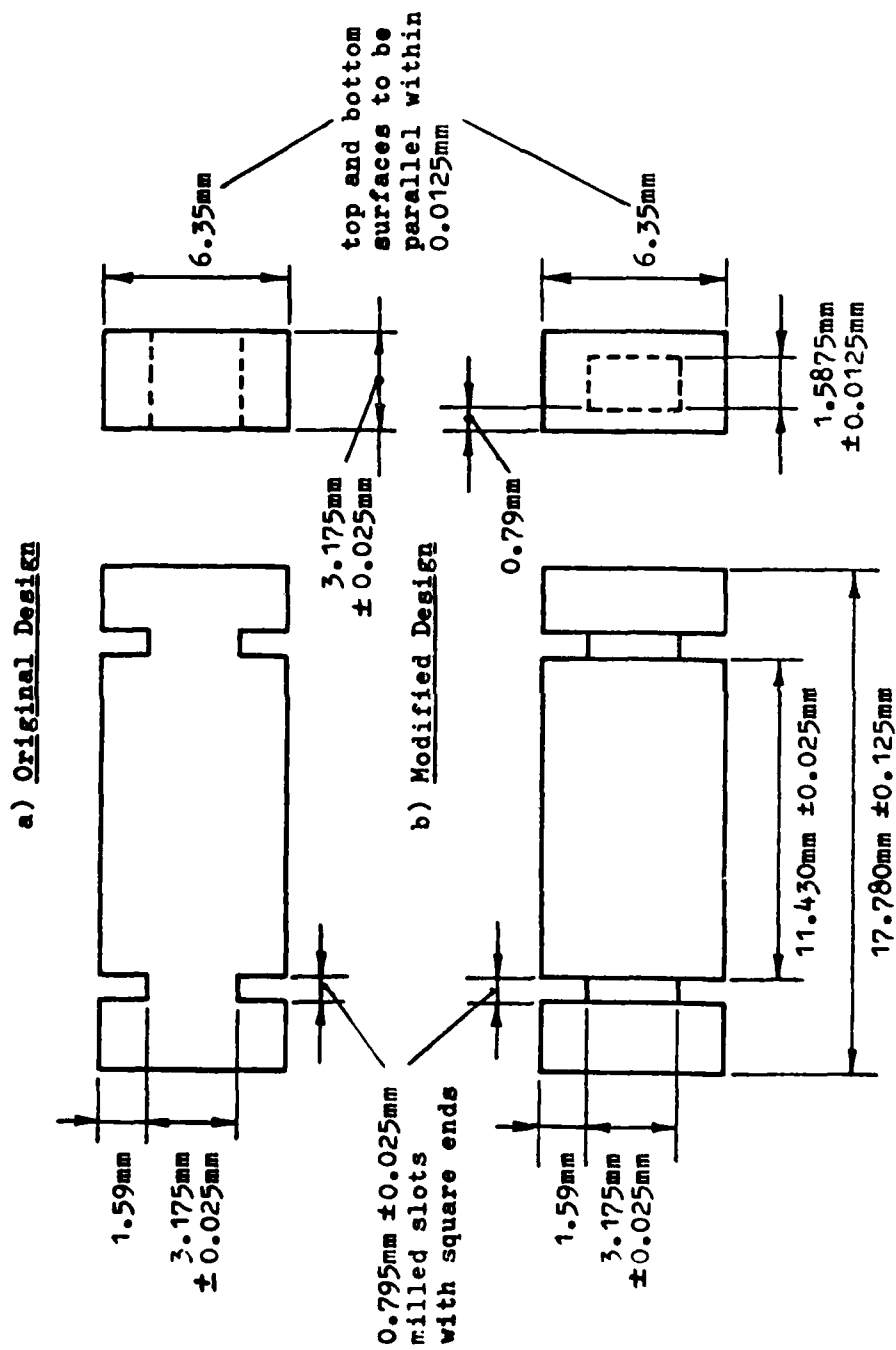


Figure 81. Designs of Double-Shear Specimens

Both metal forming and machining involve not only high strain rates but temperature effects as well; frequently they involve also shear-banding and fracture. Difficulties arise, however, in the interpretation of test results because of the nonuniformity of the stress and strain fields and the resulting complications encountered in measuring either of these quantities. During the process of metal chip removal, even at conventional machining speeds, the strain rates are very high, often increasing substantially the flow stresses opposing the progress of the tool within the work piece. A number of workers have investigated the effects of these high strain rates on the machining process, generally combining their analysis with the effects of the concomitant increase in temperature. Among the published papers on strain rate effects in machining one can cite Boothroyd and Bailey, Oxley, Spaans, and Oxley and Hastings (References 236, 237, 238 and 239). Reviews of investigations into metal cutting have been presented by von Turkovitch and Boothroyd (References 240 and 241).

An important step in the investigations into machining and forming is to estimate the strain rates in the region ahead of the tool and to determine the geometric distribution of these strain rates throughout the work piece as functions of time. Studies of this nature must include the effect on the flow stress of the temperature increase due to deformation at these high strain rates. As pointed out by Oxley (Reference 211) the problem is further complicated by the fact that machining is generally a discontinuous process. This is brought out very clearly in the work of LeMaitre et al. (Reference 242). Furthermore, at very high machining speeds the chip formation may even be accompanied by adiabatic shearing. In spite of these difficulties Oxley and coworkers have developed a model which appears to predict quite accurately the strain rates in the plastic zone in which the chip is formed in front of the cutting tool. These results are presented in a number of papers of which the latest are by Mathew et al. and Hastings et al. (References 243 and 244).

Metal forming techniques, e.g., extrusion or rolling, have probably a greater potential for dynamic plasticity studies than chip removal

because the processes do not involve fracture and are generally continuous: as the material goes by, the strain and strain rate distributions usually remain unchanged as seen by a fixed observer. Studies of hot-workability have been reviewed by Sellars and Tegart (Reference 9) and the influence of strain rate on cold forming of steels by Martensson (Reference 245). In general, the strains involved in forming are very large, and at these high strains the stress-strain relation tends to be flatter. As a result, many investigators adopt a constitutive equation relating the natural logarithm of strain rate and the hyperbolic sine of stress (Equation 34). Studies employing this constitutive relation are reviewed above in Sections V and VI. One should cite the work of Jonas and co-workers, who have shown that Equation 34 fits very well results obtained from extrusion tests. They performed experiments over a wide temperature range and with several metals, for example, their work on aluminum, Wong and Jonas and with zinc, Gagnon and Jonas (References 246 and 247).

Finally, one should mention high energy rate forming in which the material is formed explosively. When the explosive charge is not in direct contact with the work piece, then strain rates of 10^2 to 10^4 s⁻¹ are attained. When direct contact obtains, then true shock waves are formed and the strain rates are greater than 10^4 s⁻¹. As mentioned previously, the subject of high energy forming was reviewed by Orava and Otto (Reference 248).

SECTION X

COMPARISON OF THE STRAIN RATE SENSITIVITIES OF A NUMBER OF METALS

Direct comparisons of the strain rate sensitivities obtained by different authors are difficult to make, and quantitative agreement is not likely for a variety of reasons. For instance, some investigators test high purity aluminum, while others test 1100-0 aluminum, or an aluminum alloy. Differences between the various steels are even greater. Furthermore, the metal stock from which the specimens are machined may be formed in a variety of ways, e.g., cold-rolled vs. hot-rolled. The investigator may choose not to heat-treat his specimens, or else he may opt to anneal at a high temperature for a long period of time. Furthermore, there are obvious differences in the testing methods adopted. In the case of incremental strain rate tests, as pointed out above, some investigators unload their specimens completely; others avoid this practice since, as Lindholm showed, the dwell time at zero load may be of considerable importance in the subsequent behavior. Lastly, the strain rate sensitivity of a metal may well depend on the strain rates involved; yet all investigators do not test between the same strain rates nor carry their tests to the same values of strain. In view of all these differences, the agreement between various investigators' results is remarkably close. This permits a few very general conclusions as to the influence of strain rate on the behavior of various metals. These conclusions are based on data collected in tables and graphs and discussed below. Much of this material was first presented as part of the J. D. Campbell Memorial lecture, Duffy (Reference 249).

Table I lists the various papers which were used to compile the graphs. Not all investigations cited in the present review were included. More recent papers generally were favored and an attempt was made to include as many incremental strain rate results as possible. In order to compare results of shear and axial tests, all the results of axial test were converted to shear; this was effected by multiplying axial strain by $\sqrt{3}$ and dividing axial stress by the same factor. The graphs in Figures 82-87 provide two measures of the dependence of flow

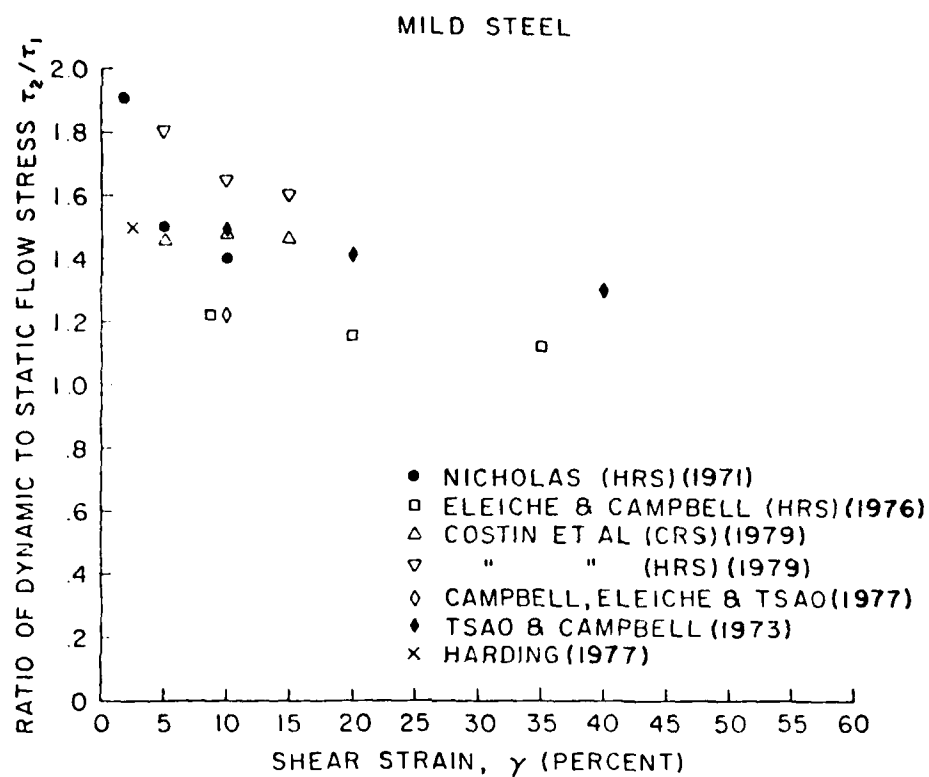


Figure 82. Ratio of Dynamic Shear Stress, τ_2 , to Static Shear Stress, τ_1 Plotted as a Function of Shear Strain. Material is Mild Steel

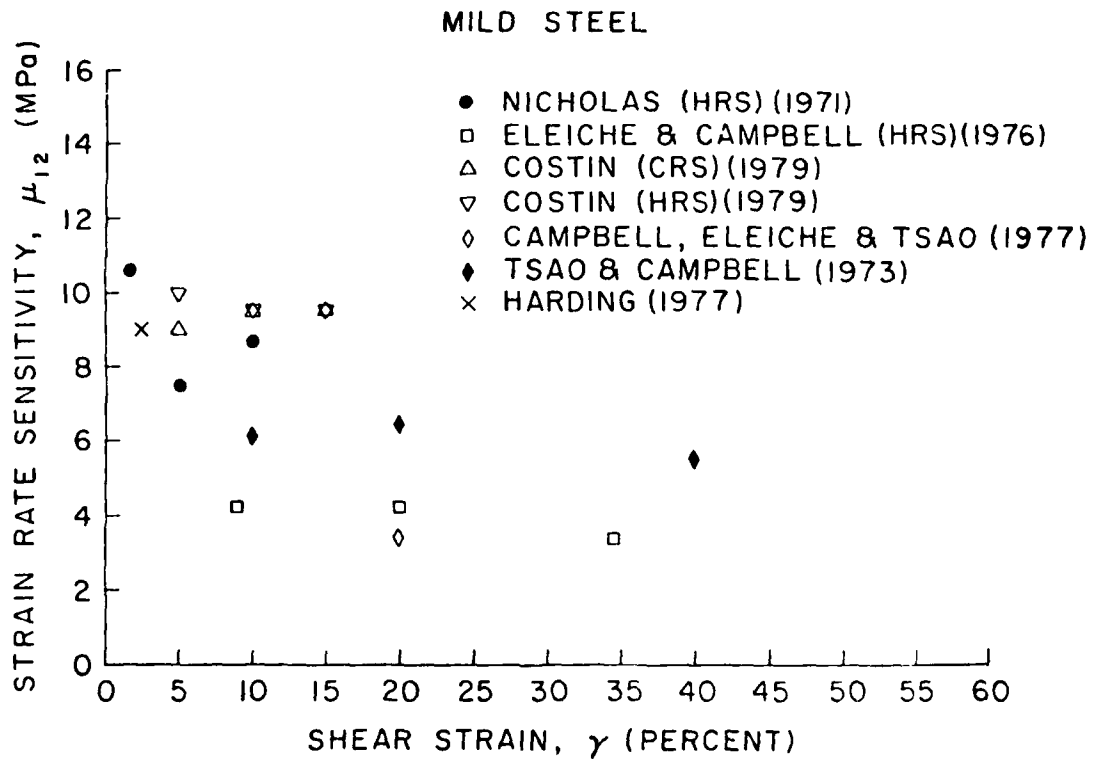


Figure 83. Apparent Strain Rate Sensitivity, μ_{12} , as a Function of Shear Strain. Material is Mild Steel

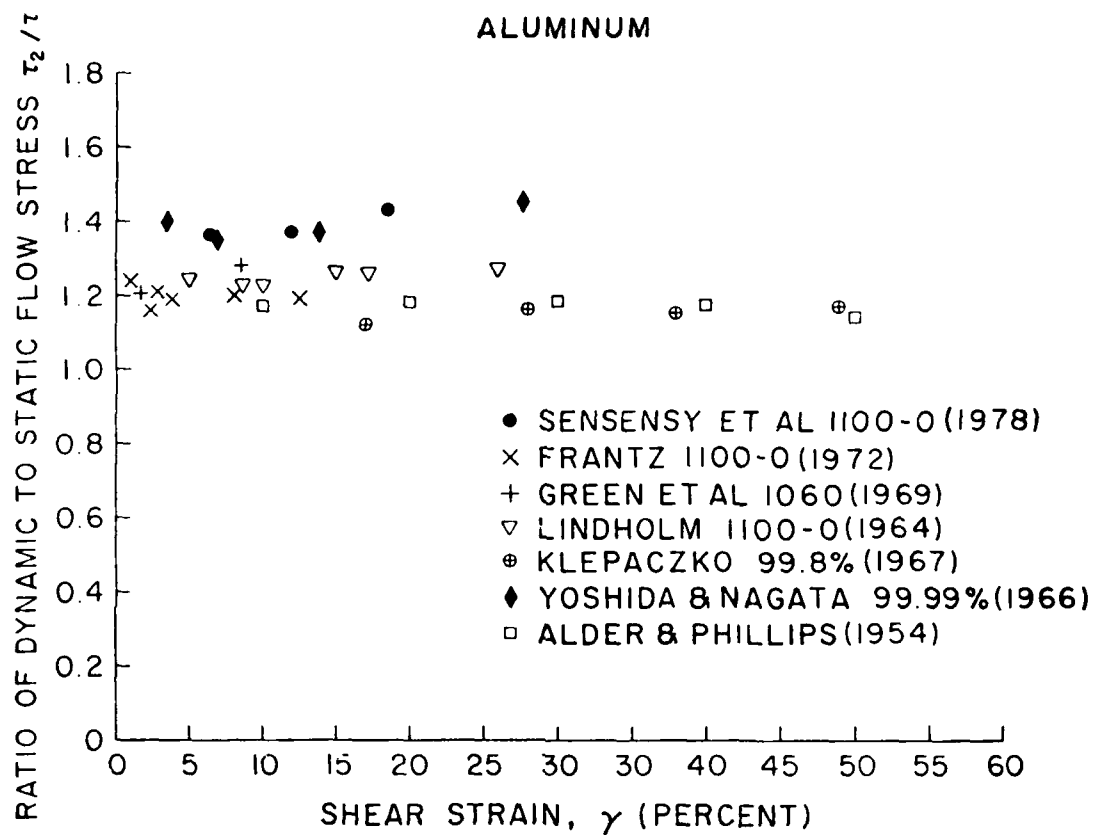


Figure 84. Ratio of Dynamic Shear Stress, τ_2 , to Static Shear Stress, τ_1 , Plotted as a Function of Shear Strain. Material is Aluminum

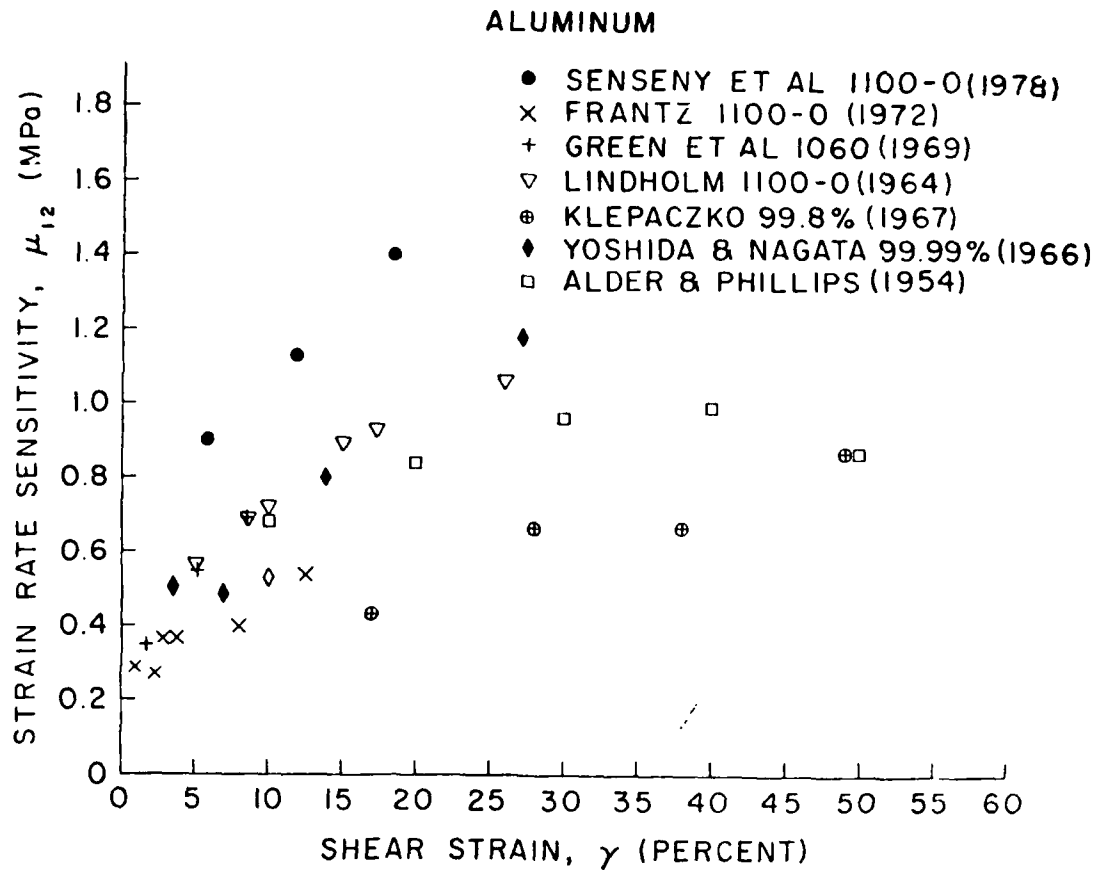


Figure 85. Apparent Strain Rate Sensitivity, μ_{12} , as Function of Shear Strain. Material is Aluminum

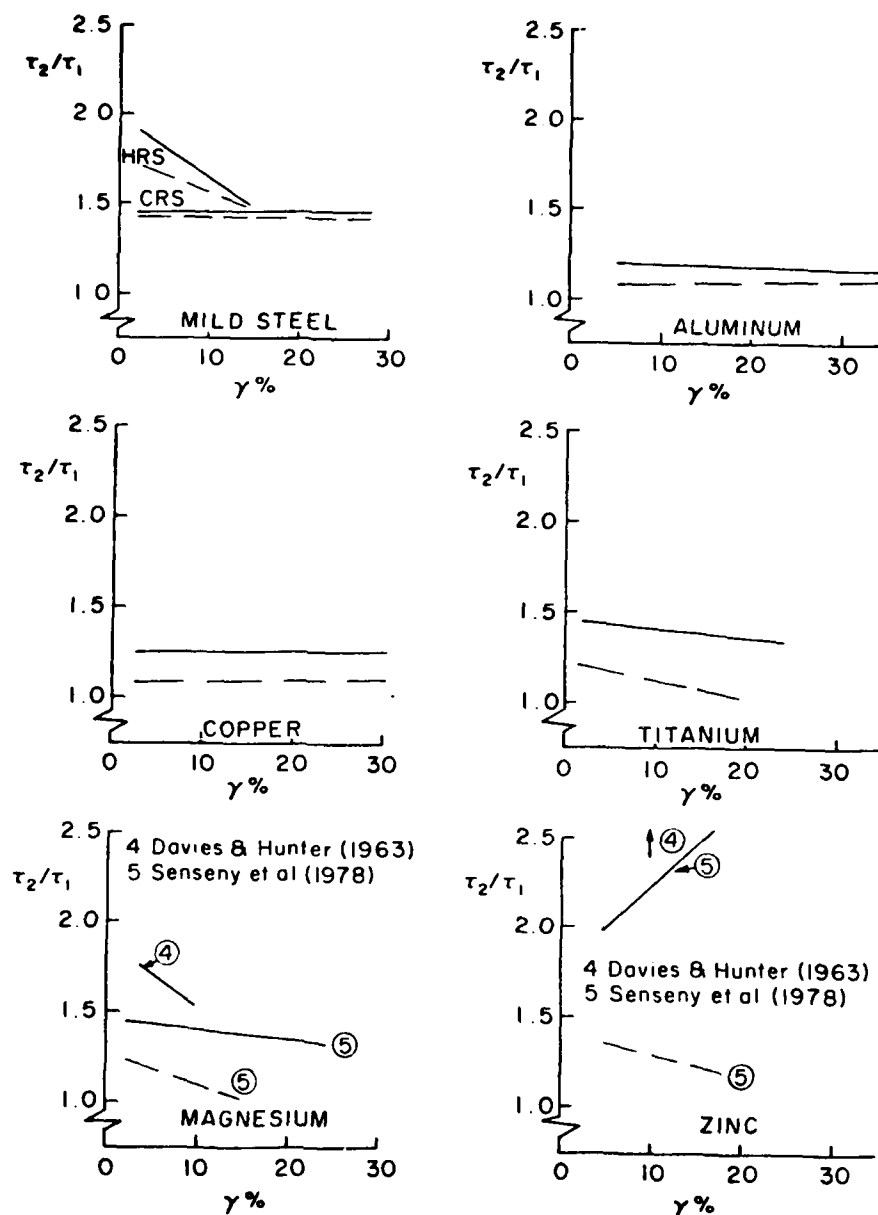


Figure 86. Ratio of Dynamic Shear Stress, τ_2 , to Static Shear Stress, τ_1 , Plotted as a Function of Shear Strain. Solid Lines Represent Results of Tests at Constant Strain Rates; Dashed Lines are Obtained from Incremental Strain Rate Tests.

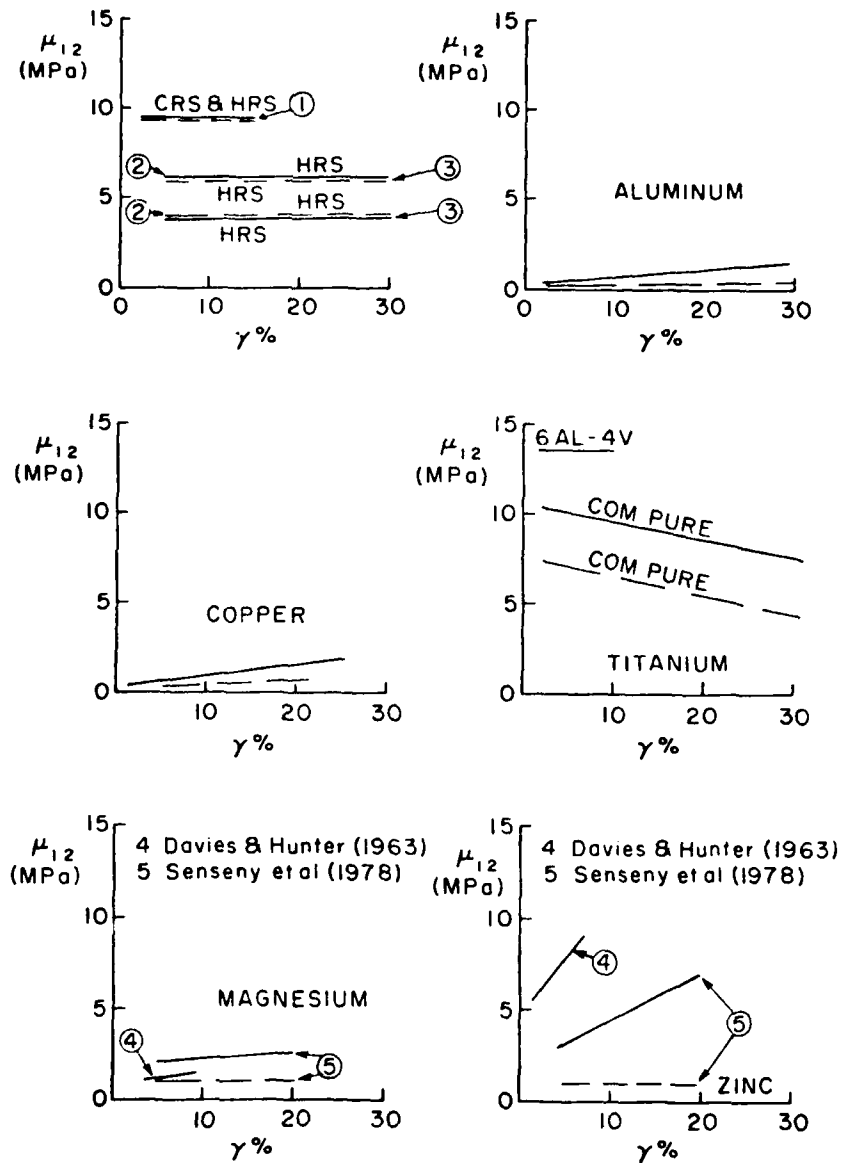


Figure 87. Strain Rate Sensitivities for Various Metals Plotted as a Function of Strain Rate. Solid Lines are Apparent and Dashed Lines are the True Strain Rate Sensitivities.

stress on strain rate, each plotted as a function of the strain accumulated during testing. Figures 82, 84 and 86 present the ratio τ_2/τ_1 , where τ_2 and τ_1 are respectively the flow stresses in shear obtained from tests at the constant strain rates $\dot{\epsilon}_2 = 10^3 \text{ s}^{-1}$ and $\dot{\epsilon}_1 = 10^{-3} \text{ s}^{-1}$. (Whenever data were not available at either of these two rates, then the nearest value was chosen; however, as indicated in Table I, in some instances it was necessary to employ values of strain rate differing considerably from 10^3 s^{-1} or 10^{-3} s^{-1} .) Figures 83, 85 and 87 present the corresponding values of the strain rate sensitivity in shear, μ_{12} , as defined through Equation 59 in Section VII. This measure of strain rate sensitivity is frequently adopted when deformation is governed by a thermally-activated mechanism, i.e. when deformation is governed by a relation such as that given by Equation 2. If, in addition, the energy of activation is a linear function of the shear stress, then μ_{12} provides a measure of the apparent activation volume, v , through

$$v = - \left(\frac{\partial \Delta G}{\partial \tau} \right)_T^* \approx - \left(\frac{\partial \Delta G}{\partial \tau} \right)_T = \frac{kT}{\mu_{12}} \quad (63)$$

where $\tau = \tau^* + \tau_u$. As defined in Figure 1, τ^* is the thermal stress component, while τ_u is the athermal component. The strain rate sensitivity defined by μ_{12} in Equation 59 was calculated on the basis of tests conducted entirely at constant strain rates. Since incremental strain rate tests are believed to give a truer measure of strain rate sensitivity, the true strain rate sensitivity, $\bar{\mu}_{12}$, defined by Equation 60, is frequently used instead. Values of $\bar{\mu}_{12}$ are also provided in the figures.

Figures 82-85, for steel and aluminum, are presented in order to show the variations in the results obtained by different investigators. These figures show the results of constant strain rate experiments only, but similar figures were made for incremental strain rate tests as well as for the other metals, i.e. copper, magnesium, titanium and zinc.

The degree of agreement shown in Figures 82-85 seems quite high when one recalls the difference in specimen preparation and in experimental techniques mentioned above. Similar agreement appears in the copper results, but not in those of the other metals. Titanium, for which insufficient data are available, shows strong differences in behavior between the commercially pure materials and the 6Al - 4V alloy. For magnesium and zinc there are only two investigations; in the case of magnesium the results happen to agree or nearly so, but they disagree in the case of zinc. There are some further disagreements with regard to history effect in steel, which are indicated below.

Figures 86 and 87 summarize the results presented in graphs such as those of Figures 82-85. It is evident immediately that aluminum and copper are considerably less sensitive to strain rate than is steel. The values of μ_{12} and $\bar{\mu}_{12}$ for the two fcc metals increase nearly linearly with accumulated strain. This may not appear very clearly on the scale used in Figure 87, but represents quite a definite trend in all the data. For steel, μ_{12} and $\bar{\mu}_{12}$ are independent of strain. Figure 87 shows that there is some disagreement as to the behavior of steel. The results of Nicholas on a hot-rolled steel and of Costin et al. with both hot-rolled and cold-rolled steels are substantially in agreement (References 115 and 152). In addition, Harding (Reference 106) using quite a different experimental technique presents a point on this curve (at $\epsilon = 2.5\%$) which agrees with the values of Nicholas and of Costin et al. On the other hand, Tsao and Campbell, Eleiche and Campbell, and Campbell et al., obtained lower values for the strain rate sensitivities (References 180, 181 and 250). The reason for this disagreement is not all clear. The only consistent difference is one of material: the higher values of μ_{12} were obtained with steels having a carbon content of about 0.20%. The steels used in the experiments of Campbell and associates had a lower carbon content, 0.075% to 0.125%. More important than the difference in the values of μ_{12} is the behavior following a sudden increment in strain rate. At room temperature, Nicholas as well as Klepaczko and Duffy find only a small effect due to strain rate history, i.e. $\mu_{12} \approx \bar{\mu}_{12}$. Eleiche and Campbell, as well as Campbell et al., find that $\bar{\mu}_{12} > \mu_{12}$. (References 152, 180, 181, and 187). This difference also remains unexplained.

Results presented for the other metals are based on fewer experiments. Maiden and Green (Reference 127) tested 6 Al - 4V titanium alloy. Even when annealed, this alloy may contain α and β phases and, in any case, its flow stress is considerably higher than one of commercially pure titanium. The latter explains why it is possible to have such a large difference in the respective values of μ_{12} , while the ratio τ_2/τ_1 is about the same for the two metals. The results of the incremental strain rate tests of Nicholas, and those of Eleiche and Campbell with commercially pure titanium, are substantially in agreement (Reference 152 and 180). As may be seen in Figures 86 and 87, the strain rate sensitivity is fairly large and there are some effects due to strain rate history. For the other hcp metals, magnesium and zinc, results are really incomplete. The work of Davies and Hunter (Reference 113) does not include incremental strain rate tests and does not specify the strain rate for the quasi-static tests. Furthermore, there is considerable disagreement between these results and those of Senseny et al. (Reference 59) in the case of zinc. Finally, with regard to the hcp metals one should point out the importance of grain size on strain rate sensitivity as brought out by the work of Prasad and Armstrong (Reference 252).

It is also of considerable interest to determine the temperature dependence of $\bar{\mu}_{12}$, particularly in view of its relationship to the apparent activation volume, v , Equation 63. Reviewing the various experiments described in Section VII, one can see that few investigators thus far have measured $\bar{\mu}_{12}$ as a function of test temperature. Eleiche and Campbell (Reference 180) calculated the value of $\bar{\mu}_{12}$ for a mild steel; their results were presented in Figure 57. Based on the test results of Klepaczko and Duffy (Reference 187); it is possible to evaluate $\bar{\mu}_{12}$ for AISI 1020 hot-rolled steel. The values agree almost precisely with those of Eleiche and Campbell. Hence, it appears that μ_{12} decreases sharply with test temperature for low carbon steel. As a result v/b^3 must increase rapidly with temperature. The values of v/b^3 found by Eleiche and Campbell are indicated in Figure 57 by the intersections of the solid and dashed lines. For copper, there may be disagreement between the results of Eleiche and Campbell, on the one

hand, and those of Senseny et al. (Reference 59) on the other. The former investigators find that $\bar{\mu}_{12}$ increases fairly rapidly with test temperature (Figure 50) while Senseny et al. obtain a smaller dependence on temperature. However, the comparison is difficult to make. In the first place, Eleiche and Campbell provide results only for a relatively restricted temperature range, 123K to 223K. Furthermore, the strain ranges are different: the maximum prestrain in the investigation of Eleiche and Campbell is over 80%, while it is under 20% in that of Senseny et al. In either case, it appears that the temperature dependence of $\bar{\mu}_{12}$ is quite different in fcc metals from that found in steel. For titanium (hcp), according to Eleiche and Campbell, the values of $\bar{\mu}_{12}$ increase with temperature up to maximum occurring in the neighborhood of 500K, above which $\bar{\mu}_{12}$ again decreases. Undoubtedly, the most thorough study of titanium at constant strain rates is that due to Harding (Reference 252). Harding performed experiments in tension with a commercially pure titanium at five temperatures from 77K to 288K. He covered a wide range of strain rates from the quasi-static to 2500 s⁻¹. The dependence of flow stress on strain rate which he obtained is shown in Figure 88 and the computed value of v/b^3 in Figure 89. These results do not seem inconsistent with those of Eleiche and Campbell. In general, all the values of v/b^3 found in high strain testing lie within the range of values obtained by other types of experiments. However, additional data are needed before firm conclusions can be drawn. To secure these data incremental strain rate experiments must be conducted over an extended temperature range.

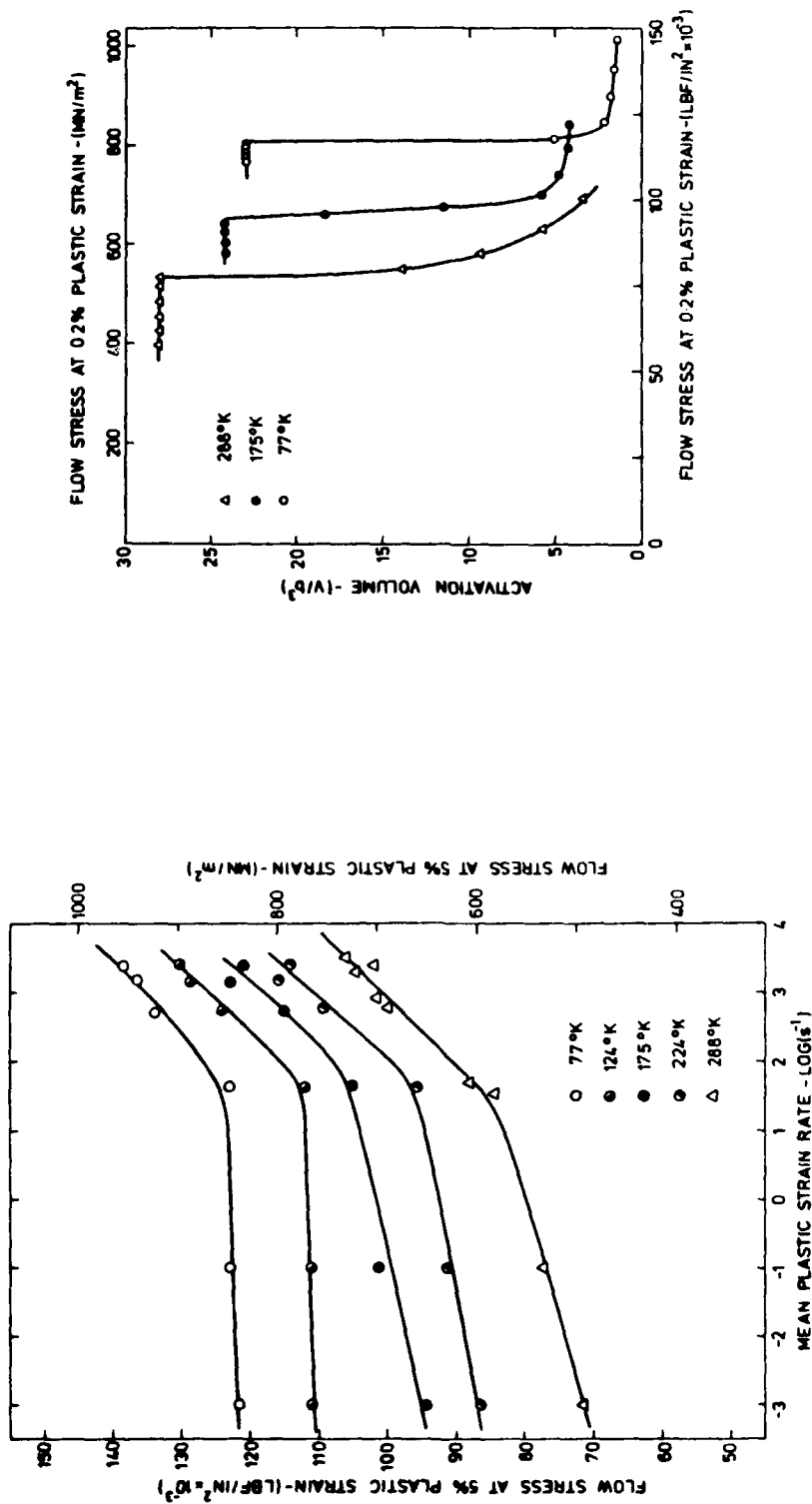


Figure 88. The Variation of Flow Stress With Strain-Rate for Commercially Pure Titanium at 5% Plastic Strain

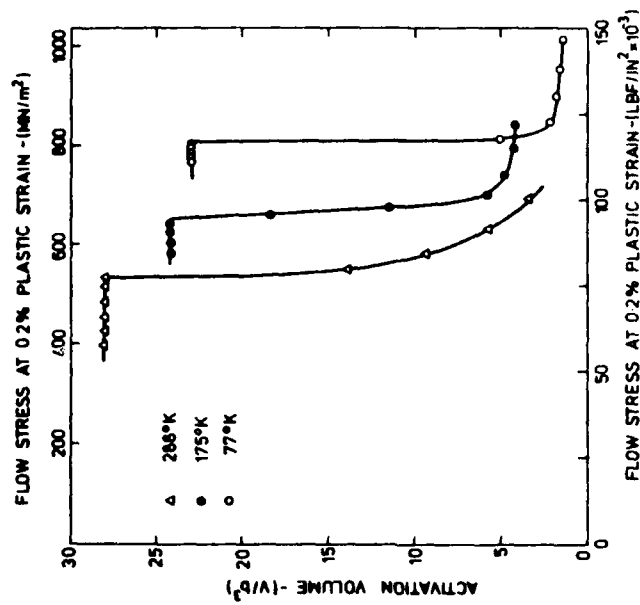


Figure 89. Variation of Activation Volume With Flow Stress in Commercially Pure Titanium at 0.2% Plastic Strain

SECTION XI

DIRECTIONS FOR FUTURE INVESTIGATIONS

It is always risky to make recommendations for future research. Nevertheless, after one has reviewed past work certain trends are apparent as well as certain gaps. Noting these recommendations are probably of value.

Since the lattice structure of a metal determines to a large extent the effect of strain rate and strain rate history on its behavior during dynamic deformation, it forms a natural classification when considering directions for future experimental research.

Fcc metals, particularly aluminum and copper, have been the subject of many investigations. As a result their dynamic response is much better understood than that of other metals. Hence, there does not appear to be a need for further uniaxial tests with these metals, if the testing is to be restricted to constant strain rates in the range from the quasi-static to 10^3 s^{-1} . There is an important need, however, to extend the range of strain rates beyond 10^3 s^{-1} for all metals, including fcc metals, both for the sake of applications and for more fundamental reasons. Furthermore, temperature and strain rate history experiments are needed particularly with single crystals of fcc metals, together with metallurgical studies of the changes that accompany deformation. Investigations of strain rate history effects should include other types of tests in addition to incremental strain rate tests. In particular, future investigations should include sudden reductions in the imposed dynamic strain rate in order to study the time-lag which apparently precedes the resulting decrease in flow stress. Experiments of this nature should be combined with studies into the effects of rapid changes in temperature and should include observations of changes in the specimen's substructure.

Among the bcc metals, only iron and steel have been the subject of frequent investigation. However, even for iron and steel additional experiments are needed, in particular, studies of temperature history and strain rate history effects. These tests should cover temperatures from the cryogenic to half the melting temperature and perhaps higher. Such experiments would enable us to categorize steels according to their strain rate sensitivity and also according to their sensitivity to history effects. Other types of experiments with steels are needed as well. These should include tests with multiple strain rate increments, as well as multiaxial loading. The significance of the time-lag observed after a drop in strain rate must be investigated for steels as well as for the fcc metals.

Aside from iron and steel, very few bcc metals have been tested at dynamic rates. It would be of value to compare strain rate history effects in other bcc metals, since a question remains as to the relative importance of impurities in determining history effects as opposed to the bcc structure itself. In general, the dynamic behavior of bcc metals, including steel, is not understood sufficiently well, either on the macroscopic or microscopic scales; this, in spite of the great practical importance of steel and of the fact that strain rate effects are more pronounced for this metal than other common metals.

A few investigators have made important studies of hcp metals, see for instance Armstrong, and a few incremental strain rate experiments with hcp metals have been conducted at lower strain rates, Santhanam et al. or de Meester et al. (References 253, 254 and 255). However, there are apparently no data with single crystals involving incremental strain rates into the dynamic range. From the fundamental research viewpoint, such work is important in order to understand better the general role played by the crystal structure. Furthermore, some of these metals, for instance titanium, do have important practical applications.

Research into the formulation of constitutive equations to describe material behavior must continue from both the phenomenological and microstructural viewpoints. Constitutive equations based on

phenomenological variables will have early applications in practice, indeed considerable success with this approach already has been achieved by a number of investigators. However, as pointed out by Sutterlin (Reference 3) what success has been achieved thus far in the inclusion of time-dependence is probably due in part to the small change in flow stress generally resulting from a comparatively large change in strain rate. For instance, for aluminum or copper, $\tau_2/\tau_1 \approx 1.2$ when $\dot{\gamma}_2/\dot{\gamma}_1 = 106$. However, for mild steel, and the same ratio of strain rates, $\tau_2/\tau_1 \approx 1.5$ to 2. Thus success to date depends again at least in part on the particular crystal structure. Furthermore, the values quoted are obtained for a maximum strain rate of about 10^3 s^{-1} , and at room temperature. In the future, many applications, e.g., metal forming and penetration, will involve increasingly higher strain rates and higher temperatures; as a result, the value of τ_2/τ_1 may change considerably. Hence, both for practical reasons and for more fundamental purposes, the formulation of constitutive equations will require that they be based on microstructural or thermodynamic considerations.

As to strain rate history effects, it must be recalled that their magnitude depends upon the particular crystal structure, temperature and perhaps mode of testing. They even appear to be absent for particular metals under the right testing conditions. Hence, progress in modelling strain rate effects has depended upon the crystal structure. Most effort has been expended on the representation of the behavior of fcc metals, and a fair degree of success has been achieved here. However, constitutive equations are needed, even for fcc metals, which will represent drops in strain rate (or sudden increases in temperature) as well as more complicated loading or temperature paths. For metals of the other crystal structures very little work has been attempted. One exception is steel and the recent work of Eleiche and Campbell, Klepaczko and Duffy, and Klepaczko (References 180, 187 and 188).

Whatever procedure may be taken in developing constitutive equations, it is essential that research be continued in the complicated problem of relating microscopic behavior to macroscopic plastic flow. Undoubtedly, considerable time will be required before results of

practical significance are attained. Research of this nature can be greatly facilitated by and may even require the participation of groups of investigators with differing backgrounds, i.e., metal physicists, metallurgists and engineers, in order to bring various points of view and various experimental methods to bear on the same problem. In this respect, the plate-impact experiment holds great promise, as do combinations of experimental techniques, as exemplified by high strain rate tests combined with SEM measurements, or by the work of Shioiri and Satoh, in which ultrasonic measurements are made during dynamic loading to obtain measurements of macroscopic variables simultaneously with a measure of dislocation behavior (References 256 and 269).

The present review does not cover multiaxial experiments; the reader is referred to the papers of Lindholm and of Hayashi and Tanimoto on the subject (References 257 and 267). Multiaxial results are of great importance for applications, as well as for more fundamental studies, and must be pursued today even though uniaxial behavior is not yet fully understood.

Metal forming and machining are hardly touched upon in the present review. This is unfortunate because they constitute a most important practical application and, furthermore, because they are potentially an excellent research tool. They involve high strain rates, large strains, and frequently, high temperatures. In particular, metal forming is very attractive as a test technique from the research viewpoint because of the high strain rates, so easily attained. Unfortunately, detailed measurements of stress, strain and strain rate are difficult to make during metal forming. This is what has made metal forming difficult to use as a research tool; yet because of its great potential it seems likely that investigators in the future will continue to use it as a test method. An added benefit is that research by means of metal forming or metal removal increases our knowledge of these processes themselves.

Research is needed into the formation of shear bands. Because of their role in machining, in fracture and in penetration, shear bands are most important, and yet neither their nature nor their causes are well

understood. The experimental techniques used in dynamic plasticity are well-suited to their study.

Finally, there appears to be very little published research into the dynamic behavior of materials following irradiation, as would be met in the core of a reactor. The few published papers on high rates of strain involving irradiated materials were published in Europe. Of direct bearing are the papers of Campbell and Harding, Dusek, Albertini and Montagnani, Harding, Bohm and Closs, and Buchar and Bilek (References 139, 256, 258, 260, 261, 262 and 263). As pointed out in the previous edition of this review, efforts in the United States apparently are limited to lower strain rates, Wronski et. al., Ring et al. and Zaverl and Lee.. (References 264, 265 and 266). This continues to be the case.

TABLE 1

REFERENCES AND DATA FOR GRAPHS TO FIGURES 82 THORUGH 87

Authors	Material, Condition, Loading Mode	Strain Rates for Graphs	Maximum Strain
<u>STEEL</u>			
Nicholas (1971)	1020 hot-rolled 1600 F for 15 min. Torsion	$\dot{\gamma}_1 = 10^{-3} \text{ s}^{-1}$ $\dot{\gamma}_2 = 25 \text{ s}^{-1}$	$\gamma = 10\%$
Tsao & Campbell (1973)	EN 2A (0.075% C) Torsion	$\dot{\gamma}_1 = 10^{-2} \text{ s}^{-1}$ $\dot{\gamma}_2 = 10^3 \text{ s}^{-1}$	$\gamma = 50\%$
Campbell, Eleiche & Tsao (1977)	EN 2A (0.075% C) Annealed at 750C Torsion	$\dot{\gamma}_1 = 10^{-3} \text{ s}^{-1}$ $\dot{\gamma}_2 = 900 \text{ s}^{-1}$	$\gamma = 90\%$
Eleiche & Campbell (1976a)	EN 1B; hot-rolled no heat treatment Torsion	$\dot{\gamma}_1 = .006 \text{ s}^{-1}$ $\dot{\gamma}_2 = 10^3 \text{ s}^{-1}$	$\gamma = 180\%$
Harding (1977)	BS 968 (0.20% C); normalized at 1173 K Compression	$\dot{\epsilon}_1 = 10^{-3} \text{ s}^{-1}$ $\dot{\epsilon}_2 = 10^3 \text{ s}^{-1}$	$\epsilon = 35\%$
Costin et al. (1979)	1018 cold-rolled 1020 hot-rolled no heat treatment Torsion	$\dot{\gamma}_1 = 5 \cdot 10^{-4} \text{ s}^{-1}$ $\dot{\gamma}_2 = 10^3 \text{ s}^{-1}$	$\gamma = 15\%$

TABLE 1 (Cont'd)

Authors	Material, Condition, Loading Mode	Strain Rates for Graphs	Maximum Strain
<u>ALUMINUM</u>			
Alder & Phillips (1954)	Commercially pure 1 hr at 400 C Compression	$\dot{\epsilon}_1 = \text{slow}$ $\dot{\epsilon}_2 = 39.3 \text{ s}^{-1}$	50% reduction in length of specimen
Davies & Hunter (1963)	> 99.83% purity 350°C for 2 hrs. Compression	$\dot{\epsilon}_1 = \text{slow}$ $\dot{\epsilon}_2 \approx 6700 \text{ s}^{-1}$	$\epsilon = 9\%$
Lindholm (1964)	Commercially pure, Annealed Compression	$\dot{\epsilon}_1 = 1.67 \cdot 10^{-3} \text{ s}^{-1}$ $\dot{\epsilon}_2 = 1.75 \cdot 10^3 \text{ s}^{-1}$	$\epsilon = 32\%$
Yoshida & Nagata (1966)	99.99% purity annealed at 450 C for min. Compression	$\dot{\epsilon}_1 = 3 \cdot 10^{-4} \text{ s}^{-1}$ $\dot{\epsilon}_2 = 200 \text{ s}^{-1}$	$\epsilon = 17\%$
Klepaczko (1967)	99.80% annealed one hour at 450°C Torsion	$\dot{\gamma}_1 = 1.66 \cdot 10^{-5} \text{ s}^{-1}$ $\dot{\gamma}_2 = 0.624 \text{ s}^{-1}$	$\gamma = 50\%$
Green, et al. (1969)	1060-0 Compression	$\dot{\epsilon}_1 = 10^{-3} \text{ s}^{-1}$ $\dot{\epsilon}_2 = 10^3 \text{ s}^{-1}$	$\epsilon = 7\%$
Campbell & Dowling (1970)	Commercially pure annealed 16 hrs at 400°C Shear	$\dot{\gamma}_1 = 5 \cdot 10^{-3} \text{ s}^{-1}$ $\dot{\gamma}_2 = 90 \text{ s}^{-1}$	$\gamma = 10\%$
Frantz & v. (1972)	1100-0; 1 1/2 hrs at 650°F Torsion	$\dot{\gamma}_1 = 5 \cdot 10^{-5} \text{ s}^{-1}$ $\dot{\gamma}_2 = 100 \text{ s}^{-1}$	$\gamma = 18\%$
Senseny, et al. (1978)	1100-0; one hour at 670 K Torsion	$\dot{\gamma}_1 = 2 \cdot 10^{-4} \text{ s}^{-1}$ $\dot{\gamma}_2 = 100 \text{ s}^{-1}$	$\gamma = 18\%$

TABLE 1 (Cont'd)

Authors	Material, Condition, Loading Mode	Strain Rates for Graphs	Maximum Strain
<u>COPPER</u>			
Alder & Phillips (1954)	Phosphorous-deoxidized copper. 2 hrs at 600°C Compression	$\dot{\epsilon}_1 = \text{slow}$ $\dot{\epsilon}_2 = 23.1$	50% reduction in length of specimen
Lindholm (1964)	Commercially pure Annealed Compression	$\dot{\epsilon}_1 = 1.67 \cdot 10^{-3} \text{ s}^{-1}$ $\dot{\epsilon}_2 = 1.60 \cdot 10^3 \text{ s}^{-1}$	$\epsilon = 22\%$
Campbell & Dowling (1970)	OFHC; 20 hrs at 550°C Shear	$\dot{\gamma}_1 = 5 \cdot 10^{-3} \text{ s}^{-1}$ $\dot{\gamma}_2 = 90 \text{ s}^{-1}$	$\gamma = 20\%$
Glenn & Bradley (1973)	OFHC; 1 1/2 hrs at 538 C <u>Note:</u> Strain rate increment is from high to low rate Compression	$\dot{\epsilon}_1 = 500 \text{ s}^{-1}$ $\dot{\epsilon}_2 = 10^{-3} \text{ s}^{-1}$	$\epsilon = 24\%$
Eleiche & Campbell (1976a)	OFHC, hot-rolled 400°C for 2 hrs (vacuum) Torsion	$\dot{\gamma}_1 = .003 \text{ s}^{-1}$ $\dot{\gamma}_2 = 900 \text{ s}^{-1}$	$\gamma = 50\%$
Senseny et al. (1978)	OFHC; 640°K for 1 1/2 hrs (argon) Torsion	$\dot{\gamma}_1 = 2 \cdot 10^{-4} \text{ s}^{-1}$ $\dot{\gamma}_2 = 150 \text{ s}^{-1}$	$\gamma = 18\%$

TABLE 1 (Cont'd)

Authors	Material, Condition, Loading Mode	Strain Rates for Graphs	Maximum Strain
<u>MAGNESIUM</u>			
Davies & Hunter (1963)	"Pure" 150°C for 1 hr Compression	$\dot{\epsilon}_1 = \text{slow}$ $\dot{\epsilon}_2 = 6000 \text{ s}^{-1}$	$\epsilon = 7\%$
Senseny et al. (1978)	AZ 31B, 670°K for 1 hr Torsion	$\dot{\gamma}_1 = 2 \cdot 10^{-4} \text{ s}^{-1}$ $\dot{\gamma}_2 = 320 \text{ s}^{-1}$	$\gamma = 20\%$
<u>ZINC</u>			
Davies & Hunter (1963)	"Pure" 100 C for 1 hr Compression	$\dot{\epsilon}_1 = \text{slow}$ $\dot{\epsilon}_2 = 4000 \text{ s}^{-1}$	$\epsilon = 4\%$
Senseny et al. (1978)	Commercially pure, no heat treatment Torsion	$\dot{\gamma}_1 = 2 \cdot 10^{-4} \text{ s}^{-1}$ $\dot{\gamma}_2 = 300 \text{ s}^{-1}$	$\gamma = 20\%$

TABLE 1 (Cont'd)

Authors	Material, Condition, Loading Mode	Strain Rates for Graphs	Maximum Strain
<u>TITANIUM</u>			
Maiden & Green (1966)	6 Al-4V; fully annealed Compression	$\dot{\epsilon}_1 = .002 \text{ s}^{-1}$ $\dot{\epsilon}_2 = 20 \text{ s}^{-1}$	$\epsilon = 8\%$
Eleiche & Campbell (1976a)	Commercially pure, hot-rolled, 1 1/2 hrs at 700°C (vacuum) Torsion	$\dot{\gamma}_1 = 0.006 \text{ s}^{-1}$ $\dot{\gamma}_2 = 900 \text{ s}^{-1}$	$\gamma = 50\%$
Nicholas (1971)	50-A; annealed as received Torsion	$\dot{\gamma}_1 = 10^{-3} \text{ s}^{-1}$ $\dot{\gamma}_2 = 25 \text{ s}^{-1}$	$\gamma = 10\%$
Harding (1974c)	Commercially pure, 1 hr at 500 C furnace cooled (vacuum) Tension	$\dot{\epsilon}_1 = 10^{-3} \text{ s}^{-1}$ $\dot{\epsilon}_2 = 10^3 \text{ s}^{-1}$	$\epsilon = 20\%$

REFERENCES

1. T. Nicholas (1981), "Material Behavior at High Strain Rates", Chapter 8 in Impact Dynamics (Ed. J. Zukas et al.), John Wiley, New York, pp. 277-331.
2. J. D. Campbell (1970), "Dynamic Plasticity of Metals", International Centre for Mechanical Sciences, Course and Lectures, No. 46, Udine, Springer-Verlag, Vienna and New York.
3. R. Sutterlin, (1972, 1973), "Sur la Plasticite Dynamique. Son Application a l'Etude du Forgeage (Dynamic Plasticity. Its Application to Studies of Forging)", Sci. et Techn. de l'Armement, Memorial de l'Artillerie francaise, Vol. 46, No. 4, pp 909-989, and Vol. 47, No. 3, pp. 567-646.
4. U. S. Lindholm (1971), "High Strain Rate Tests", in Techniques of Metals Research, (Ed. R. F. Bunshah), Vol. 5, Part 1, Measurement of Mechanical Properties, Interscience, New York, pp. 199-271.
5. P. S. Symonds, T. C. T. Ting and D. N. Robinson (1967a), "Survey of Progress in Plastic Wave Propagation in Solid Bodies", Brown University Report Contract DA-19-020-ORD-5453 (A).
6. P. S. Symonds (1967b), "Survey of Methods of Analysis for Plastic Deformation of Structures Under Dynamic Loadings", Brown University, Report BU/NSRDC/1-67.
7. H. Kolsky, (1953), Stress Waves in Solids, Oxford University Press, London.
8. R. J. Clifton (1974), "Plastic Waves: Theory and Experiment", Chapter III Mechanics Today, Vol. 1, 1972, (Ed. S. Nemat-Nasser), Pergamon Press, Oxford.
9. C. M. Sellars, and W. J. Tegart Mc G. (1972), "Hot Workability", Int. Metall. Rev., Review 158, Metals and Materials, Vol. 17, pp. 1-24.
10. K. Bitans and P. W. Whitton, (1972), "High-Strain-Rate Investigations, with Particular Reference to Stress/Strain Characteristics", Int. Metal. Rev., Vol. 17, pp 66-78.
11. P. L. B. Oxley (1974), "Allowing for Strain Rate Effects in the Analysis of Metal Working Processes", in Mechanical Properties at High Rates of Strain, (Ed. J. Harding), The Institute of Physics, pp. 359-381.
12. W. Johnson, (1972), Impact Strength of Materials, Edward Arnold, London.

REFERENCES (Cont'd)

13. M. E. Backman and W. Goldsmith (1978), "The Mechanics of Penetration of Projectiles into Targets", Inst. J. Eng. Sci., Vol. 16, pp. 1-99.
14. G. H. Jonas, and J. A. Zukas, (1978), "Mechanics of Penetration: Analysis and Experiment", Int. J. Eng. Sci., Vol. 16, pp. 879-903.
15. U. S. Lindholm, (1978), "Deformation Maps in the Region of High Dislocation Velocity", Proc. IUTAM 1977 Symposium on High Velocity Deformation of Solids, (Ed. K. Kawata and J. Shioiri), Springer-Verlag, Berlin.
16. R. W. Rohde, B. M. Butcher, J. R. Holland and C. H. Karnes, (Ed.) (1973), Metallurgical Effects at High Strain Rates, Plenum Press, New York.
17. K. Kawata and J. Shioiri, (Ed.) (1978), Proceedings IUTAM 1977 Symposium on High Velocity Deformation of Solids, Springer-Verlag, Berlin
18. J. Harding (ed.) (1974a), Mechanical Properties at High Rates of Strain, The Institute of Physics, London.
19. J. Harding, (Ed.) (1979), Mechanical Properties at High Rates of Strain, 1979, Institute of Physics, London.
20. M. E. Meyers, and L. E. Murr, (Ed.) (1981), Shock Waves and High-Strain-Rate Phenomena in Metals, Plenum Press, New York.
21. J. J. Gilman, (1969), Micromechanics of Flow in Solids, McGraw-Hill, New York.
22. U. F. Kocks, A. S. Argon, and M. F. Ashby, (1975), Thermodynamics and Kinetics of Slip, Progress in Materials Science, Vol. 19, Pergamon Press, Oxford.
23. R. W. K. Honeycombe, (1968), The Plastic Deformation of Metals, Edward Arnold, London.
24. A. R. Rosenfield, G. T. Hahn, A. L. Bement, and R. I. Jaffee, (Ed.) (1968), Dislocation Dynamics, Battelle Institute Materials Science Colloquia, McGraw-Hill.
25. M. F. Kanninen, W. F. Adler, A. R. Rosenfield and R. I. Jaffee, (Ed.) (1969), Inelastic Behavior of Solids, Battelle Institute Materials Science Colloquia, McGraw-Hill, New York.
26. J. D. Campbell (1973), "Dynamic Plasticity: Macroscopic and Microscopic Aspects", Mater. Sci. Eng., Vol. 12, pp. 3-21.

REFERENCES (Cont'd)

27. W. C. Leslie, (1973), "Microstructural Effects of High Strain Rate Deformation", in Metallurgical Effects at High Strain Rates, (Ed. R. W. Rhode, B. M. Butcher, J. R. Holland and C. H. Karnes), Plenum Press, New York, pp. 571-586.
28. A. S. Argon, (Ed.) (1975), Constitutive Equations in Plasticity, The MIT Press, Cambridge, Mass.
29. D. Klahn, A. K. Mukherjee, and J. E. Dorn (1970), "Strain-Rate Effects", Second Int. Conf. on the Strength of Metals and Alloys, Asilomar, California, ASM Vol. 3, pp. 951-982.
30. N. Cristescu, (1967), Dynamic Plasticity, North-Holland, Amsterdam.
31. Kh. A. Rakhmatulin, and Yu A. Dem'yanov, (1966), Strength Under High Transient Loads, Israel Program for Scientific Translation, Jerusalem.
32. W. K. Nowacki, (1978), Stress Waves in Non-Elastic Solids, Pergamon Press, Oxford.
33. L. S. Costin, and J. Duffy, (1979), "The Effect of Loading Rate and Temperature on the Initiation of Fracture in a Mild Rate-Sensitive Steel", Trans. ASME, Vol. 101, J. Eng. Matls. Tech., pp. 258-264.
34. L. H. Donnell, (1930), "Longitudinal Wave Transmission and Impact", Trans., ASME, Vol. 52, pp. 153-167.
35. T. Von Karman, (1942), "On the Propagation of Plastic Deformation in Solids", NDRC Report A-29 (OSRD No. 365).
36. G. I. Taylor, (1942), "The Plastic Wave in a Wire Extended by an Impact Load", Report written 1942 for the Civil Defense Research Committee, Ministry of Home Security (England), published in The Scientific Papers of G. I. Taylor, Vol. 1, Mechanics of Solids, Ed. by G. K. Batchelor, Cambridge University Press, 1958, pp. 467-479.
37. Kh. A. Rakhmatulin, (1945), "On the Propagation of Waves of Unloading", Prikl. Mat. i Mekh., Vol. 9, pp. 91-100.
38. M. P. White, and L. Griffis (1947), "The Permanent Strain in a Uniform Bar Due to Longitudinal Impact", J. Appl. Mech., Vol. 14, pp. 337-343.
39. R. Courant, and D. Hilbert, (1962), "Methods of Mathematical Physics", Vol. II, Partial Differential Equations, Interscience, New York.

REFERENCES (Cont'd)

40. N. Davids, and S. Kumar, (1958), "A Contour Method for One Dimensional Pulse Propagation in Elastic-Plastic Materials", Third U.S. Nat. Cong. of Appl. Mech., pp. 503-512.
41. T. Von Karman, and P. Duwez, (1950), "The Propagation of Plastic Deformation in Solids", J. Appl. Phys., Vol. 21, pp. 987-994.
42. L. E. Malvern, (1951a), "The Propagation of Longitudinal Waves of Plastic Deformation in a Bar of Material Exhibiting a Strain-Rate Effect", J. Appl. Mech., Vol. 18, pp. 203-208.
43. L. E. Malvern, (1951b), "Plastic Wave Propagation in a Bar of Material Exhibiting a Strain-Rate Effect", Quart. Appl. Math., Vol. 8, pp. 405-411.
44. P. Perzyna, (1966), "Fundamental Problems in Viscoplasticity", in Advances in Applied Mechanics, Vol. 9, Academic Press, pp. 243-377.
45. P. Perzyna, (1971), "Thermodynamic Theory of Biscoplasticity", in Advances in Applied Mechanics, Vol. 11, Academic Press, pp. 313-354.
46. J. M. Kelly, (1967), "Generalizations of Some Elastic-Viscoplastic Stress-Strain Relations", Trans. Soc. Rheol., Vol. 11, No. 1, pp. 55-76.
47. Yu. N. Rabotnov, (1968), "Model of Elastic-Plastic Medium with Delayed Yielding", Prk. Mech. i Techn. Phys., No. 3, pp. 45-54.
48. Yu. N. Rabotnov and J. V. Suvorova, (1972), "Deformation of Metals Under Uniaxial Loading", Izv. AN USSR Mekhanika Tverdogo Tela, (Mech. Solids), No. 4, pp. 41-54.
49. J. V. Suvorova, (1974), "Plastic Deformation of Metals Under Various Loading Rates", Izv. AN Mekhanika Tverdogo Tela, (Mech. Solids), Vol. 9, No. 1, pp. 73-79.
50. Yu. N. Rabotnov, and J. V. Suvorova, (1978), "The Non-Linear Hereditary-Type Stress Strain Relation for Metals", Int. J. Solids Structures, Vol. 14, No. 3, pp. 173-186.
51. J. F. Bell, (1951), "Propagation of Plastic Waves in Pre-Stressed Bars", The John Hopkins University Technical Report No. 5, U. S. Navy Contract N6-ONR-243.
52. E. J. Sternglass, and D. A. Stuart, (1953), "Transient Deformations in Elastoplastic Media", J. Appl. Mech., Vol. 20, No. 3, pp. 427-434.
53. U. S. Lindholm, (1964), "Some Experiments with the Split Hopkinson Pressure Bar", J. Mech. Phys. Solids, Vol. 12, pp. 317-335.

REFERENCES (Cont'd)

54. R. A. Frantz, and J. Duffy, (1972), "The Dynamic Stress-Strain Behavior in Torsion of 1100-O Aluminum Subjected to a Sharp Increase in Strain Rate", J. Appl. Mech., Vol. 39, pp. 939-945.
55. S. R. Bodner, and Y. Partom, (1972), "Dynamic Inelastic Properties of Materials. Part II: Representation of Time Dependent Characteristics of Metals", Eighth Cong. Int. Council Aero. Sci., Paper No. 72-28.
56. W. G. Johnston, and J. J. Gilman, (1959), "Dislocation Velocities, Dislocation Densities, and Plastic Flow in Lithium Fluoride Crystals", J. Appl. Phys. Vol. 30, pp. 129-144.
57. J. J. Gilman, (1960), "The Plastic Resistance of Crystals", Aust. J. Phys., Vol. 13, pp. 327-343.
58. S. R. Bodner, and A. Merzer, (1978), "Viscoplastic Constitutive Equations for Copper with Strain Rate History and Temperature Effects", Technion, Israel, MML Report No. 55.
59. P. E. Senseny, J. Duffy, and R. H. Hawley, (1978), "Experiments on Strain Rate History and Temperature Effects during the Plastic Deformation of Close Packed Metals", J. Appl. Mech., Vol. 45, pp. 60-66.
60. N. R. Patel, and M. P. Bieniek, (1979), "Analysis of Visco-Plastic Behavior of Metals", Mat. Sci. Eng., Vol. 40, pp. 123-134.
61. J. J. Gilman, (1965), "Microdynamics of Plastic Flow at Constant Stress", J. Appl. Phys., Vol. 36, pp. 2772-2777.
62. J. J. Gilman and W. G. Johnston, (1960), "Behavior of Individual Dislocations in Strain-Hardened LiF Crystals", J. Appl. Phys., Vol. 31, No. 4, pp. 687-692.
63. G. T. Hahn, (1962), "A Model for Yielding with Special Reference to the Yield-Point Phenomena of Iron and Related BCC Metals", Acta Met., Vol. 10, pp. 727-738.
64. P. P. Gillis, and J. J. Gilman, (1965), "Dynamic Dislocation Theory of Crystal Plasticity, Part I. The Yield Stress", J. Appl. Phys., Vol. 36, pp. 3370-3380.
65. B. Hopkinson, (1905), "The Effects of Momentary Stresses in Metals", Proc. Roy. Soc. (London), Vol. 74, Ser. A, pp. 498-506.
66. G. I. Taylor, (1946), "The Testing of Materials at High Rates of Loading", J. Inst. Civil Engrs., London, Vol. 26, pp. 486-519.
67. H. Kolsky and L. S. Douch, (1962), "Experimental Studies in Plastic Wave Propagation", J. Mech. Phys. Solids, Vol. 10, pp. 195-223.

REFERENCES (Cont'd)

68. G. P. DeVault, (1965), "The Effect of Lateral Inertia on the Propagation of Plastic Strain in a Cylindrical Rod", J. Mech. Phys. Solids, Vol. 13, pp. 55-68.
69. P. E. Duwez, and D. S. Clark, (1947), "An Experimental Study of the Propagation of Plastic Deformation under Conditions of Longitudinal Impact", Proc. ASTM Vol. 47, pp. 502-532.
70. D. S. Clark and P. E. Duwez, (1948), "Discussion of the Forces Acting in Tension Impact Tests of Materials", J. Appl. Mech., Vol. 15, pp. A243-A247.
71. G. Bianchi, (1964), "Some Experimental and Theoretical Studies on the Propagation of Longitudinal Plastic Waves in a Strain-Rate Dependent Material", IUTAM Symposium on Stress Waves in Anelastic Solids (Ed. H. Kolsky and W. Prager) Springer-Verlag, Berlin, pp. 101-117.
72. J. W. Craggs, (1957), "The Propagation of Infinitesimal Plane Waves in Elastic-Plastic Materials", J. Mech. Phys. Solids, Vol. 5, pp. 115-124.
73. J. W. Craggs, (1961), "Plastic Waves" in Progress in Solid Mechanics, (Ed. I. N. Sneddon and R. Hill), Vol. 2, pp. 143-197, North-Holland, Amsterdam.
74. R. J. Clifton, (1966), "An Analysis of Combined Longitudinal and Torsional Plastic Waves in a Thin-Walled Tube", Proc. Fifth Int. Cong. Appl. Mech., ASME, pp. 465-480.
75. E. H. Lee, (1970), "Constitutive Relations for Dynamic Loading and Plastic Waves", in Inelastic Behavior of Solids, (Ed. M. F. Kanninen, W. F. Adler, A. R. Rosenfield, and R. I. Jaffee), McGraw-Hill, pp. 423-446.
76. W. W. Baker, and C. H. Yew, (1966), "Strain-Rate Effects in the Propagation of Torsional Plastic Waves", J. Appl. Mech., Vol. 33, pp. 917-923.
77. C. H. Yew, and H. S. Richardson, Jr., (1969), "The Strain-Rate Effect and the Incremental Plastic Wave in Copper", Exp. Mech., Vol. 26, pp. 366-373.
78. E. Convery, and H. Pugh, L.I.D. (1968), "Velocity of Torsional Waves in Metals Stressed Staticly into the Plastic Range", J. Mech. Eng. Sci., Vol. 10, No. 2, pp. 153-164.
79. J. D. Campbell, and A. R. Dowling, (1970), "The Behavior of Materials Subjected to Dynamic Incremental Shear Loading", J. Mech. Phys. Solids, Vol. 18, pp. 43-63.
80. J. F. Bell, (1968), The Physics of Large Deformation of Crystalline Solid, Springer-Verlag, New York.

REFERENCES (Cont'd)

81. E. A. Ripperger, and H. Watson, Jr., (1968), "The Relationship Between the Constitutive Equation and One-Dimensional Wave Propagation", in Mechanical Behavior of Materials Under Dynamic Loads, (Ed. U. S. Lindholm), Springer-Verlag, New York, pp. 294-313.
82. G. I. Taylor, (1948), "The Use of Flat-Ended Projectiles for Determining Dynamic Yield Stress: I. Theoretical Considerations", Proc., Roy. Soc., (London), Vol. 194, Series A, pp. 289-299.
83. A. C. Whiffin, (1948), "The Use of Flat-Ended Projectiles for Determining Dynamic Yield Stress: II. Tests on Various Metallic Materials", Proc. Roy. Soc. (London), Ser. A, Vol. 194, pp. 300-322.
84. M. Manjoine and A. Nadai, (1940), "High Speed Tension Tests at Elevated Temperatures", Proc. ASTM, Vol. 40, pp. 822-837.
85. A. Nadai, and M. J. Manjoine, (1941), "High-Speed Tension Tests at Elevated Temperatures, Parts II and III", J. Appl. Mech., pp. A77-A91.
86. L. D. Sokolov, (1949), "On the Problem of Evaluating Materials Resistance to Plastic Deformation Depending on Strain Rate and Temperature", Doklady Akad. Nauk, SSSR, Vol. 67, No. 3, pp. 459-462.
87. J. E. Johnson, D. S. Wood, and D. S. Clark, (1953), "Dynamic Stress-Strain Relations for Annealed 2S Aluminum Under Compression Impact", J. Appl. Mech., Vol. 20, pp. 523-529.
88. D. S. Clark, and D. S. Wood, (1949), "The Time Delay for the Initiation of Plastic Deformation at Rapidly Applied Constant Stress", Proc. ASTM, Vol. 49, pp. 717-735.
89. J. D. Campbell and J. Duby, (1957), "Delayed Yield and Other Dynamic Loading Phenomena in a Medium-Carbon Steel", Proc. Conf. on the Properties of Materials at High Rate of Strain, Institution of Mechanical Engineers, London, pp. 214-220.
90. J. M. Krafft, and A. M. Sullivan, (1958), "Effect of Grain Size and Carbon Content on the Yield Delay-Time of Mild Steel", Trans., ASM, Vol. 51, pp. 643-665.
91. J. D. Campbell, and K. J. Marsh, (1962), "The Effect of Grain Size on the Delayed Yielding of Mild Steel", Phil. Mag., Vol. 7, pp. 933-952.
92. C. E. Work, and T. J. Dolan, (1953), "The Influence of Strain Rate and Temperature on the Strength and Ductility of Mild Steel in Torsion", Proc., ASTM, Vol. 53, pp. 611-626.

REFERENCES (Cont'd)

93. E. Orowan, and J. Los, (1950), Descriptions of the cam plastometer in the published literature are found in Loizou, N. and Sims, R. B., "The Yield Stress of Pure Lead in Compression," J. Mech. Phys. Solids (1953), Vol. 1, pp. 234-243, or in J. F. Adler and V. A. Phillips, (1945-55) loc. cit.
94. J. F. Alder and V. A. Phillips, (1954-55), "The Effect of Strain Rate and Temperature on the Resistance of Aluminum, Copper and Steel to Compression", J. Inst. Metals, Vol. 83, pp. 80-86.
95. P. M. Cook, (1957), "True Stress-Strain Curves for Steel in Compression at High Temperatures and Strain Rates, for Application of the Calculation of Load and Torque in Hot Rolling", in Properties Materials at High Rates of Strain, Inst. Mech. Engrs., London, pp. 86-97.
96. W. Lueg, and H. G. Muller, (1957), "Formänderungsverhalten von Stahl C45 beim Stauchen und Scheren in Abhängigkeit von Temperatur und Formänderungsgeschwindigkeit", Archiv für das Eisenhüttenwesen, pp. 505-516.
97. V. S. Zoteev, (1960), "Effect of Temperature and Deformation Rate on Carbon Steels", (translated from the Russian), Stal, Vol. 6, pp. 440-442.
98. K. J. Marsh, and Campbell (1963), "The Effect of Strain Rate on the Post-Yield Flow of Mild Steel", J. Mech. Phys. Solids, Vol. 11, pp. 49-63.
99. J. D. Campbell and W. G. Ferguson, (1970), "The Temperature and Strain-Rate Dependence of the Shear Strength of Mild Steel", Phil. Mag., Vol. 21, pp. 63-82.
100. J. A. Bailey and A.R.E. Singer, (1963-64), "Effect of Strain Rate and Temperature on the Resistance to Deformation of Aluminum, Two Aluminum Alloys and Lead", J. Inst. Metals, Vol. 92, pp. 404-408.
101. J. A. Bailey, S. L. Haas, and M. K. Shah, (1972), "Effect of Strain-Rate and Temperature on the Resistance to Torsional Deformation of Several Aluminum Alloys", Int. J. Mech. Sci., Vol. 14, pp. 735-754.
102. J. E. Hockett, (1967), "On Relating the Flow Stress of Aluminum to Strain, Strain Rate, and Temperature", Trans. Met. Soc. AIME, Vol. 239, pp. 969-976.
103. S. K. Samanta, (1968), "Resistance to Dynamic Compression of Low-Carbon Steel and Alloy Steels at Elevated Temperatures and at High Strain-Rates", Int. J. Mech. Sci., Vol. 10, pp. 613-636.

REFERENCES (Cont'd)

104. S. K. Samanta, (1969), "On Relating the Flow Stress of Aluminum and Copper to Strain, Strain-Rate and Temperature", *Int. J. Mech. Sci.*, Vol. 11, pp. 433-453.
105. H. Suzuki, Y. Yabuki, S. Hashizume, K. Kenmochi, Y. Ichihara and S. Nakajima (1968), "Studies on the Flow Stress of metals and Alloys", Report Inst. of Indust. Sci., The University of Tokyo, Vol. 18, No. 3, Ser. No. 117.
106. J. Harding, (1977), "Effect of Temperature and Strain Rate on Strength and Ductility of Four Alloys Steels", *Met. Tech.*, pp. 6-16.
107. D. P. Kendall and T. E. Davidson, (1966), "The Effect of Strain Rate on Yielding in High Strength Steels", *J. Basic Engng.*, pp. 37-34.
108. D. P. Kendall, (1972), "The Effect of Strain Rate and Temperature on Yielding in Steels", *J. Basic Engng.*, pp. 207-212.
109. H. Kolsky, (1949), "An Investigation of the Mechanical Properties of materials at Very High Rates of Loading", *Proc. Phys. Soc.*, London, V62-B, pp. 676-700.
110. R. M. Davies, (1946-48), "A Critical Study of the Hopkinson Pressure Bar", *Phil. Trans. Roy. Soc.*, (London), Vol. 240A, pp. 375-457.
111. U. S. Lindholm, and L. M. Yeakley, (1968), "High Strain Rate Testing: Tension and Compression", *Exp. Mech.*, Vol. 8, No. 1, pp. 1-9.
112. B. Bhushan and W. E. Jahsman, (1978), "Measurement of Dynamic Material Behavior Under Nearly Uniaxial Strain Conditions", *Int. J. Solids Structures*, Vol. 14, pp. 739-753.
113. E. D. H. Davies, and S. C. Hunter, (1963), "The Dynamic Compression Testing of Solids by the Method of the Split Hopkinson Bar", *J. Mech. Phys. Solids*, Vol. 11, pp. 155-179.
114. G. L. Wulf, (1974), "Dynamic Stress-Strain Measurements at Large Strains", in Mechanical Properties at High Rates of Strain, (Ed. J. Harding), *The Institute of Physics*, London, pp. 48-52.
115. L. S. Costin, E. E. Crisman, R. H. Hawley, and J. Duffy, (1979), "On the Localization of Plastic Flow in Mild Steel Tubes Under Dynamic Torsional Loading", in Mechanical Properties at High Rates of Strain 1979, (Ed. J. Harding); *The Institute of Physics*, London, pp. 90-100, see also "Strain Rate and Strain Rate History Effects in Two Mild Steels" by M. L. Wilson, R. H. Hawley and J. Duffy, Brown University Report, NSF Grant ENG 75-18532/2, March, 1979.

REFERENCES (Cont'd)

116. W. E. Jahsman (1971), "Reexamination of the Kolsky Technique for Measuring Dynamic Material Behavior", J. Appl. Mech., Vol. 38, pp. 75-82.
117. I. Nicholas, (1973), "On the Determination of Constitutive Equations from Plastic Wave Propagation Phenomena", Technical Report AFML-TR-73-73.
118. U. S. Lindholm, L. M. Yeakley, and R. L. Bessey, (1968), "An Investigation of the Behavior of Material Under High Rates of Deformation", Air Force Materials Laboratory, Technical Report 68-194.
119. S. J. Green and S. G. Babcock, (1966), "Response of Materials to Suddenly Applied Stress Loads, Part I: High Strain-Rate Properties of Eleven Reentry-Vehicle Materials at Elevated Temperatures", General Motors Defense Research Laboratories, Report TR 66-83.
120. J. L. Chiddister, and L. E. Malvern, (1963), "Compression Impact Testing of Aluminum at Elevated Temperatures", Exp. Mech., Vol. 3, pp. 81-90.
121. A. M. Eleiche and J. Duffy, (1975), "Effects of Temperatures on the Static and Dynamic Stress-Strain Characteristics in Torsion of 1100-0 Aluminum", Int. J. Mech. Sci., Vol. 17, pp. 85-95.
122. U. S. Lindholm and R. L. Bessey (1969), "A Survey of Rate Dependent Strength Properties of Metals", Air Force Materials Laboratory, Technical Report 69-119.
123. A. M. Eleiche, (1972), "A Literature Survey of the Combined Effects of Strain Rate and Elevated Temperature on the Mechanical Properties of Metals", Air Force Materials Laboratory, Technical Report 72-125.
124. T. L. Larsen, S. L. Rajnak, F. E. Hauser, and J. E. Dorn, (1964), "Plastic Stress Strain-Rate Temperature Relations in HCP Ag₂ A Under Impact Loading", J. Mech. Phys. Solids, Vol. 12, pp. 361-376.
125. F. E. Hauser, (1966), "Techniques for Measuring Stress-Strain Relations at High Strain Rates", Exp. Mech., Vol. 6, pp. 395-402.
126. F. E. Hauser, J. A. Simmons, and J. E. Dorn (1961), "Strain Rate Effects in Plastic Wave Propagation", in Response of Metals to High Velocity Deformation, (Ed. P. G. Shewmon and V. F. Zackay), Interscience, New York, pp. 93-114.
127. C. J. Maiden and S. J. Green, (1966), "Compressive Strain Rate Tests on Six Selected Materials at Strain Rates from 10^{-3} to 10^4 sec", J. Appl. Mech., pp. 496-504.

REFERENCES (Cont'd)

128. D. L. Holt, S. G. Babcock, S. J. Green, and C. J. Maiden (1967), "The Strain Rate Dependence of the Flow Stress in Some Aluminum Alloys", Trans., ASM, Vol. 60, pp. 152-159.
129. A. Kumar, C. J. Maiden, and S. J. Green, (1967), "Survey of Strain Rate Effects", The First Int. Conf. of the Center for High Energy Forming, Estes Park, Colorado.
130. S. G. Babcock and R. D. Perkins, (1968), "High Strain-Rate Response of Three Heat-Shield Materials", General Motors Corporation, Materials and Structures Laboratory, Technical Report SAMSO TR 68-71, Vol. II.
131. S. J. Green, C. J. Maiden, S. G. Babcock, and F. L. Schierloh, (1969), "The High Strain-Rate Behavior of Face Centered Cubic Metals", in Inelastic Behavior of Solids, (Ed. M. F. Kanninen, W. F. Adler, A. R. Rosenfield, and R. I. Jaffee), McGraw-Hill, New York, pp. 521-542.
132. S. K. Samanta (1971), "Dynamic Deformation of Aluminum and Copper at Elevated Temperatures", J. Mech. Phys. Solids, Vol. 19, pp. 117-135.
133. C. M. Sellars and W. J. Tegart, Mc G (1966), "La Relation entre la Resistance et la Structure dans la Deformation a Chaud", Mem. Sci. Rev. Metall., Vol. 63, pp. 731-746.
134. A. Kumar and R. G. Kumble, (1969), "Viscous Drag on Dislocations at High Strain Rates in Copper", J. Appl. Phys., Vol. 40, No. 9, pp. 3475-3480.
135. W. G. Ferguson, A. Kumar, and J. E. Dorn (1967a), "Dislocation Damping in Aluminum at High Strain Rates", J. Appl. Phys., Vol. 38, No. 4, pp. 1863-1869.
136. J. W. Edington, (1969), "The Influence of Strain Rate on the Mechanical Properties and Dislocation Substructure in Deformed Copper Single Crystals", Phil. Mag., Eighth Ser., Vol. 19, No. 162, pp. 1189-1206.
137. R. Dormeal, M. Stelly, and M. Caput, (1976), "Comportement en Traction Dynamique de Monocristaux de Cuivre", (Dynamic Traction Behavior of Copper Monocrystals), Fourth Int. Conf. on the Strength of Met. and Alloys, Nancy, pp. 1141-1145.
138. M. Stelly and R. Dormeal, (1977), "Some Results on the Dynamic Deformation of Copper", IUTAM, Symposium on High Velocity Deformation of Solids, (Ed. K. Kawata and J. Shioiri), Springer-Verlag, New York.

REFERENCES (Cont'd)

139. F. Dusek (1970), "Plastic Deformation at High Strain Rates", Czech. J. Phys., B, Vol. 20, pp. 776-789.
140. F. Dusek, (1974), "Response of Materials to High Loading Rates", In Dynamika Osrodkow Niesprezystych, (ed. P. Perzyna), Polska Akademia Nauk, pp. 125-173.
141. F. Dusek, Z. Jasinski, J. Buchar, A. Litwora, and A. Piatkowski, (1976), "Response of Cu Single Crystals to High Loading Rates", Czech. J. Phys., Vol. B26, Part I, pp. 538-558, and Part II, pp. 559-564.
142. K. Tanaka and K. Ogawa, (1979a), "The Effects of Temperature and Strain Rate on the Strength of Polycrystalline Zinc", Bulletin, Japan Soc. Mech. Engineers, Vol. 22, No. 165, pp. 300-308.
143. K. Tanaka and K. Ogawa, (1979b), "Temperature and Strain Rate Effects upon the Strength of Zinc Single Crystals", Bulletin, Japan Soc. Mech. Engineers, Vol. 22, No. 167, pp. 627-635.
144. K. Tanaka and K. Ogawa, (1980), "Effects of Temperature and Strain Rate on the Strength of Pyramidal Slip in Zinc Single Crystals", Proc. 23rd Japan Congress on Mat. Res., pp. 46-50.
145. T. Muller, (1971), "The Visco-Plastic Dynamic Behavior of Iron and Nickel at Elevated Temperatures", Acta Met., Vol. 19, pp. 691-699.
146. G. L. Wulf, (1978a), "The High Strain Rate Compression of 7039 Aluminum", Int. J. Mech. Sci., Vol. 20, pp. 609-615.
147. G. L. Wulf (1978b), "The High Strain Rate Compression of 1023 and 4130 Steels", Int. J. Mech. Sci., Vol. 20, pp. 843-848.
148. G. L. Wulf, "High Strain Rate Compression of Titanium and Some Titanium Alloys", Int. J. Mech. Sci., Vol. 21, pp. 713-718.
149. C. K. H. Dharan and F. E. Hauser, (1970), "Determination of Stress-Strain Characteristics at Very High Strain Rates", Exp. Mech., pp. 370-376.
150. C. K. H. Dharan and F. E. Hauser (1973), "High-Velocity Dislocation Damping in Aluminum", J. Appl. Phys., Vol. 44, No. 4, pp. 1468-1474.
151. U. S. Lindholm, (1978), "Deformation Maps in the Region of High Dislocation Velocity", Proc. IUTAM 1977 Symposium on High Velocity Deformation of Solids, (Ed. K. Kawata and J. Shioiri), Springer-Verlag, Berlin.

REFERENCES (Cont'd)

152. T. Nicholas (1971), "Strain-Rate and Strain-Rate History Effects in Several Metals in Torsion", *Exp. Mech.*, Vol. 11, No. 8, pp. 370-374.
153. J. Duffy, J. D. Campbell, and R. H. Hawley, (1971), On the Use of a Torsional Split Hopkinson Bar to Study Rate Effects in 1100-O Aluminum", *J. Appl. Mech.*, Vol. 38, pp. 83-91.
154. J. L. Lewis and J. D. Campbell (1972), "The Development and Use of a Torsional Hopkinson-Bar Apparatus", *Exp. Mech.*, Vol. 12, No. 11, pp. 520-524.
155. J. L. Lewis and W. Goldsmith (1973), A Biaxial Split Hopkinson-Bar for Simultaneous Torsion and Compression", *Rev. Sci. Instrum.*, Vol. 44, No. 7, pp. 811-813.
156. E. K. C. Leung, (1980), "An Elastic-Plastic Stress Analysis of the Specimen Used in the Torsional Kolsky Bar", *J. Appl. Mech.*, Vol. 47, pp. 278-282.
157. T. Trozera, O. D. Sherby, and J. E. Dorn, (1957), "Effect of Strain Rate and Temperature on the Plastic Deformation of High Purity Aluminum", *Trans. ASM*, Vol. 49, pp. 173-187.
158. H. W. Wiedersich (1957), Written Discussion to paper by T. A. Trozera, O. D. Sherby, and J. E. Dorn, "Effect of Strain Rate and Temperature on the Plastic Deformation of High Purity Aluminum", *Trans. ASM*, Vol. 49, pp. 173-187.
159. C. Zener and J. H. Holloman (1946), "Problems in Non-elastic Deformation of Metals", *J. Appl. Phys.*, Vol. 17, No. 2, pp. 69-82.
160. J. E. Dorn, A. Goldberg, and T. E. Tietz, (1949), "The Effect of Thermal-Mechanical History on the Strain Hardening of Metals", *Trans. AIME*, Vol. 180, pp. 205-224.
161. W. D. Sylwestrowicz, (1958), "The Temperature Dependence of the Yield Stress of Copper and Aluminum", *Trans., AIME*, Vol. 212, pp. 617-624.
162. D. R. Barraclough and C. M. Sellars, (1974), "The Effect of Varying Deformation Conditions During Hot Torsion Testing", in Mechanical Properties at High Rates of Strain, (Ed. J. Harding), The Institute of Physics, London, pp. 111-123.
163. E. W. Hart, (1970), "A Phenomenological Theory for Plastic Deformation of Polycrystalline Metals", *Acta Met.*, Vol. 18, pp. 559-610.

REFERENCES (Cont'd)

164. S. Yoshida and N. Negata (1966), "Deformation of Polycrystalline Aluminum at High Strain Rates", Trans. Jap. Inst. Met., Vol. 7, pp. 273-279.
165. J. Klepaczko, (1967), "Effects of Strain-Rate History on the Strain Rate Hardening Curve of Aluminum", Arch. Mech. Stosowanej, Vol. 19, No. 2, pp. 211-229.
166. J. Klepaczko, (1968), "Strain-Rate History Effects for Polycrystalline Aluminum and the Theory of Intersections", J. Mech. Phys. Solids, Vol. 16, pp. 255-266.
167. T. Shirakashi and E. Usui (1970). "Effect of Temperature and Strain Rate Upon Flow Stress of Metals in Compression. Part I", Bull. Jap. Soc. of Prec. Eng., Vol. 14, No. 4, pp. 91-100.
168. J. Klepaczko (1975), "Thermally Activated Flow and Strain Rate History Effects for Some Polycrystalline FCC Metals", Mat. Sci. Eng., Vol. 18, pp. 121-136.
169. B. Wielke, (1978), "Dislocation Dynamics During Rate Changes", Acta Met., Vol. 26, pp. 103-112.
170. J. Klepaczko, R. A. Frantz, and J. Duffy, (1977), "History Effects in Polycrystalline FCC Metals Subjected to Rapid Changes in Strain Rate and Temperature", Polska Akademia Nauk, Instytut Podstawowych problemow Techniki, Engng. Trans., Vol. 25, no. 1, pp 3-22.
171. T. Glenn and W. Bradley, (1973), "The Origin of Strain-Rate Sensitivity in OFHC Copper", Met. trans., Vol. 4, pp. 2343-2348.
172. A. Korbel and K. Swiatkowski, (1972), "The Role of Strain Rate in the Formation of Dislocation Structure and Its Influence on the Mechanical Properties of Aluminum", Met. Sci. J., Vol. 6, pp. 60-63.
173. C. W. MacGregor and J. C. Fisher, (1946), "A Velocity Modified Temperature for the Plastic Flow of Metals", J. Appl. Mech., Vol. 13, pp. A11-A16.
174. M. J. Manjoine, (1944), "Influence of Rate of Strain and Temperature on Yield Stresses of Mild Steel", J. Appl. Mech., Vol. 11, A211-218.
175. T. L. Briggs and J. D. Campbell, (1972), "The Effect of Strain Rate and Temperature on the Yield and Flow of polycrystalline Niobium and Molybdenum", Acta Met., Vol. 20, pp. 711-724.

REFERENCES (Cont'd)

176. J. D. Campbell and T. L. Briggs, (1975), "Strain-Rate History Effects in Polycrystalline Molybdenum and Niobium", *J. Less Common Metals*, Vol. 40, pp. 235-250.
177. A. M. Eleiche and J. D. Campbell, (1974), "The Influence of Strain Rate History on the Shear Strength of Copper and Titanium at Large Strains", University of Oxford, Report No. 1106/74.
178. J. Harding, (1974b), Discussion of paper by J. Klepaczko and J. Duffy, *Mechanical Properties at High Rates of Strain*, (Ed. J. Harding), The Institute of Physics, London, pp. 190-191.
179. J. E. Hockett and E. G. Zukas, (1974), "The Response of Iron to Dynamic Compression", in *Mechanical Properties at High Rates of Strain*, (Ed. J. Harding) The Institute of Physics, London, pp. 53-61.
180. A. M. Eleiche and J. D. Campbell, (1976a), "The Influence of Strain-Rate History and Temperature on the Shear Strength of Copper, Titanium and Mild Steel", University of Oxford, Report AFML-TR-76-90.
181. J. D. Campbell, A. M. Eleiche, and M. C. C. Tsao, (1977), "Strength of Metals and Alloys at High Strains and Strain Rates", in *Fundamental Aspects of Structural Alloy Design*, (Ed. R. I. Jaffee and B. A. Wilcox), Plenum Press, New York, pp. 545-563.
182. A. M. Eleiche, (1980), "The Influence of Strain-Rate History and Temperature on the Shear Strength of Commercially-Pure Titanium", Presented at Fourth International Conference on Titanium, Kyoto, Japan.
183. A. M. Eleiche, (1981), "Strain-Rate History and Temperature Effects on the Tensional-Shear Behavior of a Mild Steel", *Exp. Mech.*, Vol. 21, pp. 285-294.
184. D. Tseng and K. Tangri, (1977), "Temperature and Strain Rate Sensitivities of Flow Stress for the High Purity AISI Iron", *Scripta Met.*, Vol. 11, pp. 719-723.
185. Z. S. Basinski, (1959), "Thermally Activated Glide in Face-Centered Cubic Metals and Its Application to the Theory of Strain Hardening", *Phil. Mag.*, Vol. 4, pp. 393-432.
186. Z. S. Basinski and J. W. Christian, (1960), "The Influence of Temperature and Strain Rate on the Flow Stress of Annealed and Decarburized Iron at Subatmospheric Temperatures", *Aust. J. Phys.*, Vol. 13, pp. 299-308.

REFERENCES (Cont'd)

187. J. Klepaczko and J. Duffy, (1980), "Strain Rate History Effects in BCC Metals", presented at ASTM Symposium on Mechanical Testing, Bal Harbour, Florida. To be published in ASTM STP 765, Mechanical Testing for Deformation Model Development, (Ed. R. W. Rhode and J. C. Swearengen).
188. J. Klepaczko, (1981), "A Model for Yielding and Flow of Iron and BCC Metals Based on Thermal Activation", Brown University Report, DMR79-23257/132, NSF CME 79-23742/4.
189. U. S. Lindholm and L. Yeakley, (1965), "Dynamic Deformation of Single and Polycrystalline Aluminum", J. Mech. Phys. Solids, Vol. 13, pp. 41-53.
190. C. Y. Chiem and J. Duffy, (1981a), "Strain Rate History Effects in LiF Single Crystals During Dynamic Loading in Shear", Mater. Sci. Eng., Vol. 48, No. 2, pp. 207-222.
191. C. Y. Chiem and J. Duffy, (1981b), "Strain Rate History Effects and Observations of Dislocation Substructure in Aluminum Single Crystals Following Dynamic Deformation", Brown University Report NSF:MEA 79-23742/3.
192. J. W. Edington, (1968), "Effect of Strain Rate on the Dislocation Substructure in Deformed Niobium Single Crystals", in Mechanical Behavior of Materials under Dynamic Load, (Ed. U. S. Lindholm), Springer-Verlag, New York, pp. 191-240.
193. J. W. Edington, (1969), "The Influence of Strain Rate on the Mechanical Properties and Dislocation Substructure in Deformed Copper Single Crystals", Phil. Mag., Eight Ser., Vol. 19, No. 162, pp. 1189-1206.
194. H. J. McQueen and J. E. Hockett, (1970), "Microstructures of Aluminum Compressed at Various Rates and Temperatures", Met. Trans., Vol. 1, pp. 2997-3004.
195. A. M. Eleiche and J. D. Campbell, (1976b), "Strain-Rate Effects During Reverse Torsional Shear", Exp. Mech., pp. 281-290.
196. J. Lipkin, J. D. Campbell, and J. C. Swearengen, (1978), "The Effects of Strain-Rate Variations on the Flow Stress of OFHC Copper", J. Mech. Phys. Solids, Vol. 26, pp. 251-268.
197. D. L. Holt, (1970), "Dislocation Cell Formation in Metals", J. Appl. Phys., Vol. 41, No. 8, pp. 3197-3201.

REFERENCES (Cont'd)

198. T. H. Alden, (1976), "Microstructural Interpretation of Work Softening in Aluminum", *Met. Trans., A*, Vol. 7, pp. 1057-1063.
199. A. S. Keh and S. Weissmann, (1963), "Dislocation Substructure in Body-Centered Cubic Metals", Chapter 5 in Electron Microscopy and Strength of Crystals, (Ed. G. Thomas and J. Washburn), Interscience Publishers, New York, pp. 231-300.
200. M. R. Staker and D. L. Holt, (1972), "The Dislocation Cell Size and Dislocation Density in Copper Deformed at Temperatures between 25 and 700C", *Acta. Met.*, Vol. 20, pp. 569-579.
201. L. E. Samuels and I. R. Lamborn, (1978), "Failure Analysis of Armanent Hardware", in Metallography in Failure Analysis, (Ed. J. L. McCall and P. M. French), Plenum Press, New York, pp. 167-190.
202. A. K. Chakrabarti and J. W. Spretnak, (1975), "Instability of Plastic Flow in the Directions of Pure Shear: I. Theory", *Met. Trans. A*, Vol. 6, pp. 733-736.
203. W. K. Nowacki and J. Zarka, (1974), "Sur le Champ des Temperatures Obtenues en Thermoelastoviscoplasticite", *Arch. Mech. Stosowanej*, Vol. 26, No. 4, pp. 701-715.
204. A. Needleman and J. R. Rice, (1978), "Limits to Ductility Set by Plastic Flow Localization", Mechanics of Sheet Metal Forming, (Ed. D. P. Koistinen and N. M. Wang), Plenum Press, New York, pp. 237-267.
205. J. W. Hutchinson and K. W. Neale, (1977), "Influence of Strain-Rate Sensitivity on Necking Under Uniaxial Tension", *Acta Met.*, Vol. 25, pp. 839-846.
206. E. Smith, T. S. Cook, and C. A. Rau, (1977), "Flow Localization and the Fracture Toughness of High Strength Materials", Fracture, Vol. 1, ICF4, Waterloo, Canada, pp. 215-236.
207. R. J. Asaro, (1978), "Geometrical Effects in the Inhomogeneous Deformation of Ductile Single Crystals", Brown University Report NSF DMR 76-20642.
208. U. F. Kocks, J. J. Jonas and H. Mecking, (1978), "The Development of Strain-Rate Gradients", Report of Argonne National Laboratory, Materials Science Division.
209. H. C. Rogers, (1974), "Adiabatic Shearing; A Review", Drexel University Report for U. S. Army Research Office.

REFERENCES (Cont'd)

210. R. J. Clifton, (1978), "Adiabatic Shear", Report prepared for National Research Council Committee on Material Response to Ultra-High Loading Rates.
211. R. L. Woodward, (1978), "The Penetration of Metal Targets which Fail by Adiabatic Shear Plugging", Int. J. Mech. Sci., Vol. 20, pp. 599-607.
212. R. L. Woodward, (1979), "Metallographic Features Associated with the Penetration of Titanium Alloy Targets", Met. Trans. A, Vol. 10, pp. 569-573.
213. R. L. Woodward and R. L. Aghan, (1978), "The Structure of a White-Etching Band in an Explosively Fractured Steel", Metals Forum, Vol. 1, No. 4, pp. 180-184.
214. J. M. Yellup and R. L. Woodward, (1980), "Investigations into the Prevention of Adiabatic Shear Failure in High Strength Armour Materials", Res Mechanica, Vol. 1, pp. 41-57.
215. M. E. Beckman and S. A. Finnegan (1973), "The Propagation of Adiabatic Shear", in Metallurgical Effects at High Strain Rates, (ed. R. W. Rohde, B. M. Butcher, J. R. Holland, and C. H. Karnes), Plenum Press, New York, pp. 531-544.,
216. R. S. Culver, (1973), "Thermal Instability Strain in Dynamic Plastic Deformation", in Metallurgical Effects at High Strain Rates, (Ed. R. W. Rohde, B. M. Butcher, J. R. Holland, and C. H. Karnes), Plenum Press, New York, pp. 519-530.
217. G. L. Moss and R. B. Pond, (1975), "Inhomogeneous Thermal Changes in Copper During Plastic Elongation", Met. Trans., Vol. 6A, pp. 1223-1235.
218. M. Afzali, (1977), "Sur la Plasticite Adiabatique de Quelques Metaux Usuels", Ph. D. Thesis, Universite Pierre et Marie Curie, Paris VI.
219. T. Hayashi, H. Yamamura, and S. Okano, (1977), "Temperature Measurement of Metals Under High Velocity Deformation", Proc., Twentieth Japan Cong. on Mat. Res., Soc. of Mat. Sci., Kyoto, Japan, pp. 94-98.
220. J. Litonski, (1977), "Plastic Flow of a Tube under Adiabatic Torsion", Bulletin de l'Academie Polonaise des Sciences, Vol. 25, No. 1, pp. 7-14.
221. G. R. Johnson, (1981), "Dynamic Analysis of a Torsion Test Specimen Including Heat Conduction and Plastic Flow", J. Eng. Mat. Tech., Vol. 103, pp. 201-206.

REFERENCES (Cont'd)

222. U. S. Lindholm, A. Nagy, G. R. Johnson, and J. M. Hoegfeldt, (1980), "Large Strain, High Strain Rate Testing of Copper", Trans. ASME, J. Eng. Mat. Technol., Vol. 102, No. 4, pp. 376-381.
223. H. C. Rogers and C. V. Shastri, (1981), "Material Factors in Adiabatic Shearing in Steels", Chapter 18 in Shock Waves and High-Strain-Rate Phenomena in Metals, Plenum Press, New York, pp. 285-298.
224. G. B. Olson, J. F. Mescall, and M. Azrin, (1981), "Adiabatic Deformation and Strain Localization", Chapter 14 in Shock Waves and High-Strain-Rate Phenomena in Metals (Ed. M. A. Meyers and L. E. Murr), Plenum Press, New York, pp. 221-247.
225. K. H. Hartmann, H. D. Kunze, and L. W. Meyer, (1981), "Metallurgical Effects on Impact Loaded Materials", Chapter 21 in Shock Waves and High-Strain-Rate Phenomena in Metals, Plenum Press, New York, pp. 325-337.
226. G. L. Moss and R. B. Pond, (1975), "Inhomogeneous Thermal Changes in Copper During Plastic Elongation", Met. Trans., Vol. 6A, pp. 1223-1235.
227. M. R. Staker, (1981), "The Relation between Adiabatic Shear Instability Strain and material Properties", Acta Met., Vol. 29, pp. 683-689.
228. C. H. Karnes, (1968), "The Plate Impact Configuration for Determining Mechanical Properties of Materials at High Strain Rates", in Mechanical Behavior of Materials Under Dynamic Loads, (ed. U. S. Lindholm), Springer-Verlag, New York, pp. 270-293.
229. H. M. Berkowitz and L. J. Cohen, (1969), "A Study of Plate-Slap Technology. Part I. A Critical Evaluation of Plate-Slap Technology", Air Force Materials Laboratory Report No. AFML TR-69-106.
230. R. J. Clifton, (1976), "Some Recent Developments in Plate Impact Experiments", Propagation of Shock Waves in Solids, ASME, New York.
231. R. J. Clifton and P. Kumar, (1977), "Dislocation Configurations Due to Plate Impact", IUTAM Symposium on High Velocity Deformation of Solids (ed. K. Kawata and J. Shioiri), Springer-Verlag, New York, pp. 36-49.
232. K. S. Kim and R. J. Clifton, (1980), "Pressure-Shear Impact of 6061-T6 Aluminum", J. Appl. Mech., Vol. 47, pp. 11-16.
233. C. H. Li and R. J. Clifton, "Dynamic Stress-Strain Curves at Plastic Shear Strain Rates of 10^5 s^{-1} ", Proc. 1981 Topical Conference on Shock Waves in Condensed Matter, Amer. Phys. Soc.

REFERENCES (Cont'd)

234. J. Harding and J. Huddart, (1979), "The Use of the Double-Notch Shear Test in Determining the Mechanical Properties of Uranium at Very High Rates of Strain", in Mechanical Properties at High Rates of Strain, 1979, (ed. J. Harding), The Institute of Physics, London, pp. 490-61.
235. A. K. Ghosh, (1977), "The Influence of Strain Hardening and Strain-Rate Sensitivity on Sheet Metal Forming", Trans. ASME, J. Eng. Mat. Techn., Vol. 99, pp. 264-274.
236. G. Boothroyd and J. A. Bailey, (1966), "Effects of Strain Rate and Temperature in Orthogonal Metal Cutting", J. Mech. Eng. Sci., Vol. 8, No. 3, pp. 264-275.
237. P. L. B. Oxley, (1963), "Rate of Strain Effect in Metal Cutting", J. Engng Ind., Vol. 85, pp. 335-337.
238. C. Spaans, (1972), "A Treatise on the Streamlines and the Stress Strain, and Strain Rate Distributions, and on Stability in the Primary Shear Zone in Metal Cutting", J. Eng. Ind., Vol. 84, pp. 690-696.
239. P. L. B. Oxley and W. F. Hastings, (1977), "Predicting the Strain Rate in the Zone of Intense Shear in which the Chip is Formed in Machining from the Dynamic Flow Stress Properties of the Work Material and the Cutting Conditions", Proc. Roy. Soc., London A, Vol. 356, pp. 395-410.
240. B. F. Von Turkovich, (1972), "Metal Cutting Analysis", in Review of Material Processing Literature - 1966-1968, (ed. S. Ramalingam), J. Engng Ind., pp. 704-706.
241. G. Boothroyd, (1976), "Review of Materials Processing Literature 1971-72; Part 1: Materials Removal Practice", Trans. ASME, J. Engng Ind., Vol. 98, pp. 1-11.
242. F. LeMaitre, D. Bizeul, and R. Weill, (1974), "Contribution to the Study of Periodic Phenomena in Dynamic Deformation", C.I.R.P. 24th General Assembly, Kyoto, Japan.
243. P. Mathew, W. F. Hastings, and P. L. B. Oxley, (1979), "Machining-Study in High Strain Rate Plasticity," in Mechanical Properties at High Rates of Strain 1979, (Ed. J. Harding), The Institute of Physics, London, pp. 360-371.
244. W. F. Hastings, P. Mathew, and P. L. B. Oxley, (1980), "A Machining Theory for Predicting Chip Geometry, Cutting Forces etc. from Work Material Properties and Cutting Conditions", Proc. Roy. Soc. London, Vol. A371, pp. 569-587.

REFERENCES (Cont'd)

245. N. Martensson, (1970), "On the Influence of the Rate of Deformation at Cold Processing", Acta Polytech. Scandinavica, Mech. Engng Ser. No. 52, Stockholm, pp. 6-89.
246. W. A. Wong and J. J. Jonas, (1967), "Aluminum Extrusion as a Thermally Activated Process", Trans., Met. Soc. AIME, Vol. 242, pp. 2271-2280.
247. G. Gagnon and J. J. Jonas, (1969), "Zinc Extrusion as a Thermally Activated Process", Trans., Met. Soc. AIME, Vol. 245, pp. 2581-2589.
248. R. N. Orava and H. E. Otto, (1970), "The Effect of High Energy Rate Forming on the Terminal Characteristics of Metal - A Review", J. Metals, Vol. 22, pp. 17-31.
249. J. Duffy, (1979), "The J. D. Campbell Memorial Lecture: Testing Techniques and material Behaviour at High Rates of Strain", in Mechanical Properties at High Rates of Strain, 1979, (Ed. J. Harding), The Institute of Physics, London, pp. 1-15.
250. M. C. C. Tsao and J. D. Campbell, (1973), "Plastic Shear Properties of Metals and Alloys at High Strain Rates", Air Force Mat. Lab. Report, AFML-TR-73-177.
251. Y. V. R. K. Prasad and R. W. Armstrong, (1973), "Effect of Grain Size on the Thermal Activation Strain Rate Analysis in HCP Metals", Indian Journal of Technology, Vol. 11, No. 11, pp. 513-515.
252. J. Harding, (1974c), "The Temperature and Strain Rate Sensitivity of α -Titanium", University of Oxford, Report No. 1108/74. Published in Archiwum Mechaniki Stosowanej, 1975, Vol. 27, pp. 715-732.
253. R. W. Armstrong, (1973), "Thermal Activation Strain Rate Analysis (TASRA) for Polycrystalline metals", J. Scient. Ind. Res., Vol. 32, pp. 591-598.
254. A. T. Santhanam, V. Ramachandran, and R. E. Reed-Hill, (1970), "An Investigation of the Shape of the Titanium Stress-Strain Curves after a Strain Rate Change", Met. Trans., Vol. 1, pp. 2593-2598.
255. B. De Meester, M. Doner, and H. Conrad, (1975), "Deformation Kinetics of the Ti-6Al-4V Alloy at Low Temperatures", Met. Trans. A, Vol. 6, pp. 65-75.
256. J. Shioiri and K. Satoh, (1974), "An Ultrasonic Wave Study of the Behavior of Dislocations Under High Strain Rate Deformations" in Mechanical Properties of Materials at High Rates of Strain, (Ed. J. Harding), The Institute of Physics, London, pp. 154-162.

REFERENCES (Cont'd)

257. T. Hayashi and N. Tanimoto, (1977), "Behavior of Materials Under Dynamic Combined Stresses of Torsion and Tension", IUTAM Symposium on High Velocity Deformation of Solids, (Ed. K. Kawata and J. Shioiri) Springer-Verlag, New York, pp. 279-288.
258. J. D. Campbell and J. Harding, (1961), "The Effect of Grain Size, Rate of Strain, and Neutron Irradiation on the Tensile Strength of α -Iron", in Response of Metals to High Velocity Deformation, (Ed. P. G. Shewmon and V. F. Zackay), Interscience, New York, pp. 51-75.
259. C. Albertini and M. Montagnani, (1974), "Testing Techniques Based on the Split-Hopkinson Bar", in Mechanical Properties at High Rates of Strain, (Ed. J. Harding), The Institute of Physics, London, pp. 22-32.
260. C. Albertini and M. Montagnani, (1978), "Effect of Welding on Dynamic Response of Austenitic Stainless Steel for Nuclear Applications", Third Int. Symp., Japan Welding Society, Tokyo.
261. J. Harding, (1978), "Strain Rate Effects in Reactor Pressure Vessel Steels", University of Oxford, Report QUEL No. 1266/78.
262. J. Buchar and Z. Bilek, (1981), "Plastic Flow of Irradiated Steel at High Strain Rates", Phys. Stat. Sol. (a), Vol. 63, pp. 259-264.
263. H. Bohm and K. D. Closs, (1977), "Effects of Strain Rate on High Temperature Mechanical Properties of Irradiated Incoloy 800 and Hastelloy X", Radiation Effects in Breeder Reactor Structural Materials, (Ed. M. L. Bleiberg and J. W. Bennett), The Metallurgical Society of AIME, pp. 347-356.
264. A. S. Wronski and G. A. Sargent, and A. A. Johnson, (1965), "Irradiation Hardening and Embrittlement in Body-Centered Cubic Transition Metals", in Flow and Fracture of Metals in Nuclear Environments, ASTM, STP 380, pp. 69-85.
265. P. J. Ring, H. J. Busboom, and C. N. Spalaris, (1972), "Post-Irradiation Mechanical Properties of Austenitic Alloys and Effects of Intergranular Fission Product Attack", from International Embrittlement and Creep, The British Nuclear Engineering Society, London, pp. 197-208.
266. F. Zaverl, Sr. and D. Lee, (1978), "Constitutive Relations for Nuclear Reactor Core Materials", J. Nucl. Mat., Vol. 75, pp. 14-19.
267. U. S. Lindholm, (1968), "Some Experiments in Dynamic Plasticity Under Combined Stress", in Mechanical Behavior of Materials Under Dynamic Loads, (Ed. U. S. Lindholm), Springer-Verlag, New York, pp. 77-95.

REFERENCES (Concluded)

268. J. Shioiri and K. Satoh, (1979), "An Ultrasonic Method of Detecting Dislocation Behavior at High Strain Rates: Theoretical Basis for Data Analysis in Mechanics" Properties of Materials at High Rates of Strain, (Ed. J. Harding), The Institute of Physics, London, pp. 121-129.
269. W. G. Ferguson and F. E. Hauser, and J. E. Dorn, (1967b), "Dislocation Damping in Zinc Single Crystals", British J. Appl. Phys., Vol. 18, No. 4, pp. 411-417.

BIBLIOGRAPHY

- Afzali, M. (1977), "Sur la Plasticite Adiabatique de Quelques Metaux Usuels", Ph.D. Thesis, Universite Pierre et Marie Curie, Paris VI.
- Albertini, C. and Montagnani, M. (1974), "Testing Techniques Based on the Split-Hopkinson Bar", in Mechanical Properties at High Rates of Strain, (Ed. J. Harding), The Institute of Physics, London, pp. 22-32.
- Albertini, C. and Montagnani, M. (1978), "Effect of Welding on Dynamic Response of Austenitic Stainless Steel for Nuclear Applications", Third Int. Symp., Japan Welding Society, Toyko.
- Alden, T. H. (1976), "Microstructural Interpretation of Work Softening in Aluminum", Met. Trans., A, Vol. 7, pp. 1057-1063.
- Alder, J. F. and Phillips, V. A. (1954-55), "The Effect of Strain Rate and Temperature on the Resistance of Aluminum, Copper and Steel to Compression", J. Inst. Metals, Vol. 83, pp. 80-86.
- Argon, A. S. (Ed.) (1975), Constitutive Equations in Plasticity, MIT Press, Cambridge, Mass.
- Armstrong, R. W. (1973), "Thermal Activation Strain Rate Analysis (TASRA) for Polycrystalline Metals", J. Scient. Ind. Res., Vol. 32, pp. 591-598.
- Asaro, R. J. (1978), "Geometrical Effects in the Inhomogeneous Deformation of Ductile Single Crystals", Brown University Report NSF DMR 76-20642.
- Babcock, S. G. and Perkins, R. D. (1968), "High Strain-Rate Response of Three Heat-Shield Materials", General Motors Corporation, Materials and Structures Laboratory, Technical Report SAMSU TR 68-71, Vol. II.
- Backman, M. E. and Finnegan, S. A. (1973), "The Propagation of Adiabatic Shear", in Metallurgical Effects at High Strain Rates, (Ed. R. W. Rohde, B. M. Butcher, J. R. Holland, and C. H. Karnes), Plenum Press, New York, pp. 531-544.
- Backman, M. E. and Goldsmith, W. (1978), "The Mechanics of Penetration of Projectiles into Targets", Int. J. Eng. Sci., Vol. 16, pp. 1-99.
- Bailey, J. A. and Singer, A. R. E. (1963-64), "Effect of Strain Rate and Temperature on the Resistance to Deformation of Aluminum, Two Aluminum Alloys and Lead", J. Inst. Metals, Vol. 92, pp. 404-408.
- Bailey, J. A., Haas, S. L. and Shah, M. K. (1972), "Effect of Strain-Rate and Temperature on the Resistance to Torsional Deformation of Several Aluminum Alloys", Int. J. Mech. Sci., Vol. 14, pp. 735-754.

BIBLIOGRAPHY (Cont'd)

- Baker, W. W. and Yew, C. H. (1966), "Strain-Rate Effects in the Propagation of Torsional Plastic Waves", J. Appl. Mech., Vol. 33, pp. 917-923.
- Barracough, D. R. and Sellars, C. M. (1974), "The Effect of Varying Deformation Conditions During Hot Torsion Testing:", in Mechanical Properties at High Rates of Strain, (Ed. J. Harding), The Institute of Physics, London, pp. 111-123.
- Basinski, Z. S. (1959), "Thermally Activated Glide in Face-Centered Cubic Metals and Its Application to the Theory of Strain Hardening", Phil. Mag., Vol. 4, pp. 393-432.
- Basinski, Z. S. and Christian, J. W. (1960), "The Influence of Temperature and Strain Rate on the Flow Stress of Annealed and Decarburized Iron at Subatmospheric Temperatures", Aust. J. Phys., Vol. 13, pp. 299-308.
- Bell, J. F. (1951), "Propagation of Plastic Waves in Pre-Stressed Bars", The John Hopkins University Technical Report No. 5, U.S. Navy Contract N6-ONR-243.
- Bell, J. F. (1960), "An Experimental Study of the Applicability of the Strain Rate Independent Theory of Plastic Wave Propagation in Annealed Aluminum Copper, Magnesium and Lead", The Johns Hopkins University Technical Report No. 5, U. S. Army Contract No. DA-36-034-ORD-2366.
- Bell, J. F. (1968), The Physics of Large Deformation of Crystalline Solids, Springer-Verlag, New York.
- Berkowitz, H. M. and Cohen, L. J. (1969), "A Study of Plate-Slap Technology. Part I. A Critical Evaluation of Plate-Slap Technology", Air Force Materials Laboratory Report No. AFML TR-69-106.
- Bhushan, B and Jahsman, W. E. (1978), "Measurement of Dynamic Material Behavior Under Nearly Uniaxial Strain Conditions", Int. J. Solids Structures, Vol. 14, pp. 739-753.
- Bianchi, G. (1964), "Some Experimental and Theoretical Studies on the Propagation of Longitudinal Plastic Waves in a Strain-Rate Dependent Material", IUTAM Symposium on Stress Waves in Anelastic Solids (Ed. H. Kolsky and W. Prager) Springer-Verlag, Berlin, pp. 101-117.
- Bitans, K. and Whitton, P. W. (1972), "High-Strain-Rate Investigations, with Particular Reference to Stress/Strain Characteristics", Int. Metal. Rev., Vol. 17, pp. 66-78.
- Bodner, S. R. and Merzer, A. (1978), "Viscoplastic Constitutive Equations for Copper with Strain Rate History and Temperature Effects", Technion, Israel, MML Report No. 55.

- Bodner, S. R. and Parton, Y. (1972), "Dynamic Inelastic Properties of Materials. Part II: Representation of Time Dependent Characteristics of Metals", Eighth Cong. Int. Council Aero. Sco., Paper No. 72-78.
- Bohm, H. and Closs, K. D. (1977), "Effects of Strain Rate on High Temperature Mechanical Properties of Irradiated Incoloy 800 and Hastelloy X", Radiation Effects in Breeder Reactor Structural Materials, (Ed. M. L. Bleiberg and J. W. Bennett), The Metallurgical Society of AIME, pp. 347-356.
- Boothroyd, G. (1976), "Review of Materials Processing Literature 1971-72; Part 1: Materials Removal Practice", Trans. ASME, J. Engng Ind., Vol. 98, pp. 1-11.
- Boothroyd, G. and Bailey, J. A. (1966), "Effects of Strain Rate and Temperature in Orthogonal Metal Cutting", J. Mech. Eng. Sci., Vol. 8, No. 3, pp. 264-275.
- Briggs, T. L. and Campbell, J. D. (1972), "The Effect of Strain Rate and Temperature on the Yield and Flow of Polycrystalline Niobium and Molybdenum", Acta Met., Vol. 20, pp. 711-724.
- Buchar, J. and Bilek, Z. (1981), "Plastic Flow of Irradiated Steel at High Strain Rates", Phys. Stat. Sol. (a), Vol. 63, pp. 259-264.
- Campbell, J. D. (1970), "Dynamic Plasticity of Metals", International Centre for Mechanical Sciences, Course and Lectures, No. 46, Udine, Springer-Verlag, Vienna and New York.
- Campbell, J. D. (1973), "Dynamic Plasticity: Macroscopic and Microscopic Aspects", Mater. Sci. Eng., Vol. 12, pp. 3-21.
- Campbell, J. D. and Briggs, T. L. (1975), "Strain-Rate History Effects in Polycrystalline Molybdenum and Niobium", J. Less Common Metals, Vol. 40, pp. 235-250.
- Campbell, J. D. and Dowling, A. R. (1970), "The Behavior of Materials Subjected to Dynamic Incremental Shear Loading", J. Mech. Phys. Solids, Vol. 18, pp. 43-63.
- Campbell, J. D. and Duby, J. (1957), "Delayed Yield and Other Dynamic Loading Phenomena in a Medium-Carbon Steel", Proc. Conf. on the Properties of Materials at High Rates of Strain, Institution of Mechanical Engineers, London, pp. 214-220.
- Campbell, J. D., Eleiche, A. M., and Tsao, M. C. C. (1977), "Strength of Metals and Alloys at High Strains and Strain Rates", in Fundamental Aspects of Structural Alloy Design, (Ed. R. I. Jaffee and B. A. Wilcox), Plenum Press, New York, pp. 545-563.
- Campbell, J. D. Ferguson, W. G. (1970), "The Temperature and Strain-Rate Dependence of the Shear Strength of Mild Steel", Phil. Mag., Vol. 21, pp. 63-82.

1. Campbell, J. D. and Harding, J. (1961), "The Effect of Grain Size, Rate of Strain, and Neutron Irradiation on the Tensile Strength of α -Iron", in Response of Metals to High Velocity Deformation, (Ed. P. G. Shewmon and V. F. Zackay), Interscience, New York, pp. 51-75.
2. Campbell, J. D. and Marsh, K. J. (1962), "The Effect of Grain Size on the Delayed Yielding of Mild Steel", *Phil. Mag.*, Vol. 7, pp. 933-952.
3. Chakrabarti, A. K. and Spretnak, J. W. (1975), "Instability of Plastic Flow in the Directions of Pure Shear: I. Theory", *Met. Trans. A*, Vol. 6, pp. 733-736.
4. Chiddister, J. L. and Malvern, L. E. (1963), "Compression Impact Testing of Aluminum at Elevated Temperatures", *Exp. Mech.*, Vol. 3, pp. 81-90.
5. Chien, C. Y. and Duffy, J. (1981a), "Strain Rate History Effects in LiF Single Crystals During Dynamic Loading in Shear", *Mater. Sci. Eng.*, Vol. 48, No. 2, pp. 207-222.
6. Chien, C. Y. and Duffy, J. (1981b), "Strain Rate History Effects and Observations of Dislocation Substructure in Aluminum Single Crystals Following Dynamic Deformation", Brown University Report NSF-MEA 79-23742/3.
7. Clark, D. S. and Duwez, P. E. (1948), "Discussion of the Forces Acting in Tension Impact Tests of Materials", *J. Appl. Mech.*, Vol. 15, pp. A243-A247.
8. Clark, D. S. and Wood, D. S. (1949), "The Time Delay for the Initiation of Plastic Deformation at Rapidly Applied Constant Stress", *Proc. ASTM*, Vol. 49, pp. 717-735.
9. Clifton, R. J. (1966), "An Analysis of Combined Longitudinal and Torsional Plastic Waves in a Thin-Walled Tube", *Proc. Fifth Int. Cong. Appl. Mech.*, ASME, pp. 465-480.
10. Clifton, R. J. (1974), "Plastic Waves: Theory and Experiment", Chapter III Mechanics Today, Vol. 1, 1972, (Ed. S. Nemat-Nasser), Pergamon Press, Oxford.
11. Clifton, R. J. (1976), "Some Recent Developments in Plate Impact Experiments", Propagation of Shock Waves in Solids, ASME, New York.
12. Clifton, R. J. (1978), "Adiabatic Shear", Report prepared for National Research Council Committee on Material Response to Ultra-High Loading Rates.
13. Clifton, R. J. and Kumar, P. (1977), "Dislocation Configurations Due to Plate Impact", *IUTAM Symposium on High velocity Deformation of Solids* (ed. K. Kawata and J. Shioiri), Springer-Verlag, New York, pp. 36-49.

- Convey, E. and Pugh, H. Ll. D. (1968), "Velocity of Torsional Waves in Metals Stressed Staticly into the Plastic Range", J. Mech. Eng. Sci., Vol. 10, No. 2, pp. 153-164.
- Cook, P. M. (1957), "True Stress-Strain Curves for Steel in Compression at High Temperatures and Strain Rates, for Application of the Calculation of Load and Torque in Hot Rolling", in Properties Materials at High Rates of Strain, Inst. Mech. Engrs., London, pp. 86-97.
- Costin, L. S. and Duffy, J. (1979), "The Effect of Loading Rate and Temperature on the Initiation of Fracture in a Mild Rate-Sensitive Steel", Trans. ASME, Vol. 101, J. Eng. Matls. Tech., pp. 258-264.
- Costin, L. S., Crisman, E. E., Hawley, R. H. and Duffy, J. (1979), "On the Localization of Plastic Flow in Mild Steel Tubes Under Dynamic Torsional Loading", in Mechanical Properties at High Rates of Strain, 1979, (Ed. J. Harding); The Institute of Physics, London, pp. 90-100, see also "Strain Rate and Strain Rate History Effects in Two Mild Steels" by M. L. Wilson, R. W. Hawley and J. Duffy, Brown University Report, NSF Grant ENG 75-18532/2, March 1979.
- Courant, R. and Hilbert, D. (1962), "Methods of Mathematical Physics", Vol. II, Partial Differential Equations, Interscience, New York.
- Craggs, J. W. (1957), "The Propagation of Infinitesimal Plane Waves in Elastic-Plastic Materials", J. Mech. Phys. Solids, Vol. 5, pp. 115-124.
- Craggs, J. W. (1961), "Plastic Waves" in Progress in Solid Mechanics, (Ed. I. N. Sneddon and R. Hill), Vol. 2, pp. 143-197, North-Holland, Amsterdam.
- Cristescu, N. (1967), Dynamic Plasticity, North-Holland, Amsterdam.
- Culver, R. S. (1973), "Thermal Instability Strain in Dynamic Plastic Defirnatuib", in Metallurgical Effects at High Strain Rates, (Ed. R. W. Rohde, B. M. Butcher, J. R. Holland, and C. H. Karnes), Plenum Press, New York, pp. 519-530.
- Davids, N. and Kumar, S. (1958), "A Contour Method for One Dimensional Pulse Propagation in Elastic-Plastic Materials", Third U.S. Nat. Cong. of Appl. Mech., pp. 503-512.
- Davies, E. D. H. and Hunter, S. C. (1963), "The Dynamic Compression Testing of Solids by the Method of the Split Hopkinson Bar", J. Mech. Phys. Solids, Vol. 11, pp. 155-179.
- Davies, R. M. (1946-48), "A Critical Study of the Hopkinson Pressure Bar", Phil. Trans. Roy. Soc., (London), Vol. 240A, pp. 375-457.
- DeVault, G. P. (1965), "The Effect of Lateral Inertia on the Propagation of Plastic Strain in a Cylindrical Rod", J. Mech. Phys. Solids, Vol. 13, pp. 55-68.

- DeMeester B., Doner, M., and Conrad, H. (1975), "Deformation Kinetics of the Ti-6Al-4V Alloy at Low Temperatures", *Met. Trans. A*, Vol. 6, pp. 65-75.
- Dharan, C. K. H. and Hauser, F. E. (1970), "Determination of Stress-Strain Characteristics at Very High Strain Rates", *Exp. Mech.*, pp. 370-376.
- Dharan, C. K. H. and Hauser, F. E. (1973), "High-Velocity Dislocation Damping in Aluminum", *J. Appl. Phys.*, Vol. 44, No. 4, pp. 1468-1474.
- Donnell, L. H. (1930), "Longitudinal Wave Transmission and Impact", *Trans., ASME*, Vol. 52, pp. 153-167.
- Dormeuil, R., Steilly, M., and Caput, M. (1976), "Comportement en Traction Dynamique de Monocristaux de Cuivre", (Dynamic Traction Behavior of Copper Monocrystals), *Fourth Int. Conf. on the Strength of Met. and Alloys*, Nancy, pp. 1141-1145.
- Dorn, J. E., Goldberg, A., and Tietz, T. E. (1949), "The Effect of Thermal-Mechanical History on the Strain Hardening of Metals", *Trans. AIME*, Vol. 180, pp. 205-224.
- Dorn, J. E., Mitchell, J., and Hauser, F. (1965), "Dislocation Dynamics", *Exp. Mech.*, pp. 353-362.
- Duffy, J. (1979), "The J. D. Campbell Memorial Lecture: Testing Techniques and Material Behaviour at High Rates of Strain", in *Mechanical Properties at High Rates of Strain, 1979*, (Ed. J. Harding), *The Institute of Physics*, London, pp. 1-15.
- Duffy, J., Campbell, J. D., and Hawley, R. H. (1971), "On the Use of a Torsional Split Hopkinson Bar to Study Rate Effects in 1100-O Aluminum", *J. Appl. Mech.*, Vol. 38, pp. 83-91.
- Dusek F. (1970), "Plastic Deformation at High Strain Rates", *Czech. J. Phys., B*, Vol. 20, pp. 776-789.
- Dusek, F. (1974), "Response of Materials to High Loading Rates", In *Dynamika Osrodkow Niesprezystych*, (Ed. P. Perzyna), *Polska Akademia Nauk*, pp. 125-173.
- Dusek, F., Jasinski, Z., Buchar, J., Litwora, A., and Piatkowski, A. (1976), "Response of Cu Single Crystals to High Loading Rates", *Czech. J. Phys.*, Vol. B26, Part I, pp. 538-558, and Part II, pp. 559-564.
- Duwez, P. E. and Clark, D. S. (1947), "An Experimental Study of the Propagation of Plastic Deformation under Conditions of Longitudinal Impact", *Proc. ASTM* Vol. 47, pp. 502-532.
- Edington, J. W. (1968), "Effect of Strain Rate on the Dislocation Substructure in Deformed Niobium Single Crystals", in *Mechanical Behavior of Materials under Dynamic Loads*, (Ed. U. S. Lindholm), *Springer-Verlag*, New York, pp. 191-240.

- Edington, J. W. (1969), "The Influence of Strain Rate on the Mechanical Properties and Dislocation Substructure in Deformed Copper Single Crystals", *Phil. Mag.*, Eighth Ser., Vol. 19, No. 162, pp. 1189-1206.
- Eleiche, A. M. (1972), "A Literature Survey of the Combined Effects of Strain Rate and Elevated Temperature on the Mechanical Properties of Metals", Air Force Materials Laboratory, Technical Report 72-125.
- Eleiche, A. M. (1980), "The Influence of Strain-Rate History and Temperature on the Shear Strength of Commercially-Pure Titanium", Presented at Fourth International Conference on Titanium, Kyoto, Japan.
- Eleiche, A. M. (1981), "Strain-Rate History and Temperature Effects on the Torsional-Shear Behavior of a Mild Steel", *Exp. Mech.*, Vol. 21, pp. 285-294.
- Eleiche, A. M. and Campbell, J. D. (1974), "The Influence of Strain Rate History on the Shear Strength of Copper and Titanium at Large Strains", University of Oxford, Report No. 1106/74.
- Eleiche, A. M. and Campbell, J. D. (1976a), "The Influence of Strain-Rate History and Temperature on the Shear Strength of Copper, Titanium and Mild Steel", University of Oxford, Report AFML-TR-76-90.
- Eleiche, A. M. and Campbell, J. D. (1976b), "Strain-Rate Effects During Reverse Torsional Shear", *Exp. Mech.*, pp. 281-290.
- Eleiche, A. M. and Duffy, J. (1975), "Effects of Temperatures on the Static and Dynamic Stress-Strain Characteristics in Torsion of 1100-0 Aluminum", *Int. J. Mech. Sci.*, Vol. 17, pp. 85-95.
- Ferguson, W. G., Kumar, A. and Dorn, J. E. (1967a), "Dislocation Damping in Aluminum at High Strain Rates", *J. Appl. Phys.*, Vol. 38, No. 4, pp. 1863-1869.
- Ferguson, W. G., Hauser, F. E. and Dorn, J. E. (1967b), "Dislocation Damping in Zinc Single Crystals", *British J. Appl. Phys.*, Vol. 18, No. 4, pp. 411-417.
- Frantz, R. A. and Duffy J. (1972), "The Dynamic Stress-Strain Behavior in Torsion of 1100-0 Aluminum Subjected to a Sharp Increase in Strain Rate", *J. Appl. Mech.*, Vol. 39, pp. 939-945.
- Gagnon, G. and Jonas, J. J. (1969), "Zinc Extrusion as a Thermally Activated Process", *Trans., Met. Soc. AIME*, Vol. 245, pp. 2581-2589.
- Ghosh, A. K. (1977), "The Influence of Strain Hardening and Strain-Rate Sensitivity on Sheet Metal Forming", *Trans. ASME, J. Eng. Mat. Techn.*, Vol. 99, pp. 264-274.
- Gillis, P. P. and Gilman, J. J. (1965), "Dynamic Dislocation Theory of Crystal Plasticity, Part I. The Yield Stress", *J. Appl. Phys.*, Vol. 36, pp. 3370-3380.

- Gilman, J. J. (1960), "The Plastic Resistance of Crystals", Aust. J. Phys., Vol. 13, pp. 327-343.
- Gilman, J. J. (1965), "Microdynamics of Plastic Flow at Constant Stress", J. Appl. Phys., Vol. 36, pp. 2772-2777.
- Gilman, J. J. (1969), Micromechanics of Flow in Solids, McGraw-Hill, New York.
- Gilman, J. J. and Johnston, W. G. (1960), "Behavior of Individual Dislocations in Strain-Hardened LiF Crystals", J. Appl. Phys., Vol. 31, No. 4, pp. 687-692.
- Glenn, T. and Bradley, W. (1973), "The Origin of Strain-Rate Sensitivity in OFHC Copper", Met. Trans., Vol. 4, pp. 2343-2348.
- Green, S. J. and Babcock, S. G. (1966), "Response of Materials to Suddenly Applied Stress Loads, Part I: High Strain-Rate Properties of Eleven Reentry-Vehicle Materials at Elevated Temperatures", General Motors Defense Research Laboratories, Report TR 66-83.
- Green, S. J., Maiden, C. J., Babcock, S. G. and Schierloh, F. L. (1969), "The High Strain-Rate Behavior of Face Centered Cubic Metals", in Inelastic Behavior of Solids, (Ed. M. F. Kanninen, W. F. Adler, A. R. Rosenfield, and R. I. Jaffee), McGraw-Hill, New York, pp. 521-542.
- Hahn, G. T. (1962), "A Model for Yielding with Special Reference to the Yield-Point Phenomena of Iron and Related BCC Metals", Acta Met., Vol. 10, pp. 727-738.
- Harding, J. (Ed.) (1974a), Mechanical Properties at High Rates of Strain, The Institute of Physics, London.
- Harding, J. (1974b), Discussion of paper by J. Klepaczko and J. Duffy, Mechanical Properties at High Rates of Strain, (Ed. J. Harding), The Institute of Physics, London, pp. 190-191.
- Harding, J. (1974c), "The Temperature and Strain Rate Sensitivity of α -Titanium", University of Oxford, Report No. 1108/74. Published in Archiwum Mechaniki Stosowanej, 1975, Vol. 27, pp. 715-732.
- Harding, J. (1977), "Effect of Temperature and Strain Rate on Strength and Ductility of Four Alloys Steels", Met. Tech., pp. 6-16.
- Harding, J. (1978), "Strain Rate Effects in Reactor Pressure Vessel Steels", University of Oxford, Report QUEL No. 1266/78.
- Harding, J. (Ed.) (1979), Mechanical Properties at High Rates of Strain, 1979, Institute of Physics, London.
- Harding, J. and Huddart, J. (1979), "The Use of the Double-Notch Shear Test in Determining the Mechanical Properties of Uranium at Very High Rates of Strain", in Mechanical Properties at High Rates of Strain, 1979, (Ed. J. Harding), The Institute of Physics, London, pp. 49-61.

- Hart, E. W. (1970), "A Phenomenological Theory for Plastic Deformation of Polycrystalline Metals", *Acta Met.*, Vol. 18, pp. 599-610.
- Hartmann, K. H. Kunze, H. D. and Meyer, L. W. (1981), "Metallurgical Effects on Impact Loaded Materials", Chapter 21 in Shock Waves and High-Strain-Rate Phenomena in Metals, Plenum Press, New York, pp. 325-337.
- Hastings, W. F., Mathew, P. and Oxley, P. L. B. (1980), "A Machining Theory for Predicting Chip Geometry, Cutting Forces etc. from Work Material Properties and Cutting Conditions", *Proc. Roy. Soc. London*, Vol. A371, pp. 569-587.
- Hauser, F. E. (1966), "Techniques for Measuring Stress-Strain Relations at High-Strain Rates", *Exp. Mech.*, Vol. 6, pp. 395-402.
- Hauser, F. E., Simmons, J. A. and Dorn, J. E. (1961), "Strain Rate Effects in Plastic Wave Propagation", in Response of Metals to High Velocity Deformation, (Ed. P. G. Shewmon and V. F. Zackay), *Inter-Science*, New York, pp. 93-114.
- Hayashi, T. and Tanimoto, N. (1977), "Behavior of Materials Under Dynamic Combined Stresses of Torsion and Tension", *IUTAM Symposium on High Velocity Deformation of Solids*, (Ed. K. Kawata and J. Shioiri) Springer-Verlag, New York, pp. 279-288.
- Hayashi, T., Yamamura, H. and Okano, S. (1977), "Temperature Measurement of Metals Under High Velocity Deformation", *Proc., Twentieth Japan Cong. on Mat. Res., Soc. of Mat. Sci., Kyoto, Japan*, pp. 94-98.
- Hockett, J. E. (1967), "On Relating the Flow Stress of Aluminum to Strain, Strain Rate, and Temperature", *Trans. Met. Soc. AIME*, Vol. 239, pp. 969-976.
- Hockett, J. E. and Zukas, E. G. (1974), "The Response of Iron to Dynamic Compression", in Mechanical Properties at High Rates of Strain, (Ed. J. Harding) *The Institute of Physics*, London, pp. 53-61.
- Holt, D. L. (1970), "Dislocation Cell Formation in Metals", *J. Appl. Phys.*, Vol. 41, No. 8, pp. 3197-3201.
- Holt, D. L., Babcock, S. G., Green, S. J. and Maiden, C. J. (1967), "The Strain Rate Dependence of the Flow Stress in Some Aluminum Alloys", *Trans., ASM*, Vol. 60, pp. 152-159.
- Honeycombe, R. W. K. (1968), The Plastic Deformation of Metals, *Edwards Arnold*, London.
- Hopkinson, B. (1905), "The Effects of Momentary Stresses in Metals", *Proc. Roy. Soc. (London)*, Vol. 74, Ser. A, pp. 498-506.
- Hutchinson, J. W. and Neale, K. W. (1977), "Influence of Strain-Rate Sensitivity on Necking Under Uniaxial Tension", *Acta Met.*, Vol. 25, pp. 839-846.

- Jahsman, W. E. (1971), "Reexamination of the Kolsky Technique for Measuring Dynamic Material Behavior", J. Appl. Mech., Vol. 38, pp. 75-82.
- Johnson, G. R. (1981), "Dynamic Analysis of a Torsion Test Specimen Including Heat Conduction and Plastic Flow", J. Eng. Mat. Tech., Vol. 103, pp. 201-206.
- Johnson, J. E., Wood, D. S. and Clark, D. S. (1953), "Dynamic Stress-Strain Relations for Annealed 2S Aluminum Under Compression Impact", J. Appl. Mech., Vol. 20, pp. 523-529.
- Johnson, W. (1972), Impact Strength of Materials, Edward Arnold, London.
- Johnston, W. G. and Gilman, J. J. (1959), "Dislocation Velocities, Dislocation Densities, and Plastic Flow in Lithium Fluoride Crystals", J. Appl. Phys. Vol. 30, pp. 129-144.
- Jonas, G. H. and Zukas, J. A. (1978), "Mechanics of Penetration: Analysis and Experiment", Int. J. Eng. Sci., Vol. 16, pp. 879-903.
- Kanninen, M. F., Adler, W. F., Rosenfield, A. R. and Jaffee, R. I. (Ed.) (1969), Inelastic Behavior of Solids, Battelle Institute Materials Science Colloquia, McGraw-Hill, New York.
- Von Karman, T. (1942), "On the Propagation of Plastic Deformation in Solids", NDRC Report A-29 (OSRD No. 365).
- Von Karman, T. and Duwez, P. (1950), "The Propagation of Plastic Deformation in Solids", J. Appl. Phys., Vol. 21, pp. 987-994.
- Karnes, C. H. (1968), "The Plate Impact Configuration for Determining Mechanical Properties of materials at High Strain Rates", in Mechanical Behavior of Materials Under Dynamic Loads, (Ed. U. S. Lindholm), Springer-Verlag, New York, pp. 270-293.
- Karnes, C. H. and Ripperger, E. A. (1966), "Strain Rate Effects in Cold Worked High Purity Aluminum", J. Mech. Phys. Solids, Vol. 14, pp. 75-88.
- Kawata, K. and Shioiri, J. (Ed.) (1978), Proceedings IUTAM 1977 Symposium on High Velocity Deformation of Solids, Springer-Verlag, Berlin.
- Keh, A. S. and Weissmann, S. (1963), "Dislocation Substructure in Body-Centered Cubic Metals", Chapter 5 in Electron and Strength of Crystals, (Ed. G. Thomas and J. Washburn), Interscience Publishers, New York, pp. 231-300.
- Kelly, J. M. (1967), "Generalizations of Some Elastic-Viscoplastic Stress-Strain Relations", Trans. Soc. Rheol., Vol. 11, No. 1, pp. 55-76.

- Kendall, D. P. (1972), "The Effect of Strain Rate and Temperature on Yielding in Steels", J. Basic Engng., pp. 207-212.
- Kendall, D. P. and Davidson, T. E. (1966), "The Effect of Strain Rate on Yielding in High Strength Steels", J. Basic Engng., pp. 37-44.
- Kim, K. S. and Clifton, R. J. (1980), "Pressure-Shear Impact of 6061-T6 Aluminum", J. Appl. Mech., Vol. 47, pp. 11-16.
- Klahn, D., Mukherjee, A. K. and Dorn, J. E. (1970), "Strain-Rate Effects", Second Int. Conf. on the Strength of Metals and Alloys, Asilomar, California, ASM Vol. 3, pp. 951-982.
- Klepaczko, J. (1967), "Effects of Strain-Rate History on the Strain Rate Hardening Curve of Aluminum", Arch. Mech. Stosowanej, Vol. 19, No. 2, pp. 211-229.
- Klepaczko, J. (1968), "Strain-Rate History Effects for Polycrystalline Aluminum and the Theory of Intersections", J. Mech. Phys. Solids, Vol. 16, pp. 255-266.
- Klepaczko, J. (1975), "Thermally Activated Flow and Strain Rate History Effects for Some Polycrystalline FCC Metals", Mat. Sci, Eng., Vol. 18, pp. 121-136.
- Klepaczko, J. (1981), "A Model for Yielding and Flow of Iron and BCC Metals Based on Thermal Activation", Brown University Report, DMR79-23257/132, NSF CME 79-23742/4.
- Klepaczko, J. and Duffy, J. (1980), "Strain Rate History Effects in BCC Metals", presented at ASTM Symposium on Mechanical Testing, Bal Harbour, Florida. To be published in ASTM STP 765, Mechanical Testing for Deformation Model Development, (Ed. R. W. Rohde and J. C. Swearingen).
- Klepaczko, J., Frantz, R. A. and Duffy, J. (1977), "History Effects in Polycrystalline FCC Metals Subjected to Rapid Changes in Strain Rate and Temperature", Polska Akademia Nauk, Instytut Podstawowych Problemow Techniki, Engng. Trans., Vol. 25, No. 1, pp. 3-22.
- Kocks, U. F., Argon, A. S. and Ashby, M. F. (1975), Thermodynamics and Kinetics of Slip, Progress in Materials Science, Vol. 19, Pergamon Press, Oxford.
- Kocks, U. F., Jonas, J. J. and mecking, H. (1978), "The Development of Strain-Rate Gradients", Report of Argonne National Laboratory, Materials Science Division.
- Kolsky, H. (1949), "An Investigation of the Mechanical Properties of Materials at Very High Rates of Loading", Proc. Phys. Soc., London, V62-B, pp. 676-700.
- Kolsky, H. (1953), Stress Waves in Solids, Oxford University Press, London.

- Kolsky, H. and Douch, L. S. (1962), "Experimental Studies in Plastic Wave Propagation", J. Mech. Phys. Solids, Vol. 10, pp. 195-223.
- Korbel, A. and Swiatkowski, K. (1972), "The Role of Strain Rate in the Formation of Dislocation Structure and its Influence on the Mechanical Properties of Aluminum", Met. Sci. J., Vol. 6, pp. 60-63.
- Krafft, J. M. and Sullivan, A. M. (1958), "Effect of Grain Size and Carbon Content on the Yield Delay-Time of Mild Steel", Trans., ASM, Vol. 51, pp. 643-665.
- Kumar, A. and Kumble, R. G. (1969), "Viscous Drag on Dislocation at High Strain Rates in Copper", J. Appl. Phys., Vol. 40, No. 9, pp. 3475-3480.
- Kumar, A., Maiden, C. J. and Green, S. J. (1967), "Survey of Strain Rate Effects", The First Int. Conf. of the Center for High Energy Forming, Estes Park, Colorado.
- Larsen, T. L., Rajnak, S. L., Hauser, F. E., and Dorn, J. E. (1964), "Plastic Stress Strain-Rate Temperature Relations in HCP Ag₂ A Under Impact Loading", J. Mech. Phys. Solids, Vol. 12, pp. 361-376.
- Lee, E. H. (1970), "Constitutive Relations for Dynamic Loading and Plastic Waves", in Inelastic Behavior of Solids, (Ed. M. F. Kanninen, W. F. Adler, A. R. Rosenfield, and R. I. Jaffee), McGraw-Hill, pp. 423-446.
- LeMaitre, F., Bizeul, D. and Weill, R. (1974), "Contribution to the Study of Periodic Phenomena in Dynamic Deformations", C.I.R.P. 24th General Assembly Kyoto, Japan.
- Leslie, W. C. (1973), "Microstructural Effects of High Strain Rate Deformation", in Metallurgical Effects at High Strain Rates, (Ed. R. W. Rohde, B. M. Butcher, J. R. Holland and C. H. Karnes), Plenum Press, New York, pp. 571-586.
- Leung, E. K. C. (1980), "An Elastic-Plastic Stress Analysis of the Specimen Used in the Torsional Kolsky Bar", J. Appl. Mech., Vol. 47, pp. 278-282.
- Lewis, J. L. and Campbell, J. D. (1972), "The Development and Use of a Torsional Hopkinson-Bar Apparatus", Exp. Mech., Vol. 12, No. 11, pp. 520-524.
- Lewis, J. L. and Goldsmith, W. (1973), "A Biaxial Split Hopkinson-Bar for Simultaneous Torsion and Compression", Rev. Sci. Instrum., Vol. 44, No. 7, pp. 811-813.
- Li, C. H. and Clifton, R. J. (1981), "Dynamic Stress-Strain Curves at Plastic Shear Strain Rates of 10^5 s^{-1} ", Proc. 1981 Topical Conference on Shock Waves in Condensed Matter, Amer. Phys. Soc.

- Lindholm, U. S. (1964), "Some Experiments with the Split Hopkinson Pressure Bar", *J. Mech. Phys. Solids*, Vol. 12, pp. 317-335.
- Lindholm, U. S. (Ed.) (1968), Mechanical Behavior of Materials Under Dynamic Loads, Springer-Verlag, New York.
- Lindholm, U. S. (1968), "Some Experiments in Dynamic Plasticity Under Combined Stress", in Mechanical Behavior of Materials Under Dynamic Loads, (Ed. U. S. Lindholm), Springer-Verlag, New York, pp. 77-95.
- Lindholm, U. S. (1971), "High Strain Rate Tests" in Techniques of Metals Research, (Ed. R. F. Bunshah), Vol. 5, Part 1, Measurement of Mechanical Properties, Interscience, New York, pp. 199-271.
- Lindholm, U. S. (1978), "Deformation Maps in the Region of High Dislocation Velocity", Proc. IUTAM 1977 Symposium on High Velocity Deformation of Solids, (Ed. K. Kawata and J. Shioiri), Springer-Verlag, Berlin.
- Lindholm, U. S. and Bessey, R. L. (1969), "A Survey of Rate Dependent Strength Properties of Metals", Air Force Materials Laboratory, Technical Report 69-119.
- Lindholm, U. S. Nagy, A., Johnson, G. R. and Hoegfeldt, J. M. (1980), "Large Strain, High Strain Rate Testing of Copper", *Trans. ASME, J. Eng. Mat. Technol.*, Vol. 102, No. 4, pp. 376-381.
- Lindholm, U. S. and Yeakley, L. M. (1965), "Dynamic Deformation of Single and Polycrystalline Aluminum", *J. Mech. Phys. Solids*, Vol. 13, pp. 41-53.
- Lindholm, U. S. and Yeakley, L. M. (1968), "High Strain Rate Testing: Tension and Compression", *Exp. Mech.*, Vol. 8, No. 1, pp. 1-9.
- Lindholm, U. S., Yeakley, L. M. and Bessey, R. L. (1968), "An Investigation of the Behavior of Material Under High Rates of Deformation", Air Force Materials Laboratory, Technical Report 68-194.
- Lipkin, J., Campbell, J. D. and Swearengen, J. D. (1978), "The Effects of Strain-Rate Variations on the Flow Stress of OFHC Copper", *J. Mech. Phys. Solids*, Vol. 26, pp. 251-268.
- Litonski, J. (1977), "Plastic Flow of a Tube under Adiabatic Torsion", *Bulletin de l'Academie Polonaise des Sciences*, Vol. 25, No. 1, pp. 7-14.
- Lueg, W. and Muller, H-G (1957), "Formanderungsverhalten von Stahl C45 beim Stauchen und Scheren in Abhangigkeit von Temperatur and Formanderungsgeschwindigkeit", *Archiv fur das Eisenhutenwesen*, pp. 505-516.
- MacGregor, C. W. and Fisher, J. C. (1946), "A Velocity Modified Temperature for the Plastic Flow of Metals", *J. Appl. Mech.*, Vol. 13, pp. A11-A16.

- McQueen, H. J. and Hockett, J. E. (1970), "Microstructures of Aluminum Compressed at Various Rates and Temperatures", *Met. Trans.*, Vol. 1, pp. 2997-3004.
- Maiden, C. J. and Green, S. J. (1966), "Compressive Strain Rate Tests on Six Selected Materials at Strain Rates from 10^{-3} to 10^4 sec", *J. Appl. Mech.*, pp. 496-504.
- Malvern, L. E. (1951a), "The Propagation of Longitudinal Waves of Plastic Deformation in a Bar of Material Exhibiting a Strain-Rate Effect", *J. Appl. Mech.*, Vol. 18, pp. 203-208.
- Malvern, L. E. (1951b), "Plastic Wave Propagation in a Bar of Material Exhibiting a Strain-Rate Effect", *Quart. Appl. Math.*, Vol. 8, pp. 405-411.
- Manjoine, M. J. (1944), "Influence of Rate of Strain and Temperature on Yield Stresses of Mild Steel", *J. Appl. Mech.*, Vol. 11, A211-218.
- Manjoine, M. and Nadai, A. (1940), "High Speed Tension Tests at Elevated Temperatures", *Proc. ASTM*, Vol. 40, pp. 822-837.
- Marsh, K. J. and Campbell (1963), "The Effect of Strain Rate on the Post-Yield Flow of Mild Steel", *J. Mech. Phys. Solids*, Vol. 11, pp. 49-63.
- Martensson, N. (1970), "On the Influence of the Rate of Deformation at Cold Processing", *Acta polytech. Scandinavica, Mech. Engng Ser* No. 52, Stockholm, pp. 6-89.
- Mathew, P., Hastings, W. F. and Oxley, P. L. B. (1979), "Machining--a Study in High Strain Rate Plasticity," in Mechanical Properties at High Rates of Strain 1979, (Ed. J. Harding), The Institute of Physics, London, pp. 360-371.
- Meyers, M. E. and Murr, L. E. (Ed.) (1981), Shock Waves and High-Strain-Rate Phenomena in Metals, Plenum Press, New York.
- Moss, G. L. (1981), "Shear Strains, Strain Rates and Temperature Changes in Adiabatic Shear Bands", Chapter 19 in Shock Waves and High-Strain-Rate Phenomena in Metals, Plenum Press, New York, pp. 299-312.
- Moss, G. L. and Pond, R. B., (1975), "Inhomogeneous Thermal Changes in Copper During Plastic Elongation", *Met. Trans.*, Vol. 6A, pp. 1223-1235.
- Muller, T. (1971), "The Visco-Plastic Dynamic Behavior of Iron and Nickel at Elevated Temperatures", *Acta Met.*, Vol. 19, pp. 691-699.
- Nadai, A. and Manjoine, M. J. (1941), "High-Speed Tension Tests at Elevated Temperatures, Parts II and III", *J. Appl. Mech.*, pp. A77-A91.

- Needleman, A. and Rice, J. R. (1978), "Limits to Ductility Set by Plastic Flow Localization", Mechanics of Sheet Metal Forming, (Ed. D. P. Koistinen and Localization", Mechanics of Sheet Metal Forming, (Ed. D. P. Koistinen and N. M. Wang), Plenum Press, New York, pp. 237-267.
- Nicholas, T. (1971), "Strain-Rate and Strain-Rate History Effects in Several Metals in Torsion", *Exp. Mech.*, Vol. 11, No. 8, pp. 370-374.
- Nicholas, T. (1973), "On the Determination of Constitutive Equations from Plastic Wave Propagation Phenomena", Technical Report AFML-TR-73-73.
- Nicholas, T. (1981), "Material Behavior at High Strain Rates", Chapter 8 in Impact Dynamics (Ed. J. Zukas et al.), John Wiley, New York, pp. 277-331.
- Nowacki, W. K. (1978), Stress Waves in Non-Elastic Solids, Pergamon Press, Oxford.
- Nowacki, W. K. and Zarka, J. (1974), "Sur le Champ des Temperatures Obtenues en Thermoelastoviscoplasticite", *Arch. Mech. Stosowanej*, Vol. 26, No. 4, pp. 701-715.
- Olson, G. B. Mescall, J. F. and Azrin, M. (1981), "Adiabatic Deformation and Strain Localization", Chapter 14 in Shock Waves and High-Strain-Rate Phenomena in Metals, (Ed. M. A. Meyers and L. E. Murr), Plenum Press, New York, pp. 221-247.
- Orava, R. N. and Otto, H. E. (1970), "The Effect of High Energy Rate Forming on the Terminal Characteristics of Metal - A Review", *J. Metals*, Vol. 22, pp. 17-31.
- Orowan, E. and Los, J. (1950), Descriptions of the cam plastometer in the published literature are found in Loizou, N. and Sims, R. B., "The Yield Stress of Pure Lead in Compression," *J. Mech. Phys. Solids* (1953), Vol. 1, pp. 234-243, or in Alder, J. F. and Phillips, V. A. (1954-55) loc. cit.
- Oxley, P. L. B. (1963), "Rate of Strain Effect in Metal Cutting", *J. Engng Ind.*, Vol. 85, pp. 335-357.
- Oxley, P. L. B. (1974), "Allowing for Strain Rate Effects in the Analysis of Metal Working Processes", in Mechanical Properties at High Rates of Strain, (Ed. J. Harding), The Institute of Physics, pp. 359-381.
- Oxley, P. L. B. and Hastings, W. F. (1977), "Predicting the Strain Rate in the Zone of Intense Shear in which the Chip is Formed in Machining from the Dynamic Flow Stress Properties of the Work Material and the Cutting Conditions", *Proc. Roy. Soc., London A*, Vol. 356, pp. 395-410.

- Patel, N. R. and Bieniek, M. P. (1979), "Analysis of Visco-Plastic Behavior of Metals", *Mat. Sci, Eng.*, Vol. 40, pp. 123-134.
- Perzyna, P. (1966), "Fundamental Problems in Viscoplasticity", in Advances in Applied Mechanics, Vol. 9, Academic Press, pp. 243-377.
- Perzyna, P. (1971), "Thermodynamic Theory of Viscoplasticity", in Advances in Applied Mechanics, Vol. 11, Academic Press, pp. 313-354.
- Prasad, Y. V. R. K. and Armstrong, R. W. (1973), "Effect of Grain Size on the Thermal Activation Strain Rate Analysis in HCP Metals", *Indian Journal of Technology*, Vol. 11, No. 11, pp. 513-515.
- Rabotnov, Yu. N. (1968), "Model of Elastic-Plastic Medium with Delayed Yielding", *Prk. Mech. i Techn. Phys.*, No. 3, pp. 45-54.
- Rabotnov, Yu. N. and Suvorova, J. V. (1972), "Deformation of Metals Under Uniaxial Loading", *Izv. AN USSR Mekhanika Tverdogo Tela, (Mech. Solids)*, No. 4, pp. 41-54.
- Rabotnov, Yu. N. and Suvorova, J. V. (1978), "The Non-Linear Hereditary-Type Stress-Strain Relation for Metals", *Int. J. Solids Structures*, Vol. 14, No. 3, pp. 173-186.
- Rakhmatulin, Kh. A (1945), "On the Propagation of Waves of Unloading", *Prikl. Mat. i Mekh.*, Vol. 9, pp. 91-100.
- Rakmatulin, Kh. A. and Dem'yanov, Yu A. (1966), Strength Under High Transient Loads, Israel Program for Scientific Translations, Jerusalem.
- Ring, P. J., Busboom, H. J. and Spalaris, C. N. (1972), "Post-Irradiation Mechanical Properties of Austenitic Alloys and Effects of Intergranular Fission Product Attack", from International Embrittlement and Creep, The British Nuclear Engineering Society, London, pp. 197-208.
- Ripperger, E. A. and Watson, H., Jr. (1968), "The Relationship Between the Constitutive Equation and One-Dimensional Wave Propagation", in Mechanical Behavior of Materials Under Dynamic Loads, (Ed. U. S. Lindholm), Springer-Verlag, New York, pp. 294-313.
- Rogers, H. C. (1974), "Adiabatic Shearing; A Review", Drexel University Report for U. S. Army Research Office.
- Rogers, H. C. and Shastry, C. V. (1981), "Material Factors in Adiabatic Shearing in Steels", Chapter 18 in Shock Waves and High-Strain-Rate Phenomena in Metals, Plenum Press, New York, pp. 285-298.
- Rohde, R. W., Butcher, B. M., Holland, J. R. and Karnes, C. H. (Ed.) (1973), Metallurgical Effects at High Strain Rates, Plenum Press, New York.

- Rosenfield, A. R., Hahn, G. T., Bement, A. L., Jr. and Jaffee, R. I. (Ed.) (1968), Dislocation Dynamics, Battelle Institute Materials Science Colloquia, McGraw-Hill.
- Samanta, S. K. (1968), "Resistance to Dynamic Compression of Low-Carbon Steel and Alloy Steels at Elevated Temperatures and at High Strain-Rates", *Int. J. Mech. Sci.*, Vol. 10, pp. 613-636.
- Samanta, S. K. (1969), "On Relating the Flow Stress of Aluminum and Copper to Strain, Strain-Rate and Temperature", *Int. J. Mech. Sci.*, Vol. 11, pp. 433-453.
- Samanta, S. K. (1971), "Dynamic Deformation of Aluminum and Copper at Elevated Temperatures", *J. Mech. Phys. Solids*, Vol. 19, pp. 117-135.
- Samuels, L. E. and Lamborn, I. R. (1978), "Failure Analysis of Armament Hardware", in Metallography in Failure Analysis, (Ed. J. L. McCall and P. M. French), Plenum Press, New York, pp. 167-190.
- Santhanam, A. T., Ramachandran, V. and Reed-Hill, R. E. (1970), "An Investigation of the Shape of the Titanium Stress-Strain Curves after a Strain Rate Change", *Met. Trans.*, Vol. 1, pp. 2593-2598.
- Sellars, C. M. and Tegart, W. J. Mc G. (1966), "La Relation entre la Resistance et la Structure dans la Deformation a Chaud", *Mem. Sci. Rev. Metall.*, Vol. 63, pp. 731-746.
- Sellars, C. M. and Tegart, W. J. Mc G. (1972), "Hot Workability", *Int. Metall. Rev.*, Review 158, *Metals and Materials*, Vol. 17, pp. 1-24.
- Senseny, P. E., Duffy, J. and Hawley, R. H. (1978), "Experiments on Strain Rate History and Temperature Effect during the Plastic Deformation of Closed Packed Metals", *J. Appl. Mech.*, Vol. 45, pp. 60-66.
- Shioiri, J. and Satoh, K. (1974), "An Ultrasonic Wave Study of the Behavior of Dislocations Under High Strain Rate Deformations" in Mechanical properties of Materials at High Rate of Strain, (Ed. J. Harding), The Institute of Physics, London, pp. 154-162.
- Shirakashi, T. and Usui, E. (1970), "Effect of Temperature and Strain Rate Upon Flow Stress of Metals in Compression. Part I", *Bull. Jap. Soc. of prec. Eng.*, Vol. 14, No. 4, pp. 91-100.
- Smith, E., Cook, T. S. and Rau, C. A. (1977), "Flow Localization and the Fracture Toughness of High Strength Materials", Fracture, Vol. 1, 1CF4, Waterloo, Canada, pp. 215-236.
- Sokolov, L. D. (1949), "On the Problem of Evaluating Material Resistance to Plastic Deformation Depending on Strain Rate and Temperature", *Doklady Akad. Nauk, SSSR*, Vol. 67, No. 3, pp. 459-462.

- Spaans, C. (1972), "A Treatise on the Streamlines and the Stress, Strain, and Strain Rate Distributions, and on Stability in the Primary Shear Zone in Metal Cutting", J. Eng. Ind., Vol. 84, pp. 690-696.
- Staker, M. R. (1981), "The Relation between Adiabatic Shear Instability Strain and Material Properties", Acta Met., Vol. 29, pp. 683-689.
- Staker, M. R. and Holt, D. L. (1972), "The Dislocation Cell Size and Dislocation Density in Copper Deformed at Temperatures between 25 and 700C", Acta. Met., Vol. 20, pp. 569-579.
- Stelly, M. and Dormeal, R. (1977), "Some Results on the Dynamic Deformation of Copper", IUTAM, Symposium on High Velocity Deformation of Solids, (Ed. K. Kawata and J. Shioiri), Springer-Verlag, New York.
- Sternglass, E. J. and Stuart, D. A. (1953), "Transient Deformations in Elastoplastic Media", J. Appl. Mech., Vol. 20, No. 3, pp. 427-434.
- Suvorova, J. V. (1974), "Plastic Deformation of Metals Under Various Loading Rates", Izv. AN Mekhanika Tverdogo Tela, (Mech. Solids), Vol. 9, No. 1, pp. 73-79.
- Sutterlin, R. (1972, 1973), "Sur la Plasticite Dynamique. Son SuApplication a l'Etude du Forgeage (Dynamic Plasticity. Its Application to Studies of Forging)", Sci. et Techn. de l'Armement, Memorial de l'Artillerie francaise, Vol. 46, No. 4, pp. 909-989, and Vol. 47, No. 3, pp. 567-646.
- Suzuki, H., Yabuki, Y., Hashizume, S., Kenmochi, K., Ichihara, Y. and Nakajima, S. (1968), "Studies on the Flow Stress of Metals and Alloys", Report Inst. of Indust. Sci., The University of Tokyo, Vol. 18, No. 3, Ser. No. 117.
- Sylwestrowicz, W. D. (1958), "The Temperature Dependence of the Yield Stress of Copper and Aluminum", Trans., AIME, Vol. 212, pp. 617-624.
- Symonds, P. S. (1967b), "Survey of Methods of Analysis for Plastic Deformation of Structures Under Dynamic Loadings", Brown University, Report BU/NSRDC/1-67.
- Symonds, P. S., Ting, T. C. T. and Robinson, D. N. (1967a), "Survey of Progress in Plastic Wave propagation in Solid Bodies", Brown University Report Contract DA-19-020-ORD-5453 (A).
- Tanaka, K. and Ogawa, K. (1979a), "The Effects of Temperature and Strain Rate on the Strength of Polycrystalline Zinc", Bulletin, Japan Soc. Mech. Engineers, Vol. 22, No. 165, pp. 300-308.
- Tanaka, K. and Ogawa, K. (1979b), "Temperature and Strain Rate Effects upon the Strength of Zinc Single Crystals", Bulletin, Japan Soc. Mech. Engineers, Vol. 22, No. 167, pp. 627-635.

- Tanaka, K. and Ogawa, K. (1980), "Effects of Temperature and Strain Rate on the Strength of Pyramidal Slip in Zinc Single Crystals", Proc. 23rd Japan Congress on Mat. Res., pp. 46-50.
- Taylor, G. I. (1942), "The Plastic Wave in a Wire Extended by an Impact Load", Report written 1942 for the Civil Defense Research Committee, Ministry of Home Security (England), published in The Scientific Papers of G. I. Taylor, Vol. 1, Mechanics of Solids, Ed. by G. K. Batchelor, Cambridge University Press, 1958, pp. 467-479.
- Taylor, G. I. (1946), "The Testing of Materials at High rates of Loading", J. Inst. Civil Engrs., London, Vol. 26, pp. 486-519.
- Taylor, G. I. (1948), "The Use of Flat-Ended Projectiles for Determining Dynamic Yield Stress: I. Theoretical Considerations", Proc., Roy. Soc., (London), Vol. 194, Series A, pp. 289-299.
- Trozera, T., Sherby, O. D. and Dorn, J. E. (1957), "Effect of Strain Rate and Temperature on the Plastic Deformation of High Purity Aluminum", trans. ASM, Vol. 49, pp. 173-187.
- Tsao, M. C. C. and Campbell, J. D. (1973), Plastic Shear Properties of Metals and Alloys at High Strain Rates", Air Force Mat. Lab. Report, AFML-TR-73-177.
- Tseng, D. and Tangri, K. (1977), "Temperature and Strain Rate Sensitivities of Flow Stress for the High Purity AISI Iron", Scripta Met., Vol. 11, pp. 719-723.
- Von Karman, T. (1942), "On the Propagation of Plastic Deformation in Solids", NDRC Report A-29 (OSRD No. 365).
- Von Karman, T. and Duwez, P. (1950), "The Propagation of Plastic Deformation in Solids", J. Appl. Phys., Vol. 21, pp. 987-994.
- Von Turkovich, B. F. (1972), "Metal Cutting Analysis", in Review of Materials Processing Literature - 1966-1968, (Ed. S. Ramalingam), J. Engng Ind., pp. 704-706.
- Whiffin, A. C. (1948). "The use of Flat-Ended Projectiles for Determining Dynamic Yield Stress: II. Tests on Various Metallic Materials", Proc. Roy. Soc. (London), Ser. A, Vol. 194, pp. 300-322.
- White, M. P. and Griffis, L. (1947), "The Permanent Strain in a Uniform Bar Due to Longitudinal Impact", J. Appl. Mech., Vol. 14, pp. 337-343.
- Wiedersich, H. W. (1957), Written Discussion to paper by T. A. Trozera, O. D. Sherby, and J. E. Dorn, "Effect of Strain Rate and Temperature on the Plastic Deformation of High Purity Aluminum", Trans. ASM, Vol. 49, pp. 173-187.
- Wielke, B. (1978), "Dislocation Dynamics During Rate Change", Acta Met., Vol. 26, pp. 103-112.

- Wong, W. A. and Jonas, J. J. (1968), "Aluminum Extrusion as a Thermally Activated Process", Trans., Met. Soc. AIME, Vol. 242, pp. 2271-2280.
- Woodward, R. L. (1978), "The Penetration of Metal Targets which Fail by Adiabatic Shear Plugging", Int. J. Mech. Sci., Vol. 20, pp. 599-607.
- Woodward, R. L. (1979), "Metallographic Features Associated with the Penetration of Titanium Alloy Targets", Met. Trans. A, Vol. 10, pp. 569-573.
- Woodward, R. L. and Aghan, R. L. (1978), "The Structure of a White-Etching Band in an Explosively Fractured Steel", Metals Forum, Vol. 1, No. 4, pp. 180-184.
- Work, C. E. and Dolan, T. J. (1953), "The Influence of Strain Rate and Temperature on the Strength and Ductility of Mild Steel in Torsion", Proc., ASTM, Vol. 53, pp. 611-626.
- Wronski, A. S., Sargent, G. A. and Johnson, A. A. (1965), "Irradiation Hardening and Embrittlement in Body-Centered Cubic Transition Metals", in Flow and Fracture of Metals in Nuclear Environments, ASTM, STP 380, pp. 69-85.
- Wulf, G. L. (1974), "Dynamic Stress-Strain Measurements at Large Strains", in Mechanical Properties at High rates of Strain, (Ed. J. Harding), The Institute of Physics, London, pp. 48-52.
- Wulf, G. L. (1978a), "The High Strain Rate Compression of 7039 Aluminum", Int. J. Mech. Sci., Vol. 20, pp. 609-615.
- Wulf, G. L. (1978b), "The High Strain Rate Compression of 1023 and 4130 Steels", Int. J. Mech. Sci., Vol. 20, pp. 843-848.
- Wulf, G. L. (1979), "High Strain Rate Compression of Titanium and Some Titanium Alloys", Int. J. Mech. Sci., Vol. 21, pp. 713-718.
- Yellup, J. M. and Woodward, R. L. (1980), "Investigations into the Prevention of Adiabatic Shear Failure in High Strength Armour Materials", Res. Mechanica, Vol. 1, pp. 41-57.
- Yew, C. H. and Richardson, H. S., Jr. (1969), "The Strain-Rate Effect and the Incremental Plastic Wave in Copper", Exp. Mech., Vol. 26, pp. 366-373.
- Yoshida, S. and Nagata, N. (1966), "Deformation of Polycrystalline Aluminum at High Strain Rates", Trans. Jap. Inst. Met., Vol. 7, pp. 273-279.
- ✓ Zaverl, F., Sr. and Lee, D. (1978), "Constitutive Relations for Nuclear Reactor Core Materials", J. Nuc. Mat., Vol. 75, pp. 14-19.